University of Nottingham
UK | CHINA | MALAYSIA

Development of a Phosphate Based Glass Product for Trace Mineral Supplementation in Ruminants

By

Ellena Amiee Cartlidge

Thesis submitted to the University of Nottingham for the degree of Doctor of Philosophy

July 2021

Contents

Abstract

Optimisation of agricultural practises is essential to feed a growing global population. One method commonly used by farmers to improve livestock production outputs is the administration of mineral supplements. Delivering minerals using a bolusing method enables consistent, reliable long-term mineral supplementation of livestock whilst grazing at pasture. However, this technique heavily relies on the bolused mineral supplement delivering minerals predictably and reliably across a known duration of time. Studies assessing the mineral boluses currently commercially available in the UK suggests that their ion release is not consistent across the complete product lifespan. Therefore, there is a need to develop a bolus that meets the requirement for a reliable, long term ion supplement with consistent ion release.

The principle aim of this research was to develop a phosphate-based glass supplement to prevent trace mineral deficiency in ruminants through sustained mineral release over a 6-month period. A secondary aim of this research was to conduct competitor analysis on a commercially available phosphate-based bolus for mineral supplement in ruminants.

These two main objectives were explored by trialling multiple different product designs and phosphate glass formulations. Designs and formulations were assessed through physical characterisation techniques including differential scanning calorimetry, x-ray diffraction, energy-dispersive x-ray spectroscopy, ash fusion testing and degradation studies to assess *in vitro* ion release. As a result of extensive testing the glass formulation a sintered phosphate-based glass bolus with the formulation P50-Ca2-Na17-Cu30-Co1 was trialled *in vivo* over a 1-month and compared to the ion release profiles obtained from the *in vitro* studies using rumen fluid and blood plasma mineral concentrations to assess degradation. Functional biochemical indicators such as Vitamin B_{12} were also used to assess mineral

bioavailability, providing a more complete picture. These studies found that the proposed glass formulation (P50-Ca2-Na17-Cu30-Co1) did not adequately match the suggested Industry Partner's ideal daily ion release requirements as it degraded significantly slower than expected, likely as a result of the *in vitro* simulation conditions not replicating *in vivo* conditions closely enough.

In addition to the development of a novel bolus, the assessment of a commercially available phosphate-based bolus for mineral supplementation in ruminants was conducted to gain clarity into the degradation and ion release profile of this product *in vivo*. It was found that this bolus successfully supplemented cobalt, selenium and iodine, significantly elevating key biochemical indicators such as glutathione peroxidase.

This research generated new knowledge surrounding phosphate based glass formulations and *in vivo* simulation techniques. However, this work also highlighted the complexities of developing a multi-faceted, long term supplement product designed for *in vivo* use. As such, key areas of further work were highlighted, which include bolus prototype production improvement and experimental *in vivo* simulation refinement.

Acknowledgements

First and foremost I would like to thank my academic supervisors, without whom this work would not have been possible. To Dr Ifty Ahmed, your kindness and support have brightened the toughest of days. To Dr Nigel Kendall whose endless enthusiasm for the subject knows no bounds and is truly contagious, and to Dr Ed Lester for his patience and guidance when I was truly out of my depth.

I have been incredibly fortunate to be surrounded by countless friends and colleagues whose collective wisdom and support enabled the continuation of this work; Uresha Patel, Ronni da Silva, Andrea Clarkson, Adam Blanchard, Emma Drinkall, Andy Parsons, Zakir Hossain, Towhid Islam and Reda Felfel to name a few. Thank you to all of the technical staff in the ITRC, nmRC and Vet School for their help.

Thank you to Tangerine Holdings for giving me the opportunity to conduct this work. To Sally-Ann Emmas for her guidance throughout this project, to all of the R&D department at Tangerine. Thank you for your support during this journey, with particular mentions to Rachel Eaton, Neil Killcullen, Edd Sailsbury, Chloe Townsley, Natalie Ireland and Morgan McCabbe. A special mention to Dawn who gives the best hugs and makes the most incredible toast.

I am blessed to have been on this journey with the most wonderful friends: Caroline Morris, Lara Gosling and Alice Willett have always been on the end of the phone. Your friendship has been invaluable.

I would like to thank my family for their love with particular mention to my parents and my cousin, Brooklyn Norton, thank you for always championing me, providing rational and considered advice. I am truly blessed to have you in my life.

And lastly, thank you to James who helped me over the finish line.

I have not failed, I’ve just found 10,000 different ways that won’t work

– **Thomas Edison**

Scientific work must not be considered from the point of view of usefulness of it. It must be done for itself, for the beauty of science and then there is always a chance that a scientific discovery may become, like radium, a benefit to humanity

– **Marie Curie**

List of Abbreviations

°C	Degrees Centigrade
AFT	Ash Fusion Test
ASTM	American Society for Testing and Materials
BS	British Standard
CP	Caeruloplasmin
DEFRA	Department for Environment, Food and Rural Affairs
DSC	Differential Scanning Calorimetric Analysis
DM	Dry Matter
DTA	Differential Thermal Analysis
EDX	Energy-Dispersive X-Ray Spectroscopy
FTIR	Fourier Transmission Infrared Spectroscopy
GLM	General Linear Model
GSH-px	Glutathione Peroxidase
ICP-MS	Inductively Coupled Plasma Mass Spectrometry
ICP-OES	Inductively Coupled Plasma Optical Emission Spectrometry
ISO	International Standards Organisation
MP	Microparticle
mg/kgDM	Milligram per kilogram of dry matter
n=	Number of observations/animals
NP	Nanoparticles
$p <$	Probability is less than,,,
PlCo	Plasma cobalt

PlCu	Plasma copper
PLA	Poly Lactic Acid
PCL	Polycaprolactone
PPB	Parts Per Billion
PPM	Parts Per Million
RDI	Recommended Daily Intake
RFM	Retained Foetal Membrane
ROS	Reactive Oxygen Species
SEM	Scanning Electron Microscope
S.D	Standard Deviation
SE	Standard Error
SOD	Superoxide Dismutase
T_3	Triiodothyronine
T_4	Thyroxine
TBARS	Thiobarbituric Acid Reactive Substances
T_c	Crystallization Temperature
T_g	Transition Temperature
T_m	Melting Temperature
TEM	Transmission Electron Microscope
USP	Unique Selling Point
Wt%	Weight percent
XPS	X-Ray Photoelectron Spectroscopy
XRD	X-Ray Diffraction Analysis

List of Figures

List of Tables

Chapter 1 – Introduction and literature review

1.1 Introduction

The need for improving agricultural efficiency is part of a worldwide discussion. It is estimated that by 2050 the world's population will have increased by ~ 25 % from 7.7 billion to 9.7 billion (United Nations, 2019). In order to support the consumption requirements of the growing population it is essential that all production practices are optimised in order to meet demand. Grazing livestock such as cattle and sheep are able to utilise land unsuitable for crops to grow on, this is currently the most popular method of rearing and finishing livestock in the UK (DEFRA, 2012; Wilkinson *et al.* 2014). However, this means that farmers are reliant on the nutritional content of the pasture to meet the nutrient requirement of the animal, possibly resulting in certain deficiencies. Like humans, animals are commonly given nutritional supplements to alleviate or improve nutritional shortfalls. This in turn improves their ability to grow, reproduce and ultimately results in them being a more effective production animal.

1.2 Ruminant nutrition

Sheep and cattle are classified as ruminants: a type of animal with a multi-chamber stomach consisting of the rumen, reticulum, omasum and abomasum (Whitehead, 1979). Within the rumen exist populations of microflora essential for the metabolism and synthesis of certain vitamins or amino acids essential in the animal's diet.

1.2.1 Trace mineral supplementation

In the UK, the trace elements most likely to be in a nutritional deficit whilst grazing at pasture are cobalt, selenium, copper and iodine (Scott, 2017; McDowell, 1996).

Table 1.1: *The minimum, maximum and recommended daily values for supplementation of sheep and cattle* (Suttle, 2010)

Element	**Recommended daily intake (mg/kgDM)**		**Minimum needed to prevent deficiency (mg/kgDM)**		**Maximum tolerance limit (mg/kgDM)**	
	Sheep	**Cattle**	**Sheep**	**Cattle**	**Sheep**	**Cattle**
Cobalt	0.12	0.25	0.11	0.15	10	25
Copper	10	10	5	10	25	50
Selenium	0.3	0.1	0.05	0.1	2	5
Iodine	0.5	0.5	0.2	0.5	50	50

Table 1.1 shows that there are two different supplemental standards, the minimum needed to prevent deficiency (the lowest intake required to maintain health and prevent nutrient deficiency) and the recommended daily intake (the intake that satisfies the nutritional requirements of nearly all individuals) (Tsuboyama-Kasaoka *et al*. 2013). Therefore, meeting the recommended daily intake is required to promote optimum growth and production.

The prevalence of trace mineral deficiencies in ruminants throughout the UK fluctuates depending on the location, antagonistic element concentrations and season. The AHDB (2010) conducted a trial assessing seven different suckler beer and sheep farms across England and Wales. This study demonstrated that trace element pasture content can fluctuate with the seasons, as well as geographically. For example, one farm reviewed located in Northumberland recorded spring grass copper content of 6.33 mg/kg, but with an autumn grass copper content of 11.43 mg/kg. The

satisfactory pasture concentrations to avoid deficiency was 8 mg/kg, highlighting the complexity of suitable trace mineral supplementation throughout the year. This is in stark contrast to another farm reviewed which recorded 9.53 mg/kg and 9.18 mg/kg in the spring and autumn respectively, emphasising the importance of farmers understanding their farms trace mineral content in order to inform supplementation practises.

1.2.1.1 Cobalt Deficiency

Cobalt (Co) is an essential trace element required in ruminants for the synthesis of Vitamin B_{12} (also known as cobalamin) (Andrews, Hart and Stephenson, 1960; Smith and Marston, 1970; Kenne*dy et al*. 1994).

Vitamin B_{12} is essential in various carbon metabolic pathways, being required for the conversion of propionate to succinate via methylmalonyl-coenzyme A (CoA) in gluconeogenesis (Suttle, 2010) and acts as a cofactor for methionine synthase, needed to prevent toxic accumulation of homocysteine (Rush, Katre, and Yajnik, 2014). Thus, various physiological problems are associated with cobalt deficiency – particularly in respiration, protein synthesis and energy production.

Andrews *et al.* (1966) demonstrated the effect of cobalt supplementation on weight gains in lambs when orally dosed with either cobalt sulphate weekly (7 mg/week), cobalt sulphate monthly (300 mg/month) or cobalt oxide monthly (300 mg/month) each compared against controls over 6-months. The study found that the weekly supplemented group weighed significantly more and had significantly higher serum Vitamin B_{12} and B_{12} liver concentrations than both of the monthly supplemented groups and control group. Additionally, it was recorded that 6-weeks after the “monthly” groups were supplemented, their average serum B_{12} values were recorded as low (0.179 ng/ml and 0.197 ng/ml, for cobalt sulphate and cobalt oxide supplemented groups respectively) and their liver B_{12} concentrations registered as mildly deficient (0.136 µg/g and 0.125 µg/g for cobalt sulphate and cobalt

oxide treated groups respectively). This study showed that neither monthly treatments prevented cobalt deficiency entirely, resulting in sub-optimal growth rates compared the weekly supplemented group, as indicated by the reduced growth weight. Additionally, it emphasised that a regular supply of cobalt was more favourable for production of Vitamin B_{12} compared to sporadic monthly doses.

Vellema *et al.* (1997) supported the work of Andrews *et al.* (1966), after assessing the effect of cobalt supplementation using a bolus containing 3 g cobalt oxide against non-supplemented lambs at Co-deficient pasture. This study conducted over a 3-year period concluded that cobalt supplementation from a bolus resulted in higher serum B_{12} concentrations, better live weight gains (up to 11 kg more mean live weight) and prevented clinical symptoms and death compared to the control group. This study therefore corroborated the work of Andrews *et al.* (1966) regarding the importance of cobalt for key production parameters such as live weight gain, and that consistent supplementation through a bolus enabled more efficient production.

Table 1.2 summarises the primary disorders associated with cobalt deficiency in ruminants. As is evident from this table, not only is cobalt deficiency detrimental to production output but also animal welfare.

Table 1.2: *Primary disorders associated with cobalt deficiency in ruminants.*

Disorder	**Duration**	**Clinical sign/ feature**	**Key functional constituents**	**Biochemical dysfunction**	**References**
White liver disease	Acute	Fatty liver	Adenosyl-cobalamin, Methyl cobalamin, Homocysteine	High liver enzymes, triglyceride concentration, low red blood cell volume, low red cell haemoglobin concentration, raised concentrations of homocysteine.	(Nguyen *et al*. 2008; Kennedy *et al*. 1997; Kalhan, 2009)
Ill-thrift	Acute-Chronic	Weight loss	Methyl-cobalamin	High homocysteine, low haemoglobin concentration	(Smith, Osborne-White, and Gawthorne, 1974; Scott 1992)
Pine	Chronic	Decreased growth	Adenosyl-cobalamin	High meythylmalonic acid concentration	(Smith and Marston 1970; Gawthorne, 1968)

1.2.1.2 Copper Deficiency

Copper (Cu) is required for the synthesis of haemoglobin, as well as the enzymes: monoamine oxidase, monooxygenase, ceruloplasmin, lysyl oxidase, superoxide dismutase and tyrosine (Balemi, 2008). As such, without sufficient Cu dietary intake, growth and production are significantly affected (Suttle, 2010). Secondary copper deficiency can be induced by multiple other antagonistic elements such as molybdenum and sulphur, creating difficulty in finding a balance between supplementing to eliminate deficiency without inducing toxicity due to overcoming antagonistic interference (Clarkson, 2019; Clarkson and Kendall, 2018).

The work of Clarkson, (2019) supported work carried out by Suttle, Abrahams and Thornton, (1984) who reviewed the interaction between dietary sulphur and impaired copper absorption in sheep. This study concluded that soils high in sulphur (0.03 g/kg) can reduce copper absorption coefficient from 0.03 to 0.021, highlighting the importance of understanding the interactions between different elements and how their bioavailability may be affected.

Ledoux *et al.* (1967) assessed the relative bioavailability of different copper sources at concentrations of (20 -180 mg/kg Cu). Using initial liver biopsies as covariates, this study found that copper chloride, acetate and sulphate forms were all highly bioavailable but that cupric oxide had minimal availability. This was reflected in the low concentrations of liver Cu following cupric oxide supplementation (296 +/- 17 mg/kgDM), while copper sulphate and chloride supplementation elicited similarly high liver Cu concentration (350 +/- 38 mg/kgDM and 368 +/- 63 mg/kgDM respectively). This study demonstrated improved bioavailability through an increase in liver copper concentration, other biomarkers could have been considered that might have given a better indication that the copper was being effectively utilised. Functional biomarkers such as ceruloplasmin or superoxide dismutase (SOD) could have been indicators of functionality compared to increased liver

copper concentrations which is indicative of excessive copper supplementation (Kendall, Mackenzie, and Telfer, 2001).

Table 1.3. *Primary disorders associated with copper deficiency in ruminants.*

Disorder	**Clinical sign/ feature**	**Biochemical dysfunction**	**Reference**
Anaemia	Low erythrocyte concentrations, increased presence of Heinz bodies	Decreased activity of ferroxidase-caeruloplasmin and cytochrome c oxidase	(Suttle, Field, and Barlow, 1970; Todd, Godber, and Gunn, 2004)
Ataxia	Staggering gait, stiff movements	Demyelination of the central nervous system	(Frank, 1998)
Bone disorders	Osteochondrosis, osteoporosis	Lysyl oxidase effects formation of collagen	(Frank, 1998; Balemi, 2008)
Abnormal wool/coat growth	Loss of wool crimp	Deterioration of keratinisation	(Marston and Lee, 1948)
Reduced appetite/ reduced growth	Reduced daily intake, poorer feed conversion efficiency	Depleted peptidylglycine-alpha-amidating monoxygenase, enzyme regulate hormones that drives hunger	(Suttle, Field, and Barlow, 1970; Enjalbert *et al*. 1999)

1.2.1.3 Selenium Deficiency

Selenium (Se) is a constituent of glutathione peroxidase (GSH-Px) - one of the major endogenous antioxidants that counteract reactive oxygen species (ROS) that can be damaging to a wide range of tissues and biological processes (Rotruck *et al.* 1973). Selenium is also important for immune function deficiencies associated with white muscle disease, muscular dystrophy and stiff lamb disease *(Muth et al*. 1958; Rock, Kincaid and Carstens, 2001; Schmoelzl and Cowley, 2016), as well as reproductive function such as the synthesis of hormones and embryonic development (Guyot *et al*. 2011; Muñoz *et al.* 2008).

Selenium and Vitamin E work synergistically to reduce the oxidative damage caused by ROS that could impact overall herd health. Arechiga, Ortiz and Hansen, (1994) found that a 10 ml injection containing 500 mg Vitamin E and 50 mg selenium resulted in numerous positive production parameters, including a reduced incidence of retained foetal membrane (3 % compared to 10.1 %), an increase in the percentage of cows pregnant to the first service (41.2 % vs. 25.3 %) and a reduced interval from calving to conception (121 days vs 141 days), suggesting that this intramuscular method of Se supplementation is effective. However, it is well documented that retained placenta increases the likelihood of abnormal partus and gestation length, increasing the occurrence of postpartum diseases, consequently decreasing reproductive performance (Han and Kim, 2005). Therefore these improved parameters may not be directly linked due to sustained Se supplementation by singular injection, but rather a knock on effect of improved health in general. Similarly, it may be due to the synergistic and closely related roles of the selenium and vitamin E that caused the reduction in the retained foetal membrane (RFM). Rotruck *et al.* (1973) demonstrated that Vitamin E prevented sulphur amino acids and fatty acid hydroperoxide formation, whereas selenium is involved in peroxide elimination. Therefore, due to the similar biochemical functions, the

reduction of RFM may have been amplified by the interactions between the two compounds. Endorsing this hypothesis, Gunter, Beck and Phillips, (2003) found that selenium supplementation using sodium selenite or seleno-yeast (26 mg Se/kgDM) resulted in no significant improvement in conception rate or postpartum interval in beef cows.

Kumar *et al.* (2008) showed that supplementation of sodium selenite resulted in significantly increased glutathione peroxidase activity ($p < 0.01$) in the supplemented groups receiving 0.15 ppm or 0.3 ppm Se/day compared to the controls. This study also compared the serum antibody response, observing that those supplemented with selenium elicited a significantly higher immune response than the control ($p < 0.01$). This claim of selenium supplementation promoting a higher immune response is supported by Awadeh, Kincaid and Johnson, (1998) who demonstrated that a group of cattle and calves that received 20 ppm selenium supplementation had significantly lower concentrations of both IgG and IgM than other groups that received 60 ppm and 100 ppm selenium supplementation.

Selenium is also is crucial in the regulation of cell respiration, energy production and the rate of gene transcription (Bassett, Harvey, and Williams, 2003) via its essential role in the metabolism of the thyroid hormone type I deiodinase, required for thyroxine conversion to tri-iodthyronine (Hotz *et al.* 1997). As such, selenium incorporation in a healthy diet is an essential component for correct cellular protein synthesis and foetal development (Filettif and Rapoport, 1984).

1.2.1.4 Iodine Deficiency

Iodine (I) is an essential trace element in both animals and humans. It is required for the production of thyroid hormones such as thyroxine (T_4) and triiodothyronine (T_3), regulators of cell metabolism, growth and for brain development (Meyer *et al*. 2008). The most obvious clinical sign of iodine deficiency is goitre, the enlargement of the thyroid gland (Villar *et al*. 1998) which is most notable in neonates. Mccoy *et al*. (1997)

documented the effect of supplementing pregnant cattle diets containing 0.06 mg I/kgDM versus 0.27 mg I/kgDM, and reported an increase of 120 % thyroid weight in calves born to cattle supplemented with 0.06 mg I/kgDM diet compared to those fed 0.27 mg I/kgDM. However, despite the significant increase in weight of the thyroid gland, it is important to note neonatal survival rate was unaffected. Similarly, Andrews and Sinclair, (1962) noted that iodine deficient neonate's thyroid glands were significantly heavier than those who had received maternal supplementation, an average of 16.7 g compared to 2.7 g respectively. However, similarly to Mccoy *et al.* (1997) it was concluded that dietary iodine deficiency was not associated with the increased mortality rates.

Iodine is also important for reproduction and fertility, Todini, (2007) and Follett and Potts, (1990) demonstrated the importance of T_3 with seasonality, noting that it was due to the interactions between T_3 fluctuation, growth hormone, insulin and corticosterone that resulted in a change of metabolism initiated by the changing day length, thus effecting fertility. Sargison, West and Clark, (1998) found that iodine supplementation by injecting 1 ml of iodised oil (contained 480 mg iodine) 2-weeks before the introduction of rams each year, resulted in improved reproductive performance of ewes, stating that 21 % (year 1) and 14 % (year 2) due to increased twinning rate in the iodine supplemented animals. However, despite this improved reproduction parameter, no significant differences in T_3 orT_4 serum concentrations were observed. The author acknowledged this may have been due to the pasture being grazed having an iodine concentration of 0.31 mg/kgDM not being deficient enough to enough of an improvement in the control group.

1.2.2 Methods of supplementation

To counteract mineral deficiencies, farmers regularly supplement livestock utilising a variety of methods which include: free choice

minerals, in-feed minerals, drenches, injections, pasture dressing and boluses (Kendall, Mackenzie, and Telfer, 2001).

Indirect supplementation methods such as free choice minerals are less popular among farmers than direct methods of administration due to variability of intake (Crosby *et al*. 2004). The use of free choice minerals relies heavily on the animals innate 'nutritional wisdom' (Tait and Fisher, 1996) to select and consume minerals according to their needs

Lobato, Pearce and Beilharz, (1980) noted that over a 12-week study, sheep individual intakes of free choice minerals ranged from 0-732 g/week and that 18 % (n=8) of the population studied did not consume any of the molasses supplementation block provided. However, intake of the supplemental block was only measured during the third week with the use of chromic oxide as a marker. This measurement technique relies on four assumptions, generating significant study risk: that the molasses block and chromic oxide are homogenously mixed; all chromic oxide is excreted and all excreta is collected; and that only recording the for 1 week out of twelve is a valid representation of the entire trial. Therefore, whilst this study demonstrated the high variability of intake, the extent of variability for this trial could have been over-estimated and additional study with more reliable measurement methods is required.

In a methodologically more robust study, Muller *et al.* (1977) compared the consumption of free choice minerals between cattle fed a total mix ration (TMR) containing adequate nutritional mineral needs against those with a TMR containing no added minerals using jugular puncture blood testing. Cattle fed TMR plus minerals consumed more free choice minerals, than cattle with a TMR minus minerals Ca (94.7 g/cow/day vs 75.2 g/cow/day), Mg (56.6 g/cow/day vs 54.0 g/cow/day) and P (76.2 g/cow/day vs 59.2 g/cow/day) respectively.

Muller *et al.* (1977) suggested this supported Pamp, Goodrich and Meiske, (1977) hypothesis that ruminants do not consume minerals to

meet their requirement but rather that they consume to due to craving or appetite. However, it is well established that the effect of certain mineral deficiencies, such as cobalt, cause a reduction in appetite and lethargy (Wang *et al.* 2007; Keener *et al*. 1950). Therefore, the decreased consumption of free-choice minerals may be a direct effect caused by lack of appetite initiated by inadequate mineral concentrations (Marston, 1957; Kennedy *et al*. 1994; Stangl, Schwarz and Kirchgessner, 1999).

Topdressing pasture is a method of indirectly supplementing minerals such as cobalt, zinc and selenium by distributing a thin layer of minerals across the top of the pasture (Andrews, Hart, and Stephenson, 1960; Grace, 1975; McDowell *et al*. 1996). However, this is a costly method as minerals are often added in excess, regardless of the specific nutritional needs of the individual animal (Hybu Cig Cymru, 2011) and there are concerns regarding the high concentrations that may accumulate in pastures and the negative effects this may have on the environment. The top pasture concentration of cobalt sulphate used by Andrews, Hart and Stephenson, (1960) was 5 oz/acre, this equates to ~ 115 mg/m^3. The U.S. Department of Health and Human Services, (1998) assessed the effect of cobalt sulphate heptahydrate inhalation on rats and mice, concluding that there was clear evidence of carcinogenic activity in groups exposed to 3 mg/m^3. Whilst cattle and sheep have a higher tolerance towards cobalt before detrimental effects, it emphasised the potentially hazardous consequences of blanket supplementation to the wider environment and ecosystem. However, it is more likely that this is a less preferable option for farmers due to the higher cost compared to other methods of supplementation in the UK (Hybu Cig Cymru, 2011).

Direct methods of supplementation include drenching, in which oral doses of liquid mineral blends or pastes are administered to individual animals (McDowell, 1996) and bolusing, in which a large sequestered source of minerals known as a bolus or intraruminal device is orally

administered, allowing the minerals to be slowly released in a controlled manner for a defined period of time (Scott, 2017; Kendall, Mackenzie, and Telfer 2001).

Direct methods allow a more controlled administration of minerals to the animal (Kendall, Mackenzie, and Telfer, 2001). However, the success of methods depends on the mineral being supplemented, the dosage and the frequency.

The success of supplementation relies on the method of application being suitable for the element being supplied. Williams, Williams and Kendall, (2017) demonstrated this by assessing drenches supplying cobalt with/without Vitamin B_{12} and selenium. This research confirmed that cobalt drenches significantly increased plasma cobalt concentrations ($p < 0.001$) in a dose dependant manner, however, this did not significantly increase the vitamin B_{12} concentration. Conversely, this same study found that selenium supplied by the drenches successfully elevated plasma selenium levels to a significant degree ($p < 0.001$) across the whole 13-day experiment compared to the control group, and in turn found the erythrocyte glutathione peroxidase level significantly higher ($p < 0.05$) than the control by day 13. This observation was supported further by the declining erythrocyte glutathione peroxidase activity of the control group, suggesting that not only was the increase in the treatment group due to the supplementation but that drenching was an effective method to supply selenium. One possible reason the cobalt did not elicit a Vitamin B_{12} response may be due to the animals being unable to utilise the cobalt before it was excreted. Smith and Marston, (1970) noted that 93 % of cobalt administered was excreted in the faeces within 5 days. This suggested that whilst sporadic drenching is not an appropriate method of cobalt administration for long term benefit, it could be for selenium.

Conversely, Millar and Albyt, (1984) demonstrated that weekly drenching of cobalt containing solutions was effective at sustaining an elevated liver and plasma B_{12} concentration in sheep compared to a

control group. However, no significant difference was noted between the weekly drenched groups and an additional pelleted group. One limitation of this study that the author does not note was that there was no intermittent blood sampling between doses. Therefore, whilst the serum B_{12} concentrations appeared relatively stable across the 14-week trial, there could have been a concentration peak occurring days after the drenching and then a steady decline before the next sampling, causing the drenching to appear like it gives a constant supply when it may not. This hypothesis is supported by the work carried out by Williams, Williams and Kendall, (2017), observing an initial sharp increase in plasma cobalt concentration 23 hours after drench administration and a steady decline. Not only does this suggest that drenching may not be as effective at keeping a constant supply of minerals, but that it may result in increased cost to the farmer due to an increased handling time needed to continually dose animals, as well as potentially having a negative impact on the environment due to high levels of excreted minerals. Andrews, Hart and Stephenson, (1960) compared the ability of weekly cobalt sulphate doses, pressed cobalt oxide pellets and cobalt sulphate pasture dressing to increase Vitamin B_{12} concentrations in the liver. By the end of the trial, mean cobalt liver content for the cobalt sulphate drench and cobalt oxide pellets group was 40 µg/g and 21 µg/g respectively even though the mean total vitamin B_{12} contents for these groups were 176 µg/g and 281 µg/g. This suggested that over the 14-week trial, cobalt oxide was more efficient for the conversion of cobalt to vitamin B_{12} than for the sulphate.

However, the drench supplied contained 7 mg cobalt, whereas the amount of cobalt present in the cobalt oxide pellets is not defined, it simply states that the pellet it made of 75 % cobaltic oxide, therefore, rather than the cobalt oxide being more bioavailable to the microbes present in the rumen, it may have been due to the larger quantities of the element being available than a higher conversion rate to Vitamin B_{12}. Conversely, Kawashima *et al.* (1997) compared the efficacy of

cobalt sulphate, glucoheptonate and carbonate against cobalt oxide. All cobalt compounds were supplemented at 40 ppm, consistently recording that sulphate, carbonate and glucoheptonate were all more soluble and available to the animal than cobalt oxide.

Balemi, (2008) compared different drench formulations: copper glycine; copper amino acid chelate; and copper sulphate against a copper oxide bolus, calcium copper EDTA injection and control group receiving no treatment. This study stated that the three drenching groups demonstrated significantly higher liver copper concentrations ($p < 0.05$), compared to the injection and bolus groups. However, the author neglects to acknowledge that the amount of copper supplied for the drenches was 150 mg/day whereas the injected group only receives ~0.28 mg/day of copper from the calcium copper edetate. Therefore it was unsurprising there was no significant increase in liver copper concentration in the injected group. Whilst this study demonstrated that copper can be supplied effectively by drenching, the need for the drenches to be delivered three times a week raises the question whether there was a significant, profitable benefit to the farmer in the output of live weight gains to validate the extra labour required to supplement in this method compared to less intensive methods such as bolusing and additionally raises concerns surrounding excessive copper supplementation as indicated by the significantly higher liver copper concentrations. (Balemi, (2008) did not recorded live weight gains in their study).

Trengrove and Judson, (1985) compared five different copper treatments including: injection (Coprin, a prescription calcium copper complex), drenching and bolusing. This study noted that the glass bolus resulted in consistently higher liver copper concentrations than the drench but not compared to the injection at weeks-44 and 51, 3.99 mmol/kg and 3.65 mmol/kg compared to the glass bolus at 3.87 mmol/kg and 3.24 mmol/kg respectively. One possible reason the bolused group copper liver concentrations may have started to

decrease towards the end of the study could have been due to a decreased surface area of the bolus due to degradation and therefore a reduced amount of ion release from the bolus.

Similarly, Kendall, Mackenzie and Telfer, (2001) recorded a gradual shift in mineral status of animals in their study, that assessed elemental release of a glass bolus. The bolused animals moved from the normal range for plasma copper concentrations to the marginal at day-69 versus day-91. This supported the suggestion that ion release from the bolus decreased over time, possibly due to a reduced surface area.

There are very few pieces of literature directly comparing the efficacy of iodine supplements administered by drench and bolus. However, Donald *et al.* (1993) administered 100 mg of potassium iodide as an aqueous solution to ewes at days-54, 68, 96, 110, 124, 128 of pregnancy and 12, 28, 42 and 56 of lactation. This study found that both the ewe and lamb had significantly higher concentrations of T_3 present ($p < 0.01$ and $p < 0.05$, respectively) after being supplemented with the iodine drench compared to the control group, and that no clinical signs of iodine deficiency were exhibited by the any of the experimental animals. However, Donald *et al.* (1993) stated that the T_4 ratio in newly born lambs to its dam acts as an indicator to iodine status, that a value <1 suggests insufficient iodine. However, the mean ratio of T_4 across all treatments in this study was 1.5, suggesting there is no significant difference between supplemented and control groups.

Contrastingly, Maro and Kategile, (1980) found that supplementing with potassium iodide prior to lambing significantly reduced the incidence of goitre and increased the lambing percentage, however, the doses were of 210 mg, compared to Donald *et al.* (1993) administering 100mg, which may account for the difference in success of the drench. Ellis, George and Laby, (1983) trialled a long-term intraruminal device aiming to provide iodine supplementation for 3-years. This study compared the reproductive performance of ewes, rather than assessing their T_3/T_4 concentrations as indicators. However, when comparing ewe fertility,

lambs weaned and mean birthweight, there appeared to be no significant difference between the control and treated groups (97 % versus 96 %, 84 % versus 79 % and 3.9 kg +/- 0.7 versus 3.8 kg +/- 0.6). The author acknowledged that the lack of iodine stress in the control flock accounted for the absence of differences in the lambing performances between the two groups.

This brief review emphasises that whilst certain elements such as selenium and iodine can be effectively administered sporadically by drenches, other elements such as cobalt need sustained supplementation in order to provide effective nutrients. There is a need for a product that can effectively supply elements, in a bioavailable form, consistently over a designated period of time. This will allow farmers to formulate proactive mineral feeding regimes designed to suit their needs. Targeting optimum levels of supplementation could enable a more economically efficient, environmentally friendly, and healthier methods of production.

1.2.3 The UK bolus industry

The three largest bolus companies in the UK bolus industry are Agrimin, Animax and Bimeda (previously known as Telsol). Other boluses such as Cobalt Master™, Cobalt Complete™ and Nettex™'s Cob-I-Sel™ are available, however, they are not as dominant as the previous three. Estimated daily trace element ion release of the main boluses are disclosed in Table 1.4, calculated based on their elemental inclusion (mg) over duration (days).

Table 1.4 *Estimated trace element daily ion release rate of UK sheep boluses (mg).*

		Bolus						
		Bimeda Coselcure	**Bimeda Cosecure**	**Agrmin 24-7 Smartrace for adult sheep (48 g)**	**Agrmin 24-7 Smartrace Plus for adult sheep (52 g)**	**Animax - Tracesure traffic light sheep**	**Animax - Tracesure Se/I sheep**	**Animax - Tracesure Sheep Co**
Estimated Daily supply based on bolus elemental content (mg)	Cu	0.69	0.69	0.81	0.81	1.03	N/a	1.03
	Co	0.21	0.41	0.37	0.37	0.56	0.56	N/a
	Se	18.43	18.43	0.00	18.67	22.22	0.00	N/a
	I	1.38	N/a	4.23	4.23	3.67	3.67	N/a

Agrimin and Animax use a binding substance, like wax to press compounds such as copper oxide, cobalt carbonate, sodium selenate and calcium iodate into cylindrical blocks known as boluses (Porter, 2013; Bennison, 2010). There are two main ways boluses disintegrate when residing in the reticulum: dissolving or abrasion. Agrimin's Smartrace™ range uses abrasion: one bolus is administered, and the outer wrapper dissolves exposing two separate parts of the bolus. These fragments gradually dissolve as well as abrasion from knocking together, causing fragmentation and increased erosion. Bimeda's Cosecure™ and CoseIcure™ boluses are not unique in their method of ion release (dissolving) however, it is unique in its method of carrier, using soluble glass rather than a waxy-pressed bolus.

Kendall, Mackenzie and Telfer, (2001) investigated the efficacy of Cosecure's sintered bolus, after changing from using a monolithic glass containing selenium, to using a copper-cobalt-sodium-magnesium-polyphosphate glass. The sintered bolus significantly increased cobalt and selenium status ($p < 0.001$) in the treatment groups. However, no significant differences were recorded for the plasma copper concentration or caeruloplasmin. This was attributed to the adequate blood status of the control animals throughout the trial, reiterating Kendall's suggestion that more is not always better when aiming for optimum mineral supplementation. This redesign of bolus resulted in a much faster dissolution compared to Bimeda's previous bolus that was originally designed to last < 18-months, compared to the sintered bolus that only lasts < 6 months. This difference in duration is likely due to the sintered particles giving the bolus a rougher exterior and higher surface area, increasing the rate of degradation.

Animax and Agrimin are two of the market competitors who currently use a coated bolus. Agrimin claims that their resin coating controls release rate ensuring consistent daily supply of nutrients"(Agrmin Limited, 2020). However, the copper blood concentrations data in Parkins *et al.* (1994), assessing this bolus, suggested there were

significant differences between the blood copper concentrations of the treated cattle recorded during July, compared to September, approximately 13.0 +/- 1.0 µmol versus 17.0 +/- 1.0 µmol respectively. However, copper pasture content is not measured consistently throughout the trial, and pasture copper content is usually higher in September compared to July (Clarkson and Kendall, 2018), a similar increase in blood copper concentration was reflected in the control group as well, implying it may not necessarily been due to inconsistent ion release of the bolus.

It is possible that the design of the Agrimin Alltrace bolus has been modified since this publication, a patent published in 2010 (Bennison, 2010) by Agrimin regarding the bolus and manufacturing process discussed the possible use of resin within its manufacturing process as a binder and in another publication, the one of the authors describes the bolus as a “polymer coated cylinder” (Parkins *et al*. 1994). Therefore, whilst it was not conclusive that the coatings of these boluses are coated in the same material, it is possible.
Animax’s patent states the use of a coating, “selected from the group consisting of caster sugar, shellac, and a wax” (Porter, 1999). This coating does not claim to aid consistent ion release, and that is reflected in León, Glenn and Farver, (1999). This trial assessed copper supplementation using Copasure™ (Animax) and observed a peak in copper serum concentration one month after supplementation 1.08+/- 0.45 ppm, followed by a steady decline until serum concentration returned to within control animal range by month-5, thereby demonstrating uneven ion release profile. It should be noted that during this trial the control animals copper serum concentrations followed a similar trend overall, peaking at month-two (March). This was possibly a reflection on the seasonality of copper concentration within forage. Forage copper concentration is generally higher during winter than summer, however, so is ingestion of soil which may contain antagonistic elements (Khan *et al.* 2008). Unfortunately, as the feeding

regime was not disclosed in León, Glenn and Farver, (1999), it cannot be confirmed. Despite this, the concentration peak seen at month-two is significantly higher compared to the baseline suggesting a peak in ion release independent to the background ion levels.

The main limitation with all of the boluses currently on the market is that their elemental ion release does not stay consistent throughout the 6-month period, possibly resulting in mineral imbalances. This leads to one of the main aims of this thesis: to design and produce a nutritional supplement for ruminant nutrition that provides specific concentrations of elements (copper, cobalt, selenium and iodine) over a defined period.

1.3 Phosphate-Based Glass

Phosphate-based glasses are fully resorbable, amorphous biomaterials. Their formulations can be manipulated to alter characteristics such as degradation rate, hardness and ability to deliver controlled and sustained elemental ion release (Hoss*ain et al*. 2014). The predominant structural unit of phosphate-based glasses (PBG) is a phosphate anion (PO_4^{3-}), which forms a phosphorous backbone allowing the glass to be fully soluble in aqueous environments. Traditionally used for biomedical application due to its ability to produce microspheres (Hossain *et al.* 2018) and its chemical similarities to bone (Saad *et al*. 2019) PBGs can also be used to alleviate nutritional deficiencies as noted in (Givens *et al.* 1988; Kendall, Mackenzie, and Telfer, 2001; Kendall and Telfer, 2000).

Structures of phosphate based glasses are typically referred to using Q^n terminology, where Q^3, Q^2, Q^1 and Q^0 represent the number of bridging oxygens per tetrahedron (e.g. the number of P-O-P links per PO_4 tetrahedron) (Brow, 2000). Incorporation of modifier oxides such as metal oxides result in depolymerisation of the phosphate network through the creation of terminal oxygens, sacrificing a bridging oxygen (Brow, 2000; Knowles, 2003). Increasing the number of non-bridging

oxygens decreases the Q^n species. The addition of non-bridging oxygens strengthens the structure due to increased cohesion, caused by the cations sitting between the non-bridging oxygens (Bae and Weinberg, 1991).

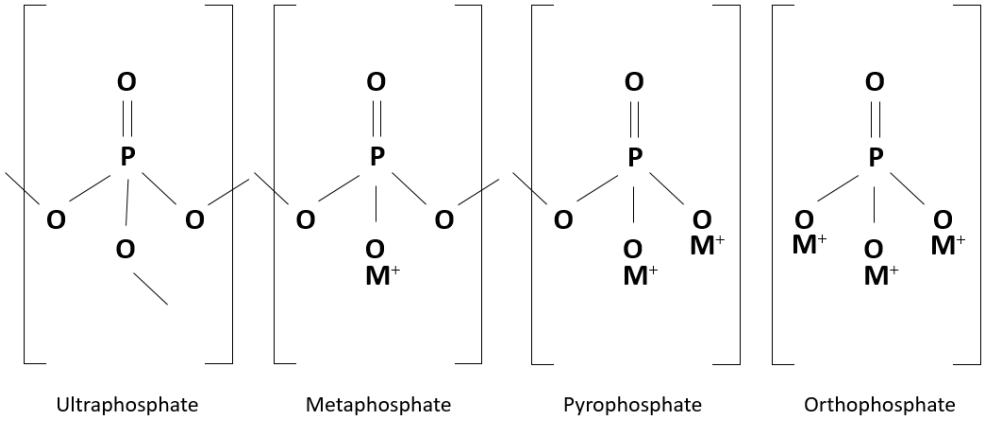

Figure 1.1: *Schematic of the Q^n species, demonstrating the structures of ultraphosphates (Q^3), metaphosphates (Q^2), pyrophosphates (Q^1), orthophosphates (Q^0) and the effect of modifier oxides (Hossain et al. 2014).*

1.3.1 Applications of phosphate-based glasses

Incorporating different metals such as copper and cobalt are relatively common within biomedical phosphate glasses due to antibacterial properties for copper (Foroutan *et al.* 2019) and hypoxia inducing cobalt ions (Raja *et al.* 2019). The addition of modifier metal ions can be used to tailor degradation rate and ion release. Lee *et al.* (2013) investigated the effect of cobalt oxide doped into titanium phosphate glass, assessing degradation and ion release. Varying glass compositions of $45P_2O_5$-$20Na_2O$-$5TiO_2$-30-xCaO-xCoO (x = 0, 5, 10, and 15 mol%) resulted in an increase in Co^{2+} ion release as cobalt content increase, despite seeing a decrease in the degradation rate. The slower degradation rate may be due to the replacement of Ca^{2+} with Co^{2+} which has a higher field strength. Fourier transform infrared spectroscopy (FTIR) was used to assess bond length finding that as Co^{2+} content increased there was a slight shift to higher wavenumber of of the v_{as} (P-O-P) mode (at approximately 890 cm^{-1}) suggesting a

change in bond length.

Similarly, Wu *et al.* (2012) found increasing the Co^{2+} content of mesoporous bioactive glass increased the release of Co^{2+} ions, whilst decreasing overall degradation rate. Bunker, Arnold and Wilder, (1984) suggested that the addition of metal oxides improves glass stability due to more stable bonds less susceptible to hydrolysis, reducing the degradation rate.

Raja *et al.* (2019) reviewed the degradation rate and ion release of Co^{2+} ions from $50P_2O_5$-$20Na_2O$-30-xCaO-xCoO (x = 0, 1, 3, 5, 10, mol%). Similar to other studies, glass weight loss was negatively correlated with an increase in CoO concentration, due to replacement of Ca-O bonds with stronger Co-O bonds. The fastest degradation rate recorded was 3.8 mg/cm^2 /day for 1 mol% CoO and the slowest degradation rate recorded was 1.4 mg/cm^2/day, at an inclusion level of 10 mol% CoO. However, the author emphasises that despite increasing the cobalt content 10-fold, it will not necessarily increase the cobalt release by a factor of 10, stressing the complexities when designing bioactive glasses compositions. Additionally, the rate of degradation is strongly dependant on the media used. Dissolution rates using distilled water are approximately twice as high when compared to nutrient broth dissolutions. The increased degradation rate is likely due to the reduced concentration gradient of the distilled water compared to buffered mediums, that may saturate, thus slowing degradation rate. This highlights the importance of using representative media for *in vitro* dissolution work.

Abou Neel *et al.* (2005) and Foroutan *et al.* (2019) found similar results to both Lee *et al.* (2013) and Raja *et al.* (2019) regarding the effect of increasing CuO content on degradation rate and copper ion release. P-O-Cu bonds were formed at the expense of P-O-Na or P-O-Ca bonds. Replacement of sodium or calcium cations with higher electronegativity copper cations resulted in denser cross-linking between phosphate chains, decreasing the rate of hydrolysis and cleavage of phosphate

chains, decreasing degradation rate (Stähli *et al.* 2014). Despite the decrease in degradation rate there was an increase in Cu^{2+} release due to the increase in copper content, similar to that observed in the cobalt-doped glass studies.

There appears to be very few studies incorporating both copper and cobalt into phosphate glasses, however, it is likely that the incorporation of copper and cobalt at the expense of calcium or sodium cations will result in a decrease in degradation rate but an increase in Cu^{2+} and Co^{2+} release. Careful consideration would need to be given to these glasses depending on the inclusion level of modifier cations present compared to network formers present, as a glass containing a P_2O_5 content lower than 40 mol% would be considered an invert glass (Walter *et al.* 2001). Invert glasses are predominantly made up of pyrophosphate (Q^1) and orthophosphate (Q^2) groups, making the glasses more prone to crystallization (Kasuga and Abe, 1999), resulting in smaller processing windows, increasing production and manufacturing difficulties (Brauer, Wilson, and Kasuga, 2012).

Ahmed *et al.* (2005) investigated the release profile of cations and anions from ternary-based glass $45P_2O_5$-55(xCaO–Na_2O) x = 30, 35, and 40 mol%, initially finding a linear relationship between an increase in calcium content with a decrease in degradation < 30 mol% CaO and then increased for the 40 mol% composition. The decrease in degradation < 30 mol% CaO is thought to be caused by cross-linking between the PO_4, P_2O_7 and P_3O_{10} branched molecules, hence why a decrease in their release is noted. Unfortunately this study did not compare any differential scanning calorimetry of these glasses, which may have reinforced this hypothesis. However, both Ahmed *et al.* (2004) and Franks *et al.* (2001) compared the thermal profiles of glass with a fixed 45 mol% P2O5 content with varying calcium and sodium content confirming that the transition temperatures of these glasses increased with a higher content of CaO, most likely due to calcium

having a higher field strength of 0.33 compared to sodium's 0.19 (Dietzel, 1942).

It is possible to incorporate selenium into glasses, however, these are not used within the biomedical field. Selenide glasses, also known as chalcogenide glasses were initially used for fiber optics due to their wide transparency range, low optical losses and stability to atmospheric moisture. These glasses are commonly made with arsenic, excluding the possibility of being used for biomedical application *(Churbanov et al.* 2011).

Research is on-going into the incorporation of iodine into glasses to aid with the management of radioactive disposal (Lemesle *et al.* 2014; Wei *et al*. 2021), however, borosilicate glass is usually used as the matrices to decrease the likelihood of leaching. Whilst it is possible to incorporate iodine into phosphate glass matrices, this is usually done by adding silver to aid glass formation at low melt temperatures (Takahashi, Nakanii, and Sakuma, 2005). The incorporation of silver into a nutritional supplement for ruminants would not be suitable due to toxicity concerns and economic viability. An alternative method to incorporating iodine into the glass matrix is through compressed glass sintering. Wei *et al.* (2021) used silver iodide as their iodine carrier, however, Bimeda also use sintering to incorporate iodine and selenium into their glass boluses, as they unable to be incorporated into the glass melt due to volatility (Telsol Limited, 2012).

1.4 Nanoparticles

Nanoparticles (NP) are defined as particulate dispersions or solid particles with a size range of 10-100 nm (Masciangioli and Zhang, 2003). Nanotechnology has been hailed by the European Commission as one of the six 'key enabling technologies' that will contribute to competitively growing, and sustaining multiple areas of industrial application (European Commision, 2012). Widely used for applications within electronics, fuel cells, and the biomedical industry (Abbas *et al.* 2008), the agricultural sector has demonstrated the utilisation of nanotechnology, ranging from fertiliser to feed additives (Parisi, Vigani, and Rodríguez-Cerezo, 2015).

At nanoscale dimensions materials exhibit novel properties different to their bulk counterparts (Albrecht, Evans, and Raston, 2006). Such differences might include their ability to melt at dramatically lower temperatures (Luo, Hu, and Xiao, 2008; Kart *et al.* 2014), elicit different light absorbing properties such as gold NP appearing red (Roduner, 2006), and due to their surface charge and increased surface area to volume ratio, NP can also be significantly more bioavailable or efficacious (Zhao *et al.* 2017; Maisel *et al.* 2015). However, the increase in bioavailability and efficacy should be treated with caution as some of the interactions and pathways are not fully understood, with longer-term effects to recipient and environment yet to be observed (Albrecht, Evans, and Raston, 2006).

1.4.1 Nanoparticles within the agricultural feed industry

Across the agricultural industry, the improved efficacy of NP compared to their micro-sized counterparts is being assessed, however, at present there is not much literature reviewing the effect of NP in ruminants. As such, other animals such as chicken and piglets are discussed but it is acknowledged that they have very different digestive systems that may not be directly comparable to ruminants.

Vijayakumar and Balakrishnan, (2014) demonstrated in broiler chickens that the supplementation of dicalcium phosphate NP compared to

conventional microparticulate dicalcium phosphate resulted in significantly ($p < 0.05$) higher body weight gain across 4-weeks in all supplemented groups compared to the control. Additionally, it was found that the group with the highest weekly body weight gains was the group fed 50 % less the dicalcium phosphate in nano-form compared to the control treatment, suggesting the optimum supplementation volume of NP was 50 % that of standard. This study supports the suggestion that supplementation with NP can decrease the volume of mineral supplementation required to improve production outputs, whilst reiterating that higher supplementation does not always equal higher outputs.

Similarly, research into the use of zinc oxide (ZnO) NP in both broilers and piglets has demonstrated an increase in growth rates, immunity and reproduction (Sahoo, Swain, and Mishra, 2014). However, inclusion rates must be carefully considered, Sahoo, Swain and Mishra, (2014) observed improved immunity by supplementing 0.06 ppm NP ZnO, compared to an inclusion rate of 15 ppm conventional organic Zn-Met. This may be due to the excess of Zn being provided in the conventional diet as the basal diet had a Zn concentration of 30 ppm, when a broiler's RDI is 30-40 ppm. So, the increase in immunity of the NP group may not be due to increased efficacy of NP, but by comparison due to the decrease in immunity of the excessive Zn conventional group. Therefore, this study does not necessarily demonstrate the efficacy of NP, but emphasises the need to appropriately dose and compare feeds. Supporting this, Zhao *et al.* (2014) assessed the growth of broilers supplemented with ZnO particles against ZnO NP. This study recorded that chickens fed 20 and 60 mg/kg ZnO NP had significantly greater weights after 14 days than the controls being fed 60 mg/kg ZnO, however, after 28 days birds being supplemented with 100 mg/kg ZnO NP noted a dramatic decrease in weight. This may be due to a decrease in catalase activity resulting in increased oxidative stress, emphasising the importance of

considering mineral inclusion levels and how excessive mineral supplementation can have a negative impact.

Likewise, Gonzales-Egui*a et al*. (2009) found a statistically significant improvement of weanling pigs supplemented with an unspecified NPCu compound compared to the control of $CuSO_4$. The study assumed that copper bioavailability was significantly improved due to increased performance and decreased faecal copper levels. This study also observed an improvement of the digestibility of crude fat of pigs supplemented the NPCu diet. Whilst this had a positive impact on the pig's production, the mechanism behind this change, an increase in the activity of lipase and phospholipase in the small intestine, should be considered as to whether it will have a similar effect on ruminants.

Romero-Pérez *et al.* (2010) carried out *in vitro* experiments, assessing selenium's release from sodium selenite, both in micro and nano-particulate, looking at different acidic environments (pH 2, 3, 4 ,6) designed to simulate the complex pH changes seen in ruminant digestion. This study demonstrated that Se is more readily released in an acidic environment of pH 2-4 compared to pH 6, emphasising that this will create more bioavailability due to Se's absorption in the abomasum and duodenum, with pH's below 4. However, the authors concluded that *in vivo* trials are needed to validate the hypothesis of increased availability. Supporting this, Sadeghian, Kojouri and Mohebbi, (2012) assessed the degree of oxidative stress, lipid peroxidation of cellular membranes and concentration of thiobarbituric acid reactive substances (TBARS) on sheep given 1 mg/kg Se as nano red selenium (SeNP) and sodium selenite. This study found the elevated thiobarbituric acid reactive substances (TBARS) activity in the NP group had decreased by day-20 unlike the sodium selenite group, which had a high TBARS value until day-30. This suggested an increase in anti-oxidative activity of the SeNP compared to the sodium selenite due to the delay of this groups return to a basal level of TBARS. Whilst this article emphasised the importance of the

incorporation of selenium into the functional enzyme as glutathione peroxidase it does not measure this as one of its haematological parameters. Therefore, whilst this study suggests that selenium NP have better anti-oxidative effects compared to sodium selenite the bioavailability and conversion to glutathione peroxidase was not assessed.

Shen, Song and Wu, (2021) investigated the effects of supplementing CuNP compared to $CuSO_4$, supplying 2 g/goat once a week, the method of supplementation is not disclosed but is likely to be as a drench due to their reference of oral supplementation. This study found that NP supplemented animals had significantly ($p < 0.01$) higher blood copper content compared to the $CuSO_4$ group, 0.89 ± 0.09 µg/g versus 0.68±0.07 µg/g respectively. Additionally, the CuNP caused a significant increase in superoxide dismutase activity compared to the $CuSO_4$, supplemented group, suggesting a higher bioavailability. However this study does compare the liver copper concentrations between the $CuSO_4$ and CuNP supplemented groups therefore it was not possible to assess whether there was excessive CuNP accumulation in the liver of the NP treated group. This is an important consideration when developing a sheep or cattle supplement as it is well-known that goats are less susceptible to copper poisoning than cattle. This is thought to be due to species specific Cu utilisation, resulting in less Cu stored in livers, resulting in a reduced risk of copper toxicity (G. Zervas, Nikolaou, and Mantzios, 1990).

Makarov *et al.* (2017) assessed the efficacy of copper and cobalt NP on live weight gain and some biochemical indicators of Holstein heifer calves. The authors administered 10 ml aqueous solutions of cobalt and copper NP at an inclusion rate of 0.02 mg/kg live weight and 0.04 mg/kg live weight respectively, at months 2, 4, 6 and 9. Calves initially weighed 57.06±0.4 kg and 57.0±0.2 kg for cobalt and copper groups respectively, estimating that elements were supplied at approximately 1.152 mg Co/day and 2.28 mg Cu/day. This study concluded that as a

result of supplementing with both NP, blood parameters such as total protein in the blood and albumins, and protein index of transaminase ferments were increased compared to the controls. Additionally, both NP groups recorded significantly higher live weight gains by the end of the experiment, 323.7±0.6 kg, 335.6±0.5 kg and 348.9±0.6 kg for the control, CuNP and CoNP groups respectively. It is unsurprising that the CoNP supplemented group had the highest live weight gains due to cobalt's role in gluconeogenesis and methionine synthesis, essential protein production (Wang *et al.* 2007). However, what is surprising is that it was only at month-7 that the CoNP group saw an increase in live weight gain compared to the control group. This might be as a result of the bacterial colonies in the rumen adapting over an initial period before being able to effectively utilise the CoNPs (Makaeva *et al*. 2019).

Ghoreish*i et al*. (2013) compared the effect of supplementing lambs with cobalt NP and cobalt chloride drenches. A dose rate of 10 mg/kg body weight was supplied daily over 25 days. Unsurprisingly, the vitamin B_{12} concentration of the NP supplied group was significantly higher ($p < 0.05$) after 25 days compared to the start, 1553 pmol/l versus 554.33 pmol/l, and compared to the cobalt chloride group measuring 1202.33 pmol/l on day-25. However, the nano-treated group exhibited granulomatous hepatitis and necrosis of hepatocytes, whereas the cobalt chloride group exhibited fatty change of hepatocytes. This suggested mild liver toxicity in the nano-group, emphasising that supplementing with NP could lead to more severe liver damage than its micro-sized counterparts. The data suggested, that when supplemented appropriately, cobalt NP can effectively increase vitamin B_{12} concentrations, but careful consideration should be given to the dose concentration to avoid toxicity. Additionally, no intermediate blood sampling was carried out across the 25-day period, suggesting that this may not have been the peak concentration of various different parameters including vitamin B_{12}.

Sadeghian, Kojouri and Mohebbi, (2012) did not directly assess the incorporation of selenium into glutathione peroxidase in sheep, but the effect of selenium supplementation on iron and its functional proteins, such as transferrin. Elemental iron is able to act as both an electron donor and acceptor, enabling it to catalyse the production of free radicals from hydrogen peroxide (Wallander, Leibold, and Eisenstein, 2006), however, incorporation of iron into proteins such as transferrin and heme prevents this. This study found significantly ($p < 0.05$) less iron serum concentration at day-20 and 30 in the SeNP group compared to the control group (168.4 µg/dL +/- 13.3 and 151.2 µg/dL +/- 17.2 vs. 211.4 µg/dL +/- 26.8 and 190.8 µg/dL +/- 18.6). However, a significant decrease ($p < 0.05$) in relative transferrin expression (% of control) was recorded at day-20 (123.7 % +/-8.1) compared to day-30 (64.8 % +/- 4.8). Therefore, whilst this suggests that at day-20 the supplementation of SeNP had a positive effect on the incorporation of iron into functional elements such as transferrin, the accumulation of daily administering of 1 mg/kg Se over 10 consecutive days may be causing detrimental effects. Unfortunately, this study does not note the blood plasma selenium concentrations throughout the study, therefore it is possible that although the SeNP may be more effective for selenium supplementation, due to the high concentrations of exposure and potential increased bioavailability an adverse response was elicited.

As with any new and emerging areas of science, regulatory frameworks are essential to safeguard the application and production of NP. The European Union have only recently specified that all companies ‘manufacturing or importing nanoforms’ must report it under REACH, listing all substances currently on the market within the EU (European Commision, 2021). Copper oxide (CuO) and cobalt oxide (Co_3O_4) are both registered with REACH, however, at present there are currently no NP mineral supplements registered on the European Feed Additives List, and the European Feed Materials Register. The only NP listed are on the European Feed Catalogue, listing milk and whey retentate and

permeate, which are currently included as “ultra, nano or micro” (European Commission, 2013) likely as a result of the argument that ultrafine and NP forms have existed for longer than it has been possible to characterise them. Quik *et al.* (2020) wrote an extensive review on the environmental risk of nanotechnology in the feed chain stressing the need for environmental exposure scenarios and modelling (Baalousha *et al.* 2016). Key areas of consideration include bioaccumulation, understanding that different forms of the same material may be accumulated in different ways; and the possible requirement of environmental risk assessments when assessing nano-feed additives as a result of residual that may be excreted, exposing soil and or water systems.

Although very few studies evaluating the efficacy of NP in ruminants have been published, their ability across multiple species to significantly increase enzymatic parameters has been established. As such, there is reasonable rationale to hypothesise that the incorporation of NP into a bolus could significantly improve animal nutrition.

Additionally, upon reviewing the available literature it was apparent that the use of NP at lower concentrations as a method of trace mineral supplementation in ruminants is not well understood. This project aimed to bridge this gap by assessing multiple methods of delivery mechanisms (drench and bolus) of NP incorporated as part of a nutritional supplement.

1.5 Aims and objectives

The main aim of this research was to develop a bolus that would enable sustained trace mineral release over a 6-month period to alleviate trace mineral deficiency. This research also aimed to understand whether NP were a beneficial method of supplementation and whether they could be incorporated into nutritional supplements by different methods of delivery, such as boluses or drenches.

The objectives included:

i. Development of phosphate-based glass formulations to deliver desired ion release profiles of copper, cobalt, selenium and iodine over a sustained period of time. Formulation characterisation such as *in vivo* and *in vitro* degradation rates, ion release profiles, thermal profiles and bioavailability using biochemical indicators such as Vitamin B_{12} and glutathione peroxidase.
ii. Understand whether NP could be incorporated into phosphate-based glass, and if they remained and could be released in their nano-form. Analysis included thermal analysis for sintering, ^{31}P-NMR and *in vitro* ion release studies.
iii. Assessment of NP bioavailability as a nutritional supplement supplied via drench to sheep. Work included synthesis and confirmation of cobalt oxide NP using hydrothermal synthesis and transmission electron microscope analysis. Followed by an *in vivo* study to investigate bioavailability using blood mineral concentrations and biochemical indicators.

The main biological outcomes of this research aimed to demonstrate that as a result of consistent mineral supplementation functional biochemical indicators such as Vitamin B_{12} and glutathione peroxidase would be consistently elevated within the optimum range for sheep, across a specified duration (1-month for prototype trials, 6-months for competitor analysis). Elevation of these metabolites would suggest that the mineral supplementation was effective. Using a variety of indicators

to analyse each element is advantageous as it indicates where in the ingestion, metabolism and storage process the element has been utilised or excreted. However, due to the dynamic nature of elements being continually utilised, metabolised and excreted, the elemental journey is not always clear.

To the knowledge of the author, no work in the literature has previously presented the incorporation of NP within phosphate-based glasses for application in ruminants as a method of trace mineral delivery.

To 1.6 Thesis outline

Due to the unusual, multi-disciplinary nature of this thesis, each chapter outlines its own introduction, methodology, results, discussion and conclusion sections. This aimed to provide clarity for the reader moving through the thesis as such a diverse breadth of work was covered throughout the duration of this PhD.

The outcomes of the aims and objectives have been divided into several chapters as outlined below:

Chapter 2: Evolution of the Bolus Design aimed to identify a suitable bolus design suitable of delivering bioavailable trace mineral elements, whilst being feasible to manufacture at mass scale. To do this, the chapter reviewed the production feasibility of multiple bolus designs, as well as the incorporation of NP into a phosphate-based glass. Physical characterisation techniques used to assess these parameters included differential scanning calorimetry, x-ray diffraction and solid-state ^{31}P nuclear magnetic resonance spectroscopy.

Chapter 3: Phosphate-Based Glass Formulation Development explored the degradation rates of 10 different glass formulations in order to identify a glass formulation that fulfilled the Industrial Partner's ideal daily release rate ahead of prototype testing. This chapter assessed physical characteristics of the glass including transition, crystallization, melt and sintering temperature, as well as *in vitro* ion release concentrations confirmed through inductively coupled plasma spectroscopy.

Chapter 4: *In vivo* Phosphate-Based Glass Formulation Assessment investigated the ion release profiles of the optimised phosphate-based glass formulation P50-Ca2-Na17-Cu30-Co1 *in vivo* compared to the ion release profiles obtained in the *in vitro* studies. Degradation of the boluses was assessed

using rumen fluid analysis and blood plasma mineral status of copper, cobalt and selenium.

Chapter 5: Competitor Bolus Review *In vivo* Trial expanded the current knowledge of the degradation time and efficacy of a commercially available sintered phosphate-based glass bolus to support future development of a similar product. The efficacy of the CoseICure bolus was assessed by reviewing rumen fluid mineral concentrations, blood plasma mineral status and biochemical indicator concentrations such as Vitamin B_{12} and glutathione peroxidase.

Chapter 6: The efficacy of Cobalt Oxide Nanoparticles in sheep reviewed the efficacy of cobalt oxide NP supplied as a drench to further explore the possibility of incorporating them into a drench product. NP efficacy was reviewed through assessment of blood plasma cobalt concentration and Vitamin B_{12} concentrations in an attempt to understand the bioavailability of NP.

Chapter 7: Conclusions and Future Work summarised the findings of all the work in this thesis and puts forward areas of future work.

Chapter 2 - Evolution of the bolus design

2.1 Introduction

In this chapter the overall design evolutions of this multi-element bolus, containing copper (Cu), cobalt (Co), selenium (Se) and iodine (I) will be discussed.

The main aim for this chapter was to identify a suitable bolus design that would enable consistent trace mineral supplementation of Cu, Co, Se and I over a 6-month period using phosphate based glass as a delivery mechanism. Additionally, this chapter aimed to understand whether nanoparticles could be incorporated into the phosphate based glass bolus design to support improved element bioavailability.

In order to achieve these aims a number of objectives were established including:

- Exploration of the incorporation of nanoparticles into phosphate based glass prior to the glass melt process to understand whether the nanoparticles retained their nano-form.
- Understanding how the nanoparticles effected the different structural and thermal characteristics of the phosphate based glasses using techniques including differential scanning calorimetry (DSC), x-ray diffraction (XRD) and solid-state ^{31}P nuclear magnetic resonance spectroscopy (^{31}P-NMR).

The product brief required the bolus to last for 6-months +/- 1 month, with a consistent daily release rate for each of the elements outlined in Table 2.1.

Table 2.1: *Industrial Partner's specified target daily elemental release rate (ppm/day).*

	Copper	**Cobalt**	**Selenium**	**Iodine**
Target	16	1.2	0.6	4.2
+10 %	17.6	1.32	0.66	4.62
-10 %	14.4	1.08	0.54	3.78

Additional physiological considerations such as oesophageal width, maximum lengths and density had to be taken into account to ensure safe delivery of the supplement and ensure bolus retention. Luginbuhl, (1983) reviewed the anatomy of a sheep's digestive tract and found that larynx's were the limiting factor in oesophageal diameter, averaging at 1.8 cm. Contrastingly, Ghirardi *et al.* (2006) found boluses up to 21 mm in diameter could be administered safely to sheep, though concluded that to ensure safe delivery of boluses to a wide range of sheep breeds and maturities that diameters should not exceed 15 mm. Additionally, this study compared the retention of boluses with different weights and specific gravity values, concluding that bolus designs with a specific gravity of 3 and above had a retention rate of > 99.5 %.

Initial designs focused on the aim of keeping a consistent surface area during degradation, which would in theory allow consistent ion release. The effect of changing surface area and subsequently ion release from a sintered phosphate-glass bolus is shown in some of the earlier Cosecure patents data (Telfer, Zervas, and Knott 1982a, 1982b). A bell-curve in the data suggested a peak in ion release at 2-3 months, followed by a steady decline until the bolus had completely dissolved, disintegrated or regurgitated. One design that may reduce ion release variability could be by using an inert, protective coating, enabling a

constant surface area and thus ion release. However, developing a suitable inert coating was beyond the scope of this thesis.

Another area of design improvement considered was the incorporation of NP within the product. The potential benefit for incorporating NP, was the assumption that their increased surface area to volume ratio would enable higher bioavailability to the animal compared to their micro-counterparts, resulting in a reduced inclusion level required for the product to exhibit similar effects. Ultimately, this could also result in lower production costs for the manufacturer (assuming increase cost in NP was offset by the reduction in concentration required), with superior bioavailability compared to the current products on the market.

Three main designs were considered to incorporate NP into the phosphate-based glass: the fruit pastille (see Figure 2.1), hollow billet (see Figure 2.2) and sintered bolus (discussed further in Chapter 3).

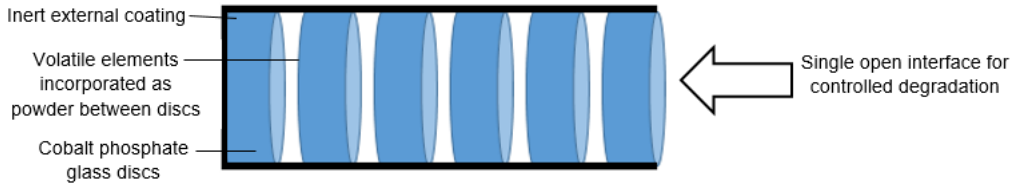

Figure 2.1: *A schematic of the proposed fruit pastille design bolus.*

Figure 2.2: *A schematic of the proposed hollow billet design bolus.*

The fruit pastille design incorporated the NP as a powder sandwiched between cut glass discs rather than being incorporated into the glass melt. However, the fruit pastille design was quickly ruled out due to a variety of reasons stated below and alternative designs were considered:

- With the proposed glass formulation that was being worked with at the time the thickness of the discs could not be consistently

cut thin enough (without cracking or breakages) for this to be feasibly mass produced.

- The cobalt concentration of the glass formula could be reduced to allow a thicker disc to be cut, however, due to the physical restriction surrounding the bolus length, this was also not a feasible option.

This chapter aimed to investigate whether NP (Co_3O_4 and CuO) could be incorporated into phosphate-based glasses during the glass melt process without merging into and becoming part of the glass matrix, and how the use of NP versus microparticles (MP) may affect the chemical and physical characteristics of the glass. An initial glass formulation with P_2O_5 fixed at 45 mol% was used as a starting point as extensive research within the group (Ahmed *et al.* 2004, 2005; Sharmin *et al.* 2017) had documented the relatively slow but controlled degradation rates of several similar formulations. Furthermore, these formulations showed sizeable processing windows and biocompatible nature suggesting that this was a logical starting point.

2.2 Materials and methodology

Table 2.2 outlined a list of materials used within this chapter, their particle sizes and manufacturers.

Table 2.2: *A list of materials, size particle sizes and manufacturer used within Chapter 2.*

Chemical	Particle size	Manufacturer
P_2O_5	< 100 µm	Fisher Scientific, UK
NaH_2PO_4	< 1 µm	Sigma Aldrich, UK
$CaHPO_4$	< 200 µm	Sigma Aldrich, UK
CuO (II) microparticle	< 44 µm	Aldrich, UK
CuO (II) nanoparticles	< 100 nm	Sigma-Aldrich, UK
CoO microparticles	< 44 µm	Acros Organics, UK
$Co(C_2H_3O_2)_2$	< 1 µm	Sigma Aldrich, UK
H_2O_2	N/a	Fisher Scientific, UK

The schematic outlined in Figure 2.3 the processes and methods used in this section.

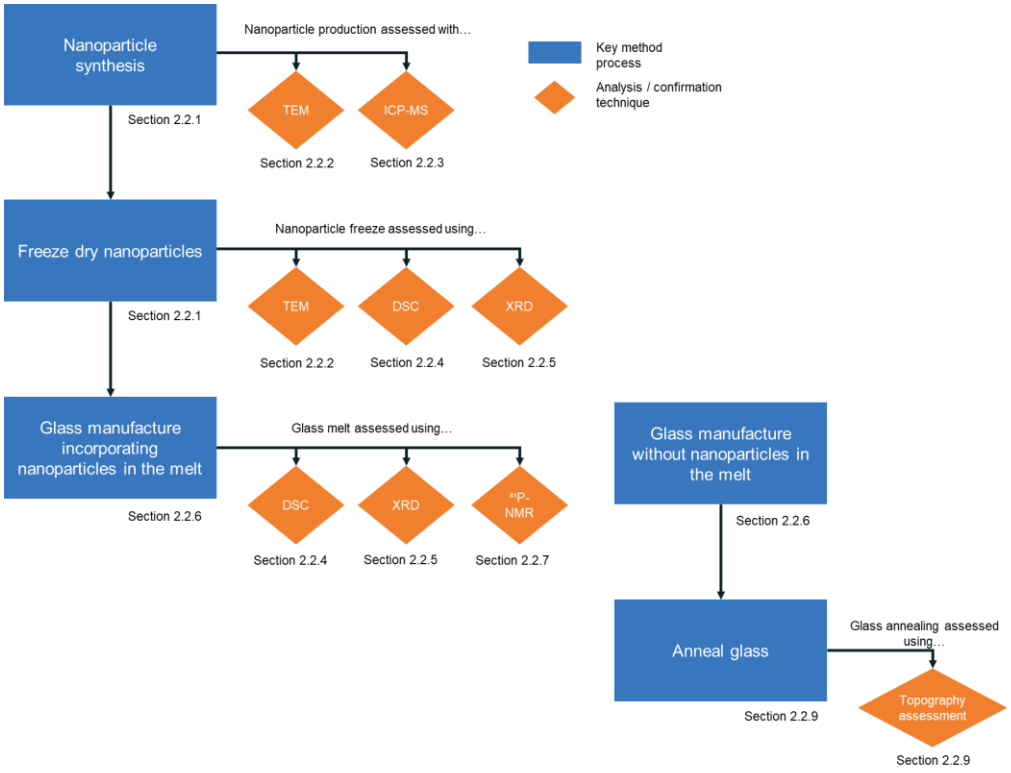

Figure 2.3: *A flow diagram to indicate the sequence of methods used within this chapter.*

2.2.1 Nanoparticle synthesis

Cubic Co_3O_4 NP were produced using a novel hydrothermal synthesis process following the method presented in (Lester *et al.* 2012). Briefly, using a high pressure water pump (Gilson HPLC piston pump 305 model, 25 SC pump head) deionised water (0.4 μΩ cm) and dilute hydrogen peroxide solution (0.25 % v/v, H_2O_2, Fisher Scientific) was fed through a preheater (1 kW) into a reactor with aqueous cobalt (II) acetate (98 %, Sigma Aldrich) to produce nanoparticles. Once fed through the reactor the cooled fluid was then freeze-dried (CoolSafe, Scanvac, UK) under low temperature vacuum (-50 °C) for more than 48 hours.

2.2.2 Transmission electron microscopy (TEM)

NP size and morphology was assessed using images obtained from a transmission electron microscope (FEI Tecnai BioTwin-12). This instrument was operated at 100 KeV and the cobalt oxide (Co_3O_4) or

copper oxide (CuO II) NP respectively, were mixed in methanol to produce an aqueous suspension. A drop of the respective suspensions was pipetted onto a 3.05 mm diameter copper mesh (300 lines per inch mesh, Agar Scientific) and allowed to dry.

2.2.3 Inductively coupled plasma mass spectrometry (ICP-MS)

Inductively coupled plasma mass spectrometry (ICP-MS) was used to confirm the production of cobalt oxide (Co_3O_4) nanoparticles via hydrothermal synthesis.

This analysis was carried out by the NuVetNA team using an XSeries^{II} (Thermo Fisher Scientific, USA) inductively coupled plasma mass spectrometer (ICP-MS). Samples and calibration standards were diluted (500 µl sample with 9.5 ml diluent). This diluent was comprised of 0.1 % non-ionic surfactant (Triton X-100 and anti-foam B, Sigma Aldrich, UK), 2 % methanol and 1 % concentrate (< 99 %) HNO_3 (Fisher Scientific, UK) including internal standards Lawrencium (5 mg/L), Rhodium (10 mg/L), Germanium (50 mg/L and Scandium (50 mg/L). All calibrations were within a range of 0-50 mg/L (Calritas-PPT grade CLMS-2 from Fisher Scientific, UK).

ICP-MS uses collision-cell technology with kinetic energy discrimination (CCT-KED), using 7 % H_2 in He as the hexapole collision cell gas, reducing polyatomic interference with aspiration through a single sample line and glass concentric nebuliser at a rate of 1 ml/minute (Thermo Fisher Scientific, UK). Results were then calibrated to concentrated solution and adjusted for background using blank correction.

2.2.4 Differential scanning calorimetry (DSC)

Three main thermal parameters were defined using differential scanning calorimetry (DSC): the glass transition temperature (T_g); the crystallization temperature (T_c); and the melt temperature (T_m). The analysis was conducted using SDT Q600 (TA Instruments, USA). Between 18-30 mg of powder was placed into a platinum pan (Birmingham Metal Company, UK) and then heated up to 1000 °C

at a heating rate of 20 °C/minute using an inert nitrogen atmosphere. In order to establish a baseline, a blank run was conducted using an empty pan. This was then subtracted from the thermal profiles using the TA Universal Analysis 2000 software.

2.2.5 X-ray diffraction analysis (XRD)

X-ray diffraction was used to assess the amorphous nature of each glass produced and the NP produced. Glass powder (< 63 µm) was analysed using a Bruker D500 X-ray diffractometer (Siemens) at room temperature using a Ni filtered Cu Kα radiation (λ = 0.15418 nm), operated at 40 kV and 25 mA. Data was collected from a range of 20º to 70º angle 2θ with a step size of 0.5 and a count time of 4s. The phases present in the NP were identified using the EVA software (DIFFRACplus) and the International Centre for Diffraction Data (ICDD) databased (2005).

2.2.6 Glass preparation

Glass formulations were prepared in batches of ~100g using the following precursors: P_2O_5 (Fisher, UK), NaH_2PO_4 (Sigma Aldrich, UK), $CaHPO_4$ (Sigma Aldrich, UK), CuO (II) MP (Aldrich, UK), CuO (II) NP (Sigma-Aldrich, UK) and CoO MP (Acros Organics).

The precursors were weighed out, mixed and transferred into a 200 ml Pt/10 % Rh crucible (type 71040, Birmingham Metal Company, Birmingham, UK). The crucible was then placed into a preheated furnace (Carbolite Gero, UK) at 350 °C for 30 minutes, before increasing up to 1150 °C for 60 minutes. The molten glass was poured onto a steel plate and left to cool to room temperature. Once cooled the glass was ground to the desired particle size (specified in each section where relevant) using a planetary ball mill (Retsch, PM100) and separated using sieves.

Glass formulations $45P_2O_5$-30CaO-$15Na_2O$-10CoO, referred to as P45-Ca30-Na15-Co10, $45P_2O_5$-30CaO-$20Na_2O$-5CoO referred to as

$45P_2O_5$-Ca30-Na20-Co5, and $45P_2O_5$-30CaO-$24Na_2O$-1CuO referred to as $45P_2O_5$-Ca30-Na24-Cu1, are explored in this Chapter.

2.2.7 Phosphorous-31 nuclear magnetic resonance spectroscopy (^{31}P-NMR)

Solid-state ^{31}P MAS NMR spectra was conducted to confirm the Q^n species of the glasses containing nanoparticles produced in Section 2.2.3. This analysis was carried out by the EPSRC UK National Solid-State NMR service at Durham University using a Varian VNMRS spectrometer and a 4 mm magic-angle spinning probe with a spin rate of 11-12 kHz. This was recorded using direct excitation at a Larmor frequency of 161.87 MHz, and the spectra was obtained with a 300s pulse delay and 4.4 µs pulse duration and was referenced to 85 % H_3PO_4. Deconvolution of peaks was carried out using the Fityk software.

2.2.8 Energy dispersive x-ray analysis (EDX)

Energy dispersive x-ray analysis (EDX) was used to confirm the elemental compositions of the glass prepared in Section 2.2.3. Glass fragments for each composition were mounted in resin and polished using SiC paper, diamond clothes and industrial methylated spirit (IMS) as lubricant. Once dry, these samples were carbon coated (thickness 10 nm) using the Polaron SC7640. EDX analysis was performed using the JEOL-6490LV SEM, using Oxford Instruments software for quantitative analysis. Each specimen's composition was analysed at three sample points using spot analysis and their average calculated. The accelerating voltage was 20 kV, using a resolution of 55 eV and an analysis time of 120 seconds. The standards used for analysis were albite for Na, GEO-MK2 apatite standard for P, Co metal for Co, Cu sulphide for Cu and wollastonite for Ca.

2.2.9 Annealing regimes

The thermal profile of P45-Ca30-Na15-Co10, was obtained using DSC analysis, identifying the T_g, T_c and T_m of the glass in order to establish potential annealing temperatures.

The glass was then cast into a hollow billet mould (see Figures 2.3a and b), machined from graphite (specification GD8878, Carbon International, UK). Table 2.2 outlines the proposed annealing regimes.

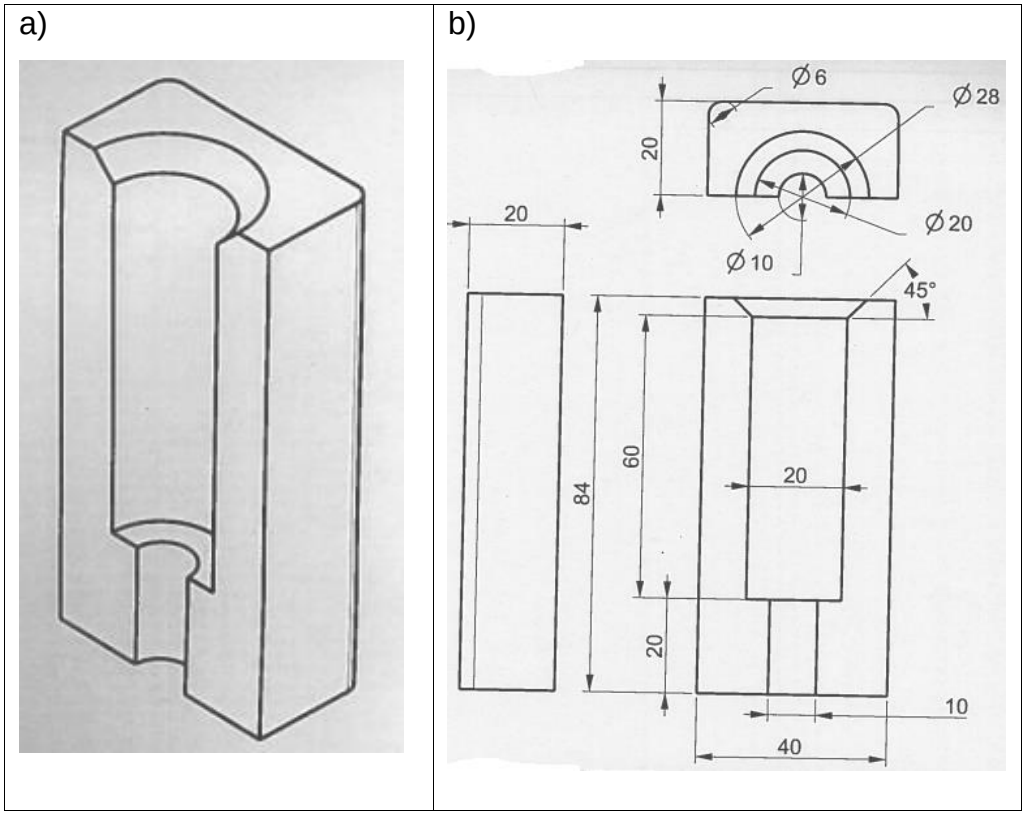

Figure 2.4*: The hollow billet graphite mould design. Image a) shows a 3D drawing of the mould without the central rod inserted, b) displays the dimensions of the mould.*

Industry standards suggest that annealing glass rods at 10 ^{o}C above glass T_g, with a hold time of 1 hour before gradually cooling (Patel *et al.* 2017) is generally sufficient to remove an residual stresses within the glass that can result in cracks or fractures. Therefore, this was the starting point for annealing trials, followed by subsequent regime alterations.

Table 2.3: *The casting and annealing regimes trialled for the hollow billet bolus with supporting literature.*

Trial	Regime	Supporting Literature
1	Cast glass into a mould preheated to 10 ºC above T_g, replace filled mould back into the heated oven, hold at 10 ºC above T_g for 1 hour before leaving to gradually cool overnight.	(Patel *et al.* 2017)
2	Cast glass into a preheated mould 100 ºC below the T_g, replace filled mould back into the preheated oven, hold at 100 ºC below the T_g for 1 hour before gradually cooling overnight.	(Tominaka *et al.* 2017; Ahmed *et al.* 2004)
3	Cast glass into a mould preheated to 100 ºC below the T_g, replace into the oven and hold for 1 hour. Then increase the temperature to 10 ºC above the T_g, and hold for an hour, before leaving to cool overnight.	(Tominaka *et al.* 2017)
4	Cast at room temperature	(Zhao *et al.* 2018; Hayden *et al.* 2000)
5	Cast glass into a mould preheated to 60 ºC below the T_g, replace into the oven an increase the temperature to 60 ºC above the T_g, and hold for 2 hours, before leaving to cool overnight.	(Chen, Zhang, and Ma, 2017)

2.3 Results

2.3.1. Transmission electron spectroscopy of cobalt oxide (Co_3O_4) nanoparticles

Image analysis results from the TEM analysis are shown in Figures 2.5. As can be seen in the first set of images (Figures 2.5) these liquid dispersed NP were arranged in a cubic crystal system, ranging in size from 4<80 nm. In order to incorporate the NP into the glass melt, they needed to be dehydrated to prevent reacting with the hygroscopic chemicals e.g. phosphorous pentoxide. Therefore, Figures 2.5a and b show the difference between the water dispersed nanoparticles (Figure 2.5a) and the freeze-dried NP (Figure 2.5b). In Figure 2.5b the NP were highly aggregated in some areas, forming clusters as large as 200 nm.

a)

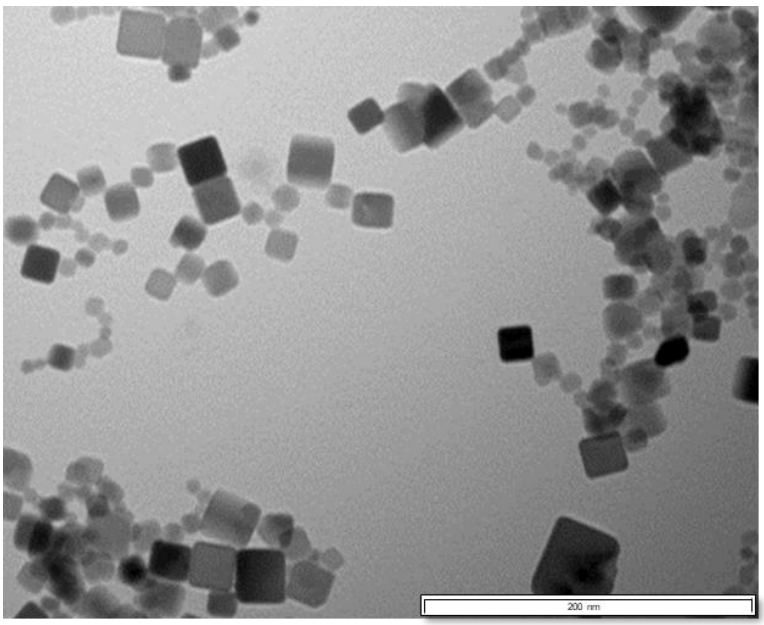

b)

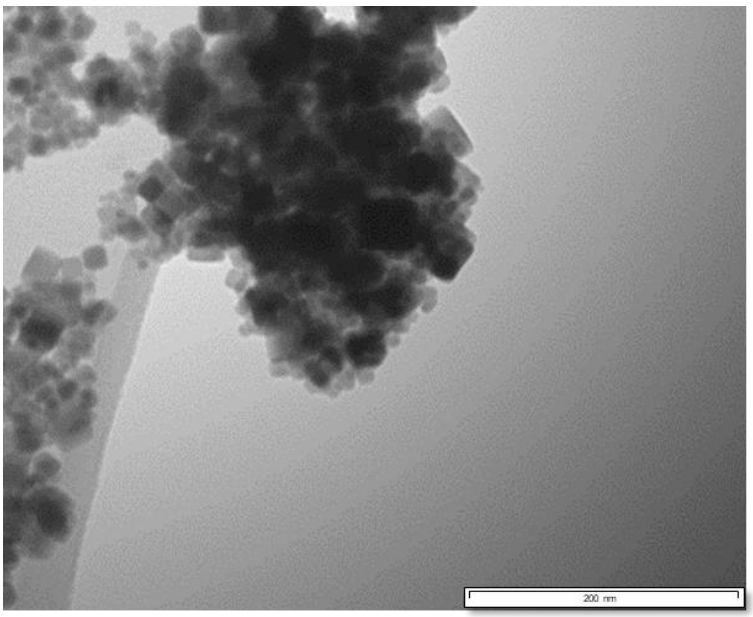

Figure 2.5: *TEM images of Co_3O_4 nanoparticles. Both samples of nanoparticles were produced from the same batch, however image a) were kept dispersed in water, whereas image b) were freeze-dried before rehydration for TEM analysis.*

2.3.2 Differential scanning calorimetry (DSC)

2.3.3.1 Cobalt Oxide (Co_3O_4) nanoparticles

The DSC profile displayed in Figure 2.6 showed the thermal parameters of the freeze-dried cobalt oxide (Co_3O_4) NP. The profile has been labelled with the respective material transition temperature (T_g), crystallization temperature (T_c), and melt temperature (T_m), with specific temperatures outlined in Table 2.4.

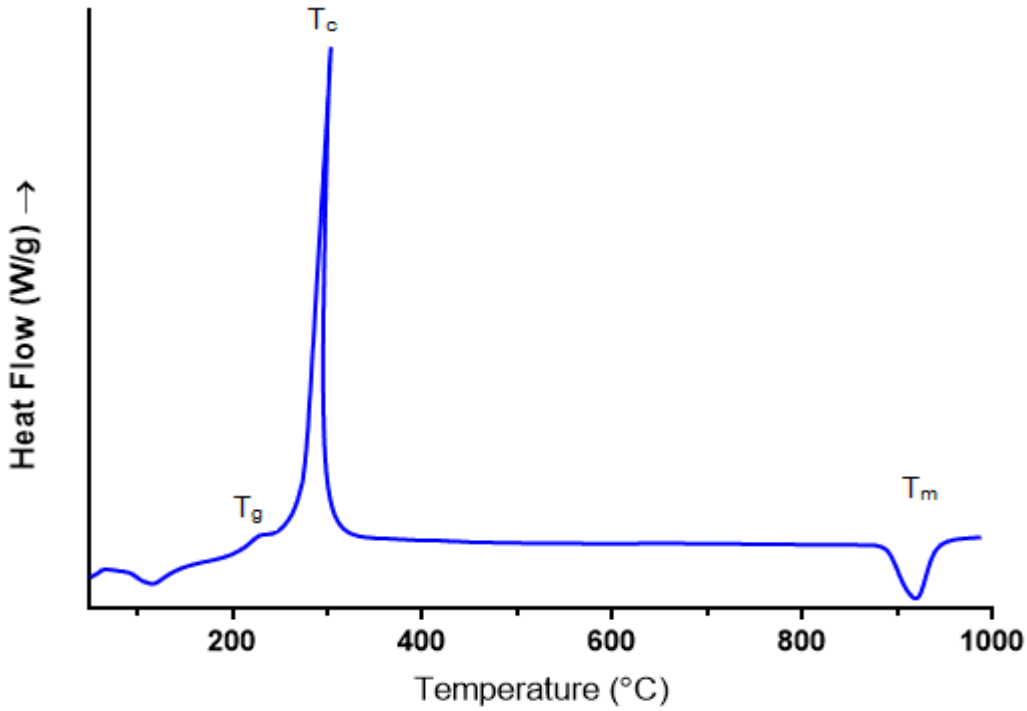

Figure 2.6: *Differential scanning calorimetry of the freeze-dried cobalt oxide (Co_3O_4) nanoparticles produced using hydrothermal synthesis*

Table 2.4: *Thermal parameters of cobalt oxide nanoparticles using DSC.*

	Onset of T_g (ºC)	**T_c (ºC)**	**Maximum T_m (ºC)**
Cobalt oxide NP (Co_3O_4)	231	303	918

2.3.3.2 Comparison between NP and MP doped cobalt glass

Figure 2.7 displayed the DSC profile for the NP and MP Co_3O_4 doped glasses. Both glasses displayed clear peaks for T_g, T_c and T_m and demonstrated similar DSC profiles, with very little difference seen the in T_g. The NP doped glass showed a slight delayed onset of crystallization, 534 ºC compared to 501 ºC for the MP glass. The delay in the onset of crystlliation resulted in the NP glass having a larger processing window, 148 ºC compared to 110 ºC for the NP and MP glasses respectively. The Co_3O_4 NP containing glass exhibited a more shouldered melt peak compared to the MP cobalt oxide doped glass, suggesting that more than one phase may be present. All thermal parameters are displayed in Table 2.5.

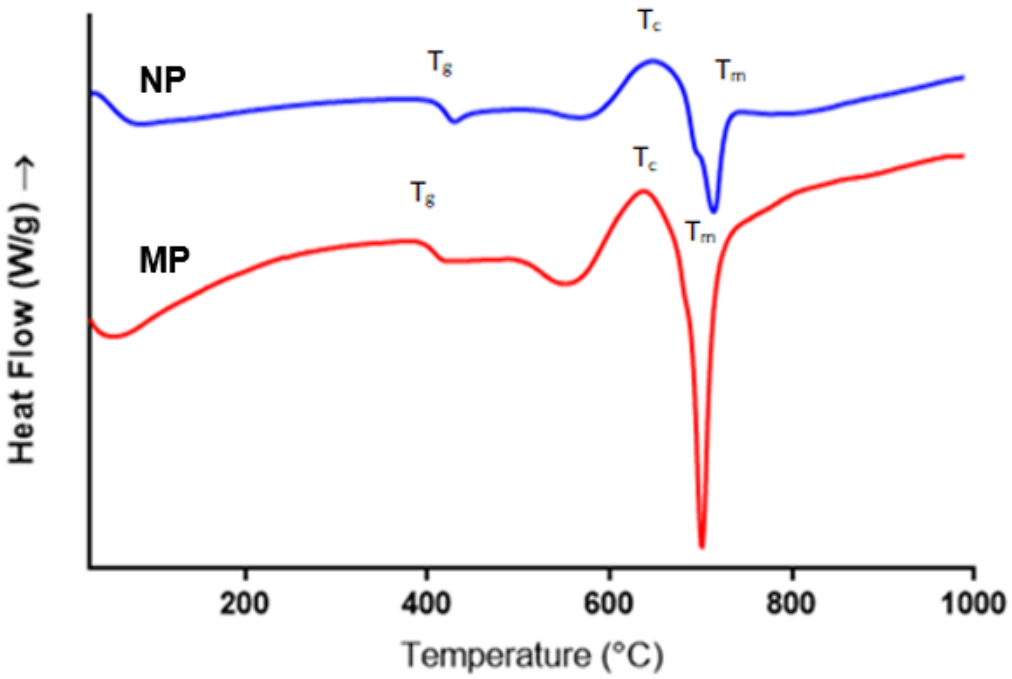

Figure 2.7: *DSC profile for glasses P45-Ca30-Na20-Co5: cobalt oxide (Co_3O_4) microparticle (red line) versus nanoparticle (blue line). Labelled: transition temperature (T_g), crystallization temperature (T_c) and melt temperature (T_m), using a heating rate of 20 ºC/minute.*

Table 2.5: *Thermal properties (T_g, T_c, and T_m) of the P45-Ca30-Na20-Co5 glasses either NP or MP cobalt oxide*

Glass	**Onset of T_g (ºC)**	**Onset of T_c (ºC)**	**T_c (ºC) peak**	**Maximum T_m (ºC)**	**Processing Window (T_c – T_g)**
P45-Ca30-Na20-Co5 MP (red line)	391	501	636	700	110
P45-Ca30-Na20-Co5 NP(blue line)	386	534	638	701	148

2.3.3.3 Comparison between NP and MP doped copper glass

The DSC profile (Figure 2.8) displayed clear peaks for transition, crystallization and melt temperatures for both NP and MP glasses. The MP containing glass revealed a larger processing (i.e. stability) window of 129 ºC, compared to the NP glass at 110 ºC. The smaller processing window for the NP glass was obtained due to the accelerated onset of crystallization at 471 ºC, compared to 506 ºC for the MP glass. Unlike the MP glass, two crystallization peaks were also observed for the NP glass, one at 500 ºC, followed by a second one at 511 ºC.

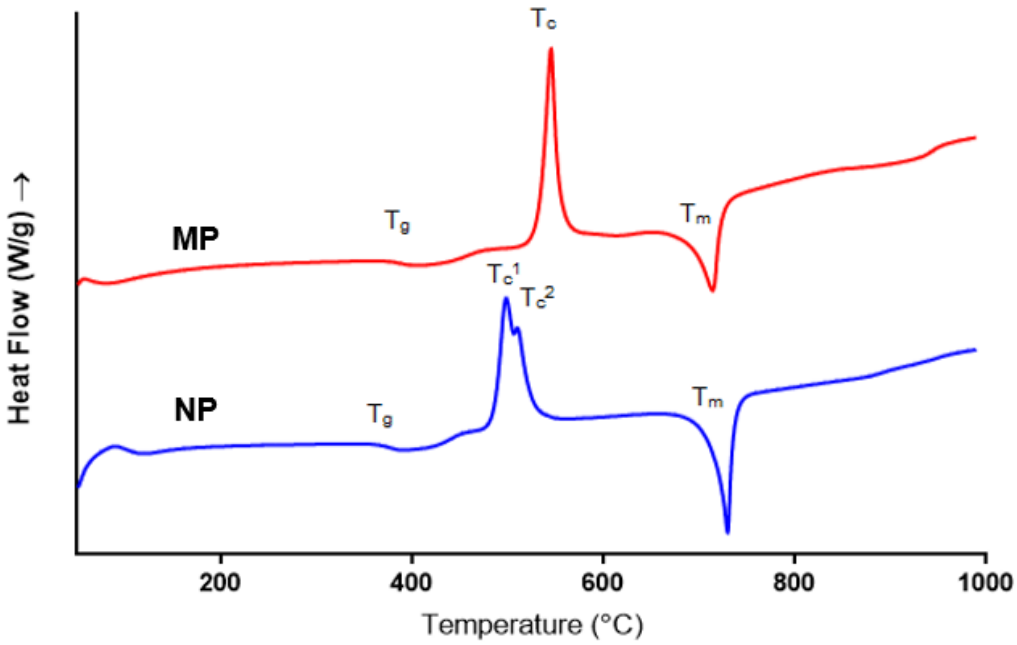

Figure 2.8: *DSC profile for glasses P45-Ca30-Na24-Cu1: microparticle (red line) versus nanoparticle (blue line). Labelled: transition temperature (T_g), crystallization temperature (T_c) and melt temperature (T_m), using a heating rate of 20 ºC minute.*

Table 2.6: *The thermal properties of glasses P45-Ca30-Na24-Cu1 containing microparticle or nanoparticle copper. MP denotes the inclusion of copper oxide as microparticle, NP denotes the inclusion of copper oxide nanoparticles into the glass melt.*

Glass	**Onset of T_g (ºC)**	**Onset of T_c (ºC)**	**T_c^1 (ºC) peak**	**T_c^2 (ºC) peak**	**Maximum T_m (ºC)**	**Processing Window ($T_c - T_g$)**
P45-Ca30-Na24-Cu1 MP (red line)	377	506	543	-	714	129
P45-Ca30-Na24-Cu1 NP (blue line)	361	471	500	511	726	110

2.3.3.4 DSC profile of P45-Ca30-Na15-Co10 glass

The DSC profile shown in Figure 2.9 displayed the T_g, T_c and two melt points T_m^2 and T_m^2 for the glass P45-Ca30-Na15-Co10. Despite having a relatively high crystallization temperature of 632 ºC for phosphate glasses, due to the broadness of the peak the onset of crystallization was much lower at 511 ºC, resulting in processing window of 110 ºC. The two different melt temperatures are recorded for this glass, one at 701 ºC and followed by a broader second peak at 737 ºC. All thermal parameters are displayed in Table 2.8.

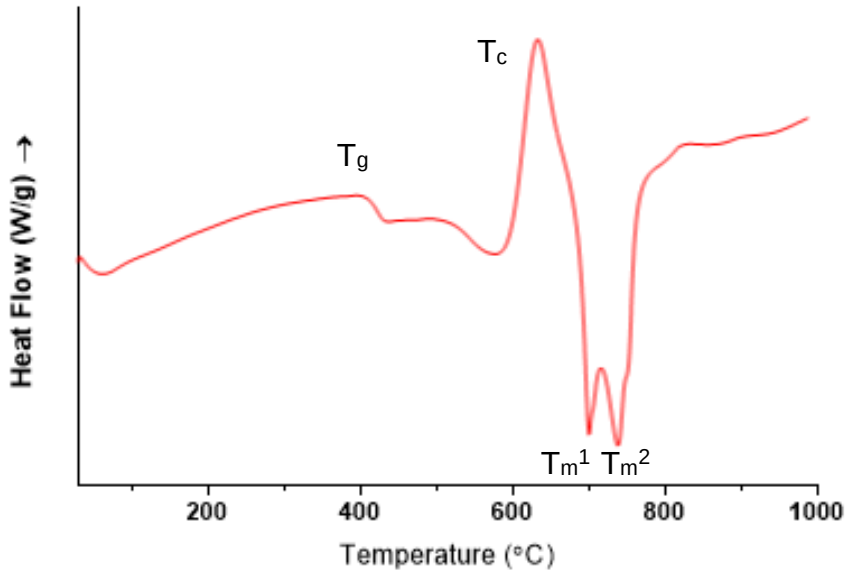

Figure 2.9: *The thermal analysis of the glass of P45-Ca30-Na15-Co10 obtained using DSC*

Table 2.7: *The thermal parameters of glass P45-Ca30-Na15-Co10*

Glass	**Onset of T_g (ºC)**	**T_c (ºC) onset**	**T_c (ºC) peak**	**T_m^1 (ºC)**	**T_m^2 (ºC)**	**Processing Window (T_c onset- T_g)**
P45-Ca30-Na15-Co10	401	511	632	701	737	110

2.3.3 X-ray diffraction (XRD)

2.3.4.1 Cobalt Oxide (Co_3O_4) nanoparticles

Figure 2.10 showed the XRD analysis, carried out to support the confirmation of the Co_3O_4 NP produced using hydrothermal synthesis.

A similar profile by Lester *et al.* (2012) suggested that the Co_3O_4 NP produced had a cubic spinel structure, which correlated with the TEM analysis in Figure 2.1. However, the peak displayed at 29.4º 2θ, is not present in Lester *et al.* (2012), or by the standard cubic Co_3O_4

according to the International Centre for Diffraction Data (ICCD) PDF 009-0418.

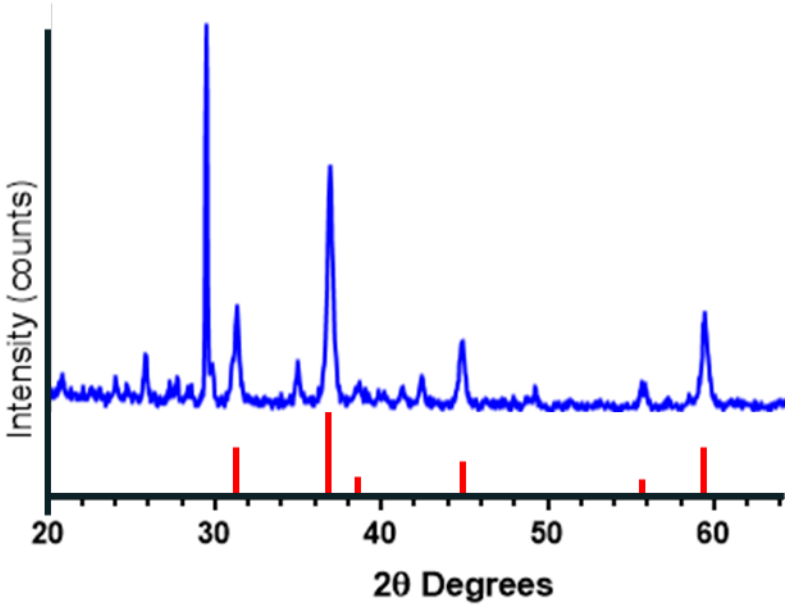

Figure 2.10: *X-ray diffraction pattern of cobalt oxide (Co_3O_4) nanoparticles dehydrated powder produced using hydrothermal synthesis (blue lines), and expected pattern for cubic Co_3O_4 (ICCD PDF 009-0418), (red ticks).*

2.3.4.2 Cobalt oxide (Co_3O_4) NP and MP doped glasses

Figure 2.11 showed that both the cobalt oxide NP and MP glasses were confirmed to be glassy and amorphous in structure due to the broad peaks between 20-40 º in 2θ values, typical of the “amorphous hump” and the absence of sharp crystalline peaks.

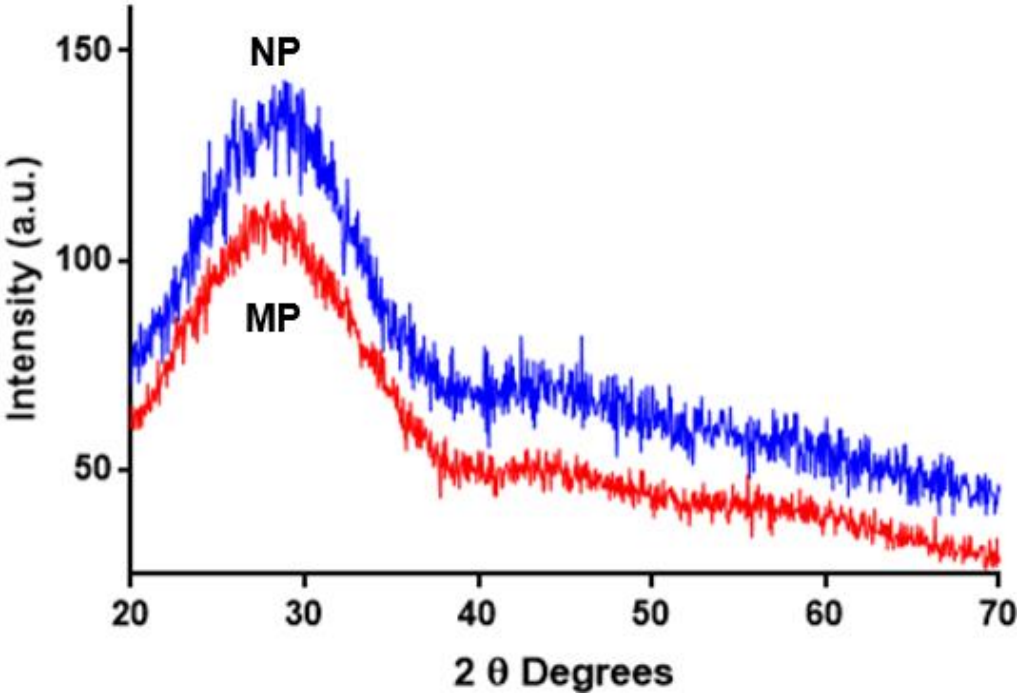

Figure 2.11: *X-ray diffraction pattern of the P45-Ca30-Na20-Co5 glasses using Co_3O_4 nanoparticles (blue line) and microparticles (red line).*

2.3.4.3 Copper Oxide (CuO) nanoparticles

The XRD pattern displayed in Figure 2.12 confirmed the crystalline nature of the copper oxide (CuO) NP, which correlated with the CuNP XRD pattern shown in Zhu *et al.* (2004) referencing powder diffraction file (PDF) *JCPDS 80-1268*.

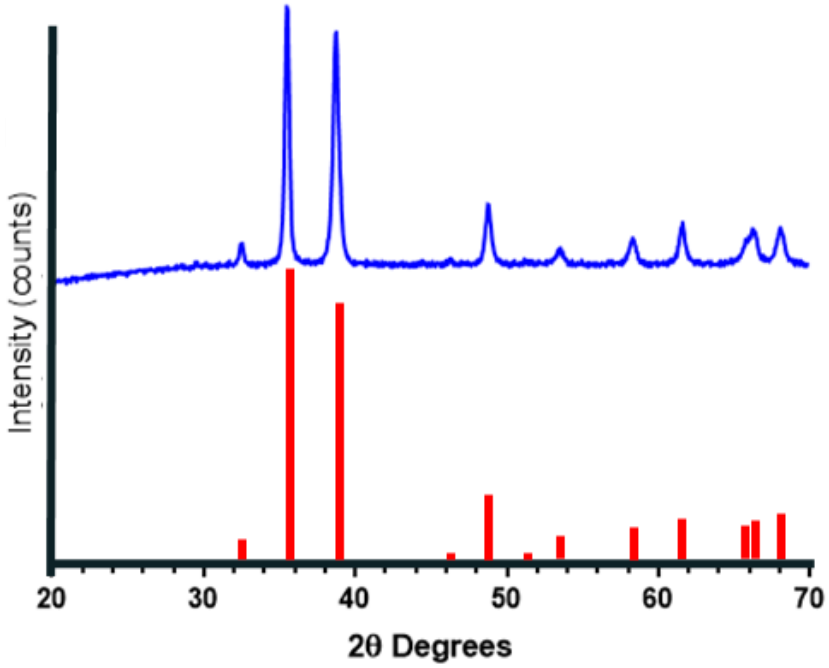

Figure 2.12: *X-ray diffraction analysis of copper oxide (CuO) powder (Sigma Aldrich, UK) (blue lines), and expected pattern for CuO (JCPDS 80-1268), (red ticks).*

2.3.4.4 Copper oxide (CuO) NP and MP doped glasses

Glasses containing copper oxide as NP and MP were confirmed to be amorphous using XRD, both glasses displayed a broad peak between 20-40 º in 2θ values, confirming the glassy amorphous states and the absence of sharp crystalline peaks (see Figure 2.13).

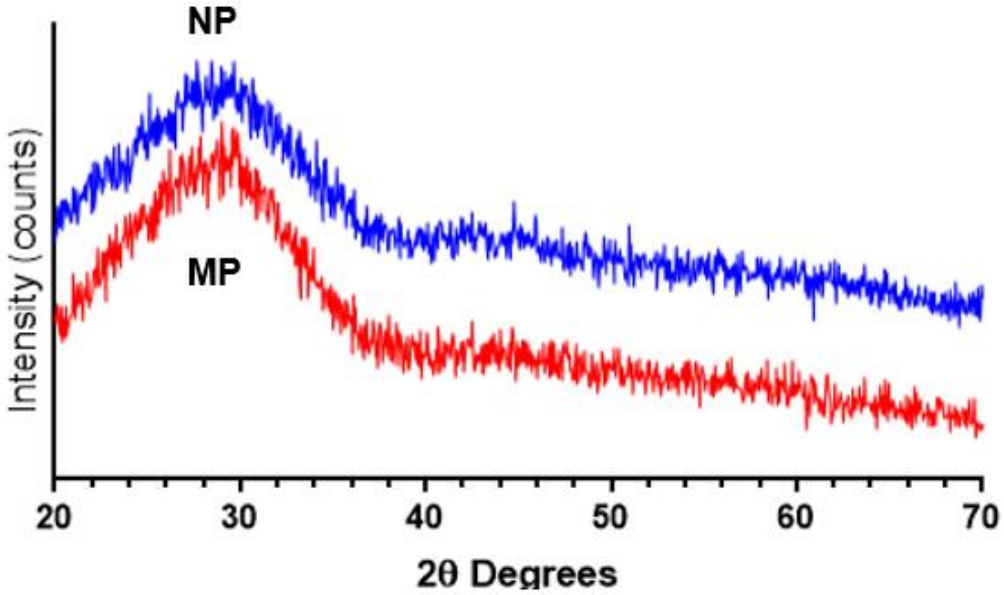

***Figure 2.13**: X-ray diffraction pattern of the P45-Ca30-Na24-Cu1 glasses using CuO nanoparticles (blue line) and CuO microparticles (red line).*

2.3.4 Phosphorous-31 nuclear magnetic resonance spectroscopy (^{31}P-NMR)

For both NP and MP Co_3O_4 glasses with a formulation of P45-Ca30-Na20-Co5, two centre-band signals were observed (see Figure 2.14). One at -2.86 and one at -23.56 ppm for the MP glass containing cobalt oxide, and one at -1.60 and -22.37 ppm for the NP containing glass. These two signals for both glasses were identified as Q^1 and Q^2 species respectively.

However, the NP glass had slightly different Q-species ratios compared to the MP glass, 17 % and 83% for Q^1 and Q^2 species for the NP glass respectively, and 21 % and 79% for Q^1 and Q^2 species for the MP glass respectively (see Table 2.8).

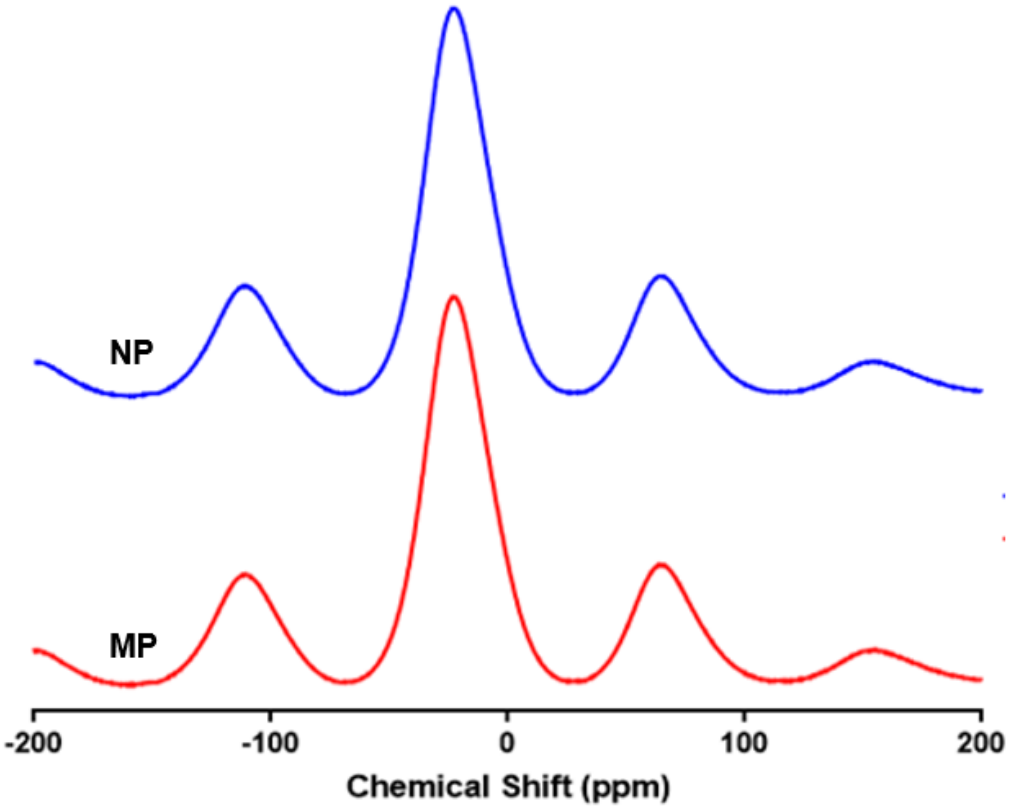

Figure 2.14: *Deconvolution spectra of solid state MAS NMR ^{31}P of the P45-Ca30-Na20-Co5 glasses using Co_3O_4 nanoparticles (blue line) and microparticles (red line).*

Table 2.8: *The Q^n obtained and identified using ^{31}P MAS NMR for P45-Ca30-Na20-Co5 glasses using Co_3O_4 nanoparticles and microparticles*

	Q^n species identified/ ppm		**Q^n species ratios obtained (%)**	
	Q^1	**Q^2**	**Q^1**	**Q^2**
Microparticle	-2.86	-23.56	21	79
Nanoparticle	-1.60	-22.37	17	83

2.3.5 Energy dispersive x-ray (EDX) analysis

2.3.2.1. Nanoparticle and microparticle comparison glasses

Presented in Table 2.9 are the EDX values of the glasses P45-Ca30-Na20-Co5 and P45-Ca30-Na24-Cu1, comparing the addition of NP versus MP used in the glass melt.

Glasses P45-Ca30-Na20-Co5 NP and MP both revealed higher phosphorous and cobalt contents, with lower sodium contents than expected. However, there was no significant difference between the two glasses formulation overall, therefore the comparison between the addition of NP and MP still stood.

Similarly, the P45-Ca30-Na24-Cu1 glasses varied slightly from their intended formulation. However, there was no significant difference between the NP and MP glasses, consequently these were also compared.

Table 2.9: *The EDX values of the glasses incorporating copper and cobalt nanoparticles studied in this Chapter, presented as mole percentage of oxides in the glass. NP denotes in the inclusion of cobalt oxide nanoparticles, MP denotes the inclusion of cobalt oxide microparticles into the glass melt.*

Glass	Mol%			
	P_2O_5	CaO	Na_2O	CoO
P45-Ca30-Na20-Co5 MP	49.7	29.1	12.6	8.6
P45-Ca30-Na20-Co5 NP	47.9	30.1	14.1	7.9
P45-Ca30-Na24-Cu1 MP	40.9	32.3	25.3	1.5
P45-Ca30-Na24-Cu1 NP	42.2	29.7	26.3	1.8

2.3.2.2 Hollow billet glass

The glass composition of the hollow billet design was confirmed using EDX analysis, showing all elements were present and within the accepted error range of 10% of the targeted elemental molar quantity.

Table 2.10: *The EDX values of the glasses studied in this Chapter used for the hollow billet, presented as mole percentage of oxides in the glass.*

Glass	P_2O_5	CaO	Na_2O	CoO
P45-Ca30-Na15-Co10	47.2	31.4	11.7	9.8

2.3.6 Annealing regimes

The images outlined in Figures 2.15a-f correspond to the annealing regimes discussed in Table 2.3.

- Trial 1 (Figure 2.15a) shows the results of annealing 10 ºC above the T_g for 1 hour. Despite macroscopically seeming to be amorphous due to its glassy appearance, this attempt was unsuccessful due to billet fragmenting into three large segments up removal from the mould.
- Trial 2 (Figure 2.15b) worked with parameters 100 ºC below the T_g, however, this yielded similar results to Trial 1 resulting in 7 large glassy looking fragments.
- Trial 3 (Figures 2.15c and d) initially appeared successful, resulting in an intact hollow billet, however, after light handling it broke into multiple shards and fragments.
- Trial 4 (Figure 2.15e) was also resulted in many smaller splintered shards of glass, with some larger fragments similar to Figures 2.15a and b.
- Trial 5 (Figure 2.15f) resulted in the glass being split into two large mottled fragments.

a)

b)

c)

d)

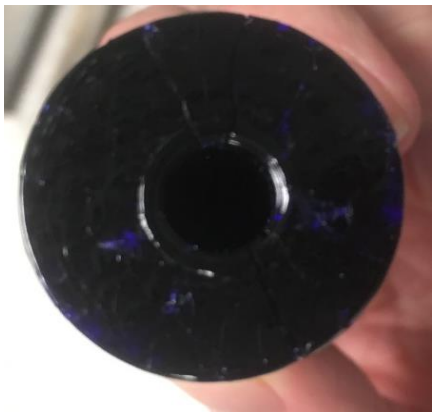

e)

f)

Figures 2.15 a-f: *Images taken of the cooled hollow billets after following different annealing regimes (outlined in Table 2.3), once removed from the mould.*

Trial 1-5 annealing regimes are outlined in Table 2.3. Figure a) followed Trial 1, b) Trial 2, images c and d) were as a result of following Trial 3, e) Trial 4 and f) Trial 5.

2.4 Discussion

2.4.1 Incorporation of nanoparticles into phosphate glass

The main aim of this chapter was identify a suitable bolus design and to establish whether NP could be incorporated into phosphate-based glasses, without integrating into the glass matrix, thus maintaining their NP form.

Section 2.3.1 showed the successful production of cubic cobalt oxide (Co_3O_4) NP dispersed in water, following the same methodology as Lester *et al.* (2012). The key advantage of the hydrothermal synthesis process is that the NP are produced in solution, thereby enabling safe transportation and handling. However, in order to be incorporated into the glass manufacturing process NP produced in solution needed to be dehydrated, and as such were subjected to a freeze-drying process. It was clear from the TEM analysis (Figure 2.5b) that the drying process led to significant agglomeration of the freeze-dried particles versus the particles that remained in solution (Figure 2.5a).

Rahman *et al.* (2008) found similar results when assessing the effect of different drying methodologies for silica NP, finding that freeze-drying resulted in bulk aggregation of loosely packed particles. It was believed that as the freeze-drying process involved a solid-gas transition evading the liquid phase, the compaction associated with capillary force observed with oven-drying was avoided, resulting in the improved dispersion and reduced agglomeration of particles. Similarly, the authors theorised that the dispersion of particles may have also contributed to the volume expansion that occurs during freezing an aqueous suspension. Therefore, this raised the question as to whether the agglomerated freeze-dried NP observed in Figure 2.5b were actually of a similar size range to the hydrated NP in Figure 2.5a.

It is therefore likely that it was due to the TEM method of size assessment that these particles appeared agglomerated and larger in size. As such, future work requiring dehydration of NP should characterise particle size using a secondary method such as dynamic light scattering that would further confirm the particle size.

Characterisation of the cobalt oxide (Co_3O_4) NP was also confirmed using XRD analysis. As mentioned in the results section all but one peak observed correlated well with cubic cobalt oxide NP documented in the *ICCD PDF 009-0418 (*Moro *et al.* 2013) however, the peak identified at 29.4 º 2Theta, was not documented. Mosheni, (2007) identified a peak at 29.5 º 2Theta, confirming it was calcite ($CaCO_3$)-Rhombohedral. However, none of the other peaks for their value correlated closely enough with XRD patterns shown in Figure 2.9 to confirm that this was the same compound. It was suggested that this unknown compound could have been caused by contamination during the drying process, or as a result of the hydrothermal reactor being used by multiple other students at the time of NP production. After speaking to University of Nottingham XRD specialist Hannah Constantin, and discussing that as a result of the high peak intensity, the anomalous peak is unlikely to be contamination, and instead a result of user error. The same batch of hydrated NP was confirmed to be correct using inductively coupled plasma mass spectroscopy (ICP-MS) during Chapter 7, Section 7.2.1, as such it is more likely that the contamination occurred during the XRD analysis than during the initial hydrothermal production of the NP. Therefore, in order to confirm whether the peak was an anomaly, or contamination, repeated XRD analysis should be conducted before these NP are used again.

The EDX values displayed in Table 2.9 show that the cobalt oxide and copper oxide glass compositions obtained were slightly different from the glass values intended. The cobalt MP and NP glasses contained 49.7 or 47.9 mol% phosphorous respectively, compared to the 45 mol% intended. Additionally, the cobalt MP and NP glasses contained lower

Na mol%, 12.6 mol% and 14.1 mol%, respectively, compared to the 20 mol% intended. The cobalt content of the MP and NP glasses was 8.6 mol% and 7.9 mol% respectively, higher than anticipated values of 5 mol%.

Patel *et al.* (2017) stated that small increases/decreases (within margins or error) are widely documented and expected with phosphate glass production and have been attributed to either the initial precursors salts (phosphate-based precursors are particularly susceptible to hydrolysis), or volatilisation losses incurred during the melt process.

After considering multiple possibilities for why the actual sodium content of the cobalt oxide glasses was lower than intended, such as the decomposition temperature and products of sodium phosphate under heating, (Banach and Makara, 2011) which resulted in a higher proportion of sodium deposit remaining in the crucible. Alternatively, localised concentration gradients of sodium within the glass which may have skewed the results of the EDX analysis, it was more likely that the discrepancy was due to user error than the process, precursors, or analysis.

Interestingly, both the copper and cobalt NP containing glasses revealed lower T_g temperatures to their MP counterparts (see Figures 2.7 and 2.8, respectively). The cobalt NP glass had a T_g of 386 ºC, compared to the MP glass that had a T_g of 391 ºC. Whereas the copper NP glass had a T_g of 361 ºC, compared to the MP glass with a T_g of 377 ºC. The decrease in T_g of the NP cobalt glass coupled with a delayed onset of crystallization from 501 ºC to 534 ºC, possibly as a result of multiple phases in the glass (Franks *et al.* 2001) resulted in a larger processing window of the glass increasing from 110 ºC to 148 ºC.

The copper NP containing glass had a decreased crystllisation temperature from 506 ºC to 471 ºC compared to the MP glass, resulting in a reduction in processing window from 129 ºC to 110 ºC, suggesting a lower stability of the NP glass. The lower crystalisation temperature of

the NP copper glass may be due to the increased surface area of the NP, resulting in a higher number of possible nucleation sites for crystllization (Ray and Day, 1996).

The copper NP containing glass displayed two cyrstallisation peaks, unlike the MP glass. One at 500 ºC and a second at 511 ºC, however, this is likely a result of subtle differences in the glass formulations such as the higher P content and lower Ca content in the NP glass, 42.2 mol% versus 40.9 mol% and 29.7 mol% versus 32.3 mol% respectively. The cobalt NP glass did reveal broader peaks, suggesting some potential phase separation could have occurred. However, this was not as well defined as the NP copper glass as it could have been masked under the broad peak observed.

NMR analysis further probed the structural differences of the cobalt oxides glasses. Previous work assessing the Q^n species of compositions with fixed P_2O_5 at 45 mol%, observed signals at -6.1 and -22.1 ppm for Q^1 and Q^2 respectively (Ahmed *et al.* 2004). The Q^n species ratios of the MP cobalt glass assessed here was consistent with the literature of other P45 glasses. The MP cobalt glass had a Q^n species ratio of 21 % and 79 % for Q^1 and Q^2 respectively. Similarly, Ahmed *et al.* (2004) showed that their P45-Ca30-Na25 glass had Q^n species ratios of 21.71 % and 78.29 % for Q^1 and Q^2 respectively. Whereas, the NP cobalt glass assessed in this chapter had a Q^n species ratio of 17 % and 83 % for Q^1 and Q^2 respectively, which was closer to the P45-Ca40-Na15 glass in Ahmed *et al.* (2004), which had Q^n species ratios of 17.04 % and 82.96 % for Q^1 and Q^2 respectively. The increase in Q^2 species compared to Q^1 for the NP cobalt glass suggested an increase in network polymerisation and longer chain structure (Ahmed *et al.* 2004), which implied that the NP cobalt is an intermediate oxide (Hoppe *et al.* 2014). Intermediate oxides are known to able to act as both network formers as well as modifiers (Azevedo *et al.* 2010), though this hypothesis would need to be confirmed with statistical significance to conclude this.

As shown in Section 2.3.5, Table 2.9, the compositions of the P45-Ca30-Na20-Co5 glasses were closer to P_2O_5 at 50 mol% with a calcium content of 40 mol%, for which a dominant signal was seen at -25.2 ppm, demonstrating Q^2 species as shown in Ahmed *et al.* (2004). This is quite different to the Q^n species identified in this work, which showed bands at -2.86 and -23.56, -1.6 and -22.37 for the Q^1 and Q^2 species for both the MP and NP containing glasses respectively. Interestingly, these bands were closer to the Q^n species observed for the P45-Ca40-Na15 glass code. It is documented that cobalt oxide can act as a network former or modifier in silicate glasses and phosphate glass depending on the concentration (Azevedo *et al*. 2010; Hoppe *et al*. 2014; Kumar Vyas *et al*. 2015). Therefore, it was suggested that the cobalt could be acting as a network former rather than a modifier. Hoppe *et al.* (2014) demonstrated that using "1393" silicate bioactive-glass, cobalt acted as both a network former when incorporated at >5 Wt% (4.19 mol%), or as a network modifier when at 1 Wt% (0.82 Mol%), therefore it is plausible that for the concentrations used in this work the Co^{2+} ions were acting as a network former. Azevedo *et al.* (2010) reported that Co^{2+} initially acted as an intermediate oxide when replacing Ca^{2+} for Co^{2+}, inducing a change in the silicate Q^2 structure towards a Q^3 structure. However, this work found the formation of $[CoO_4]^{2-}$ species increased the degree of polymerization of the silicate network, supporting the suggestion that Co^{2+} ions can act as both network modifiers and network formers depending on their concentration.

Unfortunately, no Fourier Transform Infrared Spectroscopy (FTIR) data was collected and as such it is not possible to specify whether the cobalt ions were covalently bonded into the glass network as P-O-Co, or whether it was ionic. If the cobalt was acting as a network former, in the 2+ oxidation state, then it would be more likely that it could be cross-linking chains, similar to that of Ca in the glass formulation.

Overall, the results shown in Section 2.3.2 suggested that the addition of NP into the current glass manufacturing process resulted in the NP becoming part of the glass network, either as network modifiers for copper and low inclusion levels of cobalt or possibly network formers for higher concentrations of cobalt. It is clear that there are some structural differences to the glass, such as Q-species ratios, caused by the addition of NP compared to MP. However, it is currently unclear why these differences occurred. It is possible that the NP were able to amalgamate more easily into the backbone of the structure of the glass due to their size, or that due to their small size the nanoparticles were not detected by XRD. However, Liu *et al.* (2019) found that when nickel nanoparticles were incorporated into sodium borosilicate glass, the XRD patterns displayed the peaks associated the standard JCPDS card for nickel, as well as the amorphous hump associated with glasses. Further analysis by the author using TEM showed that the nickel NP were evenly distributed through the glass matrix, whilst still retaining their spherical NP morphology.

As such, further analysis of the glasses shown in Section 2.3.4 using neutron diffraction or x-ray photoelectron spectroscopy could confirm whether the NP had become part of the glass matrix, or alternatively the use of TEM to establish whether the NP had retained their NP form, but were too small to be detected by XRD.

2.4.2 Feasibility of the hollow billet design

Two types of crack patterns are commonly observed in phosphate-based glasses. Type I cracks rarely penetrate more than a few millimetres into the casting, and do not lead directly to catastrophic fracture. Type II cracks penetrate a large fraction into the casting and make the product unusable (Hayden *et al.* 2000). As can be seen in Figures 2.15a-f, all of the annealing attempts were unsuccessful in producing uncracked specimens. However, there were a couple of common observed themes in the failed attempts: Figures 2.15a, b and f fractured into large segments (Type II cracks) whereas Figures 2.15c, d

and e splintered into smaller shards (Type I cracks); Figures 2.15a, b, c and e, appeared glassy whereas Figure 2.15f showed mottled surface indicative of surface crystallization.

It is likely that all of the cracks for the initial attempts in Figures 2.15 initiated from surface flaws (Suratwala *et al.* 2000; Crichton *et al.* 1999), possibly caused by imperfections in the graphite mould, or more likely as a result of residual stressors remaining in the glass. As a result of the Type I fractures, due to thermal gradients these then propagated into Type II fractures (Hayden *et al.* 2000). The two annealing regimes that only showed Type I fractures were regimes 3 and 4, these had the largest temperature gradients, annealing the glass at 100 ºC below T_g, for regime 3 and annealing at room temperature (approximately 25 ºC) for regime 4. Koike and Tomozawa, (2006) found that rapid cooling of soda-lime silicate glass resulted in slower crack growth rate owing to a lower viscosity, enabling plastic deformation compared to silica glasses trialled under the same conditions. This aligned with the hypothesis that rapid cooling of phosphate glasses encourages chemical stability (James *et al*. 1997).

It is likely that the reason for the annealing regime 3 failed after a short period of time after being handled may have been caused by water vapour from the atmosphere diffusing into the surface of the formed glass, causing OH-rich glass near the surface. The OH-dense layer shrinks at a higher rate than the interior of the glass, resulting in a tensile surface layer (Hayden *et al*. 2000) and as such this resulted in complete fracture after light handling due to the cracks already present. One possible method to mitigate this could be a larger central rod, which could result in a more even cooling rate across the whole of the billet, possibly decreasing the likelihood of cracking.

Regime 5 (cast glass into a mould preheated to 60 ºC below the T_g, replace into the oven an increase the temperature to 60 ºC above the T_g, and hold for 2 hours, before leaving to cool overnight) was the only glass that showed surface crystallization. This is surprising as this

regime is quite similar to regime number 3 which appeared to be the most successful of the 5 attempts, and the temperatures worked at were within the glasses relatively large processing window of 110 ºC. It is possible that the difference between these two regimes that resulted in the surface crystallization of attempt 5 may be due to the extended annealing time. If the annealing temperature was above the glasses transition temperature, then the increased duration would have enabled the rearrangement of particles into a more ordered state and hence the formation of crystallization phases (Kaminska *et al.* 2020). However, regime 5's annealing temperature was only 462 ºC, whereas the onset of crystallization is not until 511 ºC. Therefore, the surface crystallization was likely to be due to a multitude of factors: it is highly likely that in order for the furnaces used to reach the desired temperature the furnace may have exceeded the desired temperature at some point by approximately 5-10 % target temperature (485 - 508 ºC). As mentioned earlier, there is likely to be a higher proportion of OH-containing glass at the surface. It is well documented that an increased concentration of OH-bonds within phosphate glass reduces the thermal stability due to network depolymerisation (Suratwala *et al.* 2000), and as such this glass would require a lower temperature in order for the activation energy to be reached, initiating crystallization (Massera *et al.* 2015). Therefore, it is likely that the crystallization was caused by a combination of annealing too close to the onset of crystallization and holding for an extended period of time.

When comparing the DSC data displayed in Table 2.7 for P45-Ca30-Na15-Co10, the addition of 5 mol% cobalt substituted for sodium compared to the P45-Ca30-Na20-Co5 glass discussed earlier (Table 2.5), showed higher thermal processing requirements in all aspects. P45-Ca30-Na20-Co5 MP had a T_g of 391 ^oC, T_c onset of 501 ^oC and T_m of 700 ^oC, compared to P45-Ca30-Na15-Co10 MP that had a T_g of 401 ^oC, T_c onset of 511 ^oC, T_m^1 of 701 ^oC and T_m^2 of 737 ^oC. This is unsurprising due to the substitution of a monovalent cation (sodium) for

a divalent cation (cobalt), as a result the increased cross-link density would strengthen the glass network (Ahmed *et al.* 2005), resulting in higher thermal processing requirements.

Another difference in thermal characteristics between these two compositions is the presence of two melt peaks for P45-Ca30-Na15-Co10, whereas P45-Ca30-Na20-Co5 only has one. Franks *et al.* (2001) saw a similar trend that an intermediate concentration of sodium (35 mol% compared to 43 or 23 mol%) resulted in the formation of two melt peaks, whereas the lower and higher sodium containing glasses trialled had singular peaks. The authors attribute this difference to phase separation caused by differing field strength between the sodium and calcium. Cobalt has a higher field strength of 0.38 valence/Å2 (calculated using Dietzel, (1942) and Anderson *et al.* (1975)) compared to sodium's 0.19 valence/Å2 (Franks *et al.* 2001), it is likely that a similar phenomenon is occurring, thus providing stronger crosslinking between the phosphate chains, increasing the T_g, T_c and T_m of the higher cobalt containing glass. It would be interesting to see if this trend continued if increased to 15 mol% cobalt oxide, however, as this concentration would have been too high for the intended end use of the glass no further work was conducted.

As can be seen from the images presented in Figures 2.15a-f, it was possible to cast a hollow billet from the glass formulation P45-Ca30-Na15-Co10 following the annealing regime no. 3 (casting glass into a preheated mould 100 ºC below the glass T_g, followed by increasing the temperature to 10 ºC above the T_g, holding for 1 hour before slowly cooling). However light handling caused the fractures to propagate resulting in complete breakage. As a result, this design was deemed fragile to upscale, and so no further work was carried out using the hollow billet design, or P45-Ca30-Na15-Co10 formula due to practicality constraints.

2.5 Conclusion

This chapter aimed to investigate which different bolus designs may be suitable to support the uniform release of trace elements Cu, Co, Se and I over a 6-month duration. Additionally, this chapter explored whether NP (Co_3O_4 and CuO) could be incorporated into phosphate-based glasses during the glass melt process without merging into and becoming part of the glass matrix, and how the use of NP versus MPs may affect the chemical and physical characteristics of the glass.

This chapter confirmed that production of a defect-free hollow billet bolus or fruit pastille bolus was extremely challenging, and would likely to unsuitable for upscaled mass manufacturing. As a result of this, it was decided that a sintered phosphate based glass bolus would be a more appropriate bolus design by being more suitable for mass production.

Additionally, the data in this chapter suggested that it was highly likely the NP became part of the glass network due to the very similar ^{31}P-NMR data shown, while the lack of sharp peaks in the XRD analysis suggested an amorphous, glassy-state rather than crystalline ones. However, some differences in thermal characteristics were observed between the formulations, and further analysis will be required to understand this in more depth. As such, in order to further explore if NP could still be delivered using phosphate-based glass as a delivery system, a sintered phosphate-glass bolus was decided upon and used in future tests.
Due to the extensive nature of work carried out in this area, it is outlined in the next chapter.

Chapter 3 – Phosphate-based glass formulation development

3.1 Introduction

Chapter 2 outlined the merits and disadvantages of various bolus designs, confirming that in order to support mass manufacturing and the delivery of trace minerals, the sintered bolus design was the most suitable. Additionally, the sintered bolus design may still enable the incorporation of nanoparticles to enable improved trace mineral bioavailability.

As such, this chapter aimed to explore the ion release rate of multiple different glass formulations, both with and without the inclusion of nanoparticles to identify a formulation suitable of fulfilling the Industrial Partner's desired daily release rate for a prototype bolus. In order to do so, the thermal characteristics of the glasses were confirmed using DSC, and optimal sintering parameters characterised using a combination of ash fusion testing (AFT) and scanning electron microscopy (SEM). Glass formulation degradation rates were assessed using *in vitro* dissolution studies and ion release measured using inductively coupled plasma optical emission spectrometry (ICP-OES).

As discussed in Chapter 1, the supplementing of trace minerals to improve production and welfare of livestock within the agricultural industry is common practice globally (Kaufmann and Rambeck 1998). Within the United Kingdom these products are currently regulated by the European Union under Regulation (EC) No 1831/2003 (European Union 2003). This legislation stipulates the maximum permitted limits of vitamins, minerals and additives products are allowed to contain overall and on a daily release rate (Table 3.1). This legislation also outlines permitted chemical compositions for each element, such as cobalt (II) carbonate for cobalt and is updated to reflect recent scientific advances.

Table 3.1. *Maximum permitted limits for trace element inclusion in ruminants feed (MPL)* (European Commission 2015, 1999, 2014a, 2014b)

Element	**MPL based on mg/kg 88 % dry matter intake***
Copper	15
Cobalt	1
Selenium	0.5
Iodine	10

Companies supplying the European Union must abide by these regulations, therefore this was one of the major considerations when formulating and developing this product for the Industry Partner.

The majority of the competitors outlined (such as Agrimin™ and Animax™) incorporate their cobalt as cobalt carbonate, copper as copper oxide, iodine as calcium iodate and selenium as sodium selenate. These then appear to be pressed into a bolus before being encased in wax or resin-based coatings (Agrmin Limited, 2020). These coatings will then either degrade upon ingestion, or may be regurgitated once the minerals have been disintegrated. Incorporating these ingredients in this method raises two main issues: 1) the rate of mineral release is uncontrolled, relying on the abrasion of the bolus to release minerals which can be inconsistent; and 2) the copper and cobalt compounds incorporated to alleviate mineral deficiency have relatively poor bioavailability, due to their insolubility at the rumen pH (Lassiter and Bell, 1960; Kawashima, *et al.* 1997; Chapman and Bell, 1963).

As Cosecure™ boluses use phosphate-based glass as a delivery vehicle these elements are released in an ionic states, meaning they

are readily utilised by microbes, unlike their chelated counterparts such as copper oxide (Lassiter and Bell, 1960; Langlands *et al.* 1989; Kendall, Mackenzie, and Telfer, 2001).

Currently, Cosecure™ boluses appear to have the most consistent control over their degradation rate, however multiple publications trialling these boluses *in vivo*, (Black and French, 2004; Mackenzie, Moeini, and Telfer, 2001; Kendall, Mackenzie, and Telfer, 2001) recorded a bell-curve shape in the plasma mineral concentrations that suggested ion release is not consistent throughout the Cosecure™'s duration. Therefore, one of the desired characteristics of the glass developed here is to have a consistent ion release rate throughout the entire lifespan of the product.

Based on the recommended daily intake (National Research Council, 2001), and the current market competitors daily release rate (see Chapter 1, Table 1.4) the following ideal daily release rate (as seen in Table 3.2) were decided by the Industry Partner.

In an attempt to understand and stabilise ion release throughout the product's duration, coated prototypes would be trialled *in vitro* to determine ion release profiles.

Table 3.2*: Industry Partner's desired daily ion release rate (ppm/day).*

	Copper	**Cobalt**	**Selenium**	**Iodine**
Ideal daily ion release (ppm)	16	1.2	0.6	4.2

Therefore, this chapter outlines the phosphate-based glass formulation development, using a sintered bolus design in order to achieve the ideal daily release rates set by the Industry Partner (as highlighted in Table 3.2).

3.2 Materials and methodology

Table 3.3 outlined a list of materials used within this chapter, their particle sizes and manufacturers.

Table 3.3: *A list of materials, size particle sizes and manufacturer used within Chapter 3.*

Chemical	Particle size	Manufacturer
P_2O_5	< 100 µm	Fisher Scientific, UK
NaH_2PO_4	< 1 µm	Sigma Aldrich, UK
$CaHPO_4$	< 200 µm	Sigma Aldrich, UK
CuO (II) microparticle	< 44 µm	Aldrich, UK
CuO (II) nanoparticles	< 50 nm	Sigma-Aldrich, UK
$CoCO_3$	< 44 µm	Acros Organics, UK
Sodium selenate		Alfa Aesar, UK
Calcium iodate	< 44 µm	Sigma-Aldrich, UK
Acetic acid glacial	N/a	NORMAPUR, UK
$NaHCO_3$	< 100 nm	VWR Chemicals, UK
$NaHPO_4$	< 100 nm	VWR Chemicals, UK
NaCl	< 200 µm	VWR Chemicals, UK
KCl	< 200 µm	VWR Chemicals, UK
$CaCl_2$ anhydrous	< 100 nm	VWR Chemicals, UK
$MgCl_2$ anhydrous	< 100 nm	VWR Chemicals, UK

The schematic outlined in Figure 3.1 the processes and methods used in this section.

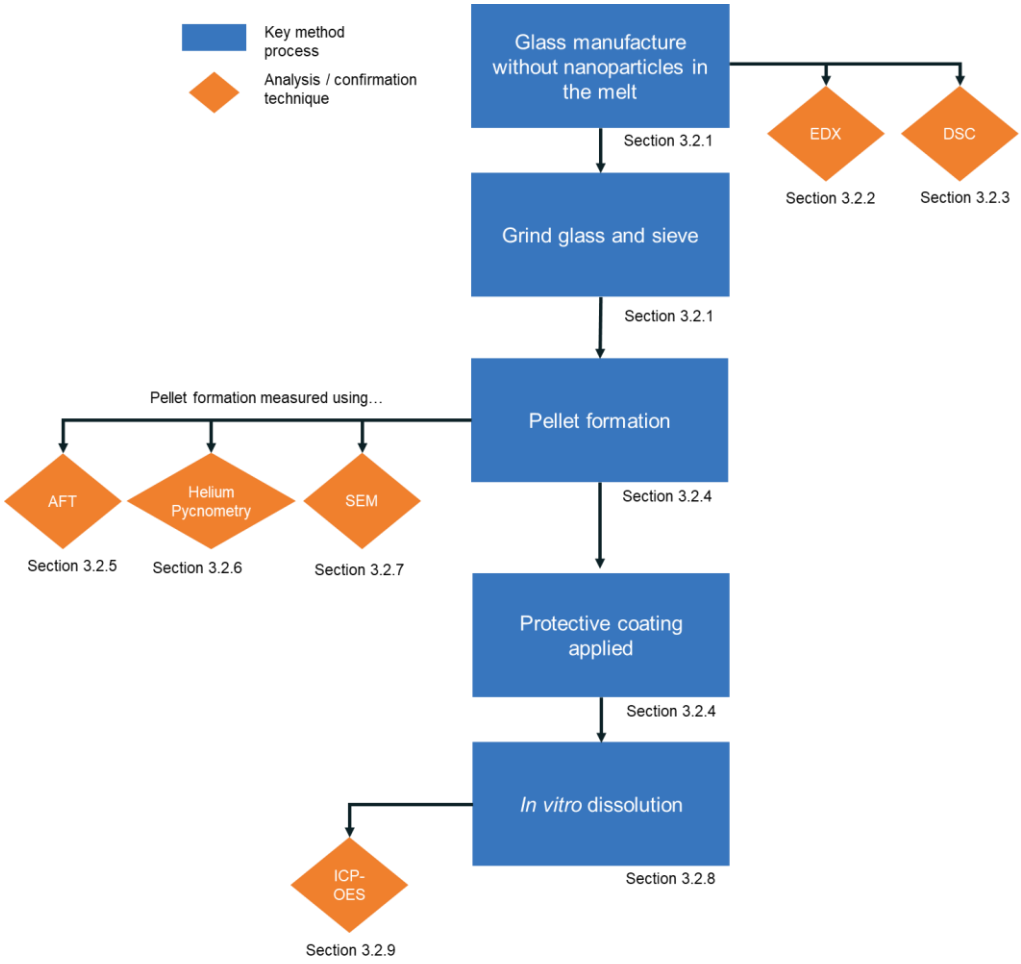

Figure 3.1: *A flow diagram to indicate the sequence of methods used in Chapter 3.*

3.2.1 Glass preparation

Glass compositions were prepared in batches of ~100g using the following precursors: P_2O_5 (Fisher, UK), NaH_2PO_4 (Sigma Aldrich, UK), $CaHPO_4$ (Sigma Aldrich, UK), CuO (Aldrich, UK), $CoCO_3$ (Acros Organics).

The precursors were weighed out, mixed and transferred into a 200 ml Pt/10 % Rh crucible (type 71040, Birmingham Metal Company, UK). The crucible was then placed in a furnace (Carbolite Gero, UK) at 350 °C for 30 minutes, before increasing up to 1150 °C for 60 minutes. The molten glass was poured onto a steel plate and left to cool to room temperature. Once cooled the glass was ground to the desired particle

size (specified in each section) using a planetary ball mill (Retsch, PM100) and separated using sieves specific to desired particle size.

The phosphate-based glass formulations outlined in Table 3.4 were devised using peer reviewed literature in Chapter 1, Section 1.3, and the results from the experimental work carried out in Chapter 2.

Table 3.4. *The glass formulations of the glasses produced and tested during Chapter 3.*

Glass formulations	Results page
P51-Ca25-Na22-1Co P52-Ca16-Na31-1Co P53-Ca26-Na19-1Co	97
P49-Ca26-Na24-Co1 P49-Ca26-Na24-Co1 plus CuNP	101
P50-Ca13-Na21-Cu15-Co1 plus additives P50-Ca9-Na16-Cu24-Co1 plus additives P50-Ca6-Na19-Co1 plus additives P50-Ca2-Na17-Cu30-Co1 plus additives	106
P48-Ca16-Na19-Cu16-Co1 plus additives	113

3.2.2 Differential scanning calorimetry (DSC)

See Chapter 2, Section 2.2.7 for methodology.

3.2.3 Energy dispersive x-ray (EDX)

See Chapter 2, Section 2.2.8 for methodology.

3.2.4 Pellet formation

Once glass compositions had been confirmed using EDX analysis, the ground glass was then mixed with additives such as copper oxide (II) NP (Sigma Aldrich, UK), sodium selenate (Alfa Aesar, UK), and calcium iodate (Sigma Aldrich, UK). Inclusion levels of each additives are disclosed in Table 3.4.

Table 3.4: *Additive inclusion level of copper oxide (II) NP, sodium selenate and calcium iodate for a 6-month sheep bolus prototype.*

Additive	Total inclusion required for bolus (g)	Inclusion level for 1g pellet
Copper oxide (II) NPs	3.605	0.141
Sodium selenate	0.444	0.017
Calcium iodate	1.161	0.045

Following the 10 mm machine pressed pellet method outlined in (Daley et al. 2019). 1 g of powdered glass (<150 µm) mixed with sodium selenate (98 %,Acros Organics, UK) and calcium iodate (> 99 % Alfa Aesar, UK) and copper oxide NP (30-50 nm particle size, Alfa Aesar, UK), hereafter referred to as “additives”. The specific inclusion rates of are outlined in each section. The glass and “additives” were pressed using a Specac die (10 mm) and an Instron Universal testing system 3360 Series using 34.47 MPa, with a hold time of 1 minute before releasing.

The pellets formed were then placed onto a steel plate and sintered using a ramp rate of 8 °C/minute up to 445 °C, holding for a duration of either 2, 4 or 8 hours, before cooling overnight to room temperature. Once cooled the pellets were dip coated following in molten refined carnauba wax (no. 1 yellow, Acros Organics, UK), heated to ~90 ^{o}C using a hotplate (IK3380000, IKA, USA). Pellets were completely submerged and removed (Araújo *et al.* 2015) and placed in a 40 ^{o}C oven for 1 hour before cooling to ambient room temperature overnight. After the pellets had dried, the bottom face of the pellet was polished using SiC paper, to completely remove any wax from the surface.

Compressed air was then used to clear any loose particles from the surface.

3.2.5 Ash fusion test (AFT)

Ash fusion testing was used to characterise the sintering temperature of the glass pellets. 10 mm pellets were made using ground glass (formulations and particle size ranges specified in each section) following the protocol used by Daley *et al.* (2019) using a pelleting pressure of 34.47 MPa (2707 N), held for 1 minute and then released. Pellets were then stored in desiccators to minimise moisture uptake.

Pellets were positioned on Carbolite Gero 25 mm x 25 mm recrystallized alumina ceramic tiles and placed into the furnace. The temperature of the furnace was increased from ambient room temperature (approximately 20 ºC) to 900 ºC at a rate of 7 ºC/minute under oxidising condition (air flowrate of 41/minute at 27.5 kPA (4 psi)).

Images were taken every 1 ºC using an integrated HD 1.3 Mb camera with an image size of 1280 x 1024 pixels. Coal Ash Fusion (CAF) Program software to measure and track pellet height during heating This software tracked height using a combination of edge detection and thresholding techniques to compare the initial height of the pellet to the relative height during heating (Daley, 2018).

Samples were run in triplicate using an average to generate the data displayed.

3.2.6 Helium pycnometry

Helium pycnometry was used to establish the density of the sintered pellets. A Micrometrics AccuPyc II 1340 gas pycnometer using helium as an inert gas was used in accordance with BS ISO 21687. Gas pycnometers use gas displacement to calculate the solid volume (V_s) of a porous material. The pycnometer was calibrated prior to each use using its internal calibration software and the AccuPyc calibration standard sphere (1 cm^3) (Micromeritics 2014).

All samples were stored in a desiccator at least 24 hours prior to testing. This ensures all moisture or volatile substance were removed from the pores.

3.2.7 Scanning electron microscopy

Glass discs from each composition were polished using SiC paper and diamond cloths using industrial methylated spirit (IMS) as lubricant. These samples were then dried and cleaned using compressed air and carbon coated using the Polaron, SC7640. Energy dispersive X-ray (EDX) analysis was conducted on the JEOL-6490LV SEM. The accelerating voltage was 20 kV, using a resolution of 55 eV, an analysis time of 120 seconds and a working distance of 10 mm. The standards used for analysis were albite for Na, GEO-MK2 apatite standard for P, Co metal for Co, Cu sulphide for Cu and wollastonite for Ca.

3.2.8 Dissolution studies

Degradation studies were conducted to assess the degradation and ion release rates of the different glass formulations. These experiments were conducted using a Cavela, 9ST (purchased from Total Laboratory Supplies, UK), see Figure 3.2, using artificial rumen fluid as dissolution media.

Following the ECow methodology (ECow, 2017), the salts outlined in Table 3.6 were weighed to 2 decimal places and emptied into a 1 L conical flask. Approximately 900 ml of deionised water (0.4 μΩ cm) was used to dissolve the salts. Working in a fume hood and slowly incorporating the acetic acid, the conical flask was then made up to 1 L liquid.

Figure 3.2: *An image of the dissolution apparatus used to conduct dissolution studies.*

Table 3.6*: The composition of the dissolution media used, "artificial rumen fluid" as outlined by the ECow methodology (ECow, 2017)*

Compound	**Quantity**	**Supplier**
Acetic acid glacial (99.8-100.5 %)	20 ml	NORMAPUR, UK
$NaHCO_3$ (99.7-100.3 %)	9.8 g	VWR Chemicals, UK
$NaHPO_4$ (>98 %)	9.3 g	VWR Chemicals, UK
NaCl (>98 %)	0.47 g	VWR Chemicals, UK
KCl (99-100.5 %)	0.57 g	VWR Chemicals, UK
$CaCl_2$ anhydrous (>94 %)	0.04 g	VWR Chemicals, UK
$MgCl_2$ anhydrous (>98 %)	0.06 g	VWR Chemicals, UK

Coated phosphate-based glass pellets were placed into air tight beakers containing 600 ml of 10 % artificial rumen fluid pH 5 (ECow, 2017) at 39 °C, with propellers rotating at a fixed speed of 20 RPM. Solution aliquots of 10 ml were taken over a 7-10 day periods (Table 3.7) outlines the sampling frequency for each experiment) to measure ion release, with no replenishing of media in during the experiment. These conditions aimed to mimic the rumen environment as closely as possible.

Table 3.7: *The sampling frequency of each dissolution experiments outlined in Chapter 3.*

Glass formulations	Sampling frequency	Figure	Page
P51-Ca25-Na22-1Co P52-Ca16-Na31-1Co P53-Ca26-Na19-1Co	Days 0, 1, 4, 10	Figure 3.9	100
P49-Ca26-Na24-Co1 P49-Ca26-Na24-Co1 plus CuNP	Days 0, 1, 4, 10	Figure 3.11	104
P50-Ca13-Na21-Cu15-Co1 plus additives P50-Ca9-Na16-Cu24-Co1 plus additives P50-Ca6-Na19-Co1 plus additives P50-Ca2-Na17-Cu30-Co1 plus additives	Days 0, 1, 2, 4, 7	Figure 3.13	110
P48-Ca16-Na19-Cu16-Co1 plus additives	Days 0, 1, 2, 4, 7, 10	Figure 3.15	116

3.2.9 Inductively coupled plasma optical emission spectrometry (ICP-OES).

For ion release analysis the ICP-OES (Optima 8000, Perkin-Elmer, UK) was used. This system allowed for the simultaneous detection of copper, cobalt and selenium. All results were calculated against a four-point calibration curve using a predefined calibration routine. Standards were prepared using 1000 ppm stock solutions of Cu, Co and Se (VWR Chemicals, UK) and diluted down to appropriate calibration range depending on the expected ion release values. For example, an ion release of 8 ppm, the calibration standards used would be 10 ppm, 5 ppm, 2.5 ppm and 1 ppm. WinLab Software (version 8) was used for data analysis.

3.2.10 Surface area estimation and extrapolation

The formula stated Equation 3.1 was used to calculate the estimated exposed surface area of the sintered pellets during dissolution.

Equation 3.1: *Surface area of a circle equation.*

$$surface\ area = \pi r^2$$

3.2.11 Statistical analysis

Mean values and standard deviation were compared for at least three replicate samples. Statistical analysis was carried out using Graphpad (Prism, version 7). Two-way analysis of variance (ANOVA) used to compare the significance of change in one factor over time. The error bars shown in the data represent standard error of mean unless stated otherwise.

3.3 Results

3.3.1 Establishing sintering parameters

EDX analysis was used to confirm the formulations produced were within the expected range due to volatility of some components during manufacture.

3.3.1.1 The effect of particle size on sintering parameters

3.3.1.1.1 Ash fusion test

Using an ash fusion furnace different particle size ranges (25-45 µm, 45-63 µm, 63-125 µm, 125-150 µm, 150-200 µm) were fired up to 900 ºC.

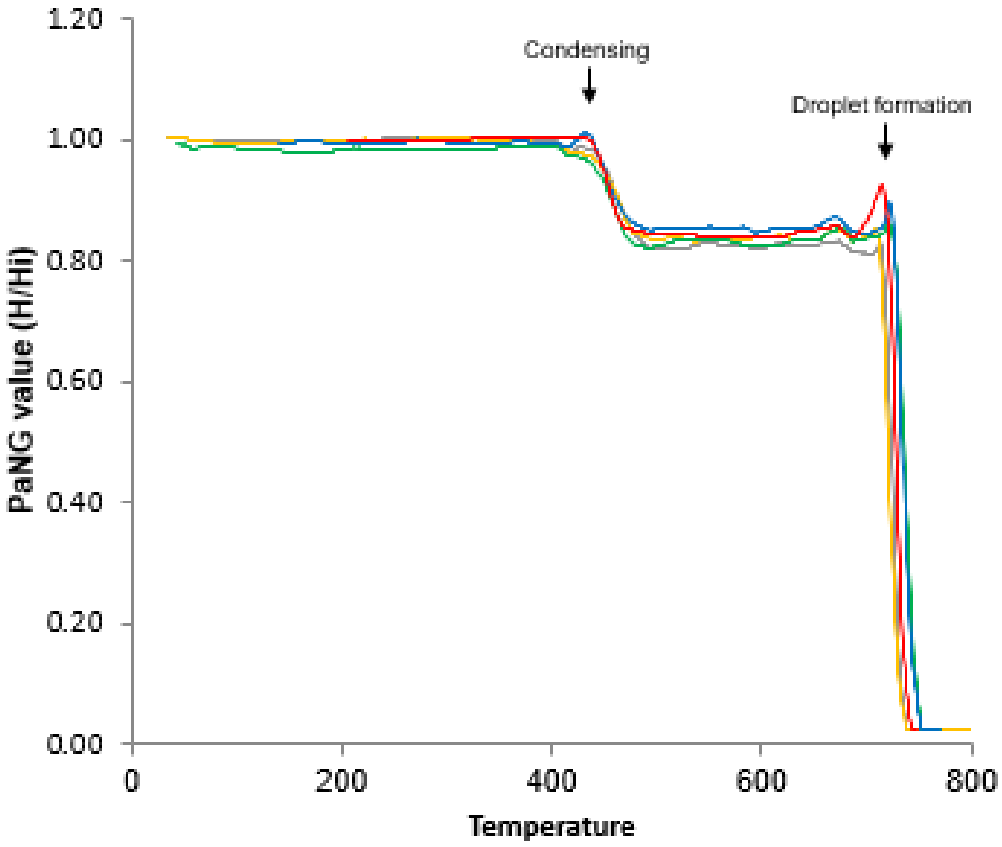

Figure 3.3: *The fluctuation of pellet height during heating < 900 ºC using AFT. The formulation of the glass pellets was P45-Ca30-Na15-Co10, particle size ranges: 25-45 µm (red line), 45-63 µm (blue line), 63-125 µm (green line), 125-150 µm (yellow line), 150-200 µm (grey line). For all particle size ranges n = 3.*

As can be seen in Figure 3.3, all the pellets decreased to approximately 85 % original of their original height around 450 ºC (Figure 3.4b). A peak was then seen at 724 ºC when a droplet shape was formed, which lead to a slight increase in height (Figure 3.4c) before melting (Figure 3.4d).

a)

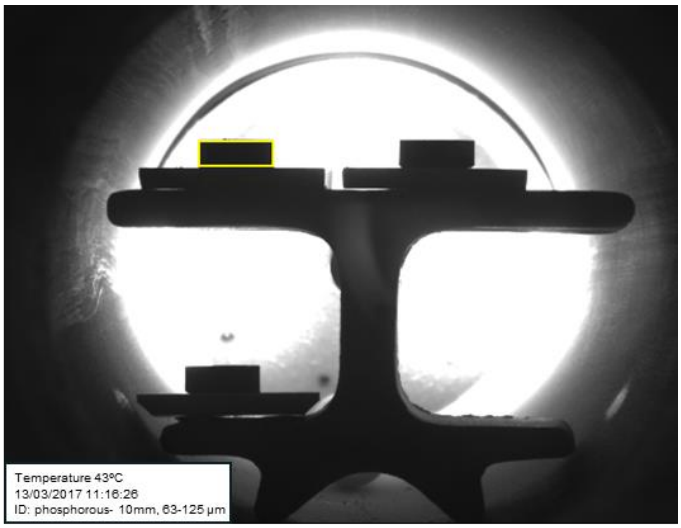
Temperature 43ºC
13/03/2017 11:16:26
ID: phosphorous- 10mm, 63-125 µm

b)

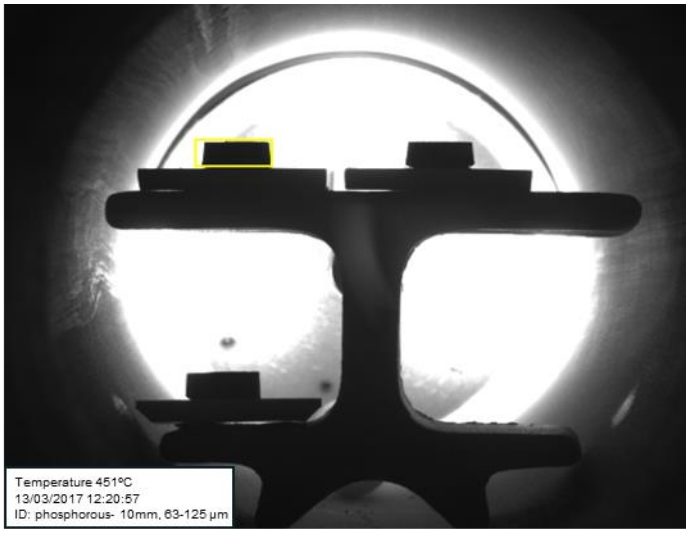
Temperature 451ºC
13/03/2017 12:20:57
ID: phosphorous- 10mm, 63-125 µm

c)

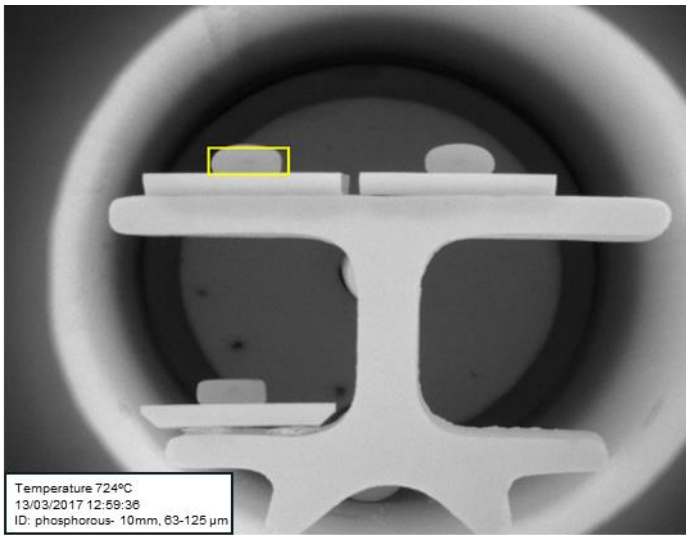

d)

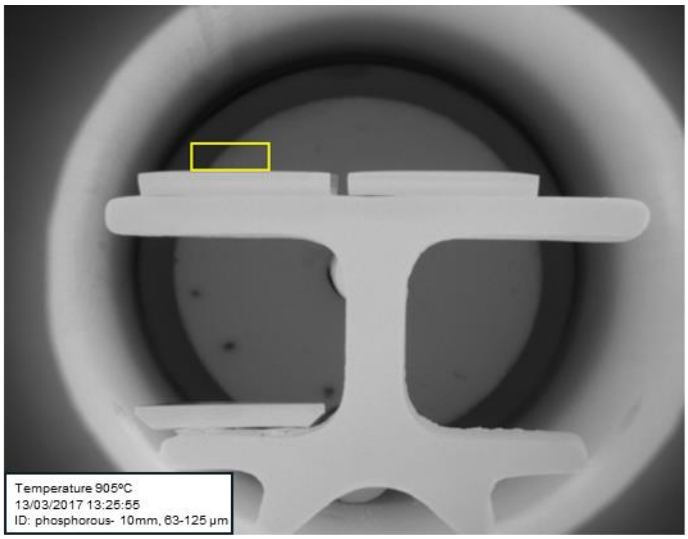

***Figures 3.4**: Images taken using the ash fusion furnace for P45-Ca30-Na15-Co10, particle size 63<125 µm to generate the green line recorded in the graph outlined in Figure 3.3. The yellow box outlines the shape of the pellet, this is box size and shape is kept constant throughout the images to demonstrate the shape change during whilst heating. a) shows the pellets at 43 ºC, this height acts as a baseline for the data analysis software (CAF), b) a reduction in the pellet size at 451 ºC, c) the pellet has melted to form a droplet at 724 ºC, d) complete melting of the pellet at the end of run at 905 ºC.*

3.3.1.1.2 Density using helium pycnometry

Table 3.8: *Density of the particle size fractioned P45-Ca30-Na15-Co10 sintered pellets shown in Figures 3.4.*

Particle size fraction (µm)	**Weight (g)**	**Average Density (g/cm^3)**	**Standard Deviation**
25-45	1.962	1.613	0.0013
45-63	1.974	1.610	0.0021
63-125	1.989	1.615	0.0024
125-150	1.968	1.619	0.0025
150-200	1.942	1.611	0.0014

No significant difference between the densities of the different particle size ranges of the sintered pellets were identified.

3.3.1.1.3 Scanning Electron Microscope

The images Figure 3.5a-f showed the difference in topography of the different particle size range pellets. Particle size ranges 25-45 µm (Figure 3.5a) 45-63 µm (Figure 3.5b) were significantly more compacted together than the larger particle size ranges 63-125 µm (Figure 3.5c), 125-150 µm (Figure 3.5d), and 150-200 µm (Figure 3.5e). A side-by-side comparison of the pellets from particle size ranges 25-45 µm versus 150-200 µm is visible in Figure 3.5f. Working at a smaller particle size range appeared to result in fewer pores present in the pellet.

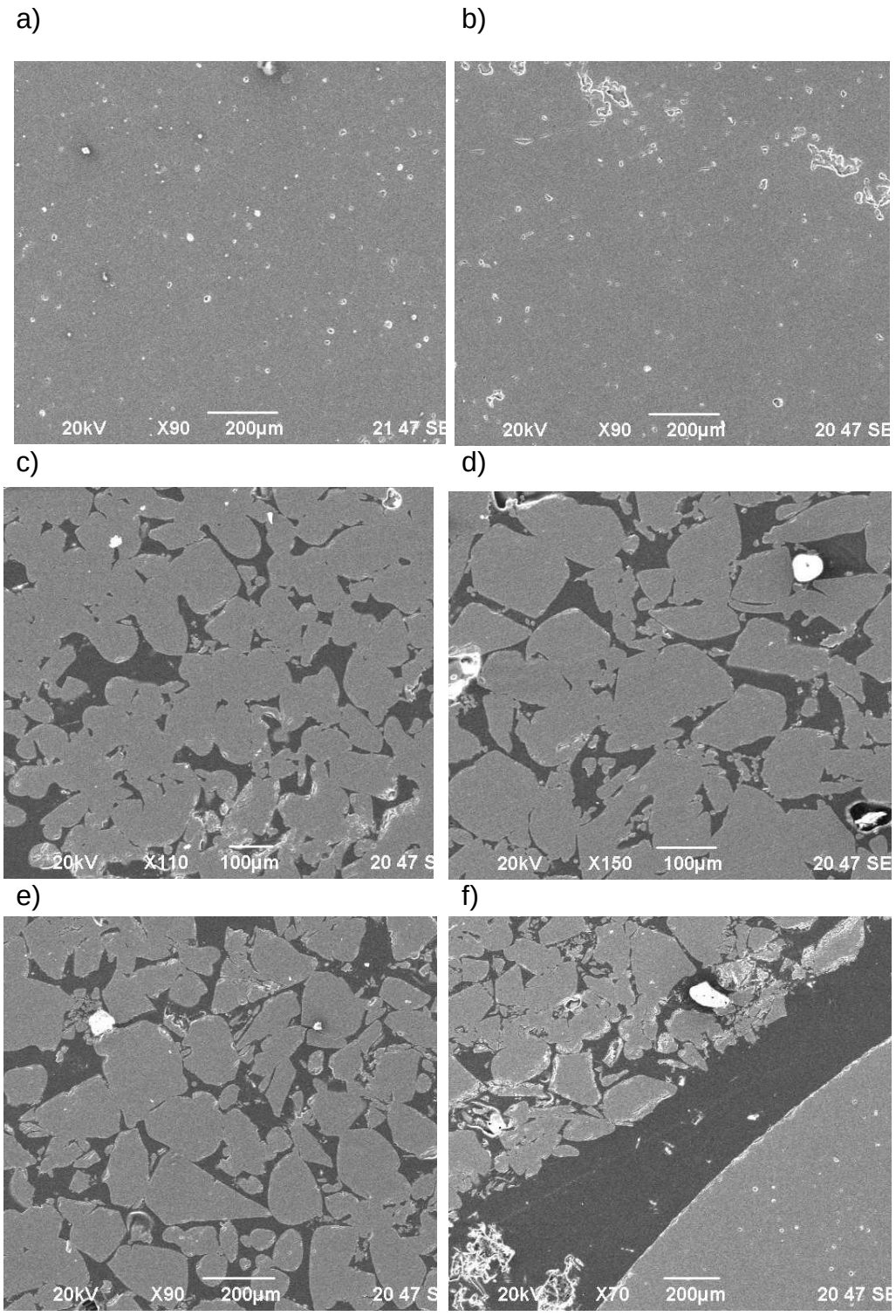

Figure 3.5: *The topography of the sintered pellets comprised of different particle size ranges P45-Ca30-Na15-Co10. Image a) 25-45 µm, b) 45-63 µm, c) 63-125 µm d) 125-150 µm, e) 150-200 µm, f) 25-45 µm versus 150-200 µm.*

3.3.1.2 Sintering Temperature

3.3.1.2.1 Differential Scanning Calorimetry (DSC)

Four key thermal parameters were identified using DSC analyses in Figure 3.6. These were glass transition (T_g), crystallization onset and peak (T_c) and melt (T_m) temperatures. The processing window (T_c-T_m) is also outlined in Table 3.9.

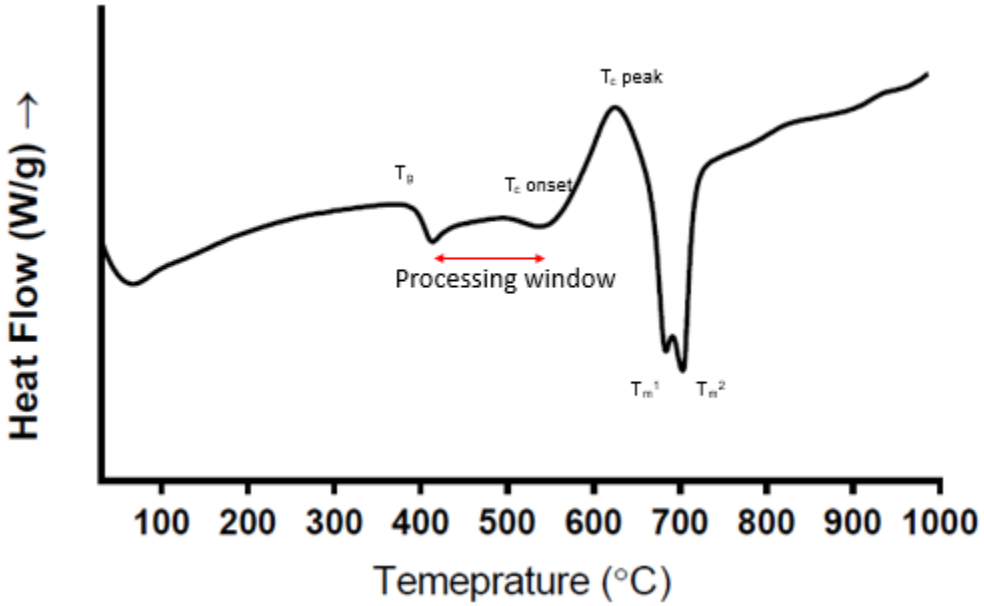

Figure 3.6: *DSC profile for the glass P45-Ca30-Na15-Co10. Labelled: transition temperature as T_g; crystallization temperature as T_c; melt temperature as T_m; and the processing window (defined as T_c- T_g), using a heating rate of 20 ºC/minute.*

Table 3.9: *Thermal properties (T_g, T_c onset and peak, and T_m) of the glass P45-Ca30-Na15-Co10 using DSC.*

	T_g (°C)	**T_c onset (°C)**	**T_c peak (°C)**	**T_m 1 (°C)**	**T_m 2 (°C)**	**Processing Window (T_c- T_g)**
P45-Ca30-Na15-Co10	374	495	625	683	703	121

3.3.1.3 Hold time

The effect of hold time duration on pellet structure was assessed using a scanning electron microscope (JEOL-6490) to show the microstructure, and helium pycnometry to establish pellet density. Despite it not being evident in the SEM images, all glass pellets changed from a light purple/blue colour before sintering to a pale pink after sintering.

3.3.1.3.1 Helium Pycnometery

Table 3.10 showed the density (measured using a helium pycnometer) of the P45-Ca30-Na15-Co10 pellets sintered using a hold time of either 2, 4 or 8 hours. These were compared against the density of the CoseIcure™ product. Despite appearing less porous in the SEM images, CoseIcure recorded a lower average density than all of the sintered pellets.

Table 3.10: *The density of P45-Ca30-Na15-Co10 pellets sintered for different durations, compared against CoseIcure™*

Sample	**Weight (g)**	**Average Density (g/cm^3)**	**Standard Deviation**
CoseIcure™	1.676	2.59913	0.006427
2 Hour	1.2483	2.94672	0.005843
4 Hour	1.2591	2.85975	0.012246
8 Hour	1.2523	2.93399	0.017377

3.3.1.3.2 Scanning Electron Microscope

The SEM images shown in Figures 3.7a-e show the cross-sectional analysis of the centre of sintered P45-Ca30-Na15-Co10 pellets after different sintering durations. The pellets sintered for 2-hours displayed a

higher frequency of more defined, separate particles that were densely packed. Whereas, the 4-hour sintered pellets displayed less distinct particle outlines that have agglomerated to form large bodies of particles. The 8-hour sinter showed contrasting results depending on whether the inner or out section was reviewed. The inner section appeared to show more distinct, larger particles, similar to the 2-hour sinter, whereas the outer image of the 8-hour sinter appeared more agglomerated like the 4-hour sinter. CoseIcure had much fewer pores present, with individual particles not distinguishable.

a) 2 Hour

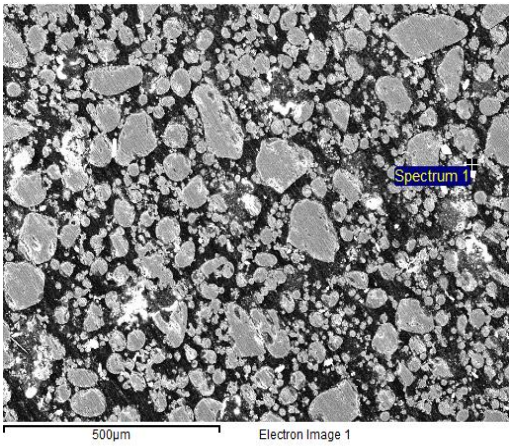

b) 4 Hour

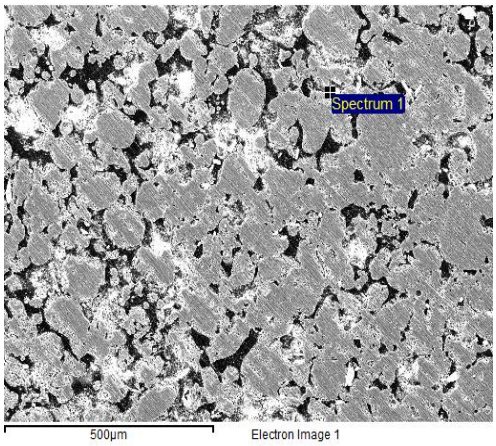

c) 8 Hour (inner section)

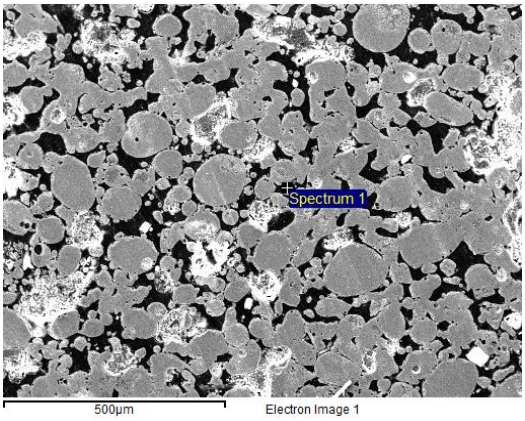

d) 8 Hour (outer section)

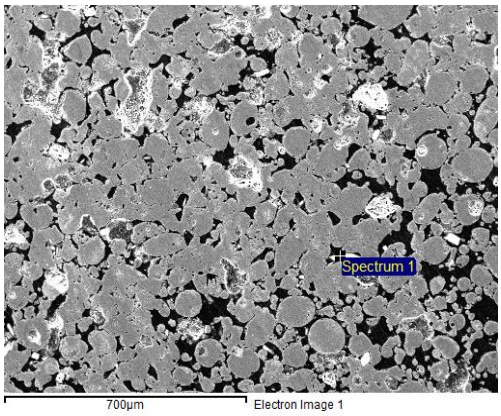

e) CoseIcure ™ sample

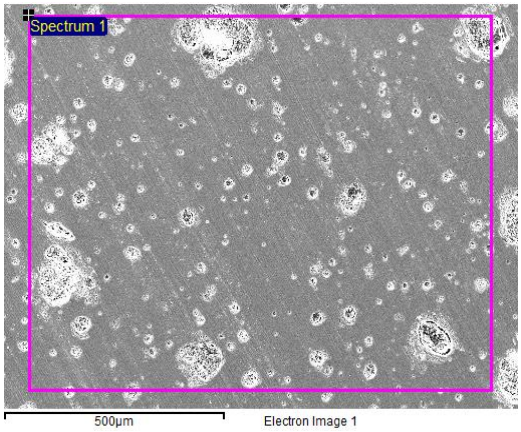

Figure 3.7: *SEM images a-d showing the effect of hold time during sintering of P45-Ca30-Na15-Co10 glass, particle size range < 150 µm at 450 ºC. Image a) 2 hour hold time (inner), b) 4 hour hold time (inner section), c) 8 hour hold time (inner section), d) 8 hour hold time (outer section), compared against e) CoseIcure™ sample.*

3.3.2 The effect of changing calcium and sodium content on ion release

Sections 3.3.2.2 and 3.3.2.3 discussed the effects of changing calcium and sodium content on the thermal properties and ion release profiles of glasses.

3.3.2.1 EDX Analysis

EDX analyses confirmed all the final glass compositions of the samples investigated. Figure 3.5 showed there was little to no difference to the effect of density by working at a lower particle size

Table 3.11: *The EDX analysis of the glasses P51-Ca25-Na22-Co1, P52-Ca16-Na31-Co1 and P53-Ca26-Na19-Co1 used in this section (mol%).*

Sample Code	P_2O_5	CaO	Na_2O	CoO
P51-Ca25-Na22-Co1	51.16	25.77	22.1	0.95
P52-Ca16-Na31-Co1	52.16	16.04	31.05	0.7
P53-Ca26-Na19-Co1	53.0	26.33	19.87	0.84

3.3.2.2 Differential Scanning Calorimetry

The DSC analysis showed (Figure 3.8) that P51-Ca25-Na22-Co1 had by far the largest processing window 108 ºC, compared to 43 ºC and 57 ºC for glass codes P52-Ca16-Na31-Co1 and P53-Ca26-Na19-Co1 respectively. The increased processing window was caused by a reduced T_g (368 ºC) and delayed onset of crystallization (476 ºC) compared to the other glasses. All glasses had broad melt peaks,

however, P52-Ca16-Na31-Co1 had two melt peaks, T_m^1 at 718 ºC and T_m^2 at 754 ºC.

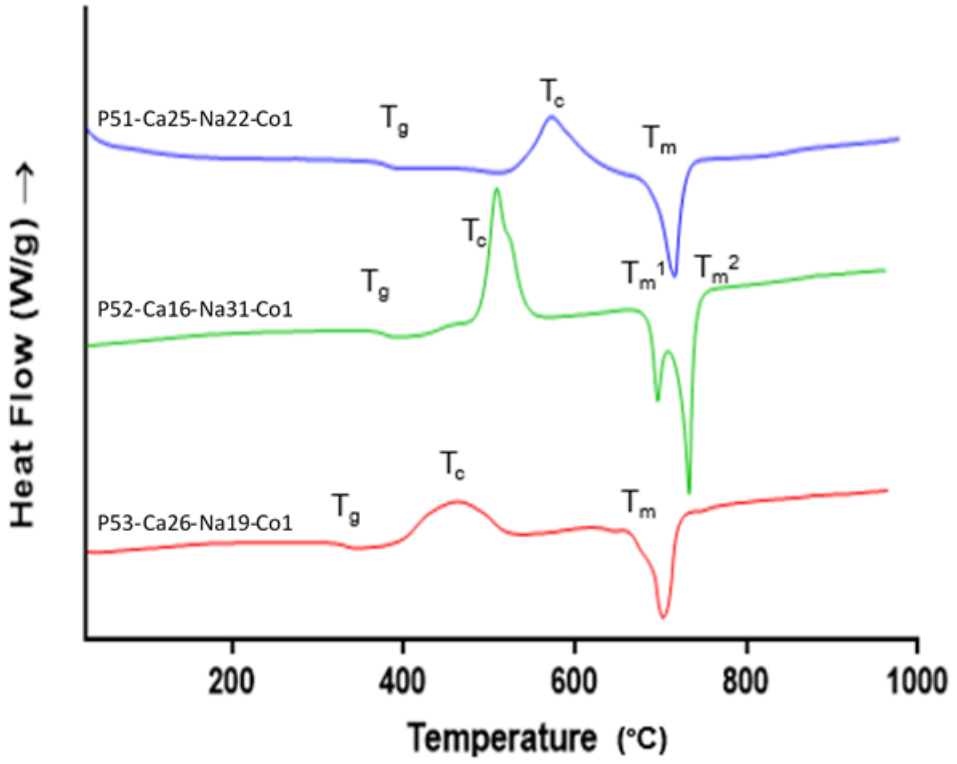

Figure 3.8: *DSC profile of glasses P52-Ca16-Na31-Co1 (blue line), P53-Ca26-Na19-Co1 (green line) and P51-Ca25-Na22-Co1 (red line). Key thermal parameters such as glass transition (T_g), crystallization (T_c) and melt (T_m) temperatures are labelled on the graph, using a heating rate of 20 ºC/minute up to 1000 ºC.*

Table 3.12: *Thermal properties of the glasses P51-Ca25-Na22-Co1, P52-Ca16-Na31-Co1, P53-Ca26-Na19-Co1 identified using DSC.*

	T_g (°C)	**T_c onset (°C)**	**T_c peak (°C)**	**T_m 1 (°C)**	**T_m 2 (°C)**	**Processing Window (T_c- T_g)**
P51-Ca25-Na22-Co1	368	476	582	721	-	108
P52-Ca16-Na31-Co1	333	376	485	734	-	43
P53-Ca26-Na19-Co1	384	441	535	718	754	57

3.3.2.3 Ion Release Profiles

Copper, cobalt and selenium ion release data is presented in Figures 3.9a-c. No significant difference was observed for copper or selenium ion release for the three different formulations. However, a significant difference ($p < 0.05$) in cobalt ion concentration was recorded at day 10 for formulation P53-Ca26-Na19-Co1 compared to both P51-Ca25-Na22-Co1 and P52-Ca16-Na31-Co1. The ideal daily release rate was based on the Industrial Partners product specification (see Chapter 2, Table 2.1).

a)

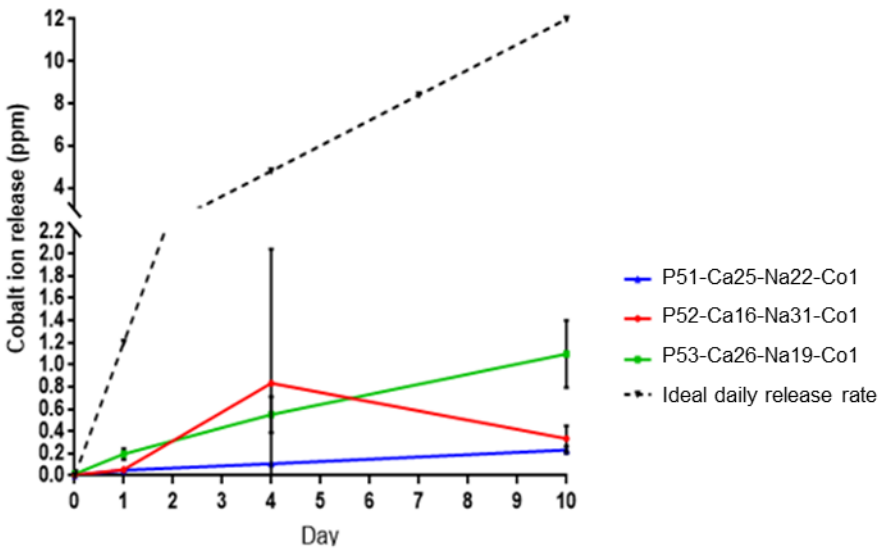

b)

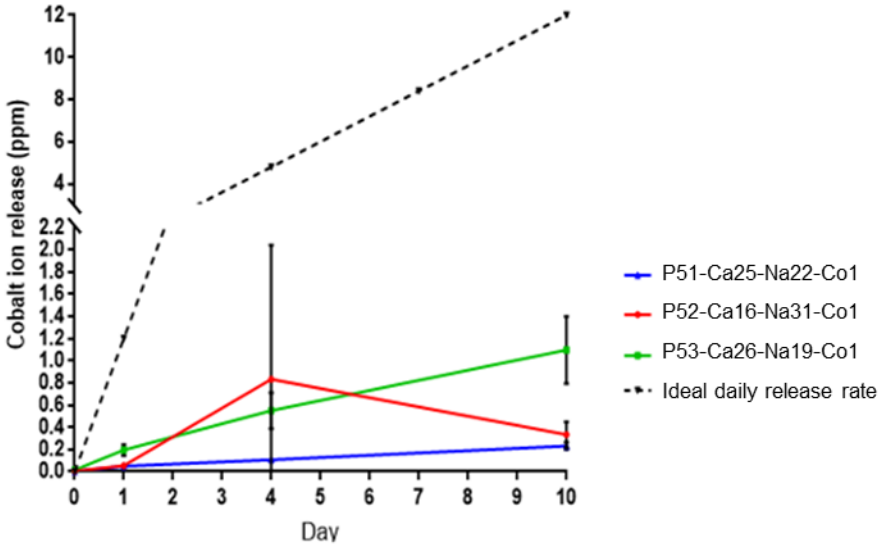

c)

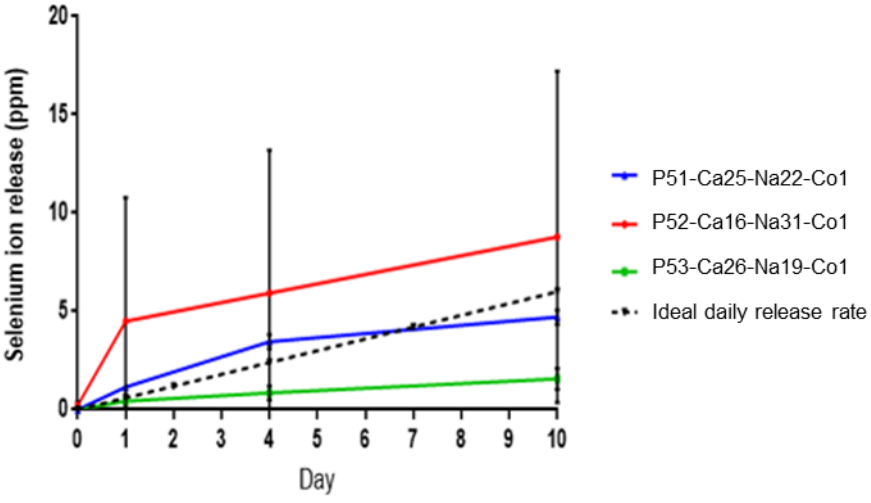

Figures 3.9. *Cumulative concentration of ion release during dissolution testing, measured using ICP-OES for the formulations used in Table 3.9*

a) copper, b) cobalt, c) selenium, investigated in artificial rumen fluid at 39 °C, over a 10-day period (n=3 for each glass formulation).

3.3.1.3 The effect of excluding CuO (II) nanoparticles from the sintered pellets on ion release

As demonstrated via dissolution experiments in Section 3.3.2 (Figures 3.9a and b) the ion release profiles of copper and cobalt were below the desired product specification set by the industry partner (see Table 3.2 for desired daily ion release). This brought into question whether the presence of CuNP were affecting the dissolution properties of the pellets, causing a reduction in degradation rates compared to what was wanted. This section aimed to identify whether the incorporation of NP into the sintered pellets had any effect on the overall ion release of the elements from the pellet.

3.3.1.3.1 EDX Analysis

Table 3.13 displayed the EDX analysis for the glass code P49-Ca26-Na24-Co1 to ensure these separately prepared glasses were within acceptable error limits of each other.

Table 3.13: *EDX analysis of glass compositions P49-Ca26-Na24-Co1 (no additives) and P49-Ca26-Na24-Co1 (plus additives), confirmed using EDX analysis (mol%). "Plus additives" indicates the inclusion of additives sodium selenate, calcium iodate and copper oxide NP for specific details on "additives" refer back to Section 3.2.4, Table 3.5.*

Sample Code	**P_2O_5**	**CaO**	**Na_2O**	**CoO**
P49-Ca26-Na24-Co1 (no additives)	49.0	25.68	24.56	0.74
P49-Ca26-Na24-Co1 (plus additives)	49.54	26.02	23.68	1.0

3.3.1.3.2 Differential Scanning Calorimetry

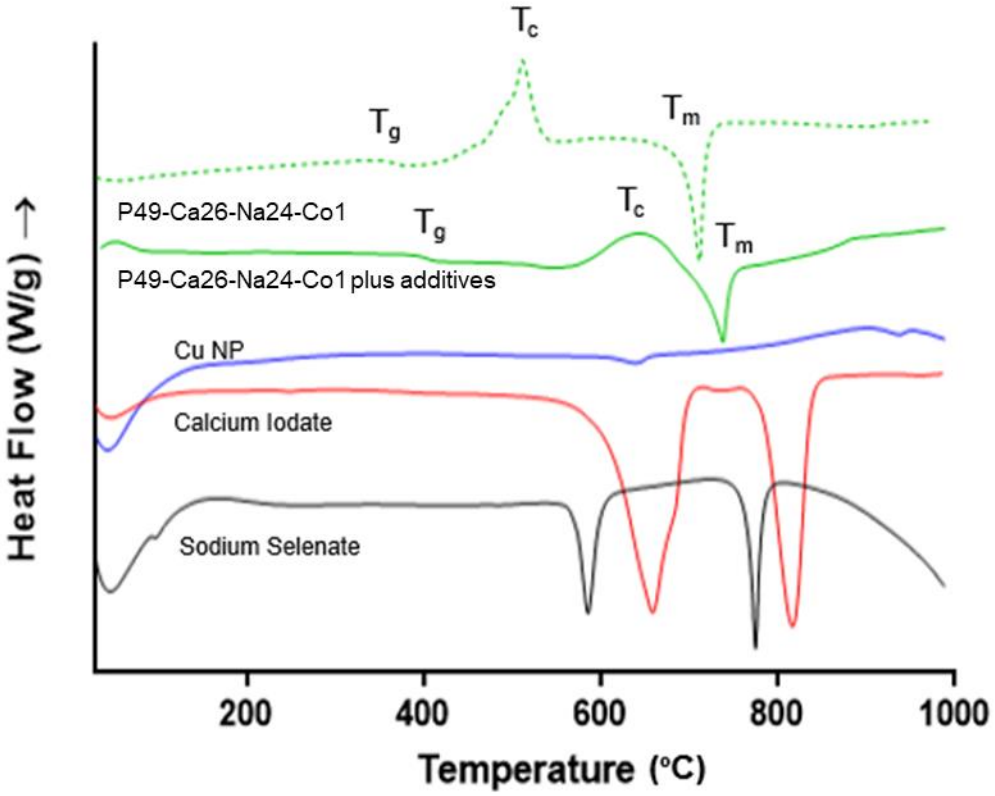

Figure 3.10: *DSC profile for the glass P49-Ca26-Na24-Co1 with the inclusion of sodium selenate, calcium iodate and copper oxide (II) nanoparticles (solid green line), and the glass with additives except the nanoparticles (broken green line).*
The independent profiles for the additives were also analysed: sodium selenate (black line), calcium iodate (red line) and copper oxide (II) nanoparticles (blue line).

Table 3.14: *The thermal properties of the glasses P49-Ca26-Na24-Co1 with and without additives. "Plus additives" indicates the inclusion of additives sodium selenate, calcium iodate and copper oxide NP for specific details on "additives" refer back to Section 3.2.4, Table 3.5.*

	T_g (°C)	**T_c onset (°C)**	**T_c peak (°C)**	**T_m (°C)**	**Processing Window (T_c- T_g)**
P49-Ca26-Na24-Co1 (no additives)	370	417	530	727	47
P49-Ca26-Na24-Co1 (plus additives)	366	483	629	723	117

The incorporation of additives seemed to significantly increase the processing window of the glass from 47 ºC to 117 ºC, which appeared to be caused by a delayed onset of crystallization temperature from 417 ºC to 483 ºC.

3.3.1.3.3 Ion Release P49-Ca26-Na24 with and without the addition of CuO (II) nanoparticles

This dissolution experiment was conducted over a 10-day period under the same conditions as the experiment in Section 3.2.8.

a)

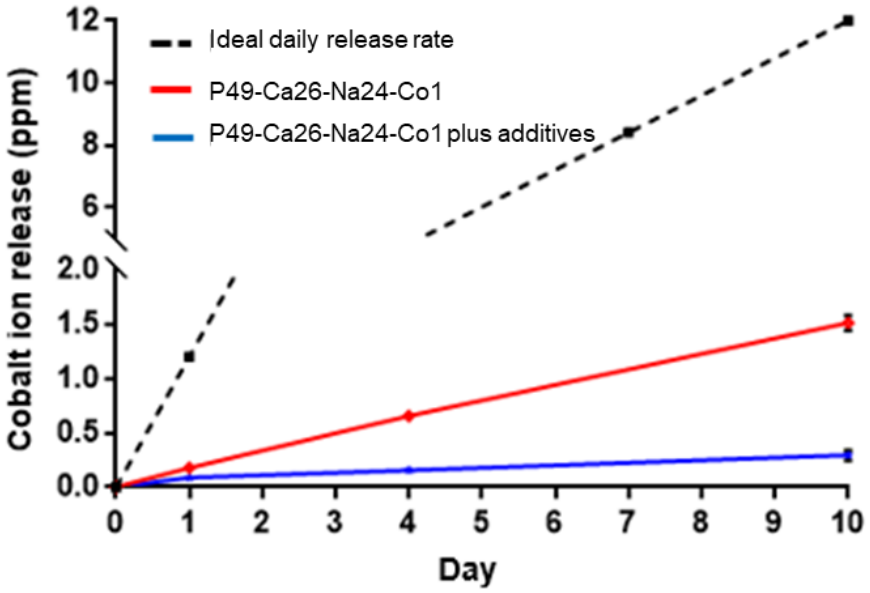

b)

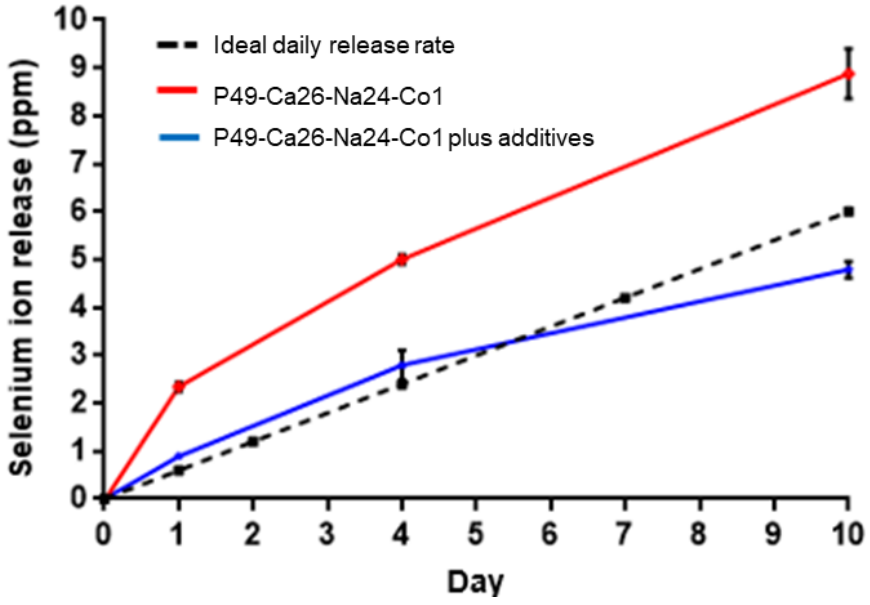

Figures 3.11: *The cumilative ion release of glass formulation P49-Ca26-Na24-Co1 with and without the addition of CuO (II) nanoparticles during dissolution experimentation. A) cobalt ion release; b) selenium ion release, measured using ICP-OES (n=3 for each glass formulation).*

Using a 2-way ANOVA to compare against both data sets, the incorporation of the CuO (II) NP resulted in a significant ($p < 0.001$) reduction in ion release of both cobalt and selenium across all data points from the glass including copper oxide (II) NP compared to the glass not containing NPs. Copper ion release was not measured for this data set due to the exclusion of copper from P49-Ca26-Na24-Co1 (no additives).

3.3.1.4 The effect of incorporating CuO (II) into the glass versus incorporating as nanoparticles

As a result of the dissolution studies conducted in Sections 3.3.1.2 and 3.3.1.3, two key factors were identified: the glass formulations outlined in these sections had a significantly lower daily ion release than the product specification required; and that the addition of copper oxide (II) NP may have reduced the overall ion release rate of the pellets. Therefore, this section assessed how the gradual incorporation of copper into the glass matrix may have affected ion release, and the ion release recorded when copper oxide (II) was incorporated as both glass and NPs.

Throughout this section all glass formulations include additives sodium selenate and calcium iodate, in quantities outlined in Section 3.2.4, Table 3.5. However, copper oxide content varies depending on the specified glass formulation outlined in Table 3.15 and Table 3.16.

3.3.1.4.1 EDX Analysis

Table 3.15: *The EDX analysis of the glass* P50-Ca13-Na21-Cu15-Co1*,* P50-Ca9-Na16-Cu24-Co1*,* P50-Ca6-Na19-Cu24-Co1 *and P50-Ca2-Na17-Cu30-Co1 (mol%)*

Sample Code	P2O5	CaO	Na2O	CuO	CoO
P50-Ca13-Na21-Cu15-Co1	52.8	13.7	17.75	15.0	0.74
P50-Ca9-Na16-Cu24-Co1	50.37	8.6	16.15	23.92	0.66
P50-Ca6-Na19-Cu24-Co1	50.48	5.82	18.9	24.23	0.58
P50-Ca2-Na17-Cu30-Co1	52.7	1.9	14.5	30.3	0.6

Table 3.16: *The pellet additive inclusion level based on the differing level of copper incorporated into the glass*

Mol% of copper in the glass	Percentage of copper incorporated as nanoparticles (%)	Mass of copper oxide nanoparticles added to glass (g)
15	50	0.0705
24	20	0.0282
30	0	0

3.3.1.4.2 Differential Scanning Calorimetry

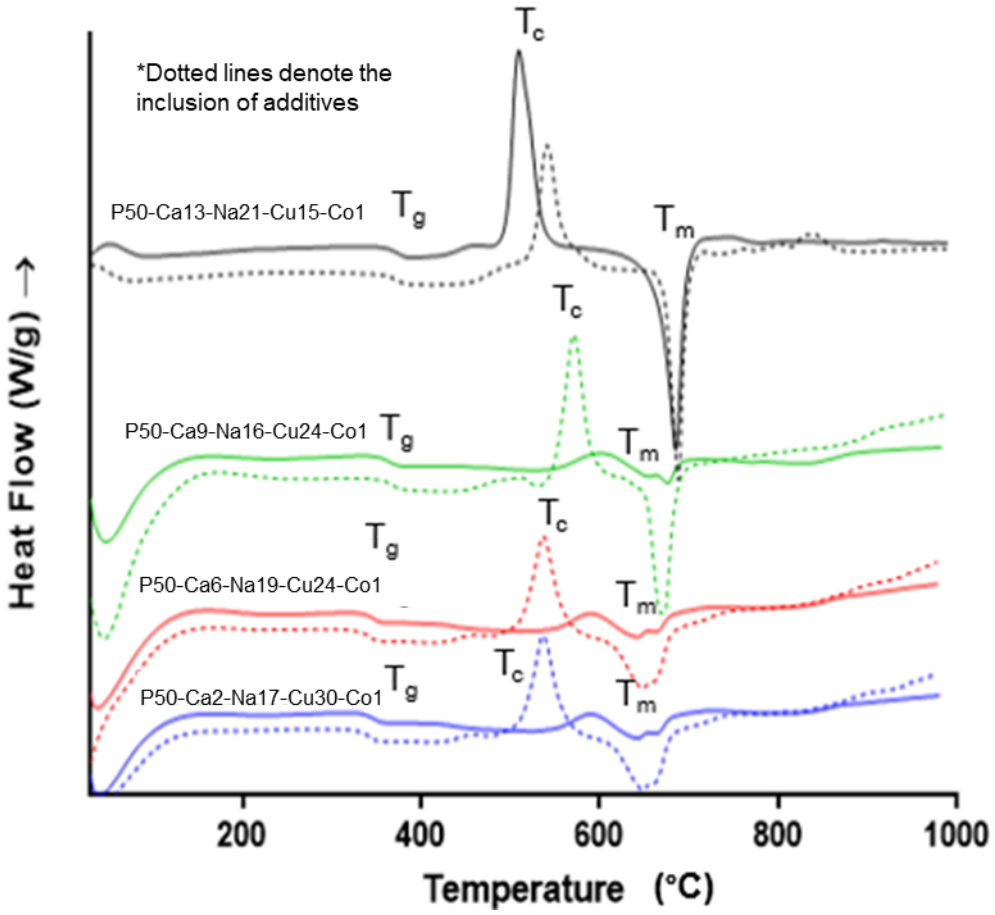

Figure 3.12: *DSC profile of glasses P50-Ca13-Na21-Cu15-Co1 (black), P50-Ca6-Na19-Cu24-Co1 (red), P50-Ca9-Na16-Cu24-Co1 (green) and P50-Ca2-Na17-Cu30-Co1 (blue). Formulations that contained just glass are solid, formulations that contained "additives", the sodium selenate, calcium iodate and copper oxide (II) nanoparticles are the broken lines.*

Table 3.17: *Thermal properties of the glasses* P50-Ca13-Na21-Cu15-Co1, P50-Ca9-Na16-Cu24-Co1, P50-Ca6-Na19-Cu24-Co1, *P50-Ca2-Na17-Cu30-Co1 (shown in Figure 3.12). The addition of "plus additives" indicates whether the glass was analysed with the inclusion of additives.*

	T_g (°C)	**T_c onset (°C)**	**T_c peak (°C)**	**T_m 1 (°C)**	**T_m 2 (°C)**	**Processing Window (T_c- T_g)**
P50-Ca13-Na21-Cu15-Co1	347	411	500	669	-	63
P50-Ca13-Na21-Cu15-Co1 plus additives	339	435	533	676	-	95
P50-Ca9-Na16-Cu24-Co1	350	566	603	658	680	216
P50-Ca9-Na16-Cu24-Co1 plus additives	353	513	625	664	-	159
P50-Ca6-Na19-Cu24-Co1	330	535	598	649	672	204
P50-Ca6-Na19-Cu24-Co1 plus additives	322	425	547	656	-	103
P50-Ca2-Na17-Cu30-Co1	337	409	511	621	683	71
P50-Ca2-Na17-Cu30-Co1 plus additives	351	429	534	642	-	78

No significant changes in glass transition temperatures were recorded between the pure glasses and glasses with the additions of sodium selenate, calcium iodate and copper oxide (II) NPs. P50-Ca9-Na16-Cu24-Co1 and P50-Ca6-Na19-Cu24-Co1 both recorded a significant decrease in the processing window duration with the addition of the additives. P50-Ca9-Na16-Cu24-Co1's processing window was reduced from 216 ºC to 159 ºC, a difference of 52 ºC, and P50-Ca6-Na19-Cu24-Co1's processing window was reduced from 204 ºC to 103 ºC, a difference of 109 ºC.

All sintered pellets containing additives (except P50-Ca13-Na21-Cu15-Co1) revealed a decrease in their glass crystallization peak, with the average shift being 25 ºC. Additional observations are outlined in the bullet points below.

- Two melt peaks were observed for glasses P50-Ca9-Na16-Cu24-Co1, P50-Ca6-Na19-Cu24-Co1 and P50-Ca2-Na17-Cu30-Co1. However once the sodium selenate, calcium iodate and copper oxide (II) particles were added, the two peaks became one broader peak.
- P50-Ca9-Na16-Cu24-Co1initial melt peak was delayed with the inclusion of additives from 658 ºC to 664 ºC, an increase of 6 ºC.
- P50-Ca6-Na19-Cu24-Co1 initial melt peak was delayed with the inclusion of additives from 649 ºC to 656 ºC, an increase of 7 ºC.
- P50-Ca2-Na17-Cu30-Co1initial melt peak was delayed with the inclusion of additives from 621 ºC to 642 ºC, an increase of 21 ºC.

3.3.1.4.3 Ion Release

a)

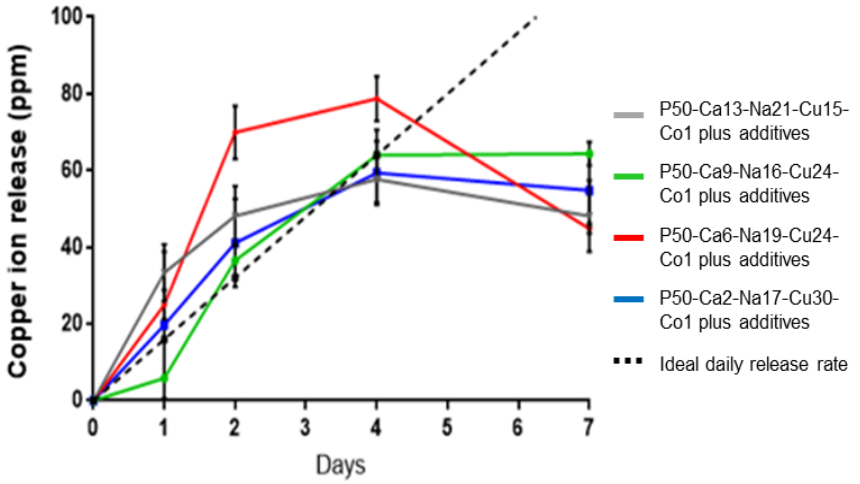

b)

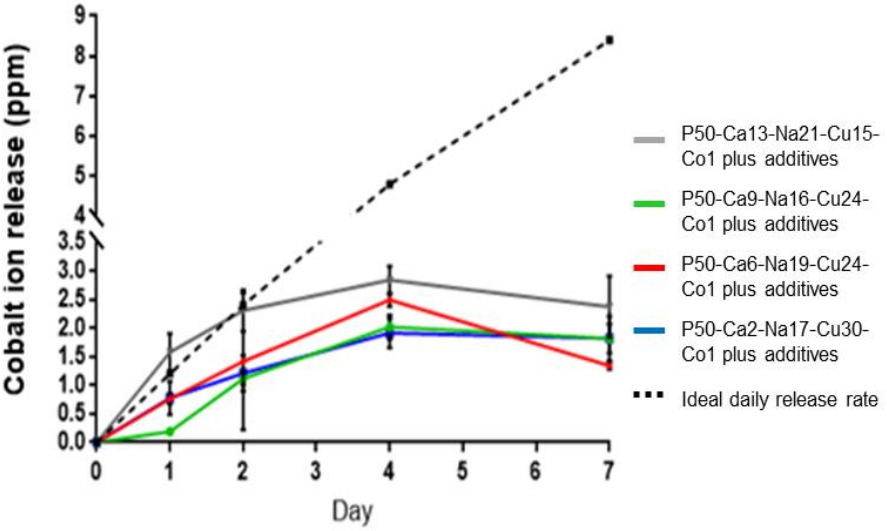

c)

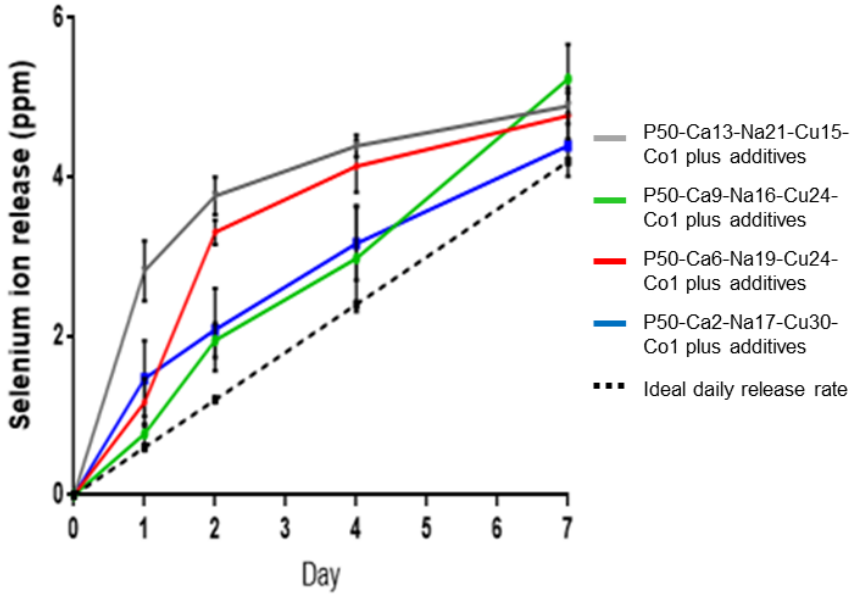

Figure 3.13: *The cumilative ion release during dissolution studies of glasses P50-Ca13-Na21-Cu15-Co1 (grey line), P50-Ca9-Na16-Cu24-Co1 (green line), P50-Ca6-Na19-Cu24-Co1 (red line), P50-Ca2-Na17-Cu30-Co1 (blue line), and ideal daily ion release rate (broken black line) (n=3 for each glass formulation). Graph a) shows copper, b) cobalt and c) selenium.*

The following observbations were derived from the data presented in Figures 3.13a-c:

Copper: A significant increase in copper release was recorded at days-2 ($p < 0.001$) and 4 ($p < 0.01$) for formulation *P50-Ca6-Na19-Cu24-Co1* compared to all other formulations (see Figure 3.13a). However, unlike all other formulations that revealed a plateau in copper ion concentration from day-4 to 7, formulation *P50-Ca6-Na19-Cu24-Co1* revealed a decrease in the cumulative copper ion concentration in the media solution between days-4 and 7.

Cobalt: Figure 3.13b showed a significant increase in cobalt ion release was recorded for formulation *P50-Ca13-Na21-Cu15-Co1* against all other formulations on days-1 ($p < 0.05$) and 2 ($p < 0.05$). On day-4, *P50-Ca13-Na21-Cu15-Co1's* cobalt ion release was still significantly higher ($p < 0.05$) than *P50-Ca6-Na19-Cu24-Co1* and *P50-Ca2-Na17-Cu30-Co1*. However, likewise, to the drop off in cumulative copper ion concentration recorded for *P50-Ca6-Na19-Cu24-Co1*, *P50-Ca13-Na21-Cu15-Co1* also revealed a decrease in cobalt concentration at day-7.

Selenium: Similarly to the results observed in the cobalt graph (Figure 3.13b), Figure 3.12c showed that *P50-Ca13-Na21-Cu15-Co1* also released significantly higher ($p < 0.0001$) selenium concentrations on day-1 compared to all other formulations. However, on day 2 *P50-Ca6-Na19-Cu24-Co1* showed a significantly higher ($p < 0.0001$) cumulative selenium concentration compared *P50-Ca2-Na17-Cu30-Co1* and *P50-Ca6-Na19-Cu24-Co1*. Whilst the results still showed significance on

day-4 for formulations *P50-Ca13-Na21-Cu15-Co1* and *P50-Ca6-Na19-Cu24-Co1* compared to the other two formulations, the rate of the ion concentration from formulations *P50-Ca9-Na16-Cu24-Co1* and *P50-Ca2-Na17-Cu30-Co1* was higher between days-4 and 7 compared to *P50-Ca9-Na16-Cu24-Co1* and *P50-Ca2-Na17-Cu30-Co1*. As a result of this no significance was recorded at day-7.

3.3.1.5 The effect of sample diameter increase on ion release profiles

The *in vitro* ion release work, shown in Section 3.3.2, Figures 3.9, 3.11 and 3.13 was determined during dissolution studies using pellets with a diameter of 10 mm, due to equipment availability at the time. However, as the end product was intended to have a diameter of 15 mm, for technical reasons outlined in Chapter 1, the formulations were remade and analysed. It was important to establish whether the data recorded from 10 mm diameter pellets was able to be extrapolated to predict the ion release of 15 mm pellets. The experiment outlined in Section 3.3.1.5.3 aimed to establish if the theoretical values of ion release for 15 mm diameter pellets based on 10 mm pellets was significantly different to the values actually obtained and recorded for 15 mm diameter pellets based on their increased surface area.

3.3.1.5.1 EDX Analysis

Table 3.18: *Glass compositions produced were confirmed as P48-Ca16-Na19-Cu16-Co1 which were analysed using EDX analysis (JEOL-6490), with the results outlined in the Table 3.18 in mol%. Sample codes indicate the pellet diameter, with 10 or 15 specifying pellet diameter of either 10 mm or 15 mm.*

Sample Code	P_2O_5	CaO	Na_2O	CuO	CoO
P48-Ca16-Na19-Cu16-Co1 (10)	48.5	16.33	18.2	16.0	0.97
P48-Ca16-Na19-Cu16-Co1 (15)	48.7	15.79	19.5	15.46	0.6

3.3.1.5.2 Differential Scanning Calorimetry

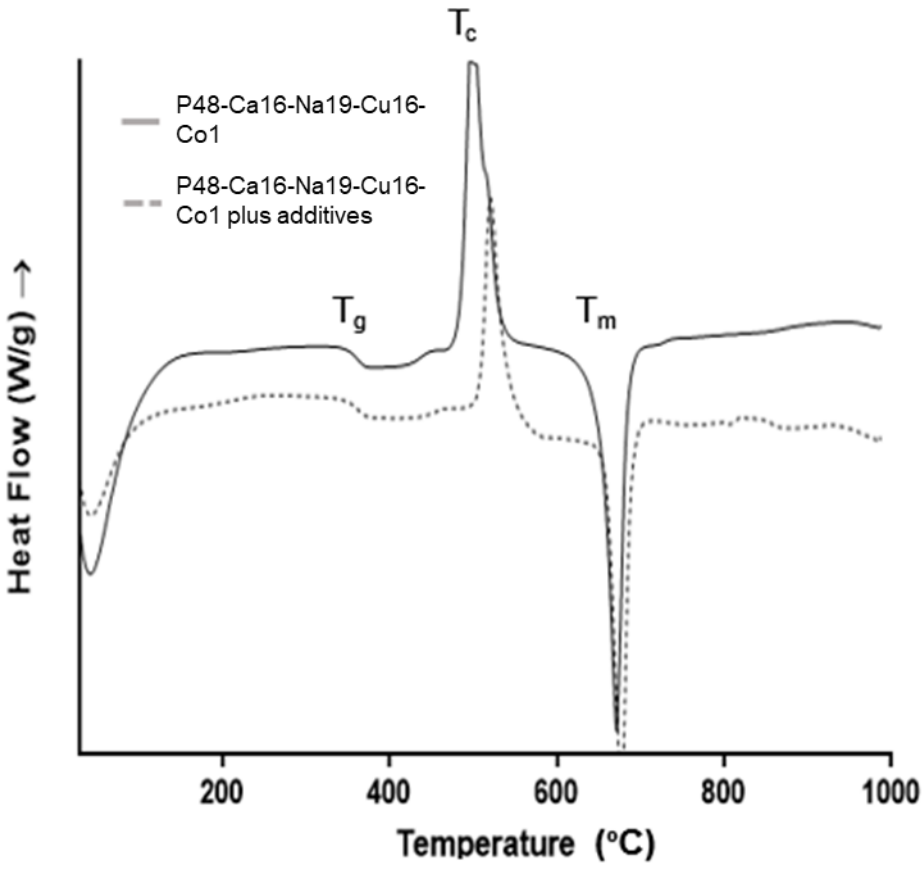

Figure 3.14: *DSC profile of P48-Ca16-Na19-Cu16-Co1 with additives (broken line) and without additives (solid line) sodium selenate, calcium iodate and copper oxide (II) nanoparticles. For specific details on "additives" refer back to Section 3.2.7, Table 3.3.*

Table 3.19: *Thermal properties of the glasses P48-Ca16-Na19-Cu16-Co1 with and without additives.*

	T_g (°C)	**T_c onset (°C)**	**T_c peak (°C)**	**T_m (°C)**	**Processing Window (T_c- T_g)**
P48-Ca16-Na19-Cu16-Co1 (no additives)	344	424	503	670	80
P48-Ca16-Na19-Cu16-Co1 (plus additives)	341	440	525	677	99

The addition of additives increased the processing window by 19 ºC, similar to the trend seen in Section 3.3.1.4.2. However, unlike the P50-Ca13-Na21-Cu15-Co1, P50-Ca9-Na16-Cu24-Co1, P50-Ca6-Na19-Cu24-Co1, P50-Ca2-Na17-Cu30-Co1 glasses, which showed a much broader melt peak with the addition of additives, this P48-Ca16-Na19-Cu16-Co1 glass revealed a narrower crystallization peak, more similar to that of just the glass profile.

3.3.1.5.3 Ion Release Rates

Linear regression was used to assess whether rates of copper, cobalt and selenium ion release from actual 15 mm diameter pellets were

significantly different from the predicted 15 mm diameter pellet ion release.

The results displayed in Figure 3.15a-c, showed that in all cases, ion release was found to be significantly higher than the predicted ion release ($p < 0.005$, $p < 0.0001$, $p < 0.001$ for copper, cobalt and selenium respectively) in 15 mm diameter P48-Ca16-Na19-Cu16-Co1 sintered glass pellets.

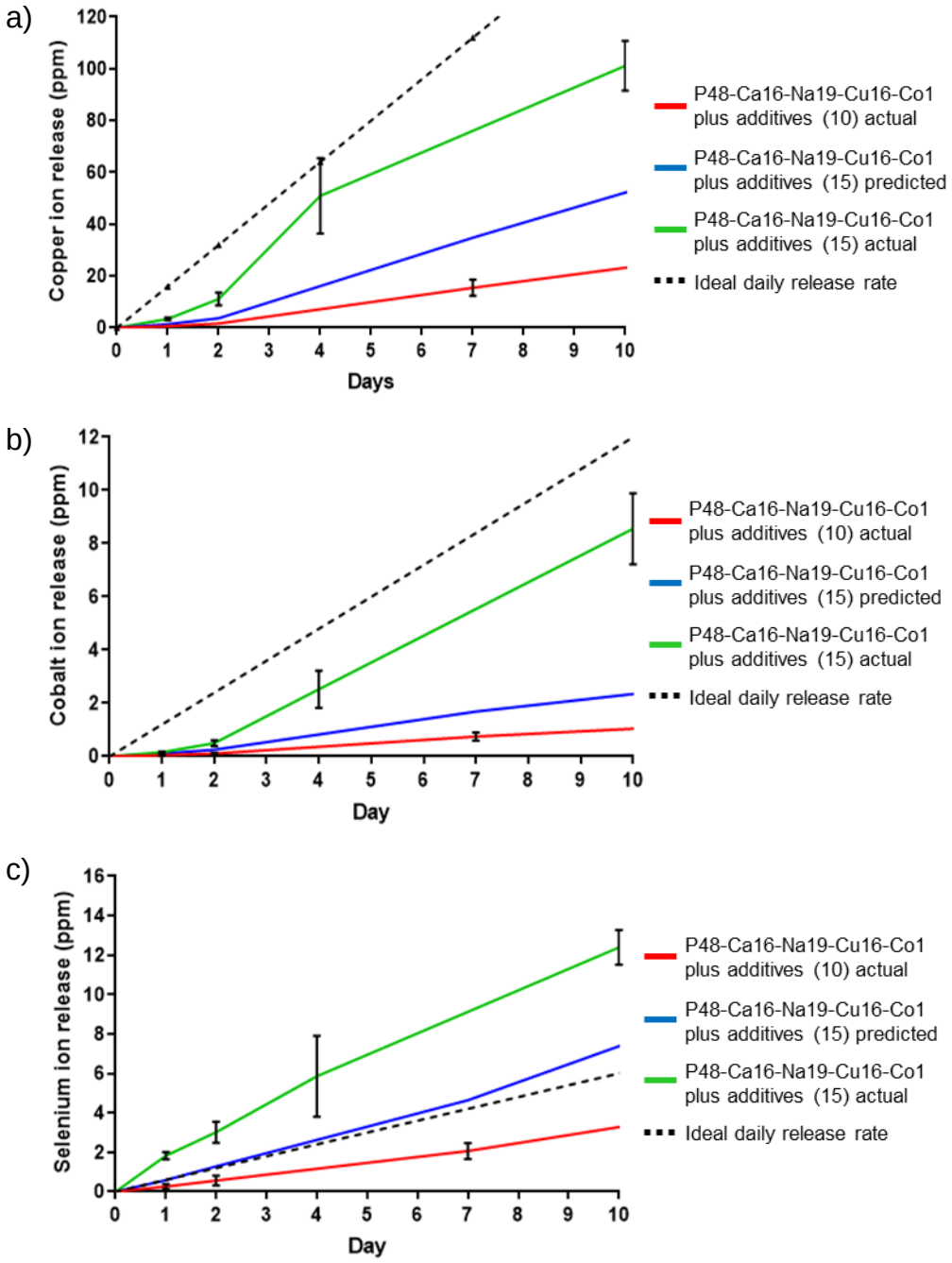

Figures 3.15: *The cumulative ion release profiles for* P48-Ca16-Na19-Cu16-Co1 *sintered glass pellets during dissolution testing. Pellet diameters are denoted using either (10) or (15) to indicate pellet diameters of either 10 mm or 15 mm. Pellet diameter of 10 mm (solid red line), and the predicted ion release of a 15 mm diameter pellet (solid blue line), the actual ion release of 15 mm diameter pellet (solid green line) and the ideal daily release rate (black dotted line) (n=3 for*

each glass formulation). Graphs a), b) and c) show copper, cobalt and selenium respectively.

3.4 Discussion

The main aim of this Chapter was to identify a suitable glass formulation that could be used as a product prototype in order to upscale and conduct further trials *in vivo*. Prior to this multiple objectives had to be achieved: establishing suitable sintering parameters such as particle size, sinter temperature and hold time duration; the inclusion of NP and effect on the microstructure and ion release of the pellets; and whether ion release data was able to be extrapolated from a 10 mm diameter pellet to a commercially preferred 15 mm diameter pellet.

3.4.1 Establishing sintering parameters

3.4.1.1 The effect of particle size on sintering parameters

The first section of this chapter investigated the sintering parameters required to form a sintered pellet. It was observed using an ash fusion furnace (see Figure 3.3) that the size of the ground glass particles (between 25<200 µm) used to form the pellet prior to sintering did not make a significant difference to the temperature at which the pellet reached its densest form. On average, pellet height decreased to 85 % original pellet height by 450 ºC regardless of initial particle size. This was surprising due to the well documented hypothesis that the reduction in particle size correlates to a reduction in the sintering temperature required. This acceleration is facilitated by the shorter distances required for particle diffusion to occur in smaller sized particles (German, Suri, and Park, 2009). One possible reason this data did not correlate with that hypothesis could have been that the particle size difference may not have been large enough for a noticeable difference to be observed. For example if the particles in this study were compared to NPs, the melting depression phenomenon may have been observed (Sun and Simon, 2007). The melting depression relies on the principle that the decrease in particle size results in an increased proportion of surface atoms exposed as the particle size reduces.

However, as the particles have been pressed into a compact pellet, the increased surface area caused by a smaller particle size may have been decreased by the pressing process, potentially resulting in no net reduction of surface atoms overall.

This data was not only useful to determine the exact temperature at which the highest density for the compact was possible, but also demonstrated that once the densest point had been reached, any additional heat or duration of heat application is excessive, and from a commercial perspective unfavourable due to the added cost of energy during production. Additionally, excessive heating could result in melting of the samples, rendering the pellets unusable.

Despite not observing a significant difference in the sintering temperature required, a large difference in pellet topography was observed (Figures 3.5a-f). Bjørk *et al.* (2013) found that when a larger particle size distribution range was used the larger grains consume the smaller grains more quickly, resulting in a reduction of the number of necks formed between particles. Consequently, this reduced the vacancy annihilation causing the main mechanism of densification to be by surface diffusion resulting in a less dense compact. This hypothesis supported the images shown as Figures 3.5a and b have a particle size range of 20 µm and 18 µm, respectively, whereas, images 3.5c-e have a large particle size range of 62 µm, 25 µm, 50 µm.

Contrastingly, the helium pycnometry data suggested that there was no difference in density of the compacts regardless of the particle size. However, the lack of difference may be attributed by a closed pore structure, preventing the helium from entering these pores. As a result the density observed was that of a skeletal density, rather than a true density (Stange, Scherf-Clavel, and Gieseler, 2013).

3.4.1.2 Hold Time

In tandem with use of the AFT data (Figure 3.5) DSC was used to assess the different thermal parameters of the glass. Within industry it

is typical that the sintering temperature of a glass lies within the processing window of the glass (Erasmus *et al*. 2017). P45-Ca30-Na15-Co10's thermal properties are outlined in Table 3.9, with the processing window annotated on the DSC profile in Figure 3.6. This data showed that this glass has a transition temperature of 374 ºC, the onset of crystallization then occurs at 495 ºC, before melting at 683 ºC. This data correlated with the images generated by the AFT, supporting the notion that the sintering temperature was located within the processing window, more specifically around 450 ºC for this glass.

After establishing the most efficient sintering temperature, the sintering duration (hold time) needed to be defined. The cross-sectional SEM images shown in Figures 3.7 a-d revealed that the optimal hold time (for durations assessed) and the glass formulation P45-Ca30-Na15-Co10, at 450 ºC to give the densest pellet was 4 hours. Interestingly, it appears that an excessive hold time may have a detrimental effect on the topography of the pellets. Figures 3.7b and c showed that an increase in hold time duration could result in higher porosity of the sintered pellet. This may be caused by an increase in grain size of the particles which is facilitated by the consumption of smaller particles, and as a result pore size and frequency was increased (Rice, Wu, and Borchelt, 1994). Another possible reason for these differences in topography may be due to the polishing of samples. Some polishing lines are visible on the samples which may have impaired the visual quality, as such, improved polishing protocols should be followed.

Similarly, to the data shown in Table 3.10, very little difference in density was seen despite seeing a large difference in microstructure observed. This could as a result of a closed pore structure and therefore a skeleton density is being shown rather than the true density. Supporting this suggestion are the side by side images, Figures 3.7 c and d that show a less densely packed core of the pellet with more pores compared to the outer section of the same pellet that appears to show less pores due to more interconnected particles. This was likely a

result of the compression process to make the pellets; the high pressure used to create the pellets caused a density variation throughout the pellet due to the uneven stress distribution of uniaxial application of a load. Yin *et al.* (2019) found that high pressure could increase the density of green compacts but led to large density variation throughout the compacts, which resulted in crack formation due to severe stress.

As a result the more densely packed particles at the edges of the pellet have a higher contact area with other particles encouraging neck formation (see Figures 3.7 c and d). This data further supported the hypothesis that the closed porous structure, potentially causing misleading density data using helium pycnometry. Therefore, SEM imaging or micro-computer tomography should be used to assess the porosity of these pellets due to the closed pore nature of this material (du Plessis *et al.* 2018).

3.4.2 The effect of changing calcium and sodium content on ion release

The thermal analysis for the formulations in Table 3.11 were shown in Figure 3.8 and Table 3.12. The large difference in thermal properties between glass formulations suggested large differences in structure. P51-Ca25-Na22-1Co has over double the processing window of P52-Ca16-Na31-1Co and nearly double that of P53-Ca26-Na19-1Co with values of 108 ºC, 43 ºC and 57 ºC, respectively. The increase in processing window suggested a greater degree of stability within the glass system (Pate*l et al*. 2017).

The increase in crystallization barrier could be due to an increase in energy barrier for the rearrangement of atoms in order to form a critical size defect (Brauer, Wilson, and Kasuga, 2012). The difference between P51-Ca25-Na22-1Co and P52-Ca16-Na31-1Co was expected due to the high calcium and lower sodium content of P51-Ca25-Na22-1Co. This disparity between the inclusion of divalent cations (calcium) in place of monovalent cations (sodium) (Gao, Tan and Wang, 2004; Ahmed *et al*. 2010; Lee *et al.* 2013) supported the trend of an

increasing T_g with an increase in calcium content in place of sodium. Divalent cations can act as cross-links between the non-bridging oxygens of two different chains, increasing glass stability (Bunker, Arnold, and Wilder, 1984). Additionally, cations with a higher field strength, such as calcium compared to sodium can decrease the dissolution rate due to increasing the covalent nature of the bonds within the glass matrix (Sharmin *et al.* 2013).

There is very little difference between the thermal properties of glass P53-Ca26-Na19-1Co and P51-Ca25-Na22-1Co as there was very little difference in their composition (see Table 3.11). What was interesting was that P53-Ca26-Na19-1Co had two melt peaks, one at 718 ºC, and a second at 754 ºC, whereas P51-Ca25-Na22-1Co only had one at 721 ºC. However, P53-Ca26-Na19-1Co had much narrower, defined peaks whereas P51-Ca25-Na22-1Co had a very broad peak. The double melt peak for P53-Ca26-Na19-1Co suggested that there could be two phases within the glass, one that requires a lower melting temperature, which then could partially crystallise and then melt at a higher temperature, resulting in the two separate peaks seen (Gracia-Fernández *et al.* 2012). It was possible that P51-Ca25-Na22-1Co was close to exhibiting this same behaviour, hence showing a broad, shouldered melt peak which could be masking more than one peak (Ahmed *et al.* 2004).

Despite seeing some differences between the glasses thermal parameters, no significant difference was observed during the dissolution study conducted. This may be for a variety of reasons, such as, there was not enough of a difference in composition between the three glasses. This may have been the case for glasses P53-Ca26-Na19-1Co and P51-Ca25-Na22-1Co but was surprising for P52-Ca16-Na31-1Co considering the differences in T_g, (56 ºC for P53-Ca26-Na19-1Co, 108 ºC for P51-Ca25-Na22-1Co and 42 ºC for P52-Ca16-Na31-1Co). Another possible reason this didn't have significantly higher ion release rate could be the possibility that due to the uniform sintering

temperature of 450 ºC for all three glasses, it was likely that these pellets could have crystallised, or at least partly crystallised (leading to glass-ceramic structure). As a result of this, the crystalline phases could have affected the solubility and dissolution kinetics of the glass (Ahmed *et al.* 2005).

Another possible reason no significant differences were observed between the three glasses was likely due to the high variation seen throughout the data sets and small duration being used to assess the ion release. For example Knowles, Franks and Abrahams, (2001) vary their glass composition in increments of 5 mol% of K_2O from 0-25 mol%, within their study the maximum difference in the calcium ion release values for 0 mol% versus 25 mol% is negligible at by day-7 (168 hours). It was only by day-10 mark onwards, that significant differences were seen in ion release, and this was still within 4 ppm range. Therefore, it may be that an extended duration of degradation was required to establish whether there were any true differences in ion release between these glasses. However, due to the time sensitive nature of this project it was a difficult compromise to make.

Another point of interest was that for formulation P52-Ca16-Na31-1Co's cobalt ion release, a peak was seen on day-4 (0.78 ppm), before seeing a reduction by day-10 (0.35 ppm), a reduction of -0.44 ppm. This was unexpected as it would be likely that ion concentration would increase with increased duration. However, the rapid increase in cobalt ion release concentration may have been indicative of a high calcium, sodium and phosphate release, based on the assumption that glasses dissolve proportionally due to the hydration of phosphate chains as the mechanism for dissolution (Bunker, Arnold, and Wilder, 1984). If this assumption was correct then the rapid release of ions could have resulted in solution saturation and then precipitation (Ducheyne, Radin, and King, 1993), consequently causing a reduction in cobalt ion concentration in the dissolution as they were incorporated into the precipitate system. Therefore, it should be considered whether it could

be beneficial to change dissolution media at frequent intervals during the experiment to prevent this ionic saturation, or whether a buffered solution, such as the artificial rumen fluid used, could have contributed to this saturation and propagated the precipitate formation and whether deionised water may have been preferable.

Despite not being able to establish whether there was any difference in ion release between these three glasses, it was observed that the ion release of these glasses was far too low compared to the desired product specification. It was due to this conclusion that no further work was investigated, or repeated with these compositions.

3.4.3 The effect of excluding copper oxide (II) nanoparticles from the sintered pellets on ion release

One of the initial desired design points of this product design was to include NP, due to the hypothesis that they would have increased bioavailability compared to their MP counterparts. However, very little research had been conducted into how the incorporation of NP into a sintered phosphate-based glass pellet may affect some of the physical characteristics. Therefore, this section of the chapter aimed to understand the effect of adding NP into the sintered phosphate-based glass formulation.

Figure 3.10 showed the DSC profile of the glass P49-Ca26-Na24-Co1 both with and without the inclusion of NP. The addition of copper oxide (II) NP to the glass mix resulted in a significant increase in processing window compared to the glass without, 117 ºC versus 47 ºC, respectively. This increase could be caused by a slightly reduced transition temperature of 366 ºC compared to 370 ºC and a delayed onset of crystallization at 483 ºC compared to 417 ºC. Choudhary, Rai and Singh, (2017) found that the incorporation of copper oxide NP into silver phosphate glasses resulted in higher stability due to the increase in covalent character of the P-O-P bonds. It was further speculated that the Cu^{2+} ions served as ionic cross-links in the glass causing an increase in thermal stability. Alternatively, if the NP had become part of

the glass matrix, similar to increasing the divalent cation content, such as Ca^{2+}, an increase in cross-linking between chains could have been observed.

Figures 3.11a and b showed that incorporation of NP into the pellets caused a significant decrease in cobalt and selenium ion release ($p < 0.001$). Inclusion of the small particle NP may have facilitated neck growth between the glass particles and aided the sintering diffusion process through the presence of a liquid phase (German, Suri, and Park, 2009). However, from the DSC profile in Figure 3.10 the NP have not melted by 450 ºC, so it is unlikely that they aided the sintering by this mechanism.

Another consideration may be that the release of cobalt and selenium was higher in the non-NP containing counterpart may be that because there was simply a high content of these elements in the pellet due to the absence of the copper oxide. The copper oxide NP accounted for nearly 1/3 of the pellets composition, therefore, it is possible that the ion release of the NP-containing pellet for cobalt and selenium concentration would be approximately 66 % of that seen in the non-NP containing pellet. On average, by day-1 the NP containing pellet had released 50.57 % of the cobalt released by the non-NP containing counterpart, and 37.88 % for selenium concentration. Interestingly, by day-10, the cobalt release compared to the non-NP pellet was reduced to 19.54 % cumulative ion release for cobalt, but increased to 53.9 % for the selenium concentration. The conflicting trends between these two elements suggested that they were being released into the solution by different mechanisms. One mechanism could be that insufficient sintering may have caused compaction of the NP into the glass, but not bonding into the glass structure, which could have caused a quicker and higher release rate. It was likely that the cobalt underwent the typical dissolution process. Bunker, Arnold and Wilder, (1984) stated that phosphate glass dissolution occurs in a three-step process: initially, H^+ and OH^- ions are taken up onto the surface of the glass, until fully

saturated; followed by a hydration process of ion exchange; and finally hydrolysis of the chain in solution. Whereas, the selenium was more likely to be dissolved purely through increased surface area exposure as degradation of the pellet increased due to being incorporated into the pellet as an additive.

Despite the increase in ion release seen with the removal of the use of NP, the overall ion release was still much lower than the desired release rate specified by the industry partner. Therefore, no continued work or experiments was done using the glass formulation P49-Ca26-Na24-Co1.

3.4.4 The effect of incorporating copper oxide (II) into the glass versus incorporating as nanoparticles

As demonstrated in Section 3.4.3 the incorporation of NP into the glass mix can not only effect the thermal parameters of the overall mixture, but can alter the ion result and degradation of the pellet as a result. Therefore, in this section the effect of gradually incorporating the copper oxide (II) NP was assessed.

Figure 3.12 showed that the incorporation of the additives had conflicting effects on the processing window of the glasses of some glasses. For example, an increased processing window was observed for P50-Ca13-Na21-Cu15-Co1 and P50-Ca2-Na17-Cu30-Co1, similar to that seen in Section 3.4.2. However, for the other two formulations, P50-Ca9-Na16-Cu24-Co1 and P50-Ca6-Na19-Co1 the processing window dramatically decreased. Choudhary, Rai and Singh, (2017) speculated that an increased number of Cu^{2+} ions may cause disruption of the glass network by depolymerisation via to the addition of more non-bridging oxygen ions, resulting in a decreased temperature required to induce crystallization. If this is the reason behind the decreased processing window for P50-Ca9-Na16-Cu24-Co1 and P50-Ca6-Na19-Co1, it is surprising that P50-Ca2-Na17-Cu30-Co1 does not also follow a similar trend. However, as P50-Ca2-Na17-Cu30-Co1 had a higher P content than anticipated 52.7 mol%, the higher ratio of

phosphorous in the formulation may counteract the higher Cu^{2+} ions present in the glass network that may have caused depolymerisation.

It could be possible the earlier onset of crystallization of P50-Ca6-Na19-Co1 and P50-Ca9-Na16-Cu24-Co1 was due to the presence of the sodium selenate. This had a crystallization peak around 580 ºC, with an onset close to 560 ºC, and as a result of these two parameters being quite close to the T_c of these two glasses, a much larger, broader crystallization peak was seen. Similarly, with P50-Ca9-Na16-Cu24-Co1 and P50-Ca6-Na19-Co1, two melt peaks were seen on the DSC profile of the glasses without the additives. However, once the calcium iodate, sodium selenate and copper oxide (II) NP were incorporated, these two peaks become one much broader peak, suggesting multiple phases close together were being masked by one another (Ahme*d et al*. 2004).

The incorporation of copper oxide into the glass matrix resulted in a much higher release of copper compared to when it was incorporated purely as copper oxide (II) NPs. This could be because copper phosphate has a higher solubility, compared to CuO. Aksu, (2009) found that $CuHPO_4$ had a much higher solubility at pH 5-6, (the range in which the dissolution experiments were carried out), compared to CuO which was more soluble at pH 10. However, by day-7, formulation P50-Ca6-Na19-Co1's copper concentration significantly decreased, despite being the highest concentration at day-4. This trend was similar to the cobalt ion release seen in Section 3.3.2.3, in which the glass with the formulation P52-Ca16-Na31-1Co had the quickest release rate of cobalt ions initially, yet by day-10 the concentration had decreased to approximately half of that seen on day-4. It was speculated that this decrease in overall concentration was caused by precipitation, lowering the overall concentration of ions in solution (Ducheyne, Radin, and King, 1993), meaning it is likely that these decreases were happening for the same reason.

The formulation P50-Ca13-Na21-Cu15-Co1 had the highest release rate of both selenium and cobalt. It is likely that this was due to the

lowest ratio of metal cations compared to the other glasses. Tan *et al.* (2017) showed that the addition of metal cations can decrease the dissolution rate of glass due to an increased cross-linking within the glass structure. This is further supported by Sharmin *et al.* (2013) finding that cations with a higher field strength can decrease the dissolution rate due to increasing the covalent nature of the bonds within the glass matrix.

Due to the high variability within all data sets and the relatively short duration during which this experiment took place, it was not possible to draw any concrete conclusions, stating that one formulation was closer to achieving the Industry Partners desired ion release rate required for the prototype. However, it was confirmed that copper oxide (II) NP, are less soluble at pH 5-6 than the copper phosphate compounds released from the glass matrix. Therefore, due to the increased complexity of processing parameters and decreased ion release, the incorporation of NP was not as advantageous as initially hoped.

3.4.5 The effect of bolus diameter on ion release

As previously mentioned, the desired diameter of a prototype bolus was 15 mm. However, during initial formulation testing only a 10 mm pellet die was available, meaning the majority of testing had to be carried out using a 10 mm pellet. Consequently, it was important to establish whether the data from the 10 mm pellets could be extrapolated to estimate a 15 mm pellet's ion release.

Figures 3.15 a-c showed that the ion release from the 15 mm diameter pellet was significantly higher ($p < 0.005$, $p < 0.0001$, $p < 0.001$) for copper, cobalt and selenium respectively than the ion release predicted using the data from the 10 mm diameter pellet. Based on these two sets of data it was estimated that the actual ion release from the 15 mm diameter pellet is 2-3 times higher than the predicted data based on a linear relationship between ion release and surface area. Therefore, this raised the question i) whether the relationship was linear, or ii) whether the surface area was higher than was accounted for. It was

plausible that it was due to the latter suggestion as there was significantly higher ion release than expected, as the larger pellets were subjected to the same sintering regime as the smaller pellets. As a result, the pellet may not have fully densified, resulting in larger pores. It is well established that an increase in porosity can result in a higher ion release and quicker degradation due to a higher surface area (Lu *et al.* 2002; Lin, Chang, and Shen, 2009; Xu *et al.* 2017).

Despite a much higher rate of ion release with an increase in the pellet diameter being recorded, these values were still much lower than the specified values set by the Industrial Partner and as such no further work was conducted using this formulation and continued development and evaluation was required.

Following exploration into the complexities and variables involved in incorporation of NP into a sintered pellet, and uncertainty surrounding legislation of feeding animals NP, the Industrial Partner made the decision to remove NP from any further product development work.

3.5 Conclusion

In this Chapter, 10 different glass formulations were trialled to find a formulation that could be used as a prototype for further research. In order to carry out dissolution experiments factors such as the effect of particle size, sintering temperature and duration needed to be established. It was concluded that a particle size range <63 µm produced a sintered pellet with the smallest pore size; the use of ash fusion furnaces can help to identify the optimum sintering temperature required to produce a fully densified pellet; and that an excessive amount of sintering time can be as detrimental to the porous structure of the pellet as not enough time.

It was also concluded that the addition of copper oxide (II) NP does not seem favourable over the incorporation of copper into the glass matrix due to the increased concentration of copper ions in the solution at the

pH 5-6, as demonstrated by the *in vitro* dissolution experiment carried out in Section 3.3.1.4.3.

As a result of the work explored in this chapter it was concluded that further consideration needs to be given as to how the current *in vitro* methodology can closer simulate an *in vivo* rumen environment. A consequence of the unrefined *in vitro* rumen simulation was the formation of precipitate, that potentially inhibited the further release of ions. Similarly, longer durations of experiment should be considered in order to more closely simulate intended degradation duration of the prototypes and establish whether there are any true differences between formulations.

Finally, due to the complexities and regulatory concern of incorporating NP into an animal feed, the Industry Partner decided to discontinue exploration of a NP containing phosphate-based glass bolus product, and as such further experimental work will use the glass formulation P50-Ca2-Na17-Cu30-Co1 containing no nanoparticles.

Chapter 4 - *In vivo* phosphate-based glass formulation assessment

4.1 Introduction

Following the *in vitro* glass formulation testing carried out in Chapter 3, P50-Ca2-Na17-Cu30-Co1 was one of the only non-NP containing glasses trialled. As a result of this it demonstrated an ion release profile most similar to the Industrial Partner's desired product specification. Following *in vitro* testing it was essential to demonstrate this same degradation profile within the animal. Additionally, it was crucial to demonstrate that boluses were retained by animals and so a preliminary trial was included before embarking on a full *in vivo* study.

As such, the aims for this chapter were:

I. Preliminary trials, were used to assess whether the combined coating and bolus density were suitable for use *in vivo*, and that they were retained in the animal for a duration long enough to properly assess the dissolution rate.
II. Determine the degradation rate of the P50-Ca2-Na17-Cu30-Co1 bolus *in vivo* by its recovery and reduction in weight and therefore establish if there was any correlation between the rate of mineral weight loss *in vivo* and *in vitro.*
III. Ensure that there was elemental release from the bolus in the rumen through assessment of the rumen fluid mineral concentrations.
IV. Establish that if there was elemental release of the bolus in the rumen, that it could be utilised into functional constituents by assessment of the blood plasma mineral concentrations.

Both rumen fluid mineral concentrations and plasma mineral

concentrations were analysed using inductively coupled plasma to confirm mineral concentrations in their respective samples.

Unfortunately, due to tight timelines it was not possible to develop and optimise bolus coatings before assessing the degradation profile *in vivo*. With the true critical factors needing evaluation to be the degradation rate and ion release profile of the glass formulation, a coating suitable for *in vivo* testing was identified from literature and utilised but not fully optimised.

The intermediate inert coating consisted of two layers comprising of an initial bottom layer of waterproof lacquer (O.P.I, USA), followed by a layer of resin for chemical resistant (Gorilla Glue, USA). It was believed that the combination of both coatings would offer a suitable protection from the rumen environment whilst remaining inert, allowing the degradation of the glass to be reviewed independently. The initial nitrocellulose lacquer was chosen due to its strong water resistance and low gas permeability properties (Ġallstedt, Törnqvist, and Hedenqvist, 2001). However, there was some concern whether the enzymes present in the rumen may degrade or impair the lacquers protective ability, due to the enzymes present in ruminants being specially adapted to break down cellulosic fibres. As such, a second chemically resistant resin was added. This layer contained a functional group called isocyanate, that readily reacts with moisture to form polyurethane (Kapp, 2014). Polyurethanes are a family of versatile polymers known for their chemical resistance and durability. Key applications of polyurethanes include adhesives, varnishes, sealants and insulators among many others (Magnin *et al.* 2020). As such, isocyanate derived polyurethane resins were selected to act as a toughening top coat.

Literature suggested that the two coating materials used in combination would be a superior approach to toughened resins being applied directly onto the glass, as both the resin and phosphate-based glass materials are hygroscopic, meaning that the resin would have to

compete with the glass for the atmospheric moisture it requires to cure and form polyurethane (Xie *et al.* 2019). This competition for moisture could have resulted in inferior curing and impaired protective properties.

Nitrocellulose lacquers are also believed to improve the structural characteristics of isocyanate derived polyurethanes (Zhang and Zhou, 1997, 1999). The mechanism behind this effect is poorly studied, though has been hypothesised that the immobilised nitrocellulose macromolecules penetrate into the polyurethane networks during curing, aiding cross-linking, and improving coating stability. The co-action of these barrier coatings would therefore be an effective way of protecting the bolus, enabling assessment of the glass ion release profile and degradation rate.

4.2 Materials and methodology

For the full list of materials used in this Chapter, see Section 3.2, Table 3.3.

The schematic outlined in Figure 4.1 the processes and methods used in this section.

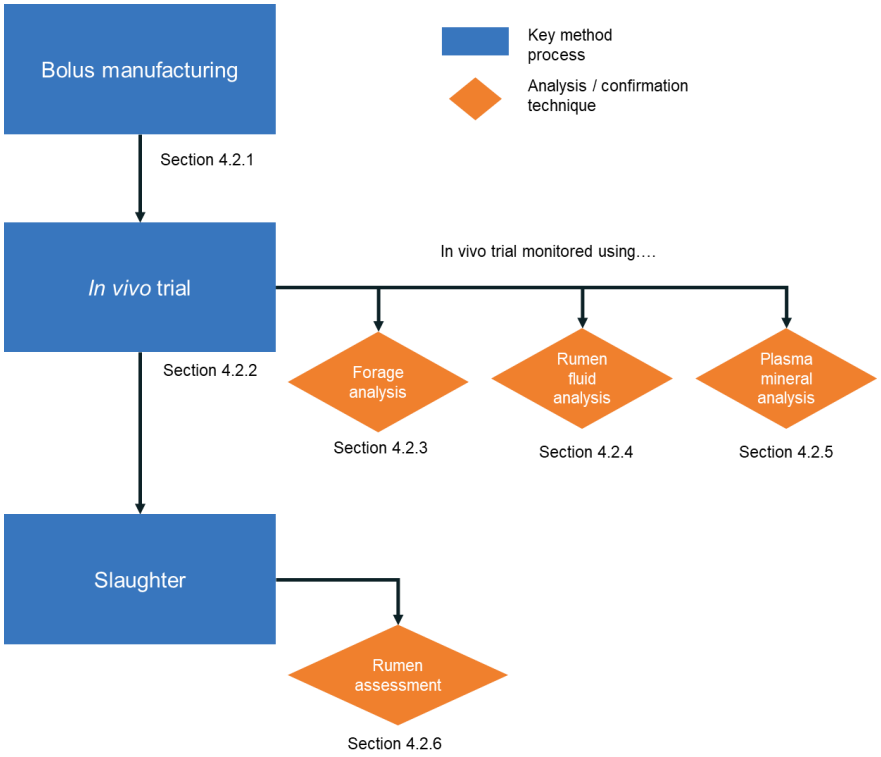

Figure 4.1: *A flow diagram to indicate the sequence of methods used in Chapter 4.*

4.2.1 Bolus manufacturing

The glass formulation P50-Cu30-Na17-Ca2-Co1 was prepared and supplied by Glass Technology Services. Upon arrival the composition was confirmed using EDX analysis (outlined in Chapter 3.3, Table 3.15). The glass was then ground and sieved to a powder with a particle size range <125 µm.

Glass and additives (see Table 4.1 for additive quantities) were weighed into glass vials before placing on a roller mixer (4010000, IKA, USA) for half an hour. Once thoroughly mixed, the vials were then

placed into a 50°C oven for half an hour to drive off any excess moisture and aid the flowability of the powder.

Table 4.1: *Bolus compositions and additive concentrations required per full sized sheep bolus.*

	Quantities of materials for 1 prototype bolus (g)		
	Cobalt and copper glass	**Sodium selenate**	**Calcium iodate**
Bolus	16.002	0.296	0.773

After glass vials were removed from the warming oven glass powder mixtures were emptied into the individual graphite mould compartments and a stainless-steel rod placed on top. Once all mould holes were filled and rods in place a flat steel plate was then bolted on top to allow even distribution of pressure when using a tensometer to compress the powders. An Instron tensometer (Instron, USA) was used to compress the powders to 35 MPa, where it was held at this pressure for 1 minute. Prior to the pressure release, wing nuts were tightened in an attempt to keep pressure on the boluses during sintering to mitigate against the shrinkage that occurs during densification.

After compression the entire graphite mould was placed centrally into a furnace (Lenton furnaces, UK) where the sintering regime outlined in Figure 4.1 was followed.

Figure 4.2: *Sintering parameters of full sized prototype sheep boluses*

The intermediate nitrocellulose coating was applied using a paint brush as disclosed in Ġallstedt, Törnqvist and Hedenqvist, (2001). Once this bottom layer (O.P.I Nail Lacquer, USA) was applied, the boluses were placed in a 40 ºC oven for 1 hour to dry, before the exterior resin coat was applied (Gorilla Glue, USA), also using a paint brush. After the resin coating had been applied, the boluses were left overnight at room temperature to cure.

After the multi-material coating was applied, the bolus weights, lengths and diameters were recorded and images captured.

4.2.2 Trial design

An initial preliminary trial was utilised to demonstrate bolus retention, *in vivo*. The key success criteria for the trial was that 4 out of 5 boluses were retained. For clarity trial design summary is displayed in Table 4.2, using a stage-gated process to determine if the extended trial would continue (Figure 4.2). Following success in bolus retention, an extended trial studying the rate of ion release would then occur.

***Table 4.2**: Summary of preliminary trial parameters.*

	Preliminary	**Extended**
Acclimatisation Period	14-days	14-days
Trial Duration	5-days	1-month
Number of Sheep	5 bolused	6 bolused 4 control
Feeding Regime	Grass silage *ad libitum*	Grass silage *ad libitum*
Trial Requirements to proceed onto the extended trial	4/5 boluses retained by sheep	N/a

Group sizes were determined using data from Kendall (2019) BSAS conference abstract. Using this data and underlying statistical assumptions, a group of 8 sheep were found to be needed to derive a statistically significant observation ($P < 0.05$), and a group of 4 sheep needed to derive a diagnostically relevant outcome ($P = 0.2$) for blood plasma levels of copper, cobalt and selenium.

As the rumen fluid analysis technique and analysis was under development, no previous work by the group was available to generate determine power.

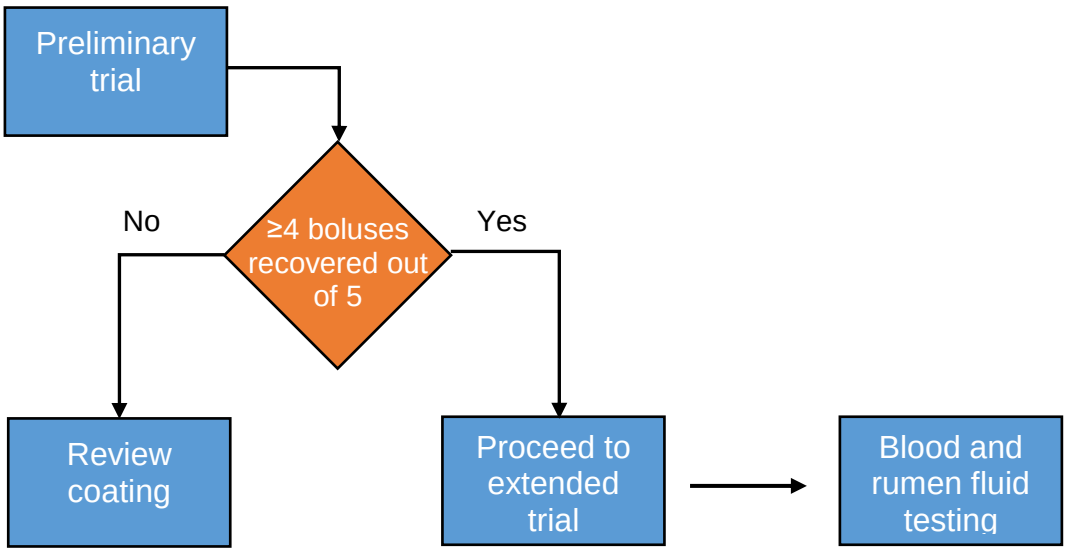

Figure 4.3. *Stage-gate process to determine whether the extended trial would occur following the preliminary trial results.*

4.2.2.1. Preliminary Trial

Multiple random samples of silage were collected and analysed for mineral concentration (full methodology discussed in Section 4.2.3). Boluses were administered to Suffolk cross cull ewes (total n = 5) following the Bimeda, (2016) bolusing protocol, using the Agrimin Sheep Applicator-A gun. Prior to bolus administration, sheep were momentarily held (~1 minute) to ensure the bolus was swallowed without instant regurgitation.

After 5-days during which animals were allowed to graze at pasture, animals were slaughtered. Entire rumens were collected and transported back to the University of Nottingham before being fully dissected and thoroughly searched to locate ingested boluses.

Assuming the successful retention of 4 out of 5 boluses during the preliminary trial, the extended trial would be conducted across 30-days, housed under the same circumstances.

4.2.2.2. Extended Trial

Suffolk cross cull ewes (total n= 10) were randomly assigned to a treatment (n= 6) or control group (n= 4). Initial blood and rumen samples were taken prior to bolus administration (following the same bolusing procedure outlined in Section 4.2.2.1). Multiple random samples of silage were collected and analysed for mineral concentration (full methodology discussed in Section 4.2.3) to control for other mineral sources.

Blood samples were taken from each sheep under ASPA license on days 0, 7, 14, 21 and 28 via jugular venepuncture, using vacuette needles (Griener Bio One Ltd, UK) and a single 9 ml lithium heparin (LH) vacuettes (Griener Bio One Ltd, UK). Rumen fluid samples were taken at the same frequency as blood samples using a syringe and tubing method (Jasmin *et al*. 2011).

Blood and rumen fluid samples were brought back into the laboratory at the University where they were initially processed, aliquoted and aliquots stored at -20 °C for subsequent analysis by the NuVetNA team. Plasma and rumen fluid minerals were analysed by ICP-MS using validated protocols (used for commercial NUVetNA analysis) (Kendall, 2021).

4.2.3 Forage analysis

Forage analysis was carried out in order to monitor the pasture mineral concentrations throughout the trial. Tangerine Holdings conducted the forage mineral analysis. Acid digestion of forage carried out by weighing 0.3 g of freeze-dried grass silage into the digestion vessels (Perkin Elmer, UK), pipetting 8 ml 70 % nitric acid (VWR International, UK) and 2 ml 30 % hydrogen peroxide and digested using the Titan MPS Microwave (Perkin Elmer, UK) and digested at 175 ºC, 30 Bar (using 10 minute ramp), 20 minute hold time and then cooled to 50 ºC, 30 Bar and held for 10 minutes at 1 minute ramp time. Digestion vessels were then emptied into a falcon tube (Fisher Scientific, UK),

ensuring the sides of the digestion vessels were washed and made up to 50 ml.

Forage mineral analysis was carried out using an Optima 8000 (Perkin Elmer, UK) inductively coupled plasma optical emission spectrometry (ICP-OES). Calibration was carried out using internal standards: Mg (100 ppm), K (1000 ppm), Na (100 ppm), S (100 ppm), Mn (100 ppm), Cu (10 ppm), Zn (10 ppm), Co (0.1 ppm), Mo (1 ppm), Se (0.1 ppm), Fe (100 ppm), Al (100 ppm), all reagents were supplied by VWR International, UK and deionised water (Normatom, VWR International, UK).

4.2.4 Rumen fluid analysis

Multiple rumen fluid samples were collected to review the ion release profiles of the boluses *in vivo*. Samples were collected following the methodology described in Petrovski (2017) “Assessment of the rumen fluid of a bovine patient”, by passing a tube orally through the mouth to the rumen. The tubing was flexible enough not to damage the oesophagus, but rigid enough to pass through the rumen mat, and of a diameter at least 10 mm to prevent blockages. Samples were retrieved using a suction pump or syringe attached to the tube.

The NuVetNA team also analysed rumen fluid samples. These samples were centrifuged for 15 minutes at 2,300 g (Allegra X-22, Beckman Coulter, UK). The supernatant was pipetted (Pasteur 3.3 ml micro bulk wrap pipette, Scientific Laboratory Supplies, UK) into a 14 ml polypropylene tube (Sarstedt, UK). From this a 500 µl sample was analysed using ICP-MS as outlined in Section 5.2.3.

4.2.5 Plasma mineral analysis

Plasma mineral analysis was conducted to confirm the release and subsequent metabolism of the target trace elements into the blood. This analysis was carried out by the NuVetNA team using an XSeries^{II} (Thermo Fisher Scientific, USA) inductively coupled plasma mass spectrometer (ICP-MS). Samples and calibration standards were

diluted (500 µl sample with 9.5 ml diluent). This diluent was comprised of 0.1 % non-ionic surfactant (Triton X-100 and anti-foam B, Sigma Aldrich, UK), 2 % methanol and 1 % concentrate (< 99 %) HNO_3 (Fisher Scientific, UK) including internal standards Lawrencium (5 mg/L), Rhodium (10 mg/L), Germanium (50 mg/L and Scandium (50 mg/L). All calibrations were within a range of 0-50 mg/L (Calritas-PPT grade CLMS-2 from Fisher Scientific, UK).

ICP-MS uses collision-cell technology with kinetic energy discrimination (CCT-KED), using 7 % H_2 in He as the hexapole collision cell gas, reducing polyatomic interference with aspiration through a single sample line and glass concentric nebuliser at a rate of 1 ml/minute (Thermo Fisher Scientific, UK). Results were then calibrated to concentrated solution and adjusted for background using blank correction.

4.2.6 Rumen dissection

On day-30 sheep were slaughtered, and the rumens of bolused sheep collected for dissection. Full rumens were placed on dissection tables at Nottingham University, and rumen digesta was thoroughly searched until boluses were located, or it concluded that they were not present within the rumen.

4.2.7 Statistical analysis

Statistical analysis of all parameters was carried out using Prism 8 (GraphPad Software, UK). Multiple T-tests were performed comparing each treatment against one another. Statistical significance was determined using the Holm-Sidak method, with an alpha value of 0.05. Each row was analysed individually, without assuming a consistent S.D.

4.3 Results

The results for both the preliminary and extended trials are outlined below.

4.3.1 Forage analysis

Forage analysis conducted by Tangerine Holdings prior to both trials starting, as can be seen in Table 4.3. Specific minerals of interest were copper, cobalt and selenium as their concentrations in rumen fluid and blood plasma were key measured parameters. The copper concentration of the forage supplied was 6.43 mg/kg DM, with cobalt and selenium measuring at 0.07 mg/kg DM and 0.01 mg/kg DM respectively. As part of their consultative forage analysis services Tangerine Holdings rated these forage mineral concentrations as low for copper and very low for both cobalt and selenium.

Table 4.3: *Mineral analysis of the forage, samples taken prior to trial commencing.*

	Concentration (mg/kgDM)		
	Copper	**Cobalt**	**Selenium**
Trial forage	6.43	0.07	0.01

Iodine was unable to be assessed as it was not part of Tangerine Holdings analysis portfolio.

4.3.2 Preliminary bolus recovery trial

Following dissection and searching, all 5 boluses were successfully located from the rumens of the preliminary trial animals, meeting the success criteria to begin the extended trial. An example of the physiological changes of the boluses is displayed in Figures 4.4.

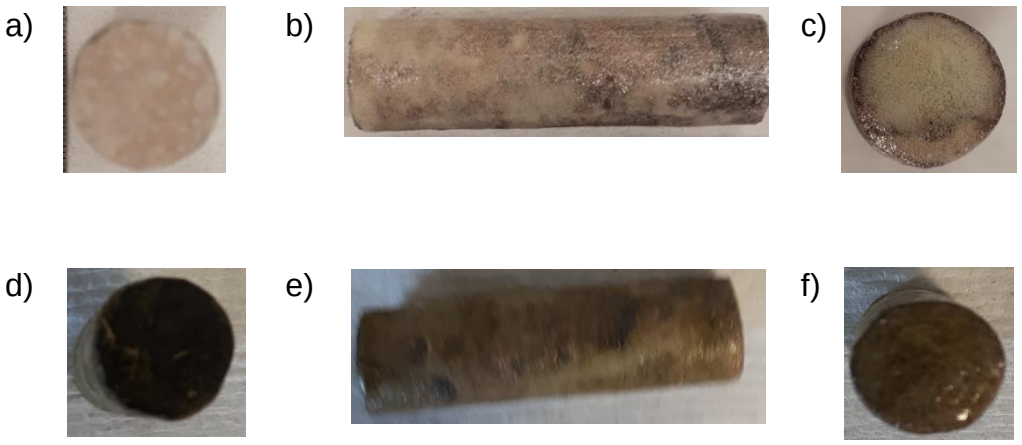

Figures 4.4: *Images 4.4a-f show a bolus used in the preliminary trial. Images 4.4 a-c showed the bolus prior to administration. 4.4a shows the radial view of the open end of the bolus, b: the axial view of the bolus and c: the radial view of the sealed end of the bolus. Images 4.4 d-f display the same bolus once retrieved after ingestion, with the images in the same order.*

Images 4.4d-f demonstrated the physiological changes that occurred subsequent to administration. Most notably is the colour change of both the coating and the glass. The glass changes from a pale pink colour to a dark green. The coating changes colour from a pale yellow to a darker yellow. Unsurprisingly, there is little change in both length and diameter after 1-week of ingestion. Some particulate matter, likely digesta, is notable in Figure 4.4d.

4.3.2 Extended trial

Following the successful retrieval of 5 out of 5 boluses from the preliminary trial, the extended trial went ahead. Section 4.3.2 discusses the physiological parameters of the recovered boluses, the rumen fluid concentrations and blood plasma concentrations during the month-long trial.

4.3.2.2 Rumen fluid

Weekly rumen fluid samples were analysed for copper, cobalt, selenium and iodine concentrations. The graphs displayed in Figures 4.5 – 4.8

compared the mineral concentrations in rumen fluids of the bolused groups against the control group across the 1-month trial.

4.3.2.2.1 Copper concentrations

There was no significant differences between the rumen fluid copper concentrations of the bolused animals compared to the control group. However, the moving average of the bolus group indicated higher rumen fluid concentration variation, compared to a relatively static control group.

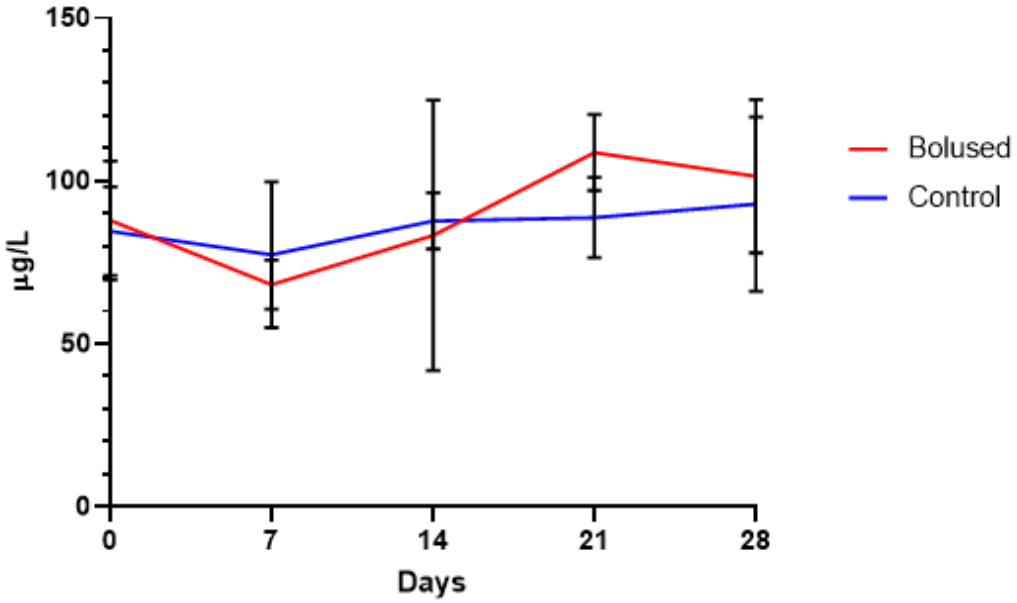

Figure 4.5: *Rumen fluid copper concentrations of the bolused (n = 6) and control animals (n = 4) during the extended trial for the prototype bolus.*

4.3.2.2.2 Cobalt concentrations

There was no significant differences between the rumen fluid cobalt concentrations of the bolused animals compared to the control group. However, both exhibit similar trends of an initial drop in rumen fluid cobalt concentration that later stabilised in weeks 1 to 4.

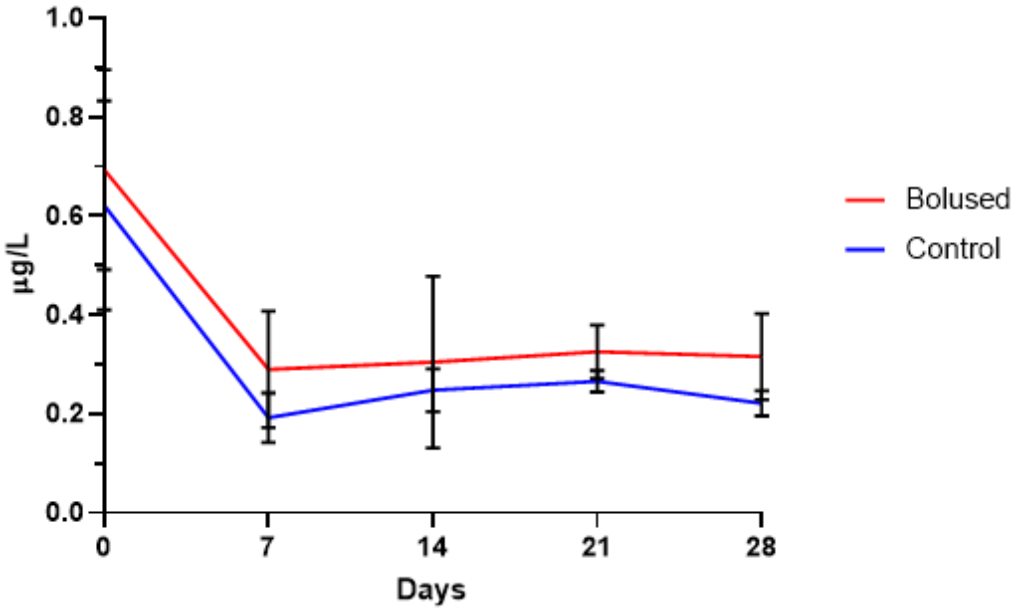

Figure 4.6: *Rumen fluid cobalt concentrations of the (n = 6) and control animals (n = 4) during the extended trial for the prototype bolus.*

4.3.2.2.3 Selenium Concentrations

Some of the most prominent effects were noted in the selenium rumen fluid concentration. By day-7 the control group recorded a drop in selenium concentration, compared to the bolused group that saw an increase. The only significant result was recorded at week three, demonstrating that the treatment group had a significantly higher ($p < 0.01$) selenium rumen fluid concentration than the control group. However, following this significant result, the selenium rumen fluid concentration of the control group increased, reducing the difference between groups to one that was not statistically significant.

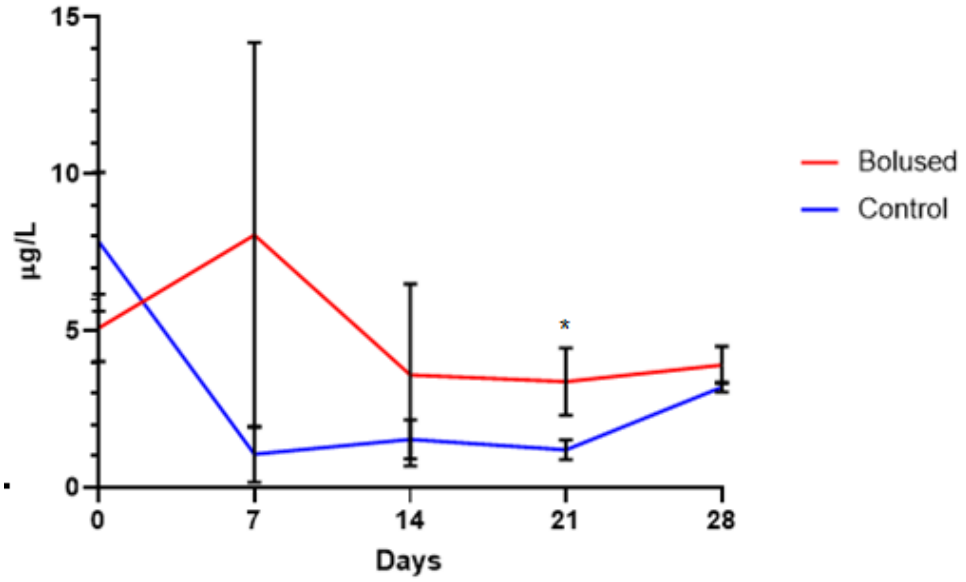

Figure 4.7: *Rumen fluid selenium concentrations of the bolused (n = 6) and control animals (n = 4) during the extended trial for the prototype bolus. Statistical significance *(p < 0.01).*

4.3.2.2.4 Iodine concentrations

No significant results were recorded for rumen fluid iodine concentrations, though both groups showed a decreased concentration over the 4-week trial. Week 2 was unable to be analysed due to sample contamination.

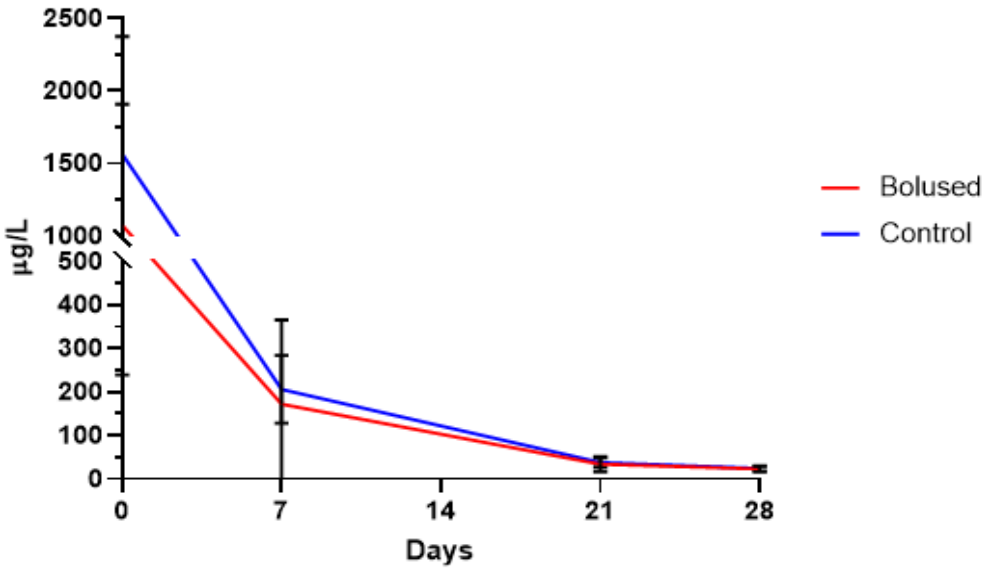

Figures 4.8: *Rumen fluid iodine concentrations of the bolused (n = 6) and control animals (n = 4) during the extended trial for the prototype bolus.*

4.3.2.3 Blood plasma

As very little difference was seen in the rumen fluid concentrations, only day-0 and day-28 blood plasmas were analysed. The expectation was that if there was a noticeable difference in blood plasmas that it would be most obvious comparing these two time points.

4.3.2.3.1 Plasma copper concentration

No significant results were observed for copper concentration in the blood plasma. Both groups recorded very little difference in plasma copper concentration over the course of the trial.

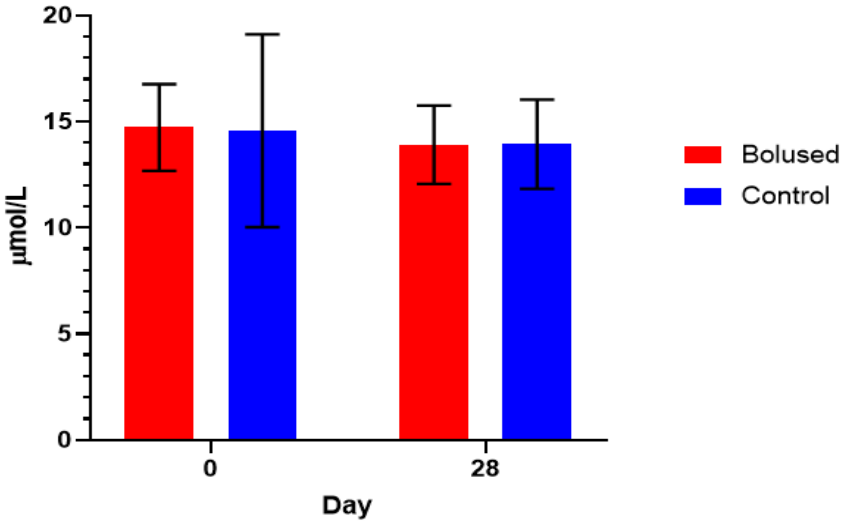

Figure 4.9: *Blood plasma copper concentrations of the bolused (n = 6) and control animals (n = 4) on days 0 and 28 during the extended trial for the prototype bolus.*

4.3.2.3.2 Plasma cobalt concentration

Displaying a similar pattern to the copper blood plasma results, the blood plasma cobalt concentrations did not exhibit any significant difference between the two time points, or between the groups despite recording a declining baseline over the course of the trial.

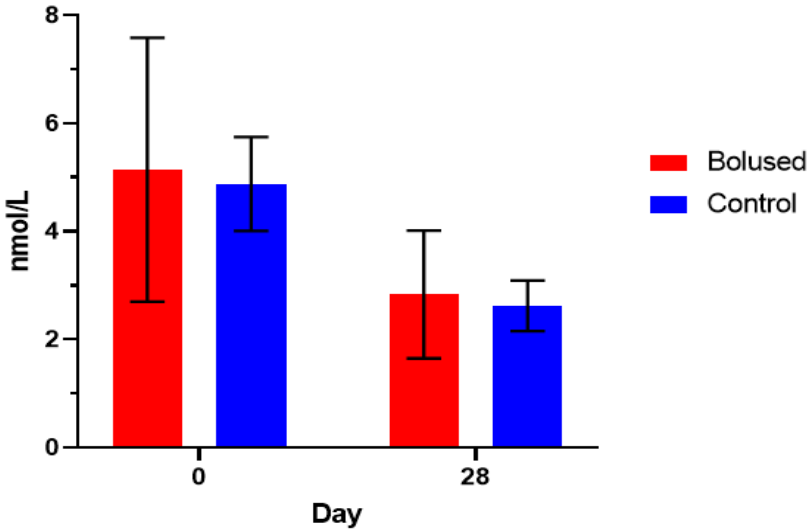

Figure 4.10: *Blood plasma cobalt concentrations of the bolused (n = 6) and control animals (n = 4) on days 0 and 28 during the extended trial for the prototype bolus.*

4.3.2.3.3 Plasma selenium concentration

Similarly to the rumen fluid data, there was a significance difference between the two groups recorded at the end of the trial. The bolused group exhibited a significantly higher ($p < 0.001$) blood plasma selenium concentration compared to the control group.

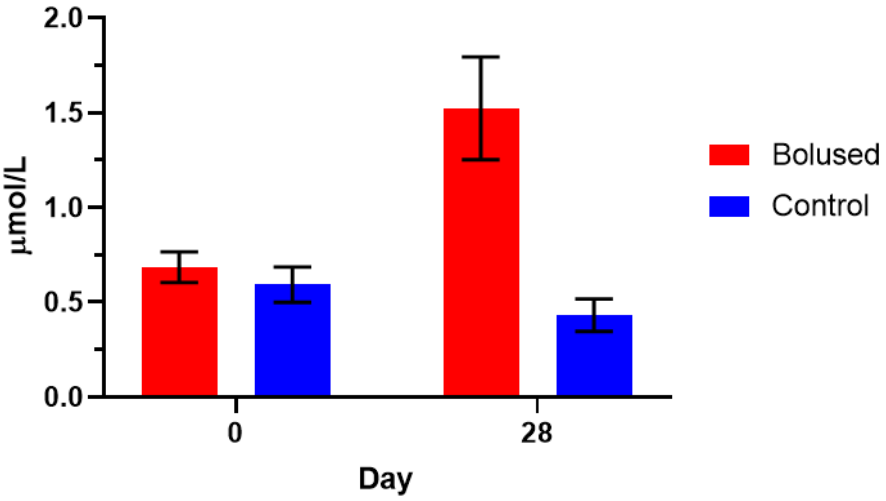

Figure 4.11: *Blood plasma selenium concentrations of the bolused (n = 6) and control animals (n = 4) on days 0 and 28 during the extended trial for the prototype bolus.*

4.3.2.1 Recovered boluses

Consistent with the findings of the preliminary trial, the extended trial boluses also exhibited colour change of the glass and coating from pink to dark green and pale yellow to dark yellow respectively. Table 4.4 outlined the changes in weight, length and diameters of the boluses following 1-month ingestion. The average weight loss of boluses was -0.42 g +/- 0.23, with an average length increase of 0.14 mm +/-0.09 (excluding bolus 2 which reduced in length -0.23 mm), as well as an average increase in diameter of 0.13 mm +/ -0.22.

Table 4.4: *Measurements of boluses weight, length and diameter before and after administration of the extended trial.*

	Before			After		
Bolus	**Weight (g)**	**Length (mm)**	**Diameter (mm)**	**Weight (g)**	**Length (mm)**	**Diameter (mm)**
1	16.03	58.57	14.59	15.48	58.85	15.15
2	16.06	56.97	14.98	15.42	56.74	15.14
3	16.16	56.25	15.05	15.43	56.38	15.26
4	15.86	53.74	15.19	15.65	53.77	15.09
5	15.94	52.74	15.16	15.82	52.80	15.16
6	15.90	52.73	15.27	15.59	52.93	15.23

4.4 Discussion

One of the most obvious differences noted during the trial was colour change of the bolus from a light pink to a dark green (see Figures 4.4a-c and 4.4d-f), accompanied by the slight colour change of the coating from pale yellow to a dark yellow. Discolouration of polyurethane coatings is common. However, this is usually as a result of photooxidation due to UV light (Rosu, Rosu, and Cascaval, 2009; Singh, Tomer, and Bhadraiah, 2001). This yellowing occurs as a result of scission of the urethane group and photooxidation of the central CH_2 group between the aromatic rings, gradually reducing protective effectiveness of the coating. It is unlikely that the degradation of the coating was due to UV radiation due to ingestion, though it is possible that the coating underwent a similar network disruption through chemical degradation by enzymes. It was also possible that following

the weakening of the network, the coating was more susceptible to highly pigmented molecules in the rumen fluid, and this contributed to the discolouration (Petrovski, 2017). Further structural analysis would be required to confirm this. However, this was deemed out of scope for this project.

It is highly likely that interaction with the rumen fluid would have changed the glass of the bolus chemically due to the hygroscopic nature of the phosphate-based glass. However, it is uncertain whether chemical interactions occurred between the coating and the rumen fluid. This type of interaction would be unlikely due to the extreme toughness and temperature resistance of isocyanate derived polyurethane's found in the resin of the coating. Polyurethane's have a much higher temperature tolerance than the bolus would have been exposed to in the rumen, the Center for the Polyurethanes Industry, (2014) stated that thermal degradation of polyurethane products doesn't begin until at least 150 ºC, with many staying stable until 250 ºC. This large, 100 ºC temperature resistance variation is due to the hard and soft segments of the polymer as a result of crystalline and amorphous phases. However, due to the aromatic nature of the polyurethane used (Magnin *et al.* 2020), this is likely to have actually improved the stability of the coating, making even more unlikely for the internal body temperature of the sheep to facilitate an interaction between the coating and rumen fluid.

The slightly acidic nature of rumen fluid, approximately pH 5.5-6.5 (Jasmin *et al.* 2011), is also unlikely to have affected the polyurethane resin coating, as polyurethanes are notoriously chemically resistant. As such, it is highly unlikely that the slightly acidic pH of the rumen would have resulted in degradation of the coating. It is possible that under highly concentrated acidic conditions polyurethanes may begin to degrade (Xie *et al*. 2019), however, the relatively neutral pH of the rumen is unlikely to have had a corrosive degradation effect on the coating. Rumen pH can become slightly more acidic when livestock are

fed concentrate or small particulate forage (Petrovski, 2017), though a change of the magnitude required is unlikely to have occurred during this trial due to the forage provided.

Another possible method of degradation could be enzymatic, whilst the biodegradation of polyurethanes is possible, it is usually as a result of being produced from precursors including polylactic acid, or polycarprolactone which result in softer, amorphous regions of the polymer that are more susceptible to hydrolysis (Magnin *et al.* 2020). However, as the polyurethane utilised in this study was produced using 4,4'methylene diphenyl isocyanate (4,4'-MDI), which forms rigid polymeric structures resistant to chemical attack, it is unlikely to be susceptible to this type of degradation.

As this multi-material coating was designed only to be utilised at a trial scale for testing the mineral release patterns of prototype boluses, and not intended to be used for the final product at manufacturing scale, no further analysis was conducted on this. However, whilst the coating functioned well during the trial, further investigation should be carried out to understand structural changes it undergoes following ingestion. This path of study would be of significant interest to better understand and characterise the full lifespan of this coating. Techniques such as XRD to understand changes in crystallinity and FTIR could have been used to explore changes in bonding over time.

The average weight loss of the boluses was -0.42 g +/- 0.23. Using this rate of degradation, it was estimated that it would take the boluses approximately 1140 days to completely degrade (assuming a constant degradation rate). This suggested that the boluses were degrading at approximately 6.3 times slower than expected compared to what was witnessed in the *in vitro* rumen simulation experiment. It is possible that this reduced rate of degradation in the *in vitro* apparatus was caused by a tolerance stack of errors including:

The dissolution apparatus was unable to simulate adequate rumen fluid turnover and contained significantly smaller volumes of liquid compared to the rumen. This potentially resulted in a more concentrated aqueous environment, a repercussion of this may have caused a drop in solution pH, commonly witnessed during phosphate glass degradation (Bunker, Arnold, and Wilder, 1984), thereby causing hydrogen ions to increase in concentration within the simulated rumen due to hydrolysis. It was interesting that this caused increased degradation of the boluses tested *in vitro*, as the converse effect could also have been plausible due to media saturation by released ions, which could have slowed degradation. In retrospect of this the *in vitro* model would need refining in order to be a more accurate reflection of the *in vivo* conditions. An *in vitro* study utilising similar methodology while continuously measuring pH and mineral ion concentration over time would elucidate these hypotheses.

Possible methods of improving the *in vitro* rumen simulation methodology could include using larger dissolutions vessels that are more indicative of the rumen's liquid volume, and/or having a continuous flow dissolution apparatus that allowed continual or more regular replenishment of dissolution media. Following this experiment, acquisition of both larger dissolution vessels and continuous flow dissolution apparatus options were explored, though were considered too costly to incorporate at this point in time.

Additionally, the greatly reduced degradation rate of 0.014 g/day compared to expected 0.89 g/day may also have accounted for the lack of biological response witnessed in the animals. Consequently, the lack of increased blood plasma minerals was potentially a result of insufficient concentrations of the element being released rather than it potentially being unable to be utilised or excreted before utilisation. It is also likely that the lack of power behind the group sizing was an additional reason no significant increase in plasma minerals was

recorded, however, the low degradation rate is likely to be the dominant factor.

Another surprising observation was the general increase in both bolus length and diameter following dissolution. It is likely that this was as a result of digesta adhering to the surface of the glass and coating, thereby increasing both of these parameters. Additionally, this may have contributed to the surprisingly low weight loss exhibited by the boluses, and possibly prevented degradation of the bolus due to a decreased surface area. Unfortunately this would be a difficult situation to mitigate against as it would be relatively constant factor *in vivo*. Therefore, it should be considered whether silage, or grass matter could be incorporated into the *in vitro* apparatus to simulate this variable.

Another possibility that may have caused an increase in the length and diameter of the boluses could be accumulation of precipitate on the surface of the boluses. This has been witnessed in other *in vivo* studies when reviewing glass bolus degradation (Kendall, 1996) as well as more other types of phosphate-based glasses. Nava*rro et al*. (2005) confirmed that the formation of the white precipitate that had formed on the surface of their glass/polymer composites was a calcium phosphate. The author hypothesised that these units formed due to the abundance of Ca^{2+} ions in the solution. As calcium content of rumen fluid was not measured, it was not possible to assess whether the calcium concentrations present in the rumen facilitated precipitate formation.

The mineral content of the forage during the trial, contained 6.43 mg/kgDM Cu, 0.07 mg/kgDM Co and 0.01 mg/kgDM Se. These forage content values are all classed as either marginal to deficient according to Suttle, (2010). Additionally, these values do not consider whether there might be any mineral antagonism, particularly of concern for copper (Suttle, 2012). Suttle, (2010) stated that copper requirements can vary 10-fold due to interactions between iron, molybdenum and

sulphur, therefore, obtaining a full forage mineral profile would have been beneficial to understand if this was a contributing factor towards the low plasma copper concentrations, as any available copper released from the bolus may have been “locked-up” (Gould and Kendall, 2011). This could also support the suggestion, that if there was not a high concentration of antagonistic elements present in the rumen, that low absorption of copper could be as a result of the low ion release from the bolus.

Surprisingly, iodine did not elicit a similar effect to selenium, despite them being incorporated into the glass in the same way. Instead, a large drop in rumen fluid iodine was observed throughout the trial duration. This was unexpected as the animals underwent an acclimatisation period to try and minimise fluctuating mineral concentrations. Another possibility is that the iodine had started to volatilise prior to bolus administration, reducing the iodine available at the surface of the bolus. As a result of the low degradation rate, little other iodine was available to be utilised.

Due to the product development nature of this thesis, it was questioned whether the coating of the bolus could be removed in an attempt to increase the degradation rate, and decrease the requirement for additional extensive formulation testing. Whilst this was considered, it was ruled out due to toxicity concerns surrounding selenium release. As can be seen in Figure 4.10, the blood plasma selenium concentration of the bolused group was significantly higher ($p < 0.001$) compared to the control group, reaching an average concentration of 1.52 µmol/L +/- 0.37. Suttle (2010) suggested that blood plasma selenium concentrations between 1-2.0 mg/L are at risk of chronic selenosis. Whilst the average concentration of the sheep used in this study is still significantly below that “at-risk threshold” it is important to consider that the blood was taken 4-weeks after administration, suggesting that it would have been significantly higher previously. Williams, Williams and Kendall, (2017) reviewed the effected of a selenium drench on the

plasma selenium concentrations. This work recorded a sharp peak in plasma selenium by day-2 of the trial and a gradual but significant decrease by the final day of the trial on day-13. Whilst these two studies are not entirely comparable due to the different methods of administration, (drench versus bolus), it still supported the suggestion that the plasma selenium peak could have been weeks before the blood samples were taken in this study. As a result of this, for further studies to understand better the degradation profile of the bolus and mitigate safety concerns surrounding toxicity limits, more frequent blood sampling should be considered.

4.5 Conclusion

This chapter aimed to further understand the degradation rate and bioavailability of the glass composition P50-Ca2-Na17-Cu30-Co1. It attempted to establish a relationship between the speed of degradation *in vitro* and *in vivo*, and potentially understand if there was a relationship between the two that could be extrapolated to improve the research and development process for current and future formulations. Unfortunately, due to multiple variables previously unaccounted for such as dissolution vessel volume, dissolution media turn-over and digesta in the media, it was not possible to compare such a dynamic environment to a static one. However, it was established that the *in vitro* system needed refining in order to more closely simulate the conditions observed in the animal.

Additionally, two further conclusions regarding the glass formulation P50-Ca2-Na17-Cu30-Co1 and temporary coating used were that: the glass formulation being used degraded too slowly when coated and should be reviewed in order to give a better degradation profile more similar to that of the Industry Partner's ideal daily release rate; and that the temporary coating was successful at providing protection to the glass. However, should this coating be used for additional trials *in vitro* or *in vivo* further characterisation of the coating following dissolution should be considered to better understand if any interactions that occurred that may be detrimental to ion bioavailability or coating robustness.

Chapter 5 – Competitor bolus review *in vivo* trial

5.1 Introduction

As previously discussed in Chapter 1, CoseIcure boluses use phosphate-based glass in order to deliver sustained ion release and consequently trace mineral nutrition. The CoseIcure manufacturers claim that the sheep boluses supply trace mineral nutrition for up to 8-months for sheep grazing at pasture (CoseICure Boluses, 2019). As this product design is the most similar available to the Industrial Partner's desired prototype (see Chapter 2) it is of great interest as to whether this product performs as well as the manufacturers claim. Whilst the effectivity of this design to supply bioavailable elements is well publicised, for example Kendall, Mackenzie and Telfer, (2001) showed that Cosecure was able to prevent deficiency of cobalt and selenium of the trial animals for up to 105 days, it was unclear whether an effect would still be seen up to 224 days (8-months). Conversely, Zervas, (1988) documents the administration of Cosecure over a longer period of 338 days, showing it can significantly increase the concentrations of plasma copper, selenium and Vitamin B_{12} for this duration. However, despite (Zervas, 1988) using a Cosecure bolus, this may be the previous monolith design, unfortunately, this is not disclosed in the paper. The effectivity and longevity supplementing cobalt, copper and selenium with Cosecure is well documented, however, the iodine supplied from the CoseIcure bolus is not as well documented. Atkins *et al.* (2020) reviewed the CoseIcure bolus in dairy heifers and concluded that the dietary iodine values were within the marginal threshold and the bolus had little effect.

Therefore, it was vital to establish how long the CoseICure bolus was able to deliver trace mineral supplementation for and whether it was at a constant release rate as claimed. It was also intended that not only was this trial to carry out a competitor analysis of CoseIcure, but to use

this data as a positive control for the prototype product when it was ready to be trialled for a full 6-months.

The main aims of this chapter was:

- To confirm that the CoseIcure bolus was able to supply consistent trace minerals to sheep at pasture.
- To establish the total duration of the CoseIcure sheep bolus lifespan, how long its elicited effects last over the 6-months.
- To refine the experimental design of this trial ahead of product prototype testing.

In order to do this CoseICure boluses were administered to ewes at pasture and using a combination of rumen fluid samples, blood plasma mineral status and biochemical indicators such as Vitamin B_{12} concentrations the duration and efficacy of the CoseICure bolus was monitored across a 6-month duration.

5.2 Materials and methodology

This trial was supervised by Dr Nigel Kendall, in accordance with ASPA guidelines (1986) and approved by the Animal Welfare and Ethical Review Board at Nottingham University.

The schematic outlined in Figure 5.1 the processes and methods used in this section.

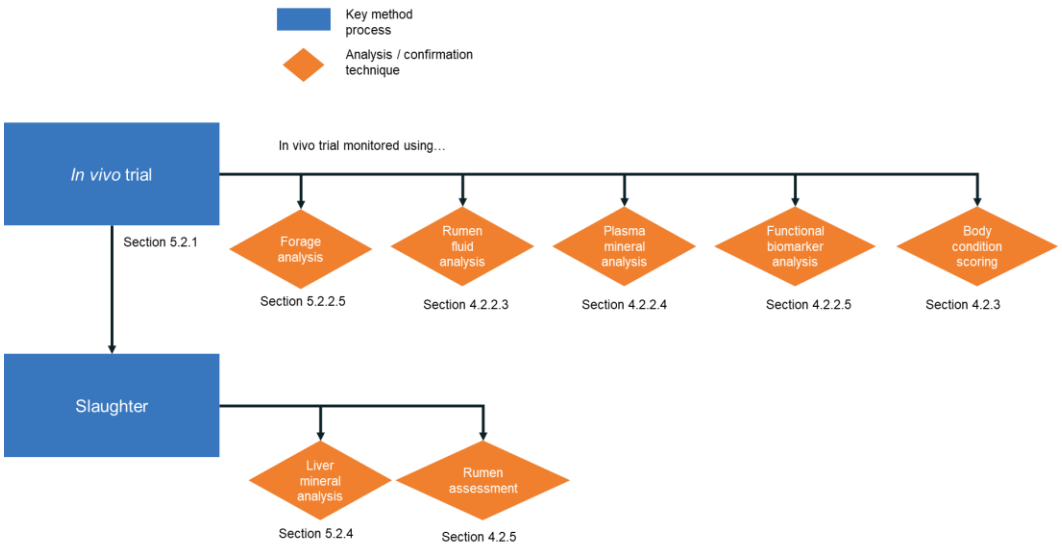

Figure 5.1: *A flow diagram to indicate the sequence of methods used within this chapter.*

5.2.1 Trial design

The trial took place over 6-months (plus an acclimatisation period of 17 days) using 20 cull mule ewes (at least 3-years old, full mouthed) grazed at pasture thought to be marginal to deficient in both selenium and cobalt content. During the acclimatisation period grass samples were taken following Clarkson and Kendall, (2018) pinch sampling protocol to establish forage mineral concentrations. Subsequently approximately monthly intervals of forage sample were taken to account for any elemental seasonality within the pasture.

Sheep were split into two equal groups using restricted randomisation of body condition scores (see Table 5.1 for groups). All treatment animals were bolused using CoseIcure (lot:161007, 2698). It was ensured that boluses were adequately administered and swallowed before releasing the animal.

Similarly to Chapter 4 group sizes were calculated based on work produced by Dr Kendall's research group, presented at the BSAS conference, 2019. This work demonstrated that for measuring plasma copper, plasma cobalt, plasma selenium, Vitamin B_{12} and glutathione peroxidase, group sizes of 4 ($P = 0.02$) and could be used for

diagnostic purposes, whereas a group size of 8 was required for statistical significance of (P = 0.05). As such in order to demonstrate significance and account for seasonal forage variation over 6-months, treatment and control group sizes of 10 were used.

Table 5.1: *Schematic of treatment and control group animals sizes.*

	Control	**Bolused**	**Total**
Group 1	N = 5	N = 5	N = 10
Group 2	N = 5	N = 5	N = 10
	*Slaughtered after 4.5-months	Slaughtered after 6-months	

*Following the assessment of blood plasma mineral concentrations, it was believed that by month-4 the boluses had been completely dissolved. Therefore, group 1 were slaughtered after 4.5 months of being on the trial to confirm this hypothesis. The remaining 10 sheep continued the trial up to 6-months and were then slaughtered.

All sheep were blood sampled by jugular venepuncture using 9 ml lithium heparin tubes (BD vacutainer, UK) and Vacuette needles (Griener Bio One Ltd, UK) and body condition scored on day-0 and subsequently at approximately monthly intervals. Group 1 animals were also sampled monthly for rumen fluid (excluding day-56 and 85 when sampling was unsuccessful due to extreme heat), following the collection method outlined in Jasmin *et al.* (2011). Table 5.2 outlined a month-by-month sampling regime, including sample analysis.

Table 5.2: *Outline of monthly samples taken and subsequent analysis. Analyses were based on: Plasma minerals - Cu, Se, Co, I (subsequently referred to as PMs) Rumen fluid - Cu, Se, Co (subsequently referred to as RFs) Biochemical indicators - Vitamin* B_{12}*, Glutathione Peroxidase (subsequently referred to as BIs).*

Month	**Samples**	**Analysis**
June- day 0	Blood samples, body condition scoring, rumen fluid samples	PMs, RFs, BIs
June- day 17	Blood samples, body condition scoring, rumen fluid samples	PMs, RFs, BIs
July – day 30	Blood samples, body condition scoring, rumen fluid samples	PMs, RFs, BIs
August – day 56	Blood samples, body condition scoring	PMs, BIs
September – day 85	Blood samples, body condition scoring	PMs, BIs
October – day 121	Blood samples, body condition scoring, rumen fluid samples	PMs, RFs, BIs
Group 1 slaughtered after day 121. Liver samples taken for mineral concentration		
October – day 144	Blood samples, body condition scoring	PMs, BIs
November – day 155	Blood samples, body condition scoring	PMs

November – 175 day	Blood samples, body condition scoring	PMs
November – day 179	Group 2 slaughtered Blood samples and liver biopsy	PMs

5.2.2 Elemental mineral analysis

5.2.2.1 Forage analysis

Pinch sampling of the pasture grazed was performed following protocol published in (Clarkson and Kendall, 2018) to mimic grazing. Grass was then freeze-dried (Modulyo, M143, UK) until no further weight loss was measured (approximately 100 hours), once dried a sample of the grass was then sent to Tangerine Holdings for multi-element analysis (excluding iodine) using acid digestion, followed by ICP-OES. Some of the sample was retained at Nottingham University to analyse the iodine concentration of the grass.

Acid digestion of forage was carried out by weighing 0.3 g of freeze-dried grass into the digestion vessels (Perkin Elmer, UK), 8 ml of 70 % nitric acid (VWR International, UK) and 2 ml 30 % hydrogen peroxide and digested using the Titan MPS Microwave (Perkin Elmer, UK) and digested at 175 ºC, 30 Bar (using 10 minute ramp), 20 minute hold time and then cooled to 50 ºC, 30 Bar and held for 10 minutes at 1 minute ramp time. Digestion vessels were then emptied into a falcon tube (Fisher Scientific, UK), ensuring to wash the side digestion vessels and made up to 50 ml.

Forage mineral analysis was carried out using an Optima 8000 (Perkin Elmer, UK) inductively coupled plasma optical emission spectrometry (ICP-OES). Calibration is carried out using internal standards: Mg (100 ppm), K (1000 ppm), Na (100 ppm), S (100 ppm), Mn (100 ppm), Cu (10 ppm), Zn (10 ppm), Co (0.1 ppm), Mo (1 ppm), Se (0.1 ppm), Fe (100 ppm), Al (100 ppm), all reagents were supplied by VWR

International, UK and deionised water (Normatom, VWR International, UK).

Elemental iodine forage analysis was conducted by the NuVetNA team following the same methodology outlined in Section 5.2.2.2.

5.2.2.2 Forage inorganic iodine content

Plasma inorganic iodine was unable to be assessed using the same ICP-MS protocol outlined in Section 4.2.5 as it requires running on a difference matrix. Therefore, 1 ml of wet sample or 0.1-0.2 g of dried sample was weighed into a 50 ml centrifuge tube (Falcon, Fisher Scientific, UK) and a 5 % solution of tetramethylammonium hydroxide (25 % w/w TMAH, VWR Ltd, UK) with deionised water (Purite h 160, Suez, UK 17 MΩ). This mixed solution is then vortex mixed and incubated for 3-4 hours at 70 ºC, vortex mixing half-way through and again at the end of incubation. After the final agitation, volumes are made up to 25ml to achieve a final TMAH concentration of 0.2 %. Samples were then mixed and centrifuged at 2000 g for 1 minutes (Allegra x22, Beckman Coulter, UK) before decanting into ICP tubes (55.538, Sarstedt, UK) for ICP analysis.

ICP-MS (Thermo-Fisher iCAP-Q) with an internal standard (5 ppb Rhenium in 1 % TMAH) incorporated into the sample stream using a T-piece. External calibration standards are within the range 0-100 µg/L (ppb). Samples are introduced using a covered auto-sampler (CetacASX-520) through a 1317090 pfa-st nebulizer (ESI, Thermo-Fisher Scientific, UK). Samples are processed using the Qtegra software (Thermo-Fisher, UK).

5.2.2.3 Rumen fluid analysis

All rumen fluid analysis was carried out by the NuVetNA team, following the same methodology used in Chapter 4, Section 4.2.4.

5.2.2.4 Plasma mineral analysis

All plasma mineral analysis was carried out by the NuVetNA team, following the same methodology used in Chapter 4, Section 4.2.5.

Plasma inorganic iodine is measured on a separate method outlined in Section 5.2.2.2

5.2.2.5 Biochemical indicator analysis

All biochemical indicator analysis was conducted by the NuVetNA team following the protocols discussed below. Biochemical indicator analysis was conducted in order to confirm the metabolism of the trace elements into their functional constituents: Vitamin B_{12} for cobalt, glutathione peroxidase for selenium and plasma inorganic iodine for iodine.

5.2.2.5.1 Vitamin B_{12}

One 25 µl aliquot of frozen plasma was sent to the Animal Health and Plant Agency (AHPA) Biochemistry Laboratory (UK) where Vitamin B_{12} concentrations were measured using the Vitamin B_{12} assay (Advia Centaur CP, Siemens, UK) according to the manufacturer's recommendations.

5.2.2.5.2 Glutathione peroxidase

One 25 µl aliquot of heparinised whole blood was diluted using 1 ml RANsel (Randox Laboratories, UK) diluent and gently agitated. This solution was then assayed using the RANsel kit (Randox Laboratories, UK) according to the manufacturer's instructions on a RX IMOLA clinical chemistry analyser (Randox Laboratories, UK). Results were expressed relative to previously estimated haematocrits as U/ml pack cell volume (PCV).

Hematocrit (PCV) is the measure of the ratio of the volume occupied by the red blood cells to the volume of whole blood. The blood sample is drawn into a capillary and centrifugated and then the ratio can be measured and expressed as a decimal or percentage fraction (Kendall, 2021) .

5.2.3 Body condition scoring (BCS)

Body condition scoring was carried out through the trial to ensure the safety of the animals used during this trial, as well as observing any

possible improvements or deterioration in animals' physical condition as a result of trace element supplementation or deficiency.

Following the standardised scoring system outlined in AHDB, (2014) "Better return programme", body condition scoring was carried out at monthly intervals by Dr Nigel Kendall to ensure consistency across the trial.

5.2.4 Liver concentration analysis

Liver concentration was measured in order to monitor storage of elements such as copper or cobalt, indicative of excessive supplementation.

Fresh liver samples were collected immediately after slaughter and stored at -20 ºC. Slices of liver approximately 1 mm thick were cleaved from the central tissue using a clean scalpel until ~0.8 g was reached. These samples were then freeze-dried (Modulyo M143, UK) until no further weight loss was measured (~100 hours). Replicates of ~0.5 g were weighed directly into Teflon microwave digestion tubes (HVT50, Anton Paar, UK) and incubated for 1 hour with 3 ml 68 % HNO_3 (Fisher Scientific, UK), 3 ml deionised water (Purite hp 160, Suez, UK, 17MΩ cm), and 2 ml 30 % H_2O_2 (< 99 %, Fisher Scientific, UK), then digested for 45 minutes (10 ramp to 140 ºC, 20 minute hold and then cooled to 55 ºC for 15 minutes) in a multi-wave 3,000 microwave (Anton Paar, UK), alongside blanks and reference material (bovine liver- 1577c, National Institute of Standards and Technology, USA). Digested samples were transferred into universal tubes (Sarstedt, UK) with 7 ml deionised water (Purite hp 160, Suez, UK, 17 Ωcm) and inverted to mix. Then following the same method as outlined in Section 5.3.2.1 500 µl was pipetted for analysis using ICP-MS.

5.2.5 Rumen dissection

See Chapter 4, Section 4.2.6 for rumen dissection details.

5.2.6 Statistical analysis

Statistical analysis of all parameters was carried out using Prism 7 (GraphPad Software, UK). An unpaired T-test using the Holm-Sidak Method, with an alpha value of 0.05 compared each row without assuming a consistent standard deviation (S.D) in order to establish significance. Log transformations for data such as plasma cobalt, Vitamin B_{12} and plasma inorganic iodine was used in order to achieve approximately normal residuals within ANOVA.

5.3 Results

5.3.1 Forage analysis

Figure 5.2 outlined the trace mineral content of the pasture grazed throughout the trial. During the trial the mineral content of copper, cobalt and selenium is recorded as low (Sciantec Analytical, 2020). The sharp decrease in cobalt and copper, and increase in selenium content on day-30 was due to the sheep being moved to different fields. Sheep also changed fields at day-85 and again on day-155. Towards the end of the trial pasture cobalt and iodine content was increasing.

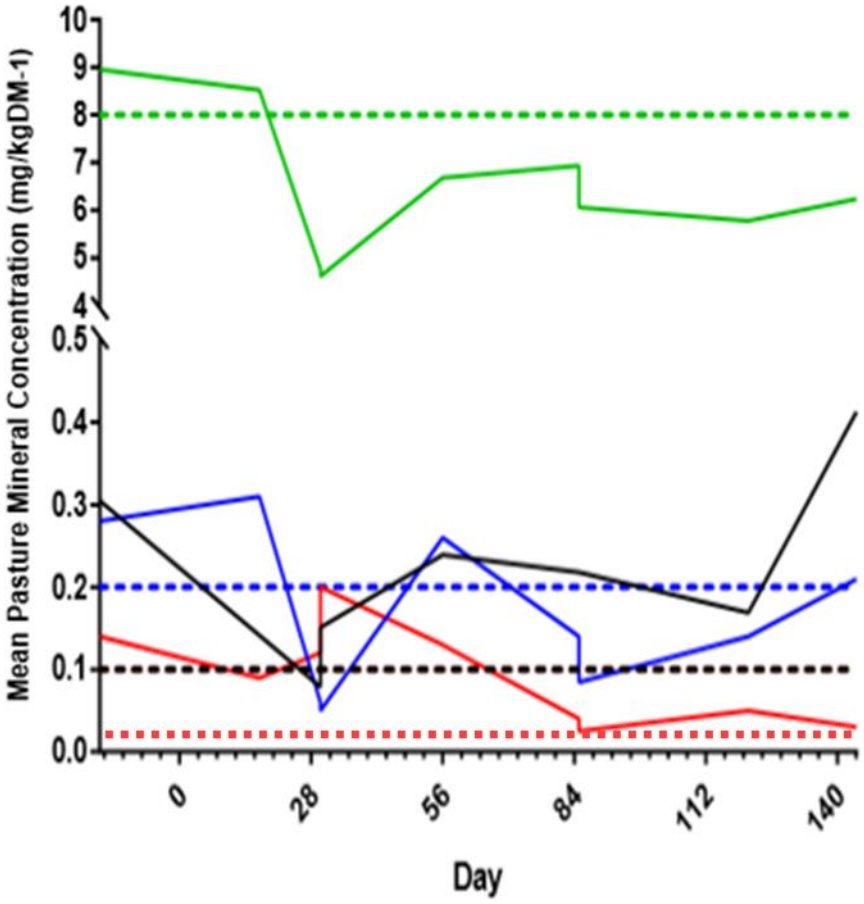

Figure 5.2: *Trace mineral content of the pasture grazed during the trial (mg/kgDM). Solid lines represent actual forage concentrations, broken lines represent indicative status of "low" mineral concentration of pastures. Copper concentration is represented by the green lines, cobalt by the blue lines, selenium by the red lines and iodine by the black lines.*

5.3.2 Rumen fluid analysis

Figure 5.3 showed the rumen fluid concentrations for cobalt, copper and selenium for both bolused and control groups. A peak in concentration was seen at day-30 for all elements, with significance shown for cobalt ($p < 0.05$) and copper ($p < 0.01$) concentrations. From day-30 onwards concentrations decreased back to or below control concentrations by day-85. No significant results were recorded for selenium concentration at any time point. Unfortunately, due to funding limitations iodine content was unable to be measured.

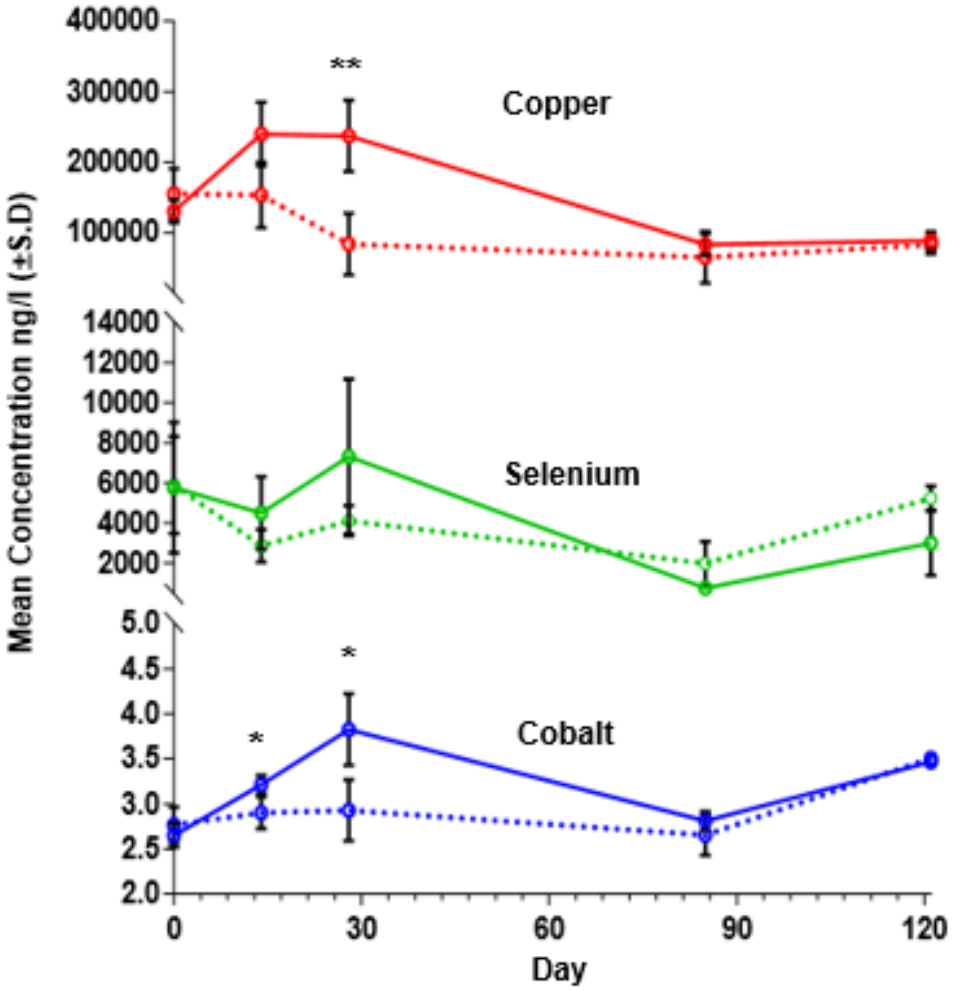

Figure 5.3: *The mean rumen fluid concentration for copper, selenium and cobalt (ng/L +/- S.D). Solid lines represent the bolused group (n = 5) and broken lines the control group (n = 5). Red shows the copper concentration, green shows the selenium concentration and blue shows the cobalt concentration Statistical significance: *(p < 0.05), **(p < 0.01)*

5.3.3 Plasma minerals and biochemical indicators

5.3.3.1 Plasma copper concentration

The blood plasma copper concentrations for the bolused group showed no statistical significance compared to the control group (Figure 5.4) at any time points. The ideal range for plasma copper concentration is 12-19 µmol/L, and 9.4 to 12 µmol/L is marginal. Values above 23 µmol/L indicate an acute phase or elevated plasma copper and are undesirable.

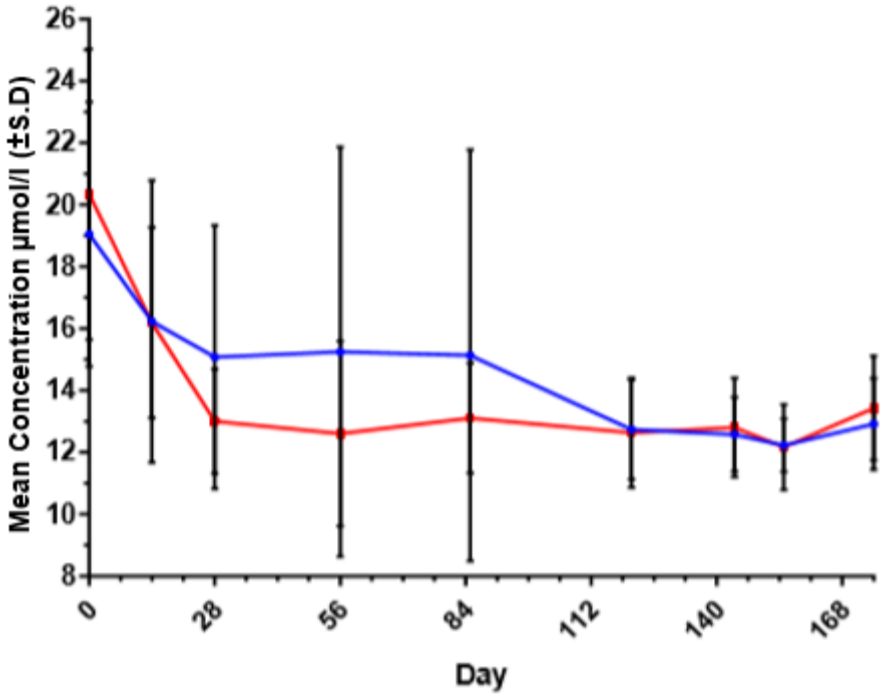

Figure 5.4: *The mean blood plasma coppers (µmol/L +/-S.D). The blue line represents the bolused group, and the red line represents the control group (for both bolused and control n = 10 up to day-121, and n = 5 from day-121 onwards).*

5.3.3.2 Plasma cobalt concentration

Blood plasma cobalt concentration (logged) ideally lies between the range 0.699-1.176 nmol/L, 0.699-0.477 nmol/L is marginal and < 0.477 nmol/L is deficient. As can be seen from Figure 5.5 the plasma cobalt concentration for the bolused animals significantly increased up to day-56 *(p* < 0.001) when the concentration peaks at 1.678 nmol/L before decreasing to similar concentrations as the control animals by day-121. This was in sharp contrast to the control animals whose plasma cobalt concentrations decreased after day-0 into the deficient range, and did not increase into the marginal range until day-144.

Towards the end of the trial both control and treated animals showed a dramatic increase in their plasma cobalt concentrations on day-175 up to 1.633 +/- 0.205 nmol/L and 1.771 +/- 0.159 nmol/L respectively.

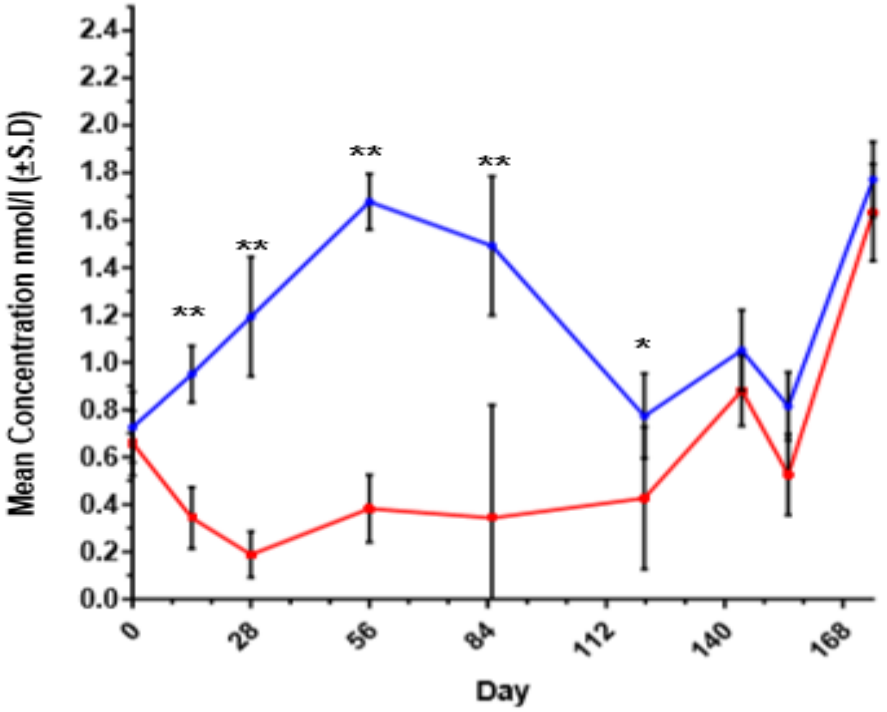

Figure 5.5: *The mean log plasma cobalt concentrations (nmol/L +/- S.D). The blue line represents the bolused, and the red line represents the control group (for both bolused and control n = 10 up to day-121, and n = 5 from day-121 onwards). Statistical significance *(p < 0.05), **(p < 0.001)*

5.3.3.3 Plasma selenium concentration

Similarly, to the plasma cobalt concentration the plasma selenium concentration demonstrated a significant increase in the treated animals compared the control animals. The plasma selenium concentrations were significantly higher ($p < 0.001$) than the control group for all days (excluding day-0) up until day-144, when significance was decreased to ($p < 0.01$). The increase in plasma selenium concentration resulted in the treated animals plasma concentrations elevating from the suboptimal range of 0.5-0.9 µmol/L into the ideal range 0.9-1.5 µmol/L, whereas the control animals remained relatively consistent in the suboptimal range. No animals decreased into a marginal <0.22 µmol/L, or deficient <0.1 µmol/L range.

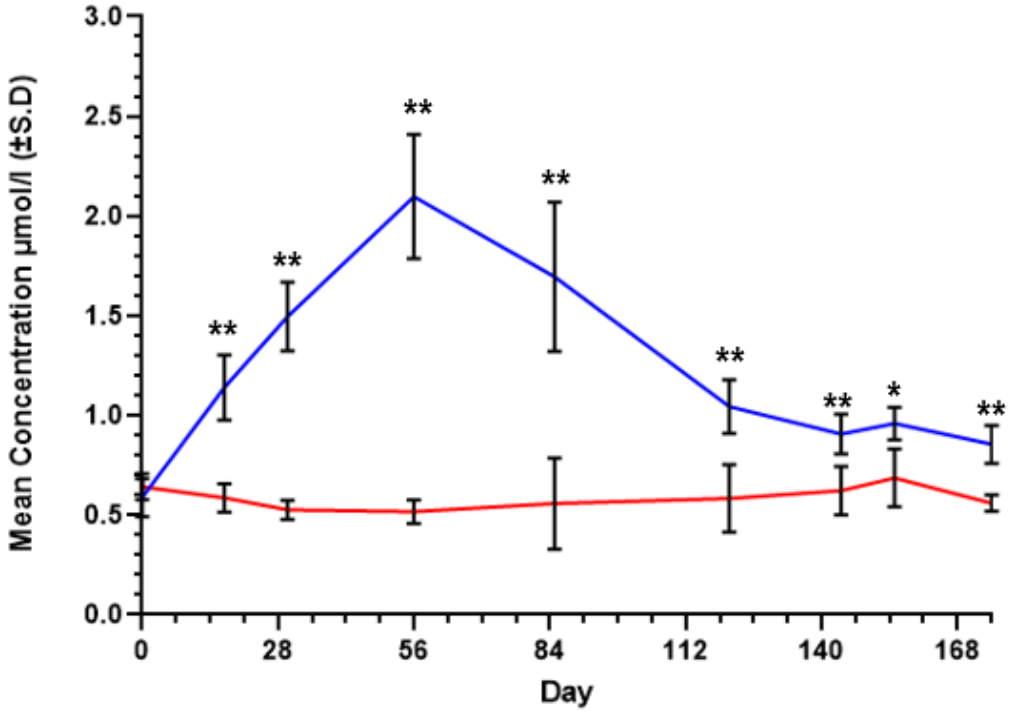

Figure 5.6: *The mean plasma selenium concentrations (µmol/L +/- S.D). The blue line represents the bolused group, and the red line represents the control group (for both bolused and control n = 10 up to day-121, and n = 5 from day-121 onwards). Statistical significance *($p < 0.01$), **($p < 0.001$).*

5.3.3.4 Plasma inorganic iodine concentration

Similarly to the both of the trends recorded for plasma cobalt and plasma selenium concentrations, the plasma inorganic iodine concentration significantly increased up to day-56 ($p < 0.001$), before it decreased back in line with the controls by day-85. Throughout the study the control animals remained within the deficient status <1.699 µg/L, unlike the bolused animals that exceed the marginal range (1.699<2 µg/L) and into adequate concentrations in excess of 2 µg/L before decreasing back into the deficient range by day-85.

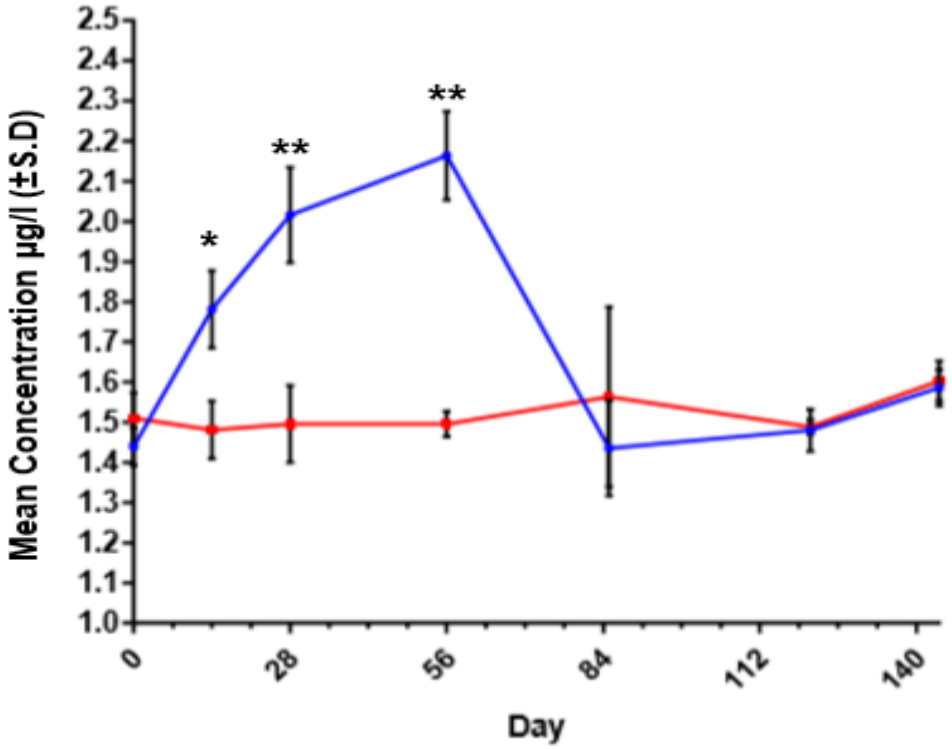

Figure 5.7: *Group 1 (n=10) mean log blood plasma inorganic iodine (µg/l +/-S.D). The blue line represents the bolused group, and the red line represents the control group (for both bolused and control n = 10 up to day-121, and n = 5 from day-121 onwards). Statistical significance *(p < 0.01), **(p < 0.001).*

5.3.3.5 Vitamin B_{12} concentration

Vitamin B_{12} significantly increased in concentration on days-17 ($p < 0.05$), 30 ($p < 0.001$), 56 ($p < 0.01$) and 85 ($p < 0.05$) compared to the control group, however, by day-121 no significant differences were

recorded. Over the duration of the trial there was an increasing baseline of Vitamin B_{12} concentration seen both in treatment and control animals.

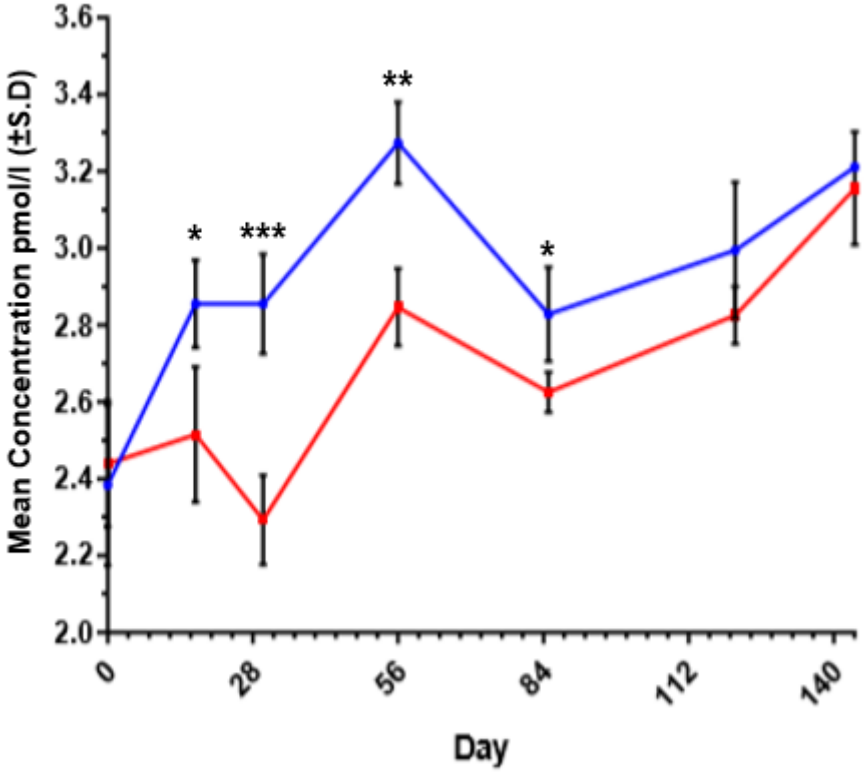

Figure 5.8: *A graph showing the mean Vitamin B_{12} concentration of group 1 (n=10) (pmol/L +/-S.D). The blue line represents the bolused group, and the red line represents the control group (for both bolused and control n = 10 up to day-121, and n = 5 from day-121 onwards). Statistical significance *($p < 0.05$), **($p < 0.01$), ***($p < 0.001$).*

5.3.3.6 Erythrocyte glutathione peroxidase activity

The biochemical indicator of selenium is erythrocyte glutathione peroxidase (GSH-Px), this significantly increased in concentration throughout the duration of the trial, and demonstrated a significance on days-17 ($p < 0.01$), ($p < 0.05$), 56 ($p < 0.01$) and days-85, 121 and 144 ($p < 0.001$).

Despite the increased concentration of GSH-Px of the bolused animals, the control animals concentration remained relatively constant at 69.753 +/- 24.97 U/ml PCV, but recorded a very small increase (non-significant) towards the end of the trial.

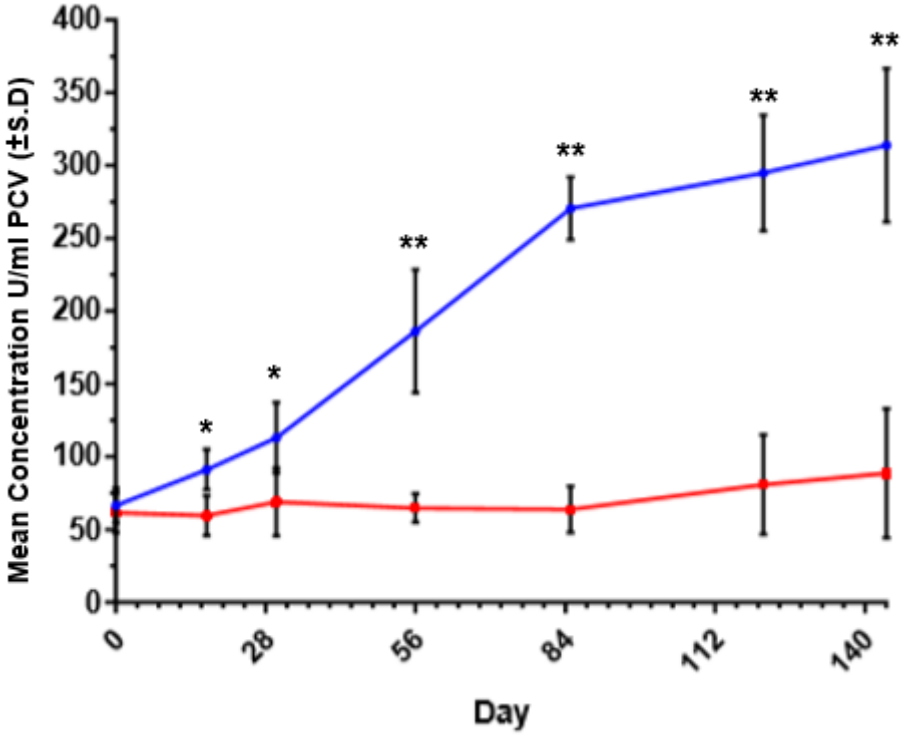

Figure 5.9: *The mean erythrocyte glutathione peroxidase activity (U/mlPCV, +/- S.D). The blue line represents the bolused group, and the red line represents the control group (for both bolused and control n = 10 up to day-121, and n = 5 from day-121 onwards). Statistical significance *(p < 0.05), **(p < 0.001).*

5.3.4 Body condition scores

At the beginning of the study, all trial animals body condition scores were between 2 and 3.5. Throughout the trial all animals remained within a healthy body score and there was no significant differences seen between the groups at any time points.

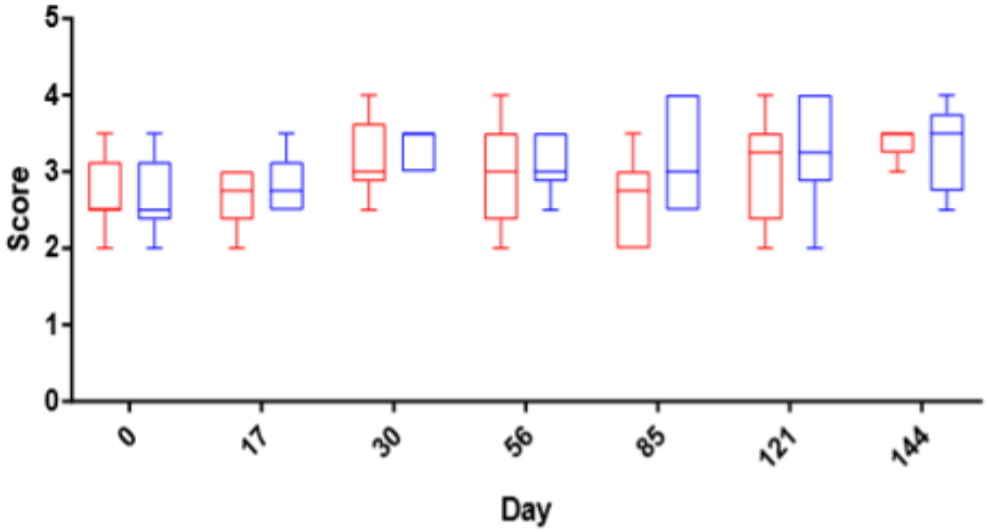

Figure 5.10: *Body condition scores of the sheep used throughout the trial. The blue boxes represent the control group, and the red boxes represent the bolused group. For both bolused and control groups n = 10 up to day-121, and n = 5 for both bolused and controls from day-121 onwards.*

5.3.5 Liver concentrations

No significant difference between the groups was observed for copper concentrations (P=0.075). However, as can be seen in Figure 5.11a, 3 out of the 5 bolused sheep in Group 1 had liver copper concentrations higher than normal (6,774 µmol /kgDM, 8,142 µmol /kgDM and 11,106 µmol/kgDM), with two exceeding the AHVLA top reference range of 8000 µmol/kgDM (Clarkson, 2019).

Figures 5.11b and c showed the liver cobalt and selenium concentrations (respectively). There was no significant differences in the liver cobalt concentration of the bolused and control group for Group 1. However, the Group 2 bolused animals liver cobalt

concentration were significantly ($p < 0.05$) higher than the bolused animals in Group 1, 6.54 µmol/kg DM and 3.14 µmol/kg DM respectively.

There was a significant difference between the control groups and their respective treatment groups for liver selenium concentration ($p < 0.001$). All control animals (excluding one who had a lower status), were within the lower marginal to deficient range for selenium (4.5 to 6.8 µmol/kgDM), whereas, treatment animals were all within the marginal (6.8<11.33 µmol/kgDM) or normal limit (11.3 to 67.3 µmol/kgDM) (Kendall, 2021).

a)

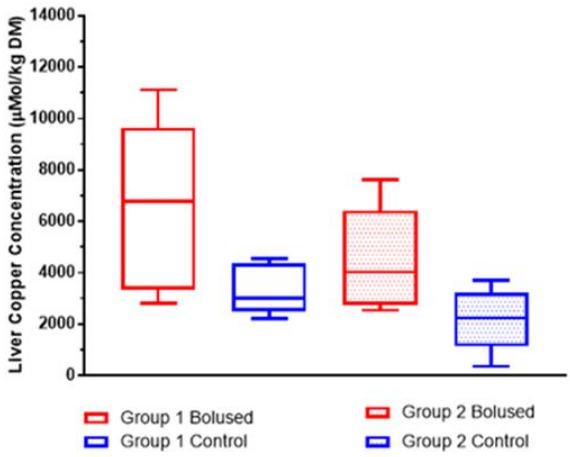

b)

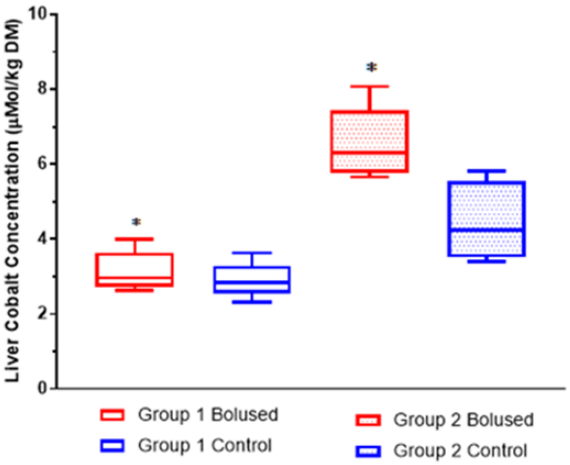

c)

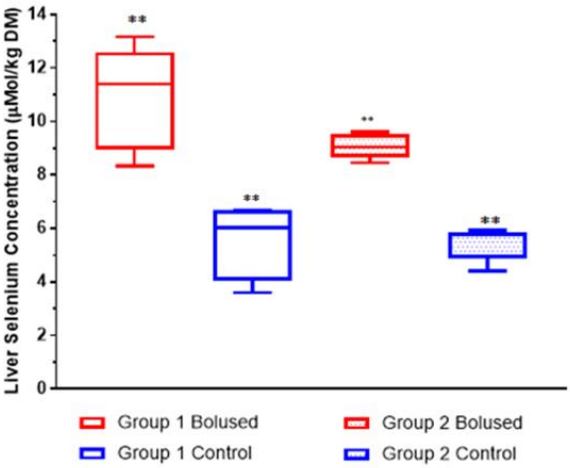

Figure 5.11*: Box and whisker plots showing the liver concentration of treatment and control groups during and after the trial. Figures 5.11 shows the liver copper concentration, b) liver cobalt concentration and*

*c) liver selenium concentration for groups 1 and 2. Group 1 was slaughtered after day-121 (n = 5 for bolused and n = 5 for control), Group 2 was slaughtered after day-179 (n = 5 for bolused and n = 5 for control). Statistical difference *(p < 0.05), **(p < 0.001).*

5.3.6 Slaughter recovery

5.3.6.1 After 4.5-months

After reviewing the 4-month plasma mineral concentration data it appeared highly likely that all the boluses had dissolved by this point. As a result of this Group 1 sheep were slaughtered on day-144 (25/10/2019), and after thorough searching of the entire rumen, it was confirmed no boluses were left in the 5 bolused sheep.

5.3.6.2 After 6-months

After 6-months Group 2 went to be slaughtered on the day-179. Whilst at the abattoir blood samples, livers and rumens were recovered. Rumens were transported back to the University of Nottingham where they were thoroughly searched for boluses, however no boluses were found.

5.3.7 Estimated ion release based on 4-month degradation

Due to the accelerated degradation of CoseIcure, (4-months instead of 8-months). It was likely that the ion release rate would be approximately double that of which the label claims assuming an even rate of ion release and degradation. The bar chart displayed in Figure 5.12 compared the daily ion release values based on an 8-month degradation, versus the estimated ion release values for a 4-month degradation.

Owing to the faster degradation rate it was possible that the daily toxicity limits (Suttle, 2010) were being exceeded and as such have been added to the graph for visualisation purposes.

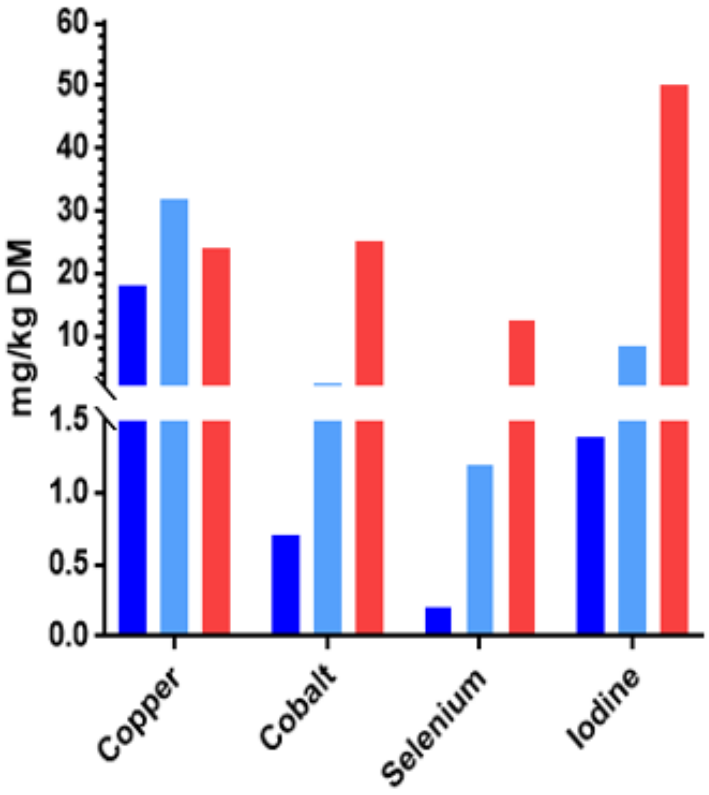

Figure 5.12: *Estimated daily ion release concentrations of CoseIcure based on their label claims of lasting 8-month (dark blue), an extrapolated ion release rate based on their product duration of 4-month (light blue) and the toxicity limits (red)* (Suttle, 2010).

5.4 Discussion

The data displayed in Figure 5.3 showed the rumen fluid concentrations for copper, cobalt and selenium. Interestingly, both copper and cobalt concentrations immediately increased, showing significant results at day-17 and day-30 ($p < 0.05$) for cobalt, and at day-30 ($p < 0.01$) for copper. However, selenium showed no significance at any time point. This is an interesting finding as the plasma selenium concentration data (Figure 5.6) and subsequent glutathione peroxidase parameters (Figure 5.9), were significantly increased from day-17 until the end of the trial. One reason selenium might have showed no significant increase in the rumen fluid concentration compared to copper may have been that the majority of the selenium absorption from sodium selenate occurs in the rumen via microbial organisms (Galbraith *et al.* 2016). Therefore it is possible that the selenium was utilised much quicker from the rumen than elements such as copper, which is more readily absorbed further down the digestive tract in the duodenum (Turner *et al.* 1987). Which could have been why the selenium concentration did not significantly increase in the rumen fluid.

On days-17, 30 and 121 the majority of treatment animals selenium status were within the optimal range (0.9-1.5 µm). However, on days-56 and 121 the majority of treatment animals status was above optimal (1.5 µm<). Suttle, (2010) stated that chronic selenium toxicity is at risk when plasma selenium concentrations are within a range of 2-3.0 mg/L (Table 5.3, shows the conversion of µm to mg/L). The values in the Table 5.3 suggest the sheep were not at risk of selenium toxicity, despite there being a significant difference between the liver selenium concentration of the control and treatment group (as seen in Figure 5.11c). Therefore, even at the boluses accelerated degradation rate, it appeared that the selenium ion release exhibited was not at risk of acute clinical toxicity, however this does suggest an oversupply. As selenium is an element that has relatively large toxicity limits and exhibits prolonged biomarker production after high doses,

supplementing this element in this method is not harmful. However, supplementing in this way demonstrates similarities to drenching and for lower toxicity threshold elements or elements requiring a consistent supply would not be recommended

Table 5.3: *Conversion of Plasma selenium concentrations from µm to mg/L.*

µm	mg/L
1.5	0.11844
2	0.15792
2.5	0.1974

(Molar mass of selenium = 78.96)

Despite a peak in plasma selenium concentration at day-56 being recorded, the biochemical indicator for selenium, glutathione peroxidase, was still significantly elevated by the end of the trial compared to the control group. It is likely that this was due to the longer half-life of selenium within sheep. Kendall *et al.* (2011) showed that administering a single drench containing 625 mg/L of selenium, resulted in a peak of plasma selenium concentrations at day-2, with an increase in glutathione peroxidase levels not recorded until day-13. This work supported the results displayed in Section 5.3.3.6 that showed a delayed but prolonged increase in glutathione peroxidase concentration compared to the more immediate but quickly declining plasma selenium concentration increase.

Similarly, Thompson *et al.* (1981) found that due to the prolonged lifespan of erythrocytes, up to 151 days in sheep (Judd and Matrone, 1962) a prolonged duration and subsequent decline of glutathione peroxidase was often observed, and as a result may not necessarily be indicative of the current animal's selenium intake. Therefore, CoseICure's label claims that the bolus lasts up to 8-months may be

derived from the extended life-span of glutathione peroxidase rather than the bolus still being present in the rumen.

Significantly increased plasma cobalt concentrations were also recorded in the treatment group compared to the controls, days-17, 30 and 85 ($p < 0.001$) and day-121 ($p < 0.01$). At day-0 the majority of animals (treatment and control) were within the marginal range for plasma cobalt, from day-17 onwards. The two groups diverge in opposite directions, control into the deficient range and treatment into adequate. This divergence carried on until day-30 when the control group's status stabilised in the deficient range, whilst the treatment group increased above the ideal range at day-56, before decreasing back into the adequate range by day-121. This suggested that peak cobalt ion release was between days-56 and 121. This hypothesis was supported by the Vitamin B_{12} data, when a peak was also seen at day-56 before decreasing. Interestingly, despite the decreased plasma cobalt concentrations seen at day-85, Vitamin B_{12} concentrations steadily increased. This is likely to be as a result of the increased cobalt content of the forage (Figure 5.2) as this increase was also seen in the control animals. As cobalt content fluctuates with seasonality, pasture cobalt content increases as weather becomes wetter (Cuesta *et al.* 1993; Sherrell, Brunsden, and McIntosh, 1987; Metherell, 1989). This may also be the cause of the significant difference between the liver cobalt concentrations of the two groups. Group 2 have a significantly ($p < 0.001$) higher liver cobalt concentration than Group 1, who were slaughtered at 6-months and at 4.5-months respectively. Therefore, it may have been caused by a cumulative effect of the combination of the bolus, coupled with the increased cobalt concentration in the forage that a higher proportion of the cobalt was stored in the liver for Group 2 treatment animals.

Figure 5.7 showed the plasma inorganic iodine significantly increased from day-17 ($p < 0.01$) until day-56 ($p < 0.001$) before it decreased back to the baseline by day-85. One possible cause for this rapid decrease

may be that plasma inorganic iodine was readily metabolised and converted to functional constituent thyroxine (T_4) (Johnsen *et al.* 2018). Iodine has relatively poor long term storage in ruminants meaning that a regular supply is essential (Suttle, 2010). The sharp decline in concentration implied that it is at this point that the bolus, or iodine within the bolus had been exhausted. This coupled with the seasonality of iodine in the forage as summer months are usually when iodine content is lowest in the UK (Alderman and Jones, 1967), means that it was highly likely iodine availability was very low, hence the rapid decrease in plasma inorganic iodine content.

Conversely to the other elements discussed, despite seeing a significant increase in copper rumen fluid concentration, plasma copper concentration showed no significant changes compared to the control group. Retrospective review of the power after analysis the standard deviation and group differences, suggested that a difference of at least 3.99 µmol/L would be required in order generate power of 0.8 and above. As a result of high variation between the groups a mean difference of only 3.37 µmol/L was recorded for plasma copper suggesting that for a group size of 10 that power would have been closer to 0.65. Therefore, as the group sizes were under powered to show significance for plasma copper, larger group sizes would be needed in future.

Unfortunately, there was no superoxide dismutase (SOD) data (samples were taken however due to a storage malfunction were unable to be analysed) to suggest whether it was due to being utilised quickly and converted to SOD that little difference was seen, similarly to selenium. However, Wooliams *et al.* (1983) showed that there was a strong correlation between the plasma copper content and SOD content, but found a decreasing rate of increase in SOD activity with increasing copper concentration at the upper end of the range. Therefore, it is plausible that due to the adequate plasma copper concentrations observed in all animas, that it is unlikely any significant

difference would have been seen in SOD activity. This suggestion was also supported by the increased copper liver concentration, showing that 3 out 5 bolused animals had copper liver concentrations higher than normal, implying that the excess copper was being stored (Goonerate *et al*. 1989). This is of great concern, as additional supplementation to animals of an adequate status is excessive and puts sheep at a greater risk of copper toxicity (Kendall *et al.* 2003).

There is a general trend that increases in cobalt, selenium and iodine blood plasma concentrations were observed up until day-56, before a gradual decrease was observed. There are potentially two theories for this peak being observed at day-56.

Day-56 may have been the point at which CoseICure's bolus had reached its maximum surface area. The bolus would still be relatively large in size macroscopically, but due to the mechanism of degradation the surface of the bolus would have been much rougher and pitted giving an even higher surface area (Kendall, Mackenzie, and Telfer, 2001). It was likely that this resulted in the bolus having its largest surface area exposed around day-56 rather than the start and as a result caused a peak in ion release. As a consequence of this, the high plasma concentrations were observed.

An alternative hypothesis was that the ion release peak could have occurred before day-56, and the high concentrations observed at day-56 were as a result of high accumulative mineral concentration present in the rumen fluid which was subsequently utilised in the following days.

This second hypothesis is unlikely due to the continual turn-over and utilisation occurring in the rumen. Thewis *et al.* (1979) showed that average ruminal turnover is between 8-11 hours depending on dry matter intake, suggesting that a concentration gradient that would be required for this hypothesis is unlikely. However, to distinguish between these two hypotheses further *in vivo* testing would be required to show the gradual degradation of the bolus during the earlier months of

supplementation. Regardless of which hypothesis was correct, it was clear these results demonstrated that the ion release supplied by the CoseIcure bolus was not uniform over the course of 8-months.

Figure 5.12 showed the theorised ion release rates of CoseIcure based on the label claims (8-month degradation), versus the estimated ion release rates based on the assumption that CoseIcure dissolves uniformly in approximately 4-months. Unfortunately, it was difficult to predict what the actual release rate from CoseIcure was, as the data collected appeared to suggest that the dissolution is not linear, peaking around day-56 before tailing off. Additionally, because the rumen is a dynamic environment, utilising elements as they become available it is unlikely definitive values would be able to be measured. Therefore, the bar chart exhibited in Figure 5.12 was intended to highlight that due to the increased rate of degradation, there was a high likelihood that the concentrations of elements being supplied may exceed acute toxicity limits. This assumption is supported by the data displayed in Section 5.3.5, Figure 5.11a, that suggested copper loading of the liver that may have been indicative of acute phase copper toxicity (Kendall *et al*. 2015).

Throughout the trial, the majority of the elements recorded remain within the lower content ranges for forage (Sciantec Analytical, 2020). This resulted in the control animal's plasma concentrations remaining around the marginal limit for their respective element, though due to some seasonality and field to field variation, large fluctuations were recorded between the sampling points. For example at day-121 the iodine content of the forage was 0.218 mg/kgDM, whereas on day-144 it was recorded as 0.413 mg/kgDM. As a result of this an increase in iodine content, both treated and control animals inorganic iodine concentrations were observed, 1.48 +/-0.05 µg/L to 1.58 +/-0.05 µg/L and 1.49 +/-0.02 µg/L to 1.59 +/-0.05 µg/L respectively. This demonstrates that it is critical to record the forage content and seasonal trends associated with the elements being assessed.

5.5 Conclusion

This trial aimed to understand the duration and efficacy of the CoseICure bolus when administered to sheep at pasture. Overall, it appeared that the CoseIcure bolus effectively supplemented trace minerals (Co, Se and I) under the trial conditions for 3 < 4 months, according to blood plasma mineral status. However, longer lasting biochemical indicators such as glutathione peroxidase remained elevated well after the bolus had degraded, and were likely to stay elevated until approximately 8-months. Both the plasma minerals and biochemical indicators suggested that there were varying levels of elemental release across the duration of the products life-span, as indicated by the bell-shaped data curves. Consequently, it was possible that due to the accelerated rate of degradation, elements with narrower toxicity limits such as copper may have been at risk of being exceeded.

Following the results outlined in this Chapter, careful consideration should be given to the inclusion levels and ion release rates of the Industry Partner's bolus if it is to continue using a similar delivery mechanism to that of the CoseIcure bolus to ensure toxicity limits are not breached.

Additionally, after reviewing the plasma copper status of animals throughout the trial, the high level of variation within groups suggested that there was not enough power in the group sizes used to show a significant difference. As such, if further work should be conducted to assess the efficacy of the Industrial Partner's prototype, a group size exceeding 10 animals would be required in order to show significance for plasma copper concentrations.

Chapter 6 - The efficacy of cobalt oxide nanoparticles in sheep

6.1 Introduction

Chapter 1 discussed that NP have shown great promise as a method of improving elemental bioavailability to animals. This could reduce supplement production costs for the manufacturer due to the reduced quantity required compared to its standard microparticulate counterparts, and reduce the volume of minerals used by farmers. As such, the Industrial Partner in this project wanted to consider the feasibility of incorporating NP into some of their existing nutritional supplements for ruminants, and the substitution of microparticles (MP) for novel nutritional NP would act as a product differentiator, giving a unique selling point (USP) and competitive advantage in market. Despite NP not being registered on the European feed additives register, the Industrial Partner had decided that if NP had significantly increased the Vitamin B_{12} concentrations of the NP treatment group compared to the cobalt sulphate group they would have applied for the addition of the cobalt oxide NP in drenches to the register.

The aims and objectives of this trial were:

- To understand whether lower concentrations of cobalt oxide (Co_3O_4) NP were bioavailable to sheep as a drench format by increasing the Vitamin B_{12} concentrations compared to the beginning of the trial and control group.
- If the cobalt oxide (Co_3O_4) NP were bioavailable to the animals, whether the NP were a more effective supplement than cobalt oxide (Co_3O_4) or cobalt sulphate ($CoSO_4.7H_2O$) MP by significantly increasing the Vitamin B_{12} concentrations compared to the NP supplemented group.

6.2 Materials and methods

Table 6.1 outlined a list of materials used within this chapter, their particle sizes and manufacturers.

Table 6.1: *A list of materials, size particle sizes and manufacturer used within Chapter 6.*

Chemical	Particle size	Manufacturer
Co_3O_4 NP	< 100 nm	Produced by hydrothermal synthesis (see Chapter 2, Section 2.2.1)
Co_3O_4 MP	< 100 µm	Sigma Aldrich, UK
$CoSO_4.7H_2O$	< 250 µm	Sigma Aldrich, UK
Xanthan Gum	N/a	Provided by the Indsutrial Partner

The trial was carried out in accordance with ASPA guidelines 1986, under license number PPL40/3677 and was approved by the Animal Welfare and Ethical Review Board at Nottingham University.

The schematic outlined in Figure 6.1 the processes and methods used in this section.

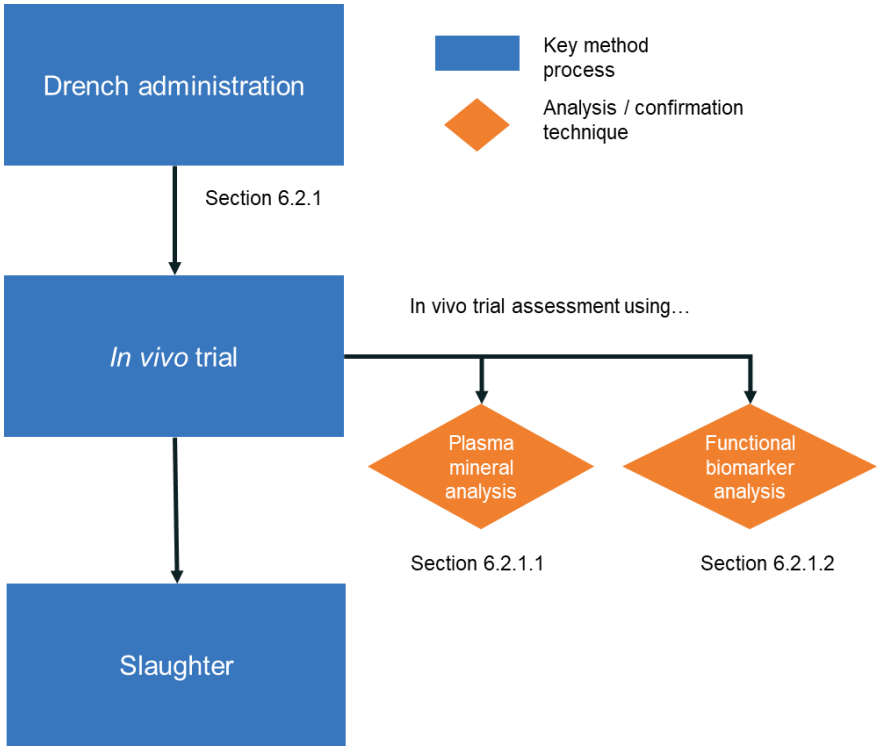

Figure 6.1: *A flow diagram to indicate the sequence of methods used within this chapter.*

6.2.1 Trial design

The trial took place over 14-days, with an additional 2-weeks prior for acclimatisation. Thirty, 7-month-old lambs were housed in a barn and fed a basal diet of grass silage *ad libitum*. The silage was analysed prior to the trial and had a cobalt content of 0.098mg/kgDM.

After acclimatisation lambs were weighed and sorted into six allocation groups, each containing a population of five animals. Groups were unbalanced and used restricted randomisation based on weight.

Similarly to Chapters 4 and 5, group sizes were calculated based on work produced by Dr Kendall's research group, presented at the BSAS conference, 2019. This work demonstrated that for measuring plasma cobalt and Vitamin B_{12}, group sizes of 4 ($P = 0.02$) and could be used for diagnostic purposes, whereas a group size of 8 was required for statistical significance of ($P = 0.05$).

As such single groups of 5 animals were assigned to the control and cobalt oxide microparticulate treatments. 2 groups of 5 animals were

assigned to the cobalt sulphate microparticulate and cobalt oxide NP treatments. The cobalt sulphate and cobalt oxide NP treatment groups had double the number of animals as there may have not been enough power within a group size of 5 to show statistical significance between the groups if there was only a small difference.

Table 6.2: *Schematic of treatment and control group animals for the trial.*

	Treatment/Control	**Total**
Group 1	Control	N= 5
Group 2	Cobalt sulphate ($CoSO_4.7H_2O$ MP)	N= 5
Group 3	Cobalt sulphate($CoSO_4.7H_2O$ MP)	N= 5
Group 4	Cobalt oxide nanoparticulate (Co_3O_4 NP)	N= 5
Group 5	Cobalt oxide nanoparticulate (Co_3O_4 NP)	N= 5
Group 6	Cobalt oxide microparticulate (Co_3O_4 MP)	N= 5

Stock solutions using xanthan gum (0.4 M, supplied by the Industrial Partner) as a carrier for each cobalt solution. Dispersions were made up to give a concentration of 0.12 mg/ 5 ml. The cobalt oxide (Co_3O_4) microparticulate (Sigma-Aldrich, UK) and the cobalt sulphate ($CoSO_4.7H_2O$) (Sigma Aldrich, UK)) were dispersed as powders, and the cobalt oxide NP were produced as an aqueous suspension by hydrothermal synthesis using the method from (Lester *et al*. 2012), see Chapter 2, Section 2.2.1 “Nanoparticle synthesis” for NP production details.

Once prepared, solutions were then tested with four replicates per treatment, using ICP-MS (XSeries^{II}, Thermo Fisher Scientific, USA) to confirm cobalt concentrations, corrected accordingly and then re-

analysed for confirmation (see Section 5.2.2.4 for mineral analysis methodology).

Blood samples were taken via jugular venepuncture using 9 ml lithium heparin (LH) tubes (BD vacutainer, UK) and Vacuette needles (Griener Bio One Ltd, UK). Samples on all days indicated (see Table 6.2) were processed and stored at -20 ºC, however, to save costs only those stated were analysed. Liver and kidney samples were stored at -20 ºC prior to analysis. Livers were then freeze-dried and digested before ICP-MS (XSeriesII, Thermo Fisher Scientific, USA) analysis.

Table 6.3: *Day by day outline of the trial, including acclimatisation period. On days 6, 8, 9, 11 and 12 no action was taken.*

Day	**Action taken**
-14	Acclimatisation period begins
-3	Sheep weighed and selenium dosed.
0	Sheep blood sampled (ICP and B_{12} analysis) and drenched.
1 – 2	Sheep blood sampled and drenched (blood not analysed unless data indicates.
3	Sheep blood sampled and drenched (ICP analysis).
4	Sheep blood sampled and drenched (blood not analysed unless data indicates.
5	Sheep blood sampled (ICP analysis).
7	Sheep blood sampled (ICP and B_{12} analysis).
10	Sheep blood sampled (blood not analysed unless data indicates.
13	Sheep weighed and blood sampled (ICP and B_{12} analysis).
14	Sheep slaughtered, livers and kidneys collected.

6.2.1.1 Plasma Cobalt Analysis

See Chapter 5, Section 5.2.2.4 for the methodology used to analyse the plasma cobalt concentrations. Analysis was carried out by the NuVetNA team.

6.2.1.2 Vitamin B_{12} Analysis

See Chapter 5, Section 5.2.2.5.1 for the methodology used to analyse the Vitamin B_{12} concentrations. Analysis was carried out by the NuVetNA team.

6.2.2 Statistical analysis

Statistical analysis of all parameters was carried out using Prism 8 (GraphPad Software, UK). Multiple T-tests were performed comparing each treatment against one another. Statistical significance was determined using the Holm-Sidak method, with an alpha value of 0.05. Each row was analysed individually, without assuming a consistent S.D. Where the data was not normally distributed the data was assessed on log transformation assessing individual treatments.

6.3 Results

6.3.1 Plasma cobalt concentration

Plasma cobalt concentrations are shown in Figure 6.2 demonstrated no significance between any of the groups. There was a general trend that showed in a slight increase in the plasma cobalt concentrations across all groups by day-13, however, due to variation within the groups no significant results are recorded.

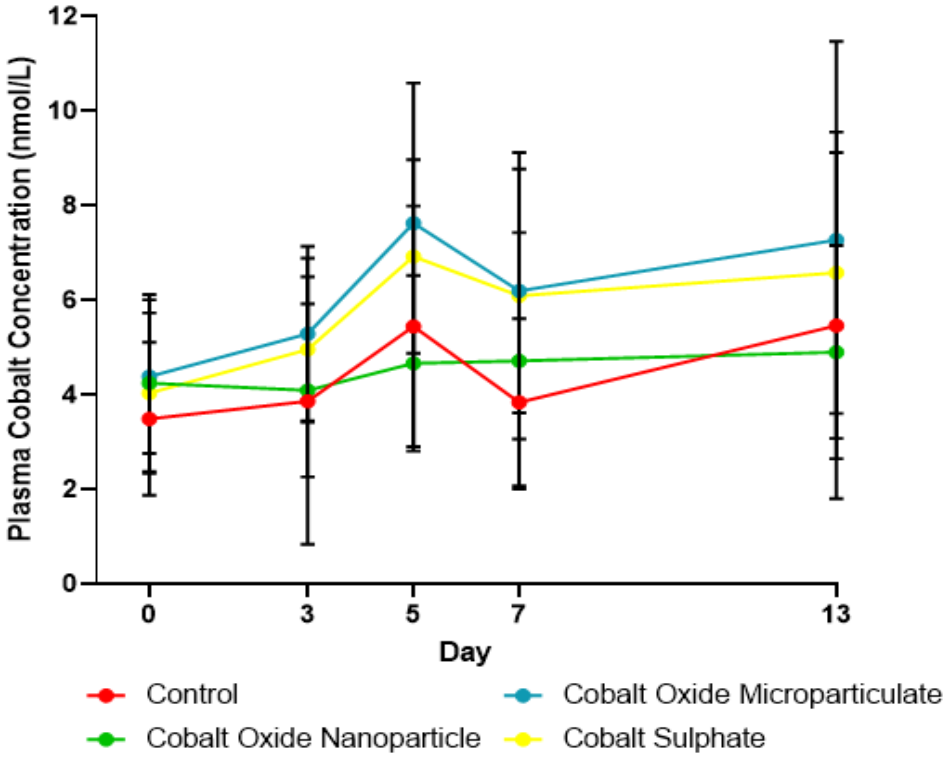

Figure 6.2: *Daily comparison of each treatment group's plasma cobalt concentrations (± S.D) across the 13-day trial. For groups control and cobalt oxide microparticulate n = 5, for groups cobalt oxide NP and cobalt sulphate n = 10.*

6.3.2 Vitamin B_{12} concentration

Unlike the plasma cobalt concentrations, Vitamin B_{12} concentrations across all groups showed an overall decline from day-0 to day-13. Natural variation within the groups prevented any statistical significance being shown due to treatments, however, a statistical significance of $p < 0.01$ was recorded for the initial Vitamin B_{12} concentrations between the control group and the cobalt sulphate group, showing concentrations of 748.6 ± 239.9 pmol/L, and 495.3 ± 96.2 pmol/L respectively.

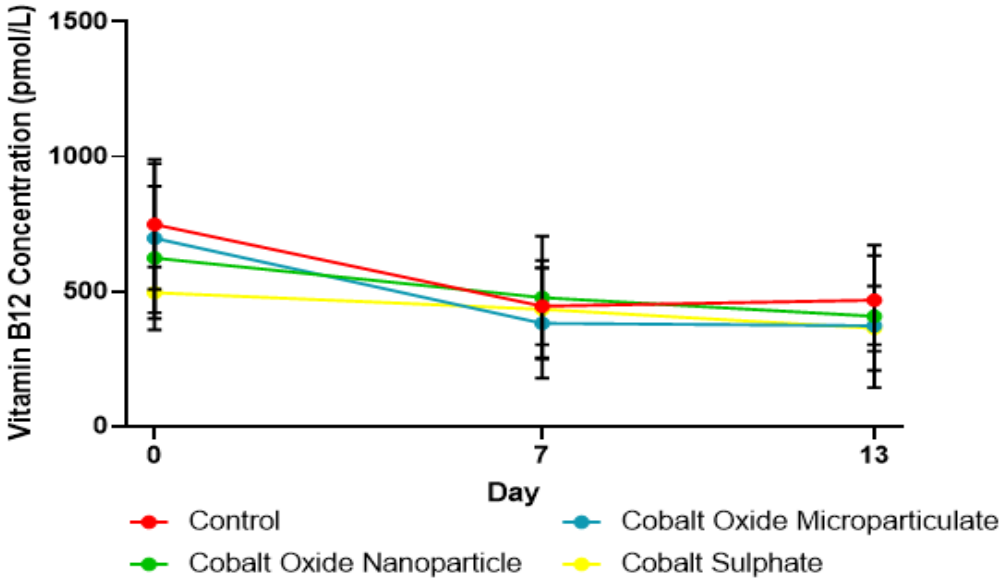

Figure 6.3: *Comparison of each treatment group's plasma Vitamin B_{12} concentration (± S.D) across the 13-day trial. For groups control and cobalt oxide microparticulate n = 5, for groups cobalt oxide NP and cobalt sulphate n = 10.*

6.3.3 Weight monitoring

Across the 13-days a general increase in weight was seen across the treatment groups compared to the control group (see Figure 6.4). Statistical significance was shown when comparing the final weights of the control group 38.1±1.1 kg against the cobalt oxide NP group 41.2±1.5 kg ($p < 0.05$) and the cobalt oxide microparticulate group 41.4± 2.0 kg ($p < 0.01$) respectively.

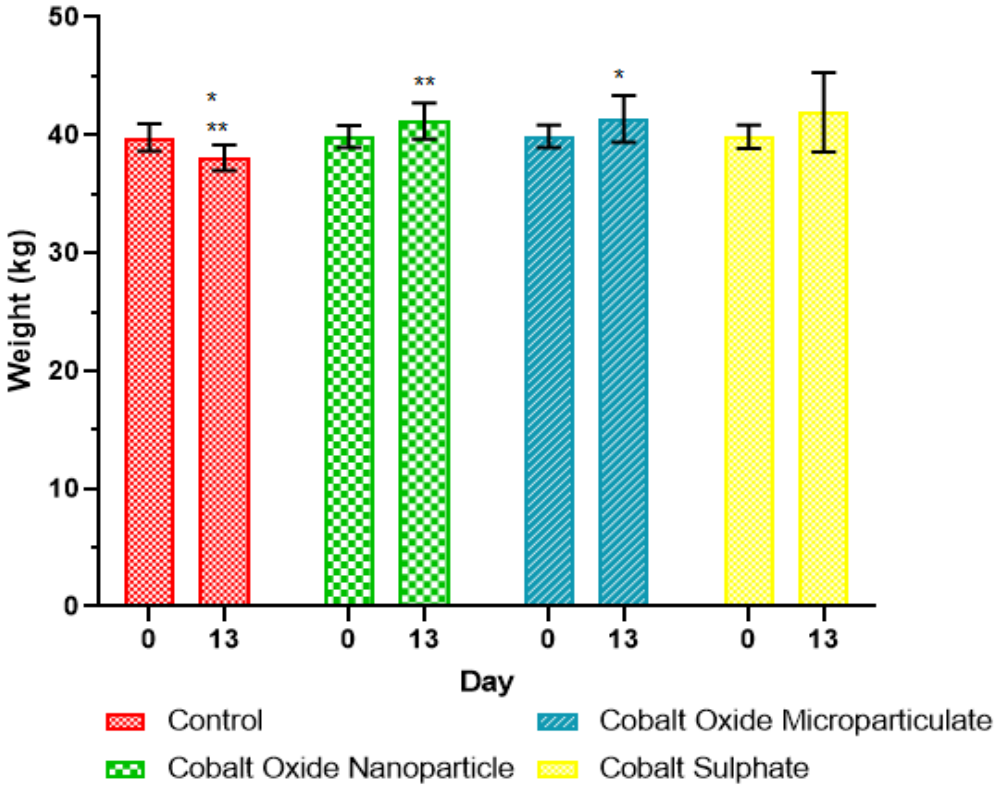

***Figure 6.4**: The initial and final mean live weights (± S.D) for each treatment group. For groups control and cobalt oxide microparticulate n = 5, for groups cobalt oxide NP and cobalt sulphate n = 10. Statistical significance of *(p < 0.01), **(p < 0.05).*

6.4 Discussion

The results showed mixed outcomes as a result of the supplementation with multiple different cobalt containing compounds.

No significant differences in plasma cobalt were shown across the 13-day trial, however, a spike in plasma cobalt concentration at day-5 across the microparticulate groups and control group was observed. This spike was to be expected as it was likely to be the day when cobalt concentrations within the body were likely to be highest due to being the final day of drenching after five consecutive days of treatments. However as this spike was also present for the control group, suggested it may have been due to forage cobalt content. The cobalt content of the forage, 0.098mg/kg DM, contained above “adequate” cobalt concentrations required by sheep (0.03-0.05 mg/kgDM) (Suttle, 2010). Whilst the control group had a lower average plasma cobalt concentration compared to the cobalt oxide MP and cobalt sulphate groups (5.45 ± 2.55 nmol/L, 7.64 ± 2.97 nmol/L, 6.93 ± 2.05 nmol/L, respectively), due to variation within the groups no statistical significance was recorded. The overall graph trend suggested that the steady increase in plasma cobalt concentration may have been independent of the supplements. This may have been due to the rumen microflora becoming more efficient at absorbing the low concentrations of cobalt as Smith and Marston, (1970) found that there was a linear decrease in cobalt conversion to cobalamins from 15 % in animals deficient in cobalt, compared to 3 % when supplemented daily with 1 mg cobalt. Additionally, it is also highly likely that it was due to the already adequate cobalt concentrations of the forage, highlighting that supplementing higher concentrations of minerals is not always better.

Alternatively, one possible reason for this steady background incline may have been due to the cobalt deficient ruminal cultures stabilising. McDonald and Suttle, (1986) experimented with continuous cultures from cobalt-rich and cobalt-deficient diets and the effect of cobalt supplementation. This study found that cobalt supplementation to

cultures that were previously on Co-deficient diets caused a shift in the rumen bacterial population, so that lower cobalt sources could be utilised more efficiently. Therefore, the bacterial colonies in this study may have started to adapt to the concentrations of cobalt in the forage, enabling a higher utilisation of cobalt over time. However, this trial might have been the lag-phase before improve conversion efficiency of cobalt to plasma cobalt, but, due to the short trial duration it's not possible to confirm this hypothesis without further study.

Despite the trial appearing to have quite high variation within groups, it is likely that this is representative of natural variation within the population. Williams, Williams and Kendall, (2017) observed a similar level of variability in both control and treatment groups to that observed in this study, implying this level of variation could readily be expected in a study of this type. However, due to the larger concentrations of cobalt utilised as treatments by Williams, Williams and Kendall, (2017), the doses applied still elicited statistically significant results. Therefore, it would be essential to have a larger sample size to take into account the population variance, or ensure that animals were in a marginal-deficient status before the beginning of the trial in order to show maximum effects in future work to confirm this hypothesis. Previous work in Chapter 5 suggested it was possible to demonstrate statistical significance for plasma cobalt and Vitamin B_{12} concentrations for group sizes of 10, however, as only cobalt sulphate and cobalt oxide nanoparticle groups had 10 animals within them, it demonstrated that the control and cobalt oxide microparticle groups would have been under powered, explaining why no significance would have been seen.

Interestingly, despite seeing a gradual increase in plasma cobalt concentrations in the control group and microparticulate supplemented groups (cobalt oxide and cobalt sulphate) Vitamin B_{12} concentrations showed a declining baseline from day-0 to 7, before seeming to stabilise by day-13. It is possible, as mentioned previously that due to Vitamin B_{12} being synthesised there is a lag seen between the

conversions of cobalt containing compounds to the functional vitamin due to the rumen microbial population needing to stabilise. Zervas, (1988) saw a significant drop in Vitamin B_{12} concentrations following supplementation with a bolus, only seeing an increase by day-134 compared to the initial starting concentrations. This bacterial stabilisation may significantly affect the Vitamin B_{12} contents of the rumen. Smith and Marston, (1970) found that *Escherichia coli* may degrade cobalamin to a by-product called cofactor B. This coliform was most concentrated in the rumen of sheep throughout the digestive system (Bryant, 1959), particularly in housed animals compared to pasture fed (Smith and Marston, 1970). Therefore, one hypothesis as to why supplementation had little observed effect on rumen Vitamin B_{12} was that the abundance of *E.coli* in the rumen acted to metabolise and degrade Vitamin B_{12} before it was measured. It may be possible to negate this in future trials by keeping animals at pasture, however, due to pasture availability and seasonality this protocol would not always be feasible.

An increase in plasma cobalt concentration does not always correlate to an increase in Vitamin B_{12} (Williams, Williams and Kendall, 2017). Indeed, blood plasma cobalt concentration is not necessarily an indication of the amount of cobalt absorbed into the bloodstream as cobalt has multiple other physiological applications other than Vitamin B_{12} synthesis, meaning 100 % conversion rate to Vitamin B_{12} cannot be assumed.

Cobalt is also used to synthesis Vitamin B_{12} analogues such as cobalamide. Cobalamide lacks the base ribose and phosphate groups possessed by cobalamin (Vitamin B_{12}) (Girar*d et al*. 2009). The phosphorous content of forage was not assessed, so it is not possible to conclude whether phosphorous concentration had a limiting effect on the rate of cobalt conversion to Vitamin B_{12} or to other materials such as cobalamide. Further testing to evaluate the conversion rates of cobalt to

downstream metabolites could include excretion studies on cobalt to estimate cobalt conversion into Vitamin B_{12}.

The cobalt supplements administered in this trial contained 0.12 mg Co/day, the recommended daily intake (Suttle, 2010). Literature assessing the effects of cobalt concentration generally evaluates the effects of higher concentrations compared to the work carried out in this study. Wang *et al.* (2010) supplemented 0.3 mg/kgDM/day cobalt and did not see a significant difference between the treatment and control groups Vitamin B_{12} concentrations (initially 594.5± 29.82 pmol/L, increased to 877.5 ± 47.9 pmol/l after 2 weeks, compared to the control 512.75±41.23 pmol/L increased to 807.2±71.7 pmol/L).

Millar and Albyt, (1984) elicited a significant response by supplying a much larger dose than Wang *et al.* (2010) with supplementation of 1 mg Co/day over two-weeks. Results of this higher dose were that the control groups Vitamin B_{12} concentration decreased from 405±147 pmol/L to 217±86 pmol/L, whereas the cobalt sulphate supplemented group had increased from 372 ± 278 pmol/L to 476 ± 149 pmol/L.

As such, a higher supplementation dose, more similar to Millar and Albyt, (1984) may have resulted in a significant response within 2-weeks. Alternatively, ensuring the animals were in a marginal to deficient concentration range before the trial started, so that any affects were highly noticeable could have improved the supplementation response. In this trial the lowest starting Vitamin B_{12} concentration recorded was 359 pmol/L, meaning that all animals were above the marginal to deficient parameters, as the suggested range for that is 150-300 pmol/L (Vellema et al. 1997).

It is possible that the supplements being administered by oral drenching resulted in the cobalt being excreted quicker than the microbes were able to adjust to the higher concentrations present, and were therefore unable to metabolise it.

It is also possible that the supplements being administered by drenching resulted in the cobalt being excreted quicker than the microbiome populations in the rumen were able to adapt to its continued presence and alter their metabolic pathways or species distribution towards a population that thrived in a cobalt rich environment.

Smith and Marston, (1970) found that the half-life for the decline of Co^{60} in the rumen contents was 17.5 hours, and suggested that only 1.2 % of the cobalt supplied would be present 28 hours after the dose. This would fit with the trend of the declining baseline seen in Figure 6.2, which suggested that all groups were insufficiently being supplied with cobalt to be metabolised. It could also be reasoned that due to blood sampling occurring approximately 24 hours after each treatment, troughs were being measured and therefore may not have given a true value of plasma cobalt concentration.

Xanthan gum is a polysaccharide used to stabilise emulsions. It was used as a carrier for this experiment to ensure a homogenous mix of stock solutions, intended to prevent the particles from dropping out of suspension.

As cobalt sulphate is a highly soluble salt, it is likely to readily dissolve in xanthan gum. However, Talukdar and Kinget, (1997) found when comparing hydrophilic polymers, xanthan gum (XG) and hydroxypropylmethyl cellulose (HPMC) that XG had a higher ability to hinder drug transport through its gel due to a difference in its matrices. Xanthan gum matrices swell due to acetyl side chains of the polymer network during hydration (Jaipal *et al*. 2013). As such the xanthan gum present may have hindered cobalt's bioavailability during this study.

Despite not seeing significant improvements in biochemical indicators such as plasma cobalt and Vitamin B_{12}, a significant difference in weight was observed between the control group and the cobalt oxide

NP group, and between the control group and the cobalt oxide microparticulate group ($p < 0.01$, and $p < 0.05$ respectively).

This suggested that the Vitamin B_{12} generated from the supplements was being utilised within the body to aid muscle generation, compared to the control group which saw an average reduction in weight from 39.8 ± 1.2 kg to 38.1 ± 1.1 kg. This also suggested that the cobalt MP and NP may be being utilised by different metabolic pathways, resulting in higher plasma cobalt of the microparticulate group, but increased weight gain in the NP group.

For example, Maisel *et al.* (2015) demonstrated that NP were able to penetrate deeper into certain mucus membranes of mice than their microparticulate counterparts, enabling enhanced delivery for utilisation. It was hypothesised that alternative metabolic pathways were being utilised in order to elicit this effect. It is possible, a similar effect was being caused by the cobalt oxide NP in the rumen. However, these live weight gain values to be treated with caution as, sheep's weight can easily fluctuate due to gut fill, with Chittock, (1994) finding that rumen contents can contribute up to 17 % of animal weight. Therefore, for short-term trials such as this, fasting should be considered prior to weighing in an attempt to reduce gut-fill variation.

6.5 Conclusion

It was not possible to definitively conclude whether cobalt oxide NP were more bioavailable than microparticulate cobalt oxide, or whether their supplementation at low concentrations in a drench format is a feasible method of alleviating mineral deficiencies.

It can be concluded that assessment and characterisation of these interactions requires further work over longer durations. This would allow the observation of rumen microflora stabilisation which would demonstrate how utilisation may differ across the supplements.

Increased trial length would also give a better indication of weight loss and gain, lowering the error incurred by gut-fill. Increasing the

concentration of the supplements supplied could possibly elicit a more pronounced and effect measurable to a statistically significant degree.

Finally, conducting the study in a cobalt-deficient pasture with a larger sample size may result in any supplementing effects being more noticeable due to the deficient status of the animals prior to supplementation, and the group sizes having enough power to demonstrate significance across all treatment groups. Furthermore, the possibility that any deleterious effects caused by bacteria more prevalent in housed conditions would be reduced, and the reduced variance in population could provide a higher power to statistical analysis.

Chapter 7 – Conclusions and future directions

7.1 Conclusions

The purpose of this work was to design and develop a long-term, mineral release product intended to release ions consistently and predictably over a 6-month period to alleviate mineral deficiencies.

New scientific knowledge was consistently generated in each of the four principle focus areas – bolus design, glass formulation, *in-vivo* testing and competitor evaluation (packaged into independent chapters 2, 3, 4, 5 and 6 respectively). However, there are multiple opportunities to improve the depth and coverage of research on each of these areas.

The research discussed in this thesis highlighted the complexities involved when developing a multi-disciplinary product, designed to be commercially launched. It considered the merits and draw-backs of different designs, taking into account feasibility to upscale; the characterisation of multiple different phosphate-based glass formulations including thermal and structural analysis; and finally it explored the possibility of incorporating NP into a supplement suitable for alleviating nutritional deficits in sheep.

As a result of the very tight timelines, the opportunities to generate wider learnings were narrow, and focus was consistently placed on pace and movement through the milestones required to validate each of the highly complex individual focus areas needed for bolus product design. Any and each of the five principle focus areas presents ample scope for an entire thesis of research and optimisation.

Whilst it was not possible to fully develop a product fit for market, this work acts an initial block to build further research upon, stressing the importance of understanding key scientific interactions before pressing forward.

Conclusions specific to each Chapter and further areas of learning are discussed in Sections 7.1.1-7.1.5.

7.1.1 The evolution of the bolus design

Chapter 2 suggested that it was highly likely the NP became part of the phosphate-based glass network due to the similar XRD analysis of the MP and NP glasses.

During the XRD analysis, it was expected that Bragg peaks, indicating a crystalline structure of NP would be clearly visible (Patel *et al.* 2017). However, no sharp peaks were visible on the spectrum results. This indicated that the structure was amorphous and glassy.

Despite this similarity, it was likely there was some slight structural differences due to the different thermal profiles of the glasses with and without NPs. The increased processing window of the CoNP-doped glass as a result of a decreased transition temperature and a delayed onset of crystallization suggested a more stable glass structure. Conversely, this trend was not consistent for the CuNP-doped glass that showed a decrease in processing window due to an accelerated onset of crystallization. The ^{31}P-NMR analysis on the CoNP-doped glass, this supported the DSC data that there were structural differences in the glasses due to the differences in Q-species ratios. However, it is important to note that due to cobalt's ability to act as an intermediate oxide, the CuNP-doped glass may not have exhibited similar differences in its Q-species ratio.

Opportunities for future work to understand these structural differences would utilise neutron diffraction to explore the atomic structure of the glasses, and x-ray photoelectron spectroscopy to understand the chemical states of its elements (Patel, 2017; Khattak *et al.* 1995). Insights from these analyses would aid understanding of exactly how the incorporation of NP affected the overall glass structure.

7.1.2 Phosphate-based glass formulation development

Chapter 3 explored the effect of different manufacturing parameters and glass formulations on ion release. It concluded that ash fusion furnaces were a highly effective tool when attempting to optimise sintering conditions to produce a denser pellet, making the pellet much less likely to be regurgitated by the animal while ruminating.

In the particle size ranges tested (25 < 200 µm), there were no major differences in sintering profiles, meaning the glass bolus could be produced with a wide range of particle sizes, making the manufacturing process easier. Pellets were then evaluated using helium pycnometry to assess their density, finding that there was no significant difference between the different particle size ranges. However, when combining this work with cross-sectional SEM image analysis of the structure and specifically the degree of porosity suggested that a particle size range <63 µm produced a sintered pellet with the smallest pores out of the particle sizes tested. The SEM analysis also highlighted that all sintered pellets had closed pore structure regardless of their size or frequency.

As such, an alternative quantitative density measurement would be required to properly evaluate the pore structure and how they may contribute to density of the finished product. Mercury porosimetry is regularly used within the group and academia (Hossain *et al.* 2018; Ravelingien *et al.* 2010) to quantify porosity of phosphate-based glass microspheres, however, this would not be suitable for this work due to the closed pore structure.

Instead, micro-computer tomography (microCT) could be used as part of further confirmation work to identify internal pore structures and the “true density” of boluses or pellets (du Plessis *et al.* 2018).

The *in vitro* ion release studies in this chapter highlighted the variability in the data set. This variability was likely due to a variety of inconsistent factors in the individual pellets including the degree of crystallinity, porosity and coating interactions. Due to time restrictions, it was not

possible to fully review each different glass formulations optimum sintering regime, and as a result of this it is highly likely there were crystalline phases throughout the pellets. Amorphous phases are preferentially hydrolysed compared to crystalline phases (Knowles, Franks, and Abrahams, 2001), as such a pellet with a higher proportion of crystallinity would likely have had a lower ion release rate. Therefore, to mitigate this variable moving forwards it would be important to produce consistent amorphous pellets before trialling *in vitro* degradation studies. This should be assessed by grinding sintered pellets to a powder to enable an overall assessment, and not just peripheral, of crystallinity when using XRD analysis to ensure that the sintered pellets are amorphous.

While the multi-material lacquer and resin barriers utilised for bolus protection functioned adequately across the study, there is significant scope for further research and optimisation of these barriers – especially when considering the manufacture of boluses and barrier application at an industrial scale.

In further testing, the initial coating methodology could be vastly improved upon by using an automated dip-coating tool, and a specified rate of withdrawal to ensure regular and consistent coating thickness (Fang *et al*. 2008). This would better control coat thickness and drying rate than application of coatings with a paintbrush.

As lack of adhesion between the coating and the pellet may result in micro-climates of low pH solutions due to the hydrolysis of phosphate glass, which in turn could exacerbate the rate of degradation in localised pockets, adhesion is another important variable to research further. As it would be important to measure not just adhesion strength, but also adhesion coverage over the bolus surface, combination approaches of SEM analysis and mechanical adhesion pulling-off testing could be utilised (Gartner, Li, and Almenar, 2015).

The starting point for glass formulations was based on existing literature and a competitive outlook on existing products in market. While the glass formulations reached were judged to be of sufficient quality for future trials, it is essential to look further into glass formulation.

The vast majority of glass formulations may have been based too closely on existing products, though due to tight timescales, it was infeasible to innovate fully in this area.

Key starting points of this additional research include structural analysis and studying of the interactions and physical properties of the glasses as well as their manufacturing parameters (such as sintering conditions) should be initiated, with the aim of building knowledge into novel glass products and formulations. Looking more widely may enable the identification and creation of novel glass formulations with better characteristics than the current market competitor, providing the Industry Partner with a competitive advantage in-market.

Lastly, a large proportion of this work was dedicated to incorporating NP into the sintered bolus design. Due to regulatory concerns regarding the incorporation of NP into animal feed, and secondarily, the complexity of incorporating NP into the sintered bolus the Industry Partner decided to discontinue the exploration of a phosphate-based glass bolus containing NP. It was possible that this commercially-motivated decision could have been made in advance of such extensive NP incorporation work being carried out, which would have enabled review other glass formulations. Had more in-depth work into non-NP containing sintered boluses been carried out, novel or improved glass formulations that may have been closer to the Industry Partner's desired release rate may have been found. Whilst this was not something that could have been altered, it stressed the importance of obtaining a specific and considered product brief before starting development work.

7.1.3 *In vivo* phosphate-based glass formulation assessment

Chapter 4 aimed to better characterise the P50-Ca2-Na17-Cu30-Co1 glass formulation, and understand if it would be suitable as a bolus prototype and whether there was a repeatable relationship between ion release in the *in vitro* dissolution apparatus and ion release in the rumen of sheep. This study concluded that the P50-Ca2-Na17-Cu30-Co1 glass formulation degraded too slowly within the rumen to meet the Industry Partner's desired daily release rate and that the current *in vitro* dissolution design was not representative of simulating *in vivo* conditions.

Upon review, multiple factors impacted on the ability to establish a relationship between these two environments. As the *in vivo* conditions of the rumen are a complex and dynamic environment, it is extremely difficult to build accurate *in vitro* model. The static environment created by the dissolution apparatus utilised resulted in accelerated degradation rates compared to *in vivo*. Additionally, the absence of digestive materials and rumen microorganisms meant that interactions that would naturally occur within the animal, such as mineral chelation and absorption were unable to be replicated within the *in vitro* system. These factors may have accounted for the differences in ion release profiles observed.

Moving forward it would be logical to improve the *in vitro* experimental dissolution design, so that the degradation profiles *in vitro* are more representative of the degradation rates observed *in vivo*. This is an essential step as it is important to minimise animal testing where necessary. This could also decrease the risk of moving from an *in vitro* environment to an *in vivo*, from a toxicity perspective of the animal and commercial risk to the Industry Partner.

An initial starting-point for improvement of the dissolution design could be by using the CoseIcure bolus as a control for refinement of the dissolution conditions. Work outlined in Chapter 5 showed that the CoseIcure boluses had dissolved by approximately month-4 of the *in*

vivo trial. Using this data it could be possible to replicate conditions of a similar dissolution rate for CoseIcure *in vitro*, and use this to inform dissolution protocol.

Additional areas of improvement for the *in vitro* study could be to increase the frequency of media replenishment, simulating rumen fluid turnover. Alternatively, the use of recovered rumen fluid from the abattoir or fistulated sheep, similar to the work carried out by Kawashima *et al.* (1997) could be used as dissolution media that may simulate some of the interactions within the rumen.

An intermediate transition between the dissolution apparatus and administering boluses to sheep could be using fistulated sheep. Fistulated sheep could enable regular review of bolus degradation over weeks and/or months without having to sacrifice sheep (Kendall, 1996). Sampling of rumen fluid could be easily conducted, as well as retrieving boluses for regular physiological review could be hugely beneficial before launching into long-term *in vivo* studies.

However, the use of fistulated sheep includes limitations such as the requirement of an ASPA license to create and maintain these “surgical models”, as well as ensuring healthy upkeep. Fistulated animals can be prone to necrotic lesions around the rumen cannula and so must be carefully monitored due to welfare concerns (Girardi *et al.* 2017). Additionally, consideration surrounding bolus retrieval when carrying out the intermediate reviews of the boluses should be considered. Some studies use dacron bags, though this may not be representative of “true” rumen parameters as the slightly enclosed environment is likely to be more concentrated and possibly acidic compared to the actual rumen, and possibly not exposed to physical abrasion (Orskov, Hovell, and Mould, 1980) it could be subjected to in the rumen. Manual searching could be performed though this may be difficult depending on gut-fill and may not be preferable from an animal welfare perspective.

7.1.4 Competitor bolus review *in vivo* trial

Chapter 5 showed that the CoseIcure bolus could effectively supplement trace minerals Co, Se and I which were then successfully metabolised to their functional constituents. However, under the trial conditions carried out, plasma mineral data and biochemical indicator data suggested the bolus may have fully dissolved closer to 3 < 4 months, rather than 8-months. This suggestion was supported by the slaughter recovery finding that boluses were no longer present within the rumens by month-4. It is possible that the boluses may have been regurgitated, however, biochemical metabolites such as plasma iodine showed a gradual decline in concentration suggesting boluses were releasing a reduced amount of ions over time. However, despite the bolus no longer being present a positive correlation in glutathione peroxidase concentrations were estimated to be adequate up until 8-months, supporting their label claims.

Additionally, the data collected suggested that the bolus does not deliver sustained and uniform release over its duration demonstrated by peaks in rumen fluid concentrations by day-28 and peaks in biochemical indicators concentrations by day-56. Unfortunately, it was not possible to review the biochemical indicator status for copper though liver copper concentrations supported the suggestion that an initial peak in copper release resulted in liver copper accumulation of treated animals. This work highlighted the importance of supplementing a nutritional deficit and how over-supplementation can raise concerns for narrower toxicity limit elements, such as copper.

This study could be improved by using a larger number of bolused sheep, enabling more frequent slaughter recovery of boluses, (possibly on a monthly basis). This would give greater detail into the degradation process and duration of the CoseIcure bolus. Alternatively, fistulated sheep could be used to gain this insight, however, it is likely only a very small number of fistulated sheep would be available for use, reducing sampling size and possibly statistical power. Additionally, fistulated

sheep would need to be kept in secure research facilities to be carefully monitored, reducing the simulation of realistic grazing at pasture that would be expected of a bolused animal. Differences might include housed sheep having different microflora present in their rumen that can be antagonistic or degrading towards functional biomarkers such as Vitamin $B_{12,}$ (Smith and Marston, 1970), or a less stable rumen pH (Jasmin *et al*. 2011) that may exacerbate bolus degradation, skewing ion release data.

7.1.5 The efficacy of cobalt oxide nanoparticles in sheep

Chapter 6 aimed to understand whether cobalt oxide NP were more bioavailable than their micro-sized counterparts and if drenched cobalt oxide NP would be a suitable method of cobalt supplementation. Unfortunately, this study was unable to definitively answer either question, though multiple valuable learnings were highlighted which should be explored in future work.

A key improvement to future work utilising a similar trial design would be to extend its length. Cobalt is utilised by rumen microflora, and it is well documented that in order for the microflora to effectively utilise changing cobalt sources or concentrations, the microflora need to adapt (Smith and Marston 1970). As such it can take up to 6 days for microflora to stabilise following changes to supplementation (Kawashima *et al.* 1997), meaning that an extended trial would have better characterised the longer term effects of the NP as a cobalt source.

Additionally, a longer trial could have assessed the live weight gains of lambs more efficiently, reducing the effect of gut fill variation. A longer trial may have also resulted in more prominent accumulation of NP in tissues, or abnormal histology of tissues associated with toxicity (Ghoreishi *et al.* 2013). These are important areas of consideration when developing a product designed to give long-term exposure of a compound, one that was previously overlooked.

Finally, an additional area to assess would be the effect of different CoNP concentrations in drenches. Supplementing at different concentrations of NP could have potentially shown the minimum dose required to elicit a biochemical effect compared to microparticles.

After this knowledge had been established, it could then be build upon to validate that the concentration is safe to supplement over a long-term period and how it could improve production parameters in the long-run.

7.2 Future Directions

There is significant opportunity for future work to build upon the findings of this thesis. Due to limited time scale, opportunities for investigating wider avenues of research could not be followed, and peripheral information that would be extremely valuable to the longer-term development and optimisation of the bolus product was not generated. Instead, an accelerated prototype development process was required by the Industry Partner in order to meet their research and development milestones.

Sections 7.2.1 – 7.2.3 outlined the main areas of expanded research that could have been beneficial in the long-run for product development.

7.2.1 Sintering optimisation

Sintering is a highly complex process. Incorporating multiple different additives and particles had a direct impact on the thermal profiles of the phosphate-based glasses trialled (see figures 3.9, 3.11 and 3.13). Further development could look at understanding the individual effects of incorporating these additives into the formulation to understand the interactions between the different chemicals. Adding multiple variables at once may have masked certain effects or characteristics.

For example, the DSC analysis shown in Figure 3.9 showed that the incorporation of additives delayed the onset of crystallization and increased the processing window. The mechanisms behind the increased stability of the glass could be a useful characteristic to understand to aid processing and manufacturing at scale in the future. However, without individually testing and assessing the effect of incorporating each compound individually is it not possible to confirm the interactions occurring.

Another area that was significantly overlooked was the colour change of pellets before and after sintering. Cobalt is a transition metal, capable of existing as either a tetrahedral or octahedral configuration

that affects its colour (Abdelgh*any et al*. 2014). Le, Eng and Navrotsky, (2006) studied the thermal behaviour and relative stability differences between α-$NaCoPO_4$ (pink phase), β- $NaCoPO_4$ (blue phase) and red $NaCoPO_4$. This paper reviewed the different coordination states of the cobalt in these compounds, and concluded that cobalt in $NaCoPO_4$ (pink phase) was in the octahedral coordination, whereas, β- $NaCoPO_4$ (blue phase) was in the tetrahedral coordination. It is likely that the pink colour of the sintered boluses used in this thesis was as a result of the cobalt in $NaCoPO_4$ existing in a octahedral coordination, rather than in the tetrahedral coordination (blue phase). Le, Eng and Navrotsky, (2006) stated that cobalt in a tetrahedral environment is more stable than an octahedral environment, and so this may have affected degradation rate. However, to support this suggestion XPS analysis would need to be performed and compared against the work carried out by Le, Eng and Navrotsky, (2006).

Another area of further exploration could be the optimisation of sintering conditions. Sintering conditions for the glass formulation P50-Ca2-Na17-Cu30-Co1 plus additives likely resulted in the formation of some crystalline phases throughout the bolus/pellet due to the close proximity of sintering temperature to the onset of crystallization temperature (see Figure 3.11). It is likely this impacted ion release studies due to the preferential hydrolysis of amorphous phases over crystalline phases. Therefore, prior to performing dissolution studies, sintered pellets should have been confirmed as amorphous following optimised sintering regimes to prove this hypothesis.

The use of techniques such as microCT to establish the internal porosity and structure of pellets could be useful for confirming a fully densified pellet and reducing the potential for regurgitation during rumination. This technique could have supported the identification of more effective sintering parameters by mapping the reduction of internal porosity. Additionally, Yin *et al.* (2019) used modelling to confirm density and pressure disparities of compacts when sintering

under pressure and optimised their sintering methodology. A similar model could have been developed to aid the uniform sintering of the boluses and/or pellets to potentially produce a more consistent sinter.

Ultimately, further work to improve sintering repeatability would be the most beneficial continuation of work as it is highly likely this would consequently reduce the variability of the ion release data observed.

7.2.2 In vivo simulation refinement

The *in vivo* experiment conducted to assess the ion release profile of the P50-Ca2-Na17-Cu30-Co1 formulation highlighted multiple shortcomings of the *in vitro* dissolution system. One of the improvements for *in vitro* experiments included larger dissolution vessels in an attempt to closer replicate the volumes observed within the rumen. The dissolution apparatus held 6x 1 L vessels, and whilst the possibility of using larger vessels was considered, it was not possible to adapt the dissolution apparatus. As such, it was deemed that the heating and agitating function of the dissolution apparatus was of a higher importance compared to the smaller volume. It was also considered whether this work could be outsourced to a larger scale dissolution facility, such as the Alltech IFM model recently installed at Harper Adams University. This equipment simulates rumen fermentation and evaluates the digestibility of feed. Therefore, using this equipment in future would enable assessment of bolus degradation in an environment that would also be able to simulate microbial interactions, a parameter not previously able to be assessed in the *in vitro* experiments carried out in this work.

An alternative to both of these refinements could be replenishing dissolution media more frequently to simulate rumen fluid turn-over. The RUSITEC system replenishes media daily, using recovered rumen fluid from cannulated (fistulated) sheep (Czerkawski and Breckenridge, 1977; Sol*iva et al*. 2011). This could improve overall rumen simulation due to the inclusion of microbes that may chelate or utilise ions

released by the boluses or pellets, simulating a more realistic environment.

Finally, conducting dissolution studies for longer periods of time would have been beneficial to assess the extended ion release profiles of glass formulations. Knowles, Franks and Abrahams, (2001) only recorded significant differences in their glass formulations ion release from day-10 onwards. As such it may have been that the experiments in this thesis were not conducted for long enough for the glass formulations to exhibit their true ion release rate. It was believed that by reviewing a higher number of glass formulations ion release in shorter dissolution studies, an ideal glass formulation would have been established quicker. However, such short durations of dissolution experiment, particularly when considering the intended duration of the product, were not representative and may have been misleading.

7.2.3 Nanoparticle bioavailability

Despite the Industry Partner deciding the incorporation of NP into an animal feed supplement was commercially too high risk to pursue, in the coming years pushes for higher yields and optimisation for raw material usage for environmental reasons may mean that regulations change as NP technologies become better understood by the public, governing bodies and the food industry.

This research highlighted that there is a need to understand the effects of lower concentration supplementation of NPs, over an increased duration of time in ruminants in order to be well prepared for movements in novel NP technologies.

At present multiple studies demonstrate the efficacy of NP within animals, eliciting significantly higher plasma mineral status, or biochemical indicator concentrations. However, these studies supplement with excessively high concentrations of minerals, often exceeding those set out in EU regulatory legislation in standard practice. Whilst this work is important and potentially demonstrates

“worst case scenarios”, extrapolating this into real life situations can be limited.

There are multiple opportunities to further understand the efficacy and viability of cobalt oxide NP in sheep covered in chapter 6 with additional *in vivo* testing.

The first key area of improvement would be to increase the study duration. While the trial conducted took place over 14-days, increasing trial duration may enable rumen microflora to stabilise, generating results more representative of ruminants grazing at pasture in an industrial farming environment.

This microflora stability is an important consideration as a stable microflora population that have been exposed to a consistent concentration of CoNP and adapted to them are more likely to demonstrate the actual utilisation of cobalt in a long-term supplement. Additionally, a longer study assessing live weight gains as a key performance indicator would be less susceptible to gut-fill variation skewing the data.

The concentration of CoNP supplied in the *in vivo* trial in Chapter 6 was 0.12 mg Co/day, the recommended daily intake. However, Ghoreishi *et al.* (2013) supplemented with significantly higher concentrations of 10 Co mg/kg body weight. The lambs studied by Ghoreishi *et al.* (2013) weighed between 18-20 kgs, estimating that lambs were supplemented between 180-200 mg Co/day. This level of supplementation is excessive, vastly exceeding toxicity limits of 10 Co mg/kgDM (National Research Council, 2007). Therefore, it is unsurprising the lambs supplemented to this level by Ghoreishi *et al.* (2013) exhibited hepatocyte necrosis. Whilst this study is useful to show the pathogenesis of excessive cobalt supplementation, it does stress the requirement for realistic supplementation concentrations of NP when accessing NP efficacy.

Similarly to Ghoreishi *et al.* (2013), it would be important to monitor the histological differences and accumulation of cobalt in different tissues, to understand whether different pathways are utilised by the NP as a result of long-term supplementation of cobalt NPs. Zhou *et al.* (2009) found that carp had a higher accumulation of Se in muscle when supplemented with nano-Se compared to selenomethionine. The authors hypothesised that this may have been due to a different metabolic pathway being used for nano-Se than that of selenomethionine. Therefore, it is important that this be considered when measuring the effects of supplementation, as well as plasma cobalt concentrations, Vitamin $B_{12,}$ and live weight gains.

Finally, should any further NP studies be conducted it would be essential to assess the concentration excreted. The long-term effects of NP on the environment are yet to be confirmed, however, it is highly likely that eutrophication and bioaccumulation is a real concern. As such, it would be crucial to understand the concentrations of NP excreted, and how this may compare to the microparticles. However, even if the levels of cobalt excreted are similar, this would not account for the NP being utilised through different metabolic pathways as mentioned in Zhou *et al.* (2009) and so the effects of NP on plant metabolism and soil bio-systems should be considered.

The assessment of NP being incorporated into animal feed and their effect on the environment is an area of science that could be greatly expanded. However, this exceeds the current scope of work.

Chapter 8 – References

Abbas, Z, C Labbez, S Nordholm, and E Ahlberg. 2008. “Size-Dependent Surface Charging of Nanoparticles.” *Journal of Physical Chemistry C* 112 (15): 5715–23. https://doi.org/10.1021/jp709667u.

Abdelghany, A M, F H Elbatal, H A Elbatal, and F M EzzElDin. 2014. “Optical and FTIR Structural Studies of CoO-Doped Sodium Borate, Sodium Silicate and Sodium Phosphate Glasses and Effects of Gamma Irradiation - A Comparative Study.” *Journal of Molecular Structure* 1074 (September): 503–10. https://doi.org/10.1016/j.molstruc.2014.06.011.

Abou Neel, E A, I Ahmed, J Pratten, S N Nazhat, and J C Knowles. 2005. “Characterisation of Antibacterial copper Releasing Degradable Phosphate Glass Fibres.” *Biomaterials* 26 (15): 2247–54. https://doi.org/10.1016/j.biomaterials.2004.07.024.

Agrmin Limited. 2020. “Trace Element Boluses for Cattle.” Www.Agrimin.Co.Uk. 2020.

AHDB 2010 " Trace element case studies for cattle and sheep" https://ahdb.org.uk/trace-element-supplementation

AHDB. 2014. “Managing Ewes for Better Returns.” *Better Returns Programme*, 2014. http://beefandlamb.ahdb.org.uk/wp/wp-content/uploads/2014/08/brp-manual-4-Managing-ewes080814.pdf.

Ahmed, I., M. Lewis, I. Olsen, and J. C. Knowles. 2004. “Phosphate Glasses for Tissue Engineering: Part 1. Processing and Characterisation of a Ternary-Based P2O5-CaO-Na 2O Glass System.” *Biomaterials* 25 (3): 491–99. https://doi.org/10.1016/S0142-9612(03)00546-5.

Ahmed, I, M P Lewis, S N Nazhat, and J C Knowles. 2005.

"Quantification of Anion and Cation Release from a Range of Ternary Phosphate-Based Glasses with Fixed 45 Mol% P2O5." *Journal of Biomaterials Applications* 20 (1): 65–80. https://doi.org/10.1177/0885328205049396.

Ahmed, I, A Parsons, A Jones, G Walker, C Scotchford, and C Rudd. 2010. "Cytocompatibility and Effect of Increasing MgO Content in a Range of Quaternary Invert Phosphate-Based Glasses." *Journal of Biomaterials Applications* 24 (6): 555–75. https://doi.org/10.1177/0885328209102761.

Aksu, S. 2009. "Electrochemical Equilibria of copper in Aqueous Phosphoric Acid Solutions." *Journal of the Electrochemical Society* 156 (11): c387–94. https://doi.org/10.1149/1.3215996.

Albrecht, M A, C W Evans, and C L Raston. 2006. "Green Chemistry and the Health Implications of Nanoparticles." *Green Chemistry* 8 (5): 417–32. https://doi.org/10.1039/b517131h.

Alderman, G, and D IH Jones. 1967. "The Iodine Content of Pastures." *Journal of the Science of Food and Agriculture* 18 (5): 197–99. https://doi.org/10.1002/jsfa.2740180506.

Anderson, J B, E Kostiner, M C Miller, and J R Rea. 1975. "The Crystal Structure of Cobalt Orthophosphate $Co_3(PO_4)_2$." *Journal of Solid State Chemistry* 14 (4): 372–77. https://doi.org/10.1016/0022-4596(75)90058-4.

Andrews, E D, L I Hart, and B J Stephenson. 1960. "Vitamin B12 and Cobalt in Livers from Grazing Cobalt-Deficient Lambs and from Others given Various Cobalt Supplements." *New Zealand Journal of Agricultural Research* 3 (2): 364–76. https://doi.org/10.1080/00288233.1960.10418091.

Andrews, E D, and D P Sinclair. 1962. "Goitre and Neonatal Mortality in Lambs." *Proceedings of the New Zealand Society of Animal Production* 22: 123–32.

Andrews, E D, B J Stephenson, C E Isaacs, and R H Register. 1966. "The Effects of Large Doses of Soluble and Insoluble Forms of Cobalt given at Monthly Intervals on Cobalt Deficiency Disease in Lambs." *New Zealand Veterinary Journal* 14 (11): 191–96. https://doi.org/10.1080/00480169.1966.33668.

Araújo, M, M Miola, E Bertone, G Baldi, J Perez, and E Verné. 2015. "On the Mechanism of Apatite-Induced Precipitation on 45S5 Glass Pellets Coated with a Natural-Derived Polymer." *Applied Surface Science* 353: 137–49. https://doi.org/10.1016/j.apsusc.2015.06.088.

Arechiga, C F, O Ortiz, and P J Hansen. 1994. "Effect of Prepartum Injection of Vitamin E and Selenium on Posrtpartum Reproductive Function of Dairy Cattle." *Theriogenology* 41: 1251–58.

Atkins, N E, E C L Bleach, A M Mackenzie, P R Hargreaves, and L A Sinclair. 2020. "Mineral Status, Metabolism and Performance of Dairy Heifers Receiving a Combined Trace Element Bolus and out-Wintered on Perennial Ryegrass, Kale or Fodder Beet." *Livestock Science* 231 (October 2019): 103865. https://doi.org/10.1016/j.livsci.2019.103865.

Awadeh, F T, R L Kincaid, and K A Johnson. 1998. "Effect of Level and Source of Dietary Selenium on Concentrations of Thyroid Hormones and Immunoglobulins in Beef Cows and Calves." *American Society of Animal Science* 76: 1204–15.

Azevedo, M M, G Jell, R V Law, R G Hill, and M M Stevens. 2010. "Synthesis and Characterization of Hypoxia-Mimicking Bioactive Glasses for Skeletal Regeneration." *Journal of Materials Chemistry*, no. 40.

Baalousha, M, G Cornelis, T A J Kuhlbusch, I Lynch, C Nickel, W Peijnenburg, and N W Van Den Brink. 2016. "Modeling Nanomaterial Fate and Uptake in the Environment: Current Knowledge and Future Trends." *Environmental Science: Nano* 3

(2): 323–45. https://doi.org/10.1039/c5en00207a.

Balemi, S C. 2008. “An Evaluation of the Efficacy of Orally Administered copper Glycine Complex, Copper Amino Acid Chelate, Copper Sulphate, a Copper Oxide Wire Particle Bolus and a Copper Edetate Injection in New Zealand Dairy Cows.” Massey University, New Zealand.

Banach, M, and A Makara. 2011. “Thermal Decomposition of Sodium Phosphates.” *Journal of Chemical and Engineering Data* 56 (7): 3095–99. https://doi.org/10.1021/je200381z.

Bassett, J H D, C B Harvey, and G R Williams. 2003. “Mechanisms of Thyroid Hormone Receptor-Specific Nuclear and Extra Nuclear Actions.” *Molecular and Cellular Endocrinology* 213 (1): 1–11. https://doi.org/10.1016/j.mce.2003.10.033.

Bennison, J J. 2010. Bolus and manufacturing process. *EP Patent 0879946A2*, issued 2010. http://info.sipcc.net/files/patent/fulltext/EP/200605/EP2099194A1/EP2099194A1.PDF.

Bitencourt da Silva A, Regina de Moura M, Zadorosny R. 2022. " Formation of copper oxide II in polymer solution-blow-spun fibers and the successful non-woven ceramic production" Materials Chemistry and Physics 278

Bjørk, R, V Tikare, H L Frandsen, and N Pryds. 2013. “The Effect of Particle Size Distributions on the Microstructural Evolution during Sintering.” *Journal of the American Ceramic Society* 96 (1): 103–10. https://doi.org/10.1111/jace.12100.

Black, D H, and N P French. 2004. “Effects of Three Types of Trace Element Supplementation on the Fertility of Three Commercial Dairy Herds.” *Veterinary Record* 154 (May): 652–58. https://doi.org/10.1136/vr.154.21.652.

Brauer, D S, R M Wilson, and T Kasuga. 2012. “Multicomponent

Phosphate Invert Glasses with Improved Processing." *Journal of Non-Crystalline Solids* 358 (14): 1720–23. https://doi.org/10.1016/j.jnoncrysol.2012.04.027.

Brow, R K. 2000. "Review : The Structure of Simple Phosphate Glasses." *Journal of Non-Crystalline Solids* 263&264: 1–28.

Bryant, M P. 1959. "Bacterial Species of the Rumen." *Bacteriological Reviews* 23 (3): 125–53. https://doi.org/10.1128/mmbr.23.3.125-153.1959.

Bunker, B C, G W Arnold, and J A Wilder. 1984. "Phosphate Glass Dissolution in Aqueous Soltuions." *Journal of Non-Crystalline Solids* 64: 291–316.

Center for the Polyurethanes Industry. 2014. "Polyurethanes and Thermal Degradation Guidance." *American Chemistry Council*, 2014.

Chapman, H L, and M C Bell. 1963. "Relative Absorption and Excretion by Beef Cattle of Copper from Various Sources." *Journal of Animal Science* 22 (1): 82–85.

Chen, H, T Zhang, and Y Ma. 2017. "Effect of Applied Stress on the Mechanical Properties of a Zr-Cu-Ag-Al Bulk Metallic Glass with Two Different Structure States." *Materials* 10 (7): 1–14. https://doi.org/10.3390/ma10070711.

Chittock, D G. 1994. "Lincoln University Digital Dissertation." *Researcharchive.Lincoln.Ac.Nz*. https://researcharchive.lincoln.ac.nz/bitstream/10182/1073/7/chittock_mps.pdf.txt.

Choudhary, B P, S Rai, and N B Singh. 2017. "Structure and Properties of Silver Phosphate Glasses Doped with Copper Oxide Nanoparticles." *Emerging Materials Research* 6 (2): 285–95. https://doi.org/10.1680/jemmr.16.00152.

Churbanov, M F, G E Snopatin, V S Shiryaev, V G Plotnichenko, and E M Dianov. 2011. “Recent Advances in Preparation of High-Purity Glasses Based on Arsenic Chalcogenides for Fiber Optics.” *Journal of Non-Crystalline Solids* 357 (11–13): 2352–57. https://doi.org/10.1016/j.jnoncrysol.2010.11.057.

Clarkson, A H. 2019. “The Copper Conundrum: Elucidating the Modes of Copper Antagonism in the Rumen.” *PhD. Thesis. University of Nottingham*.

Clarkson, A H, and N R Kendall. 2018. “Seasonality of Copper and Its Antagonsist Elements in Grazing Pasture.” In *British Society of Animal Science Annual Conference*, 1.

CoseCure Boluses. 2016. “Sheep Bolus Applicator Instructions.” Bimeda UK. 2016.

CoseICure Boluses. 2019. “CoseICure Sheep Bolus Data Sheet.” Bimeda UK. 2019. https://www.cosecureboluses.com/images/documents/1COS011_Data_Sheet.pdf.

Crichton, S N, M Tomozawa, J S Hayden, T I Suratwala, and J H Campbell. 1999. “Subcritical Crack Growth in a Phosphate Laser Glass.” *Journal of American Ceramic Society* 82 (11): 3097–3104.

Crosby, T F, T M Boland, P O Brophy, P J Quinn, J J Callan, and D Joyce. 2004. “The Effects of Offering Mineral Blocks to Ewes Pre-Mating and in Late Pregnancy on Block Intake , Pregnant Ewe Performance and Immunoglobulin Status of the Progeny.” *Animal Science* 79: 493–504.

Cuesta, P A, L R McDowell, W E Kunkle, N S Wilkinson, F Bullock, D Drew, and F G Martin. 1993. “Seasonal Variation of Soil and Forage Mineral Concentrations in North Florida.” *Communications in Soil Science and Plant Analysis* 24 (3–4): 335–47. https://doi.org/10.1080/00103629309368803.

Czerkawski, J W, and G Breckenridge. 1977. “Design and Development of a Long-Term Rumen Simulation Technique (Rusitec).” *The British Journal of Nutrition* 38 (3): 371–84. https://doi.org/10.1079/BJN19770102.

Daley, P J. 2018. “AN OPTIMISED ADVANCED ASH FUSION TEST FOR POWER GENERATORS.” University of Nottingham.

Daley, P J, O Williams, C Heng Pang, T Wu, and E Lester. 2019. “The Impact of Ash Pellet Characteristics and Pellet Processing Parameters on Ash Fusion Behaviour.” *Fuel* 251 (April): 779–88. https://doi.org/10.1016/j.fuel.2019.03.142.

DEFRA. 2012. “Agriculture in the United Kingdom.”

Dietzel, A. 1942. “Die Kationenfeldstärken Und Ihre Beziehungen Zu Entglasungsvorgängen, Zur Verbindungsbildung Und Schmelzpunkten von Silikaten.” *Zeitschrift Für Elektrochemie Und Angewandte Physikalische Chemie* 48 (1): 9–23. https://doi.org/10.1002/bbpc.19420480104.

Donald, G E, J P Langlands, J E Bowles, and A J Smith. 1993. “Subclinical Selenium Insufficiency 4 . Effects of Selenium , Iodine , and Thiocyanate Supplementation of Grazing Ewes on Their Selenium and Iodine Status , and on the Status and Growth of Their Lambs.” *Australian Journal of Experimental Agriculture* 33: 411–16.

Ducheyne, P, S R Radin, and L King. 1993. “The Effect of Calcium Phosphate Ceramic Composition and Structure on *in vitro* Behavior. I. Dissolution.” *Journal of Biomedical Materials Research* 27 (1): 25–34. https://doi.org/10.1002/jbm.820270106.

ECow Limited 2017. “Procedure to Make 1 L of Artificial Rumen Fluid.”

Ellis, K J, J M George, and R H Laby. 1983. “Evaluation of an Intraruminal Device to Provide an Iodine Supplement for Sheep.” *Australian Journal of Experimental Animal Husbandry* 23: 369–73.

Enjalbert, J, P Lebreton, O Salat, and F Schelcher. 1999. “Effects of Pre- or Postpartum Selenium Supplementation on Selenium Status in Beef Cows and Their Calves.” *Journal of Animal Science* 77 (1): 223–29.

Erasmus, E P, O T Johnson, I Sigalas, and J Massera. 2017. “Effects of Sintering Temperature on Crystallization and Fabrication of Porous Bioactive Glass Scaffolds for Bone Regeneration.” *Scientific Reports* 7 (1): 1–12. https://doi.org/10.1038/s41598-017-06337-2.

European Commision. 2012. “A European Strategy for Key Enabling Technologies-A Bridge to Growth and Jobs’.” Brussels. http://ipts.jrc.ec.europa.eu/publications/pub.cfm?id=3780.

———. 2021. “European Observatory for Nanomaterials.” European Union. 2021. https://euon.echa.europa.eu/es/regulation.

European Commission. 1999. *Commission Directive Amending the Annexes to Council Directive 70/S24/EEC Concerning Additives in Feedstuffs*. *Official Journal of the European Union*.

———. 2013. *Commission Regulation (EU) No 68/2013 of 16 January 2013 on the Catalogue of Feed Materials*. *Official Journal of the European Union*.

———. 2014a. *Commission Implementing Regulation (EU) No 1230/2014 Concerning the Authorisation of Copper as a Feed Additive for All Animal Species*. *Official Journal of the European Union*.

———. 2014b. *Commission Implementing Regulation (EU) No 131/2014 Concerning the Authorisation of Cobalt as a Feed Additive*.

———. 2015. *Commission Implementing Regulation (EU) 2015/861 of 3 June 2015 Concerning the Authorisation of Potassium Iodide, Calcium Iodate Anhydrous and Coated Granulated Calcium Iodate Anhydrous as Feed Additives for All Animal Species*. *Official*

Journal of the European Union. Vol. 2015/861.

European Union. 2003. *European Union Register of Feed Additives Pursuant to Regulation (EC) No 1831/2003 Annex I, List of Additives*.

Fang, Hsu Wei, Kuo Yen Li, Tai Lun Su, Thomas Chun Kuang Yang, Ji Sheng Chang, Po Liang Lin, and Wen Chung Chang. 2008. “Dip Coating Assisted Polylactic Acid Deposition on Steel Surface: Film Thickness Affected by Drag Force and Gravity.” *Materials Letters* 62 (21–22): 3739–41. https://doi.org/10.1016/j.matlet.2008.04.046.

Filettif, S, and B Rapoport. 1984. “Autoregulation by Iodine of Thyroid Protein Synthesis: Influence of Iodine on Amino Acid Transport in Cultured Thyroid Cells*.” *The Endocrine Society* 114 (4): 1379.

Follett, B K, and C Potts. 1990. “Hypothyroidism Affects Reproductive Refractoriness and the Seasonal Oestrous Period in Welsh Mountain Ewes.” *Journal of Endocrinology* 127: 103–9.

Foroutan, F, J McGuire, P Gupta, A Nikolaou, B A Kyffin, N L Kelly, J V Hanna, et al. 2019. “Antibacterial Copper-Doped Calcium Phosphate Glasses for Bone Tissue Regeneration.” *ACS Biomaterials Science and Engineering* 5 (11): 6054–62. https://doi.org/10.1021/acsbiomaterials.9b01291.

Frank, A. 1998. “‘Mysterious’ Moose Disease in Sweden. Similarities to Copper Deficiency and/or Molybdenosis in Cattle and Sheep. Biochemical Background of Clinical Signs and Organ Lesions.” *Science of the Total Environment* 209 (1): 17–26. https://doi.org/10.1016/S0048-9697(97)00303-3.

Franks, K, I Abrahams, G Georgiou, and J C Knowles. 2001. “Investigation of Thermal Parameters and Crytallisation in a Ternary CaO-Na2O-P2O5 Based Glass System.” *Biomaterials* 22: 497–501.

Galbraith, M L, W R Vorachek, C T Estill, P D Whanger, G Bobe, T Z

Davis, and J A Hall. 2016. “Rumen Microorganisms Decrease Bioavailability of Inorganic Selenium Supplements.” *Biological Trace Element Research* 171 (2): 338–43. https://doi.org/10.1007/s12011-015-0560-8.

Ğallstedt, M., J. Törnqvist, and M. S. Hedenqvist. 2001. “Properties of Nitrocellulose-Coated and Polyethylene-Laminated Chitosan and Whey Films.” *Journal of Polymer Science, Part B: Polymer Physics* 39 (10): 985–92. https://doi.org/10.1002/polb.1075.

Gao, H, T Tan, and D Wang. 2004. “Effect of Composition on the Release Kinetics of Phosphate Controlled Release Glasses in Aqueous Medium.” *Journal of Controlled Release* 96: 21–28. https://doi.org/10.1016/j.jconrel.2003.12.030.

Gartner, Hunter, Yana Li, and Eva Almenar. 2015. “Improved Wettability and Adhesion of Polylactic Acid/Chitosan Coating for Bio-Based Multilayer Film Development.” *Applied Surface Science* 332: 488–93. https://doi.org/10.1016/j.apsusc.2015.01.157.

Gawthorne, J M. 1968. “The Excretion of Methylmalonic and Formiminoglutamic Acids during the Induction and Remission of Vitamin B12 Deficiency in Sheep.” *Australian Journal of Biological Science* 21: 789–94.

German, R M, P Suri, and S J Park. 2009. “Review: Liquid Phase Sintering.” *Journal of Materials Science* 44 (1): 1–39. https://doi.org/10.1007/s10853-008-3008-0.

Ghirardi, J J, G Caja, D Garin, M Hernández-Jover, O Ribó, and J Casellas. 2006. “Retention of Different Sizes of Electronic Identification Boluses in the Forestomachs of Sheep.” *Journal of Animal Science* 84 (10): 2865–72. https://doi.org/10.2527/jas.2006-157.

Ghoreishi, S M, H Najafzadeh, B Mohammadian, E Rahimi, M R Afzalzadeh, M K Varnamkhasti, and H G Darani. 2013. “Effect of

Cobalt Nano-Particles on Serum Biochemical and Histopathological Changes in Liver and Kidney of Lambs." *Iranian Journal of Veterinary Science and Technology* 5 (2): 1–8.

Girard, C L, D E Santschi, S P Stabler, and R H Allen. 2009. "Apparent Ruminal Synthesis and Intestinal Disappearance of Vitamin B12 and Its Analogs in Dairy Cows." *Journal of Dairy Science* 92 (9): 4524–29. https://doi.org/10.3168/jds.2009-2049.

Girardi, Annita Morais, Samuel Santos Sousa, Amanda Festa Sabes, Gabriela Marchiori Bueno, Tiago José Caparica Módolo, Yuri da Silva Bonacin, Beatriz de Assis Pimenta, José Antônio Marques, and Luiz Carlos Marques. 2017. "One-Stage Rumen Fistulation With Permanent Silicone Cannula in Sheep." *Nucleus Animalium* 9 (1): 91–96. https://doi.org/10.3738/21751463.2140.

Givens, D I, G Zervas, V R Simpson, and S B Telfer. 1988. "Use of Soluble Glass Rumen Boluses to Provide a Supplement of Copper for Suckled Calves." *The Journal of Agricultural Science* 110 (1): 199–204. https://doi.org/10.1017/S0021859600079843.

Gonzales-Eguia, A, C M Fu, F Y Lu, and T F Lien. 2009. "Effects of Nanocopper on Copper Availability and Nutrients Digestibility, Growth Performance and Serum Traits of Piglets." *Livestock Science* 126 (1–3): 122–29. https://doi.org/10.1016/j.livsci.2009.06.009.

Gould, L, and N R Kendall. 2011. "Role of the Rumen in Copper and Thiomolybdate Absorption." *Nutrition Research Reviews* 24 (02): 176–82. https://doi.org/10.1017/S0954422411000059.

Grace, N D. 1975. "Studies on the Flow of Zinc, Cobalt, Copper and Manganese along the Digestive Tract of Sheep given Fresh Perennial Ryegrass, or White or Red Clover." *British Journal of Nutrition* 34 (1): 73–82. https://doi.org/10.1017/S0007114575000104.

Gracia-Fernández, C A, S Gómez-Barreiro, J López-Beceiro, S Naya, and R Artiaga. 2012. “New Approach to the Double Melting Peak of Poly(l-Lactic Acid) Observed by DSC.” *Journal of Materials Research* 27 (10): 1379–82. https://doi.org/10.1557/jmr.2012.57.

Grovum, L W, and V J Williams. 1979. “Rate of Passage of Digesta in Sheep - The Effect of Level of Food Intake on Mathematical Predications of the Kinetics of Digesta in the Reticulorumen and Intestines.” *British Journal of Nutrition* 38 (2–3): 425. https://doi.org/10.1079/bjn19770107.

Gunter, S A, P A Beck, and J M Phillips. 2003. “Effects of Supplementary Selenium Source on the Performance and Blood Measurements in Beef Cows and Their Calves.” *Journal of Animal Science* 81: 856–64.

Guyot, H, L A de Oliveira, E Ramery, J F Beckers, and F Rollin. 2011. “Effect of a Combined Iodine and Selenium Supplementation on I and Se Status of Cows and Their Calves.” *Journal of Trace Elements in Medicine and Biology* 25 (2): 118–24. https://doi.org/10.1016/j.jtemb.2011.02.003.

Han, Y, and I Kim. 2005. “Risk Factors for Retained Placenta and the Effect of Retained Placenta on the Occurrence of Postpartum Diseases and Subsequent Reproductive Performance in Dairy Cows.” *Journal of Veterinary Science* 6 (1): 53–59.

Hayden, J S, A J Marker III, T I Suratwala, and J H Campbell. 2000. “Surface Tensile Layer Generation during Thermal Annealing of Phosphate Glass.” *Journal of Non-Crystalline Solids* 264: 228–39.

Hoppe, A, B Jokic, D Janackovic, T Fey, P Greil, S Romeis, Jochen Schmidt, et al. 2014. “Cobalt-Releasing 1393 Bioactive Glass-Derived Scaffolds for Bone Tissue Engineering Applications.” *ACS Applied Materials and Interfaces* 6 (4): 2865–77. https://doi.org/10.1021/am405354y.

Hossain, K M Z, M S Hasan, R Felfel, and I Ahmed. 2014. "Development of Phosphate-Based Glass Fibers for Biomedical Applications." In *Hot Topics in Biomaterials*, 104–15. Future Medicine Ltd. https://doi.org/10.4155/EBO.13.352.

Hossain, K M Z, U Patel, A R Kennedy, L Macri-Pellizzeri, V Sottile, D M Grant, B E Scammell, and I Ahmed. 2018. "Porous Calcium Phosphate Glass Microspheres for Orthobiologic Applications." *Acta Biomaterialia* 72: 396–406.

Hotz, C S, D W Fitzpatrick, K D Trick, and M R L Abbe. 1997. "Dietary Iodine and Selenium Interact To Affect Thyroid Hormone Metabolism of Rats." *American Society for Nutritional Sciences* 127: 1214–18.

Hybu Cig Cymru. 2011. "Trace Element Supplementation of Beef Cattle and Sheep."

Jaipal, A, M M Pandey, A Abhishek, S Vinay, and S Y Charde. 2013. "Colloids and Surfaces B : Biointerfaces Interaction of Calcium Sulfate with Xanthan Gum: Effect on *in vitro* Bioadhesion and Drug Release Behavior from Xanthan Gum Based Buccal Discs of Buspirone." *Colloids and Surfaces B: Biointerfaces* 111: 644–50. https://doi.org/10.1016/j.colsurfb.2013.06.052.

James, P F, Y Iqbal, U S Jais, S Jordery, and W E Lee. 1997. "Crystallisation of Silicate and Phosphate Glasses." *Journal of Non-Crystalline Solids* 219: 17–29. https://doi.org/10.1016/S0022-3093(97)00247-0.

Jasmin, B H, R C Boston, R B Modesto, and T P Schaer. 2011. "Perioperative Ruminal PH Changes in Domestic Sheep (Ovis Aries) Housed in a Biomedical Research Setting." *Journal of the American Association for Laboratory Animal Science* 50 (1): 27–32.

Johnsen, L, N B Lyckegaard, P Khanal, B Quistorff, K Raun, and M O Nielsen. 2018. "Fetal Over-and Undernutrition Differentially

Program Thyroid Axis Adaptability in Adult Sheep.” *Endocrine Connections* 7 (5): 777–90. https://doi.org/10.1530/EC-18-0014.

Judd, J T, and G Matrone. 1962. “Sheep Erythrocyte Life Span in Estimation of Hemoglobin Turnover in Iron Metabolism Studies.” *The Journal of Nutrition* 77 (3): 264–68. https://doi.org/10.1093/jn/77.3.264.

Kalhan, S C. 2009. “Metabolism of Methionine *in vivo* : Impact of Pregnancy , Protein Restriction , and Fatty Liver Disease.” In *Emerging Societies- Coexistence of Childhood Malnutrition and Obesity*, 63:121–33.

Kaminska, E, A Minecka, M Tarnacka, B Hachu, K Kaminski, and M Paluch. 2020. “Influence of Annealing in the Close Vicinity of T on the Reorganization within Dimers and Its Impact on the Crystallization Kinetics of Gemfibrozil.” *Molecular Pharmaceutics* 17 (3): 990–1000. https://doi.org/10.1021/acs.molpharmaceut.9b01244.

Kapp, R W. 2014. “Isocyanates.” In *Encyclopedia of Toxicology: Third Edition*, 2:1112–31. https://doi.org/10.1016/B978-0-12-386454-3.00865-4.

Kart, H H, H Yildirim, S Ozdemir Kart, and T Çağin. 2014. “Physical Properties of Cu Nanoparticles: A Molecular Dynamics Study.” *Materials Chemistry and Physics* 147 (1–2): 204–12. https://doi.org/10.1016/j.matchemphys.2014.04.030.

Kasuga, T, and Y Abe. 1999. “Calcium Phosphate Invert Glasses with Soda and Titania.” *Journal of Non-Crystalline Solids* 243 (1): 70–74. https://doi.org/10.1016/S0022-3093(98)00820-5.

Kaufmann, S, and W A Rambeck. 1998. “Iodine Supplementation in Chicken, Pig and Cow Feed.” *Journal of Animal Physiology and Animal Nutrition* 80 (1–5): 147–52. https://doi.org/10.1111/j.1439-0396.1998.tb00517.x.

Kawashima, T, P R Henry, D G Bates, C B Ammerman, R C Littell, and J Price. 1997. “Bioavailability of Cobalt Sources for Ruminants 3: i*n vitro* Ruminal Production of Vitamin B12 and Total Corrinoids in Response to Different Cobalt Sources and Concentrations.” *Nutrition Research* 17 (6): 975–87.

Kawashima, T, P R Henry, RC Littell, and J Price. 1997. “Bioavailability of Cobalt Sources for Rumiants 2: Estimation of the Relative Value of Reagent Grade and Feed Grade Cobalt Sources from Tissue Cobalt Accumilation and Vitamin B12 Concentrations.” *Nutrition Research* 17 (6): 957–74.

Keener, H A, G P Percival, G H Ellis, and K C Beeson. 1950. “A Study of the Function of Cobalt in the Nutrition of Sheep.” *Journal of Animal Science* 9 (3): 404–13.

Kendall N R. 1996. "The delivery and utilisation of prophylactic doses of zinc in ruminant animals" PhD Thesis, University of Leeds, United Kingdom

Kendall N R. 2015. " A determination of sample number requirements for nutritional analyses in sheep" BSAS Conference Proceedings

Kendall, N. R., H. R. Holmes-Pavord, P. A. Bone, E. L. Ander, and S. D. Young. 2015. “Liver Copper Concentrations in Cull Cattle in the UK: Are Cattle Being Copper Loaded?” *Veterinary Record* 177 (19): 493. https://doi.org/10.1136/vr.103078.

Kendall, N R. 2021. “Nutritional Analysis - The University of Nottingham.” University of Nottingham. 2021.

Kendall, N R, A M Mackenzie, and S B Telfer. 2001. “Effect of a Copper, Cobalt and Selenium Soluble Glass Bolus given to Grazing Sheep.” *Livestock Production Science* 68: 31–39. www.elsevier.com/locate/livprodsci.

Kendall, N R, and S B Telfer. 2000. “Induction of Zinc Deficiency in Sheep and Its and Its Correction With a Soluble Glass.” *The*

Veterinary Record 146: 637–340.

Kennedy, D G, S Kennedy, W J Blanchflower, J M Scott, D G Weir, A M Molloy, and P B Young. 1994. “Cobalt-Vitamin B12 Deficiency Causes Accumulation of Odd- Numbered , Branched-Chain Fatty Acids in the Tissues of Sheep.” *British Journal of Nutrition* 71: 67–76.

Kennedy, S, S McConnell, H Anderson, D G Kennedy, P B Young, and W J Blachflower. 1997. “Histopathologic and Ultrastructural Alterations of White Liver Disease in Sheep Experimentally Depleted of Cobalt.” *Veterinary Pathology* 34: 575–84.

Khan, Z I, A Hussain, M Ashraf, K Ahmad, M Danish, and L R McDowell. 2008. “Effect of Seasonal Variation on the Copper Status in a Soil-Plant-Animal System.” *Acta Agronomica Hungarica* 56 (1): 55–67. https://doi.org/10.1556/AAgr.56.2008.1.6.

Khattak, G D, M A Salim, A B Hallak, M A Daous, E E Khawaja, L E Wenger, and D J Thompson. 1995. “Study of Valence States of Copper in Copper-Phosphate Glasses.” *Journal of Materials Science* 30: 4032–36.

Knowles, J C. 2003. “Phosphate Based Glasses for Biomedical Applications.” *Journal of Materials Chemistry* 13 (10): 2395–2401. https://doi.org/10.1039/b307119g.

Knowles, J C, K Franks, and I Abrahams. 2001. “Investigation of the Solubility and Ion Release in the Glass System K2O-Na2O-CaO-P2O5.” *Biomaterials* 22: 3091–96.

Koike, A, and M Tomozawa. 2006. “Fictive Temperature Dependence of Subcritical Crack Growth Rate of Normal Glass and Anomalous Glass.” *Journal of Non-Crystalline Solids* 352 (52–54): 5522–30. https://doi.org/10.1016/j.jnoncrysol.2006.09.023.

Langlands, J P, G E Donald, J E Bowles, and A J Smith. 1989. “Trace Element Nutrition of Grazing Ruminants. III. Copper Oxide Powder

as a Copper Supplement.” *Australian Journal of Agricultural Research* 40 (1): 187–93. https://doi.org/10.1071/AR9890187.

Lassiter, J W, and M C Bell. 1960. “Availability of Copper to Sheep from Cu-64 Labelled Inorganic Compounds.” *Journal of Animal Science* 19 (3): 754–62.

Le, S N, H W Eng, and A Navrotsky. 2006. “Energetics of Cobalt Phosphate Frameworks: α, β, and Red NaCoPO4.” *Journal of Solid State Chemistry* 179 (12): 3731–38. https://doi.org/10.1016/j.jssc.2006.08.007.

Ledoux, D R, E B Pott, P R Henry, C B Ammerman, A M Merritt, and J B Madison. 1995. “Estimation of the Relative Bioavailability of Inorganic Copper Soruces for Sheep.” *Nutrition Research* 15 (12): 1803–13.

Lee, I H, S H Shin, F Foroutan, N J Lakhkar, M S Gong, and J C Knowles. 2013. “Effects of Magnesium Content on the Physical, Chemical and Degradation Properties in a MgO-CaO-Na2O-P2O5 Glass System.” *Journal of Non-Crystalline Solids* 363 (1): 57–63. https://doi.org/10.1016/j.jnoncrysol.2012.11.036.

Lee, I, H Yu, N J Lakhkar, H Kim, M Gong, J C Knowles, and I B Wall. 2013. Development, characterisation and biocompatibility testing of a cobalt-containing titanium phosphate-based glass for engineering of vascularized hard tissues, 33 Materials science & Engineering C 2104–12.

Lemesle, T, F O Méar, L Campayo, O Pinet, B Revel, and L Montagne. 2014. “Immobilization of Radioactive Iodine in Silver Aluminophosphate Glasses.” *Journal of Hazardous Materials* 264 (January): 117–26. https://doi.org/10.1016/j.jhazmat.2013.11.019.

León, A, J S Glenn, and T B Farver. 1999. “Copper Oxide Wire Particles for the Treatment of Copper Deficiency in Sheep.” *Small Ruminant Research* 35 (1): 7–12. https://doi.org/10.1016/S0921-

4488(99)00034-6.

Lester, E, G Aksomaityte, J Li, S Gomez, J Gonzalez-Gonzalez, and M Poliakoff. 2012. “Controlled Continuous Hydrothermal Synthesis of Cobalt Oxide (Co_3O_4) Nanoparticles.” *Progress in Crystal Growth and Characterization of Materials* 58 (1): 3–13. https://doi.org/10.1016/j.pcrysgrow.2011.10.008.

Lin, Kaili, Jiang Chang, and Ruxiang Shen. 2009. “The Effect of Powder Properties on Sintering, Microstructure, Mechanical Strength and Degradability of β-Tricalcium Phosphate/Calcium Silicate Composite Bioceramics.” *Biomedical Materials* 4 (6). https://doi.org/10.1088/1748-6041/4/6/065009.

Liu M, Zhong J, Ma X, Huang Y, Xiang W. 2019. " Sodium borosilicate glass doped with Ni nanoparticles: Structure, formation mechanism and nonlinear optical properties" Journal of Non-Crystalline Solids 522, 15.

Lobato, J F P, G R Pearce, and R G Beilharz. 1980. “Effect of Early Familiarization with Dietary Supplements on the Subsequent Ingestion of Molasses-Urea Blocks by Sheep.” *Applied Animal Ethology* 6: 149–61.

Lu, J, M Descamps, J Dejou, G Koubi, P Hardouin, J Lemaitre, and J P Proust. 2002. “The Biodegradation Mechanism of Calcium Phosphate Biomaterials in Bone.” *Journal of Biomedical Materials Research* 63 (4): 408–12. https://doi.org/10.1002/jbm.10259.

Luginbuhl, J. 1983. “Comparative Anatomy of the Digestive Tract in Cattle, Sheep and Goats: A Review.” Raleigh.

Luo, Wenhua, Wangyu Hu, and Shifang Xiao. 2008. “Size Effect on the Thermodynamic Properties of Silver Nanoparticles.” *Journal of Physical Chemistry C* 112 (7): 2359–69. https://doi.org/10.1021/jp0770155.

Mackenzie, A M, M M Moeini, and S B Telfer. 2001. “The Effect of a

Copper, Cobalt and Selenium Bolus on Fertility and Trace Element Status of Dairy Cattle." *British Society of Animal Science* 26 (2): 423–27. https://doi.org/10.1017/s0263967x00034030.

Magnin, A, E Pollet, V Phalip, and L Avérous. 2020. "Evaluation of Biological Degradation of Polyurethanes." *Biotechnology Advances* 39 (April 2019): 107457. https://doi.org/10.1016/j.biotechadv.2019.107457.

Maisel, K, L Ensign, M Reddy, R Cone, and J Hanes. 2015. "Effect of Surface Chemistry on Nanoparticle Interaction with Gastrointestinal Mucus and Distribution in the Gastrointestinal Tract Following Oral and Rectal Administration in the Mouse." *Journal of Controlled Release* 197: 48–57. https://doi.org/10.1016/j.jconrel.2014.10.026.

Makaeva, A M, E S Aleshina, E A Sizova, and K N Atlanderova. 2019. "Cattle' Microbiocoenosis of Rumen While Various Feed Ultrafine Particles Release." In *IOP Conference Series: Earth and Environmental Science*, 341:1–10. https://doi.org/10.1088/1755-1315/341/1/012194.

Makarov, P M, I A Stepanova, A A Nazarova, S D Polishchuk, and G I Churilov. 2017. "Physiological and Biochemical Parameters of Holstein Heifers When Adding to Their Diet Bio-Drugs Containing Cuprum and Cobalt Nanoparticles." *Nano Hybrids and Composites* 13: 123–29. https://doi.org/10.4028/www.scientific.net/nhc.13.123.

Maro, J K, and J A Kategile. 1980. "Studies on Copper and Cobalt in Dairy Calves." *British Journal of Nutrition* 44: 25.

Marston, H R, and H J Lee. 1948. "Nutritional Factors Involved in Wool Production by Merino Sheep." *Australian Journal of Agricultural Research* 1: 376–87.

Masciangioli, T, and W X Zhang. 2003. "Environmental Technologies at the Nanoscale." *American Chemical Society - Environmental Science and Technology* 37 (5): 102A-108A.

https://doi.org/10.1021/es0323998.

Massera, J., M. Mayran, J. Rocherullé, and L. Hupa. 2015. “Crystallization Behavior of Phosphate Glasses and Its Impact on the Glasses’ Bioactivity.” *Journal of Materials Science* 50 (8): 3091–3102. https://doi.org/10.1007/s10853-015-8869-4.

Mccoy, M A, J A Smyth, W A Ellis, J R Arthur, and D G Kennedy. 1997. “Experimental Reproduction of Iodine Deficiency in Cattle.” *Veterinary Record* 141: 544–47. http://veterinaryrecord.bmj.com/.

McDonald, P, and N F Suttle. 1986. “Abnormal Fermentations in Continuous Cultures of Rumen Micro-Organisms given Cobalt-Deficient Hay or Barley as the Food Substrate.” *British Journal of Nutrition* 56: 369–78.

McDowell, L R. 1996. “Feeding Minerals to Cattle on Pasture.” *Animal Feed Science and Technology* 60 (3–4): 247–71. https://doi.org/10.1016/0377-8401(96)00983-2.

McDowell, L R, G Valle, L Cristaldi, P A Davis, O Rosendo, and N S Wilkinson. 1996. “Selenium Availability and Methods of Selenium Supplementation for Grazing Ruminants.” In *Proceedings 13th Annual Florida Ruminant Nutrition Symposium*, 86–101.

Metherell, A K. 1989. “The Cobalt Engima - Some Observations and Strategies for Otago and Southland.” In *Proceedings of the New Zealand Grassland Association*, 50:101–8.

Meyer, U, K Weigel, F Schöne, M Leiterer, and G Flachowsky. 2008. “Effect of Dietary Iodine on Growth and Iodine Status of Growing Fattening Bulls.” *Livestock Science* 115 (2–3): 219–25. https://doi.org/10.1016/j.livsci.2007.07.013.

Micromeritics. 2014. “AccuPyc II Operator Manual.”

Millar, K R, and A T Albyt. 1984. “A Comparison of Vitamin b 12 Levels in the Liver and Serum of Sheep Receiving Treatments Used to

Correct Cobalt Deficiency.” *New Zealand Veterinary Journal* 32 (7): 101–8. https://doi.org/10.1080/00480169.1984.35083.

Moro F, Tang S, Tuna F, Lester E. 2013. " Magnetic properties of cobalt oxide nanoparticles synthesised by a continuous hydrothermal method" Journal of Magnetism and Magnetic Materials 348 (1-7)

Mosheni, K. 2007. “Characterization of Precipitated Calcium Carbonate (PCC) Compounds on the Basis of Powder X-Ray Diffraction Data.” *University of Karlsruhe*. https://doi.org/10.1515/9783110928723.341.

Muller, L D, L V Schaffer, L C Ham, and M J Owens. 1977. “Cafeteria Style Free-Choice Mineral Feeder for Lactating Dairy Cows.” *Journal of Dairy Science* 60 (10): 1574–82. https://doi.org/10.3168/jds.S0022-0302(77)84073-3.

Muñoz, C., A. F. Carson, M. A. McCoy, L. E.R. Dawson, N. E. O’Connell, and A. W. Gordon. 2008. “Nutritional Status of Adult Ewes during Early and Mid-Pregnancy. 1. Effects of Plane of Nutrition on Ewe Reproduction and Offspring Performance to Weaning.” *Animal* 2 (1): 52–63. https://doi.org/10.1017/S1751731107001048.

Muth, O H, J E Oldfield, L F Remmert, and J R Schubert. 1958. “Effects of Selenium and Vitamin E on White Muscle Disease.” *Science* 128 (3331): 1090.

National Research Council. 2001. *Nutrient Requirements of Dairy Cattle*.

National Research Council. 2007. *Nutrient Requirements of Small Ruminants : Sheep, Goats, Cervids, and New World Camelids*. Book. Edited by National Research Council (U.S.). Committee on Nutrient Requirements of Small Ruminants. Animal Nutrition Series (Washington, D.C.). Washington, D.C.: National Academies Press.

Navarro, M, M P Ginebra, J A Planell, C C Barrias, and M A Barbosa.

2005. “*in vitro* Degradation Behavior of a Novel Bioresorbable Composite Material Based on PLA and a Soluble CaP Glass.” *Acta Biomaterialia* 1 (4): 411–19. https://doi.org/10.1016/j.actbio.2005.03.004.

Nguyen, P, V Leray, M Diez, S Serisier, J Le Bloc’H, B Siliart, and H Dumon. 2008. “Liver Lipid Metabolism.” *Journal of Animal Physiology and Animal Nutrition* 92 (3): 272–83. https://doi.org/10.1111/j.1439-0396.2007.00752.x.

Orskov, E R, F D D Hovell, and F Mould. 1980. “The Use of Nylon Bag Tehnique in the Evaluation of Feedstuffs.” *Tropical Anim. Prod.* 5: 195–213.

Pamp, D E, R D Goodrich, and J C Meiske. 1977. “Free Choice Minerals for Lambs Fed Calcium- or Sulfur-Deficient Rations.” *Journal of Animal Science* 45 (6): 1458–66.

Parisi, C, M Vigani, and E Rodríguez-Cerezo. 2015. “Agricultural Nanotechnologies : What Are the Current Possibilities ?” *Nano Today* 10 (2): 124–27. https://doi.org/10.1016/j.nantod.2014.09.009.

Parkins, J J, R G Hemingway, D C Lawson, and N S Ritchie. 1994. “The Effectiveness of Copper Oxide Powder as a Component of a Sustained-Release Multi-Trace Element and Vitamin Rumen Bolus System for Cattle.” *British Veterinary Journal* 150 (6): 547–53. https://doi.org/10.1016/S0007-1935(94)80038-3.

Patel, U, R M Moss, K M Z Hossain, A R Kennedy, E R Barney, I Ahmed, and A. C. Hannon. 2017. “Structural and Physico-Chemical Analysis of Calcium/Strontium Substituted, near-Invert Phosphate Based Glasses for Biomedical Applications.” *Acta Biomaterialia* 60 (September): 109–27. https://doi.org/10.1016/j.actbio.2017.07.002.

Patel, Uresha. 2017. “Manufacture and Structural Characterisation of

Novel Resorbable Phosphate-Glass Microspheres for Bone Repair Applications," no. June.

Persson, Kristin. 2016. "Calculated X-Ray Diffraction Patterns of Cubic Co_3O_4." *Materials Project Database*.

Petrovski, K R. 2017. "Assessment of the Rumen Fluid of a Bovine Patient." *Journal of Dairy & Veterinary Sciences* 2 (3): 1–7. https://doi.org/10.19080/jdvs.2017.02.555588.

Plessis, A du, P Sperling, A Beerlink, L Tshabalala, S Hoosain, Ntombi Mathe, and S G le Roux. 2018. "Standard Method for MicroCT-Based Additive Manufacturing Quality Control 2: Density Measurement." *MethodsX* 5 (September): 1117–23. https://doi.org/10.1016/j.mex.2018.09.006.

Porter, W L. 1999. Bolus for supplying biologically beneficial substances to ruminant animals, issued 1999.

Porter, William Leslie. 2013. Improvements in or relating to release of a beneficial substance from a bolus, issued 2013.

Quik, J T K, J A J Meesters, W J G M Peijnenburg, W Brand, and E A J Bleeker. 2020. "Environmental Risk Assessment (ERA) of the Application of Nanoscience and Nanotechnology in the Food and Feed Chain." *EFSA Supporting Publications*. Vol. 17. https://doi.org/10.2903/sp.efsa.2020.en-1948.

Rahman, I A, P Vejayakumaran, C S Sipaut, J Ismail, and C K Chee. 2008. "Effect of the Drying Techniques on the Morphology of Silica Nanoparticles Synthesized via Sol-Gel Process." *Ceramics International* 34 (8): 2059–66. https://doi.org/10.1016/j.ceramint.2007.08.014.

Raja, F N S, T Worthington, M A Isaacs, L Forto Chungong, B Burke, O Addison, and R A Martin. 2019. "The Antimicrobial Efficacy of Hypoxia Mimicking Cobalt Oxide Doped Phosphate-Based Glasses against Clinically Relevant Gram Positive, Gram Negative Bacteria

and a Fungal Strain." *ACS Biomaterials Science and Engineering* 5 (1): 283–93. https://doi.org/10.1021/acsbiomaterials.8b01045.

Ravelingien, M, S Mullens, J Luyten, M D'Hondt, J Boonen, B De Spiegeleer, T Coenye, C Vervaet, and J P Remon. 2010. "Vancomycin Release from Poly(d,l-Lactic Acid) Spray-Coated Hydroxyapatite Fibers." *European Journal of Pharmaceutics and Biopharmaceutics* 76 (3): 366–70. https://doi.org/10.1016/j.ejpb.2010.08.010.

Ray, C S, and D E Day. 1996. "Identifying Internal and Surface Crystallization by Differential Thermal Analysis for the Glass-to-Crystal Transformations." *Thermochimica Acta* 280–281 (SPEC. ISS.): 163–74. https://doi.org/10.1016/0040-6031(95)02640-1.

Rice, R W, C C M Wu, and F Borchelt. 1994. "Hardness-Grain-Size Relations in Ceramics." *Journal of American Ceraminc Society* 77 (10): 2549–53.

Rock, M J, R L Kincaid, and G E Carstens. 2001. "Effects of Prenatal Source and Level of Dietary Selenium on Passive Immunity and Thermometabolism of Newborn Lambs." *Small Ruminant Research* 40: 129–38.

Roduner, E. 2006. "Size Matters: Why Nanomaterials Are Different." *Chemical Society Reviews* 35 (7): 583–92. https://doi.org/10.1039/b502142c.

Romero-Pérez, A, E García-García, A Zavaleta-Mancera, J E Ramírez-Bribiesca, A Revilla-Vázquez, L M Hernández-Calva, R López-Arellano, and R G Cruz-Monterrosa. 2010. "Designing and Evaluation of Sodium Selenite Nanoparticles *in vitro* to Improve Selenium Absorption in Ruminants." *Veterinary Research Communications* 34 (1): 71–79. https://doi.org/10.1007/s11259-009-9335-z.

Rosu, D, L Rosu, and C N Cascaval. 2009. "IR-Change and Yellowing

of Polyurethane as a Result of UV Irradiation." *Polymer Degradation and Stability* 94 (4): 591–96. https://doi.org/10.1016/j.polymdegradstab.2009.01.013.

Rotruck, J T, A L Pope, H E Ganther, A B Swanson, D G Hafeman, and W G Hoekstra. 1973. "Selenium: Biochemical Role as a Component of Glutathione Peroxidase." *Science, New Series*. Vol. 179.

Rush, E C, P Katre, and C S Yajnik. 2014. "Vitamin B12 : One Carbon Metabolism , Fetal Growth and Programming for Chronic Disease." *European Journal of Clinical Nutrition* 68 (1): 2–7. https://doi.org/10.1038/ejcn.2013.232.

Saad, A P, A T Prakoso, M A Sulong, H Basri, D A Wahjuningrum, and A Syahrom. 2019. "Impacts of Dynamic Degradation on the Morphological and Mechanical Characterisation of Porous Magnesium Scaffold." *Biomechanics and Modeling in Mechanobiology* 18 (3): 797–811. https://doi.org/10.1007/s10237-018-01115-z.

Sadeghian, S, G A Kojouri, and A Mohebbi. 2012. "Nanoparticles of Selenium as Species with Stronger Physiological Effects in Sheep in Comparison with Sodium Selenite." *Biological Trace Element Research* 146 (3): 302–8. https://doi.org/10.1007/s12011-011-9266-8.

Sahoo, A, R Swain, and S K Mishra. 2014. "Effect of Inorganic , Organic and Nano Zinc Supplemented Diets on Bioavailability and Immunity Status of Broilers." *International Journal of Advanced Research* 2 (11): 828–37.

Sargison, N. D., D. M. West, and R. G. Clark. 1998. "The Effects of Iodine Deficiency on Ewe Fertility and Perinatal Lamb Mortality." *New Zealand Veterinary Journal* 46 (2): 72–75. https://doi.org/10.1080/00480169.1998.36060.

Schmoelzl, S, and F Cowley. 2016. “The Case for Pre-Parturient Selenium and Iodine Supplementation of Ewes for Improving Lamb Survival.” *Animal Production Science* 56 (8): 1263–74. https://doi.org/10.1071/AN15362.

Sciantec Analytical. 2020. “Dietary Minerals Report.”

Scott, J M. 1992. “Folate-Vitamin B12 Interrelationships in the Central Nervous System.” *Proceedings of the Nutrition Society* 51 (2): 219–24.

Scott, P. 2017. “Element Deficiencies in Sheep.”

Sharmin, N, F Gu, I Ahmed, and A J Parsons. 2017. “Compositional Dependency on Dissolution Rate and Cytocompatibility of Phosphate-Based Glasses: Effect of B2O3 and Fe2O3 Addition.” *Journal of Tissue Engineering* 8: 1–10. https://doi.org/10.1177/2041731417744454.

Sharmin, N, M S Hasan, A J Parsons, D Furniss, C A Scotchford, I Ahmed, and C D Rudd. 2013. “Effect of Boron Addition on the Thermal, Degradation, and Cytocompatibility Properties of Phosphate-Based Glasses.” *BioMed Research International* 2013: 12. https://doi.org/10.1155/2013/902427.

Shen, X, C Song, and T Wu. 2021. “Effects of Nano-Copper on Antioxidant Function in Copper-Deprived Guizhou Black Goats.” *Biological Trace Element Research* 199 (6): 2201–7. https://doi.org/10.1007/s12011-020-02342-1.

Sherrell, C J, P Brunsden, and P D McIntosh. 1987. “Pasture Cobalt Concentration and Its Effect on Vitamin B12 Status of Sheep Grazing Upland and Lowland Pastures in the Kaiwera District, Eastern Southland, New Zealand.” *New Zealand Journal of Agricultural Research* 30 (3): 325–31. https://doi.org/10.1080/00288233.1987.10421891.

Singh, R P, N S Tomer, and S V Bhadraiah. 2001. “Photo-Oxidation

Studies on Polyurethane Coating: Effect of Additives on Yellowing of Polyurethane." *Polymer Degradation and Stability* 73 (3): 443–46. https://doi.org/10.1016/S0141-3910(01)00127-6.

Smith, R. M., and Late H. R. Marston. 1970. " Production, Absorption, Distribution and Excretion of Vitamin B 12 in Sheep ." *British Journal of Nutrition* 24 (4): 857–77. https://doi.org/10.1079/bjn19700092.

Smith, R M, W S Osborne-White, and J M Gawthorne. 1974. "Folic Acid Metabolism in Vitamin B12-Deficient Sheep." *Biochemical Journal* 142: 105–17.

Soliva, C R, S L Amelchanka, S M Duval, and M Kreuzer. 2011. "Ruminal Methane Inhibition Potential of Various Pure Compounds in Comparison with Garlic Oil as Determined with a Rumen Simulation Technique (Rusitec)." *British Journal of Nutrition* 106 (1): 114–22. https://doi.org/10.1017/S0007114510005684.

Stähli, C, M Shah Mohammadi, K E Waters, and S N Nazhat. 2014. "Characterization of Aqueous Interactions of Copper-Doped Phosphate-Based Glasses by Vapour Sorption." *Acta Biomaterialia* 10 (7): 3317–26. https://doi.org/10.1016/j.actbio.2014.03.015.

Stange, U, M Scherf-Clavel, and H Gieseler. 2013. "Application of Gas Pycnometry for the Density Measurement of Freeze-Dried Products." *Journal of Pharmaceutical Sciences* 102 (11): 4087–99. https://doi.org/10.1002/JPS.23723.

Stangl, G I, F J Schwarz, and M Kirchgessner. 1999. "Moderate Long-Term Cobalt Deficiency Affects Liver, Brain and Erythrocyte Lipids and Lipoproteins of Cattle." *Nutrition Research* 19 (3): 415–27.

Sun, J, and S L Simon. 2007. "The Melting Behavior of Aluminum Nanoparticles." *Thermochimica Acta* 463 (1–2): 32–40. https://doi.org/10.1016/j.tca.2007.07.007.

Suratwala, T I, R A Steele, G D Wilke, J H Campbell, and K Takeuchi.

2000. “Effects of OH Content, Water Vapor Pressure, and Temperature on Sub-Critical Crack Growth in Phosphate Glass.” *Journal of Non-Crystalline Solids* 263 & 264: 213–27. www.elsevier.com/locate/jnoncrysol.

Suttle, N F. 2010. *Mineral Nutrition of Livestock, 4th Edition*. 4th ed. Cambridge.

Suttle, N F, P Abrahams, and I Thornton. 1984. “The Role of a Soil x Dietary Sulphur Interaction in the Impairment of Copper Absorption by Ingested Soil in Sheep.” *The Journal of Agricultural Science* 103 (1): 81–86. https://doi.org/10.1017/S0021859600043343.

Suttle, N F, A C Field, and R M Barlow. 1970. “Experimental Copper Deficiency in Sheep.” *Journal of Comparative Pathology* 80 (1): 151–62. https://doi.org/10.1016/0021-9975(70)90042-3.

Suttle, Neville F. 2012. “Copper Imbalances in Ruminants and Humans: Unexpected Common Ground.” *Advances in Nutrition* 3 (5): 666–74. https://doi.org/10.3945/an.112.002220.

Tait, R M, and L J Fisher. 1996. “Variability in Individual Animal’s Intake of Minerals Offered Free-Choice to Grazing Ruminants.” *Animal Feed Science and Technology* 62 (1 SPEC. ISS.): 69–76. https://doi.org/10.1016/S0377-8401(96)01007-3.

Takahashi, H, H Nakanii, and T Sakuma. 2005. “Effect of Iodide Addition on the Ionic Conduction in Silver Metaphosphate Glasses.” *Solid State Ionics* 176 (11–12): 1067–72. https://doi.org/10.1016/j.ssi.2005.01.007.

Talukdar, M M, and R Kinget. 1997. “Comparative Study on Xanthan Gum and Hydroxypropylmethyl Cellulose as Matrices for Controlled-Release Drug Delivery II. Drug Diffusion in Hydrated Matrices.” *International Journal of Pharmaceutics* 151: 99–107.

Tan, C, I Ahmed, A J Parsons, N Sharmin, C Zhu, J Liu, C D Rudd, and X Liu. 2017. “Structural, Thermal and Dissolution Properties of

MgO- and CaO-Containing Borophosphate Glasses: Effect of Fe2O3 Addition." *Journal of Materials Science* 52 (12): 7489–7502. https://doi.org/10.1007/s10853-017-0981-1.

Telfer, S B, G Zervas, and P Knott. 1982a. Water soluble glass article. GB2116424A, issued 1982.

———. 1982b. Water soluble glass article. 4482541, issued 1982.

Telsol Limited. 2012. "Coseicure Sheep Bolus Safety Data Sheet." *Telsol Limited*.

Thompson, K G, A J Fraser, B M Harrop, J A Kirk, J Bullians, and D O Cordes. 1981. "Glutathione Peroxidase Activity and Selenium Concentration in Bovine Blood and Liver as Indicators of Dietary Selenium Intake." *New Zealand Veterinary Journal* 29 (1–2): 3–6. https://doi.org/10.1080/00480169.1981.34776.

Todd, L M, I M Godber, and I R Gunn. 2004. "Case Report Iatrogenic Copper Deficiency Causing Anaemia and Neutropenia." *Annals of Clinical Biochemistry* 41: 414–16.

Todini, L. 2007. "Thyroid Hormones in Small Ruminants: Effects of Endogenous, Environmental and Nutritional Factors." *Animal* 1 (7): 997–1008. https://doi.org/10.1017/S1751731107000262.

Tominaka, S, K Kawakami, M Fukushima, and A Miyazaki. 2017. "Physical Stabilization of Pharmaceutical Glasses Based on Hydrogen Bond Reorganization under Sub-Tg Temperature." *Molecular Pharmaceutics* 14 (1): 264–73. https://doi.org/10.1021/acs.molpharmaceut.6b00866.

Trengrove, L C, and G J Judson. 1985. "Trace Element Supplementation of Sheep : Evaluation of Various Copper Supplements and a Soluble Glass Bullet Containing Copper , Cobalt and Selenium." *Australian Veterinary Journal* 62 (6527): 321–24.

Tsuboyama-Kasaoka, N, A Takizawa, M Tsubota-UtsugiI, M Nakade, E Imai, A Kondo, K Yoshida, N Okuda, Nobuo Nishi, and H Takimoto. 2013. “Dietary Intake of Nutrients with Adequate Intake Values in the Dietary Reference Intakes for Japanese.” *Journal of Nutritional Science and Vitaminology* 59: 584–95.

Turner, J C, V Shanks, P J Osborn, and S M Gower. 1987. “Copper Absorption in Sheep.” *Comparative Biochemistry and Physiology.* 86C (1): 147–50. https://doi.org/10.1016/0742-8413(87)90157-5.

U.S. Department of Health and Human Services. 1998. “NTP Technical Report on the Toxicology and Carcinogenesis Studies of in F344 / N Rats and B6C3F 1 Mice.” *National Institutes of Health*.

United Nations. 2019. “Growing at a Slower Pace, World Population Is Expected to Reach 9.7 Billion in 2050.” Growing at a Slower Pace, World Population Is Expacted to Reach 9.7 Billion in 2050. 2019. https://www.un.org/development/desa/en/news/population/world-population-prospects-2019.html.

Vellema, P, L Moll, H W Barkema, and Y H Schukken. 1997. “Effect of Cobalt Supplementation on Serum Vitamin B12 Levels, Weight Gain and Survival Rate in Lambs Grazing Cobalt-Deficient Pastures.” *Veterinary Quarterly* 19 (1): 1–5. https://doi.org/10.1080/01652176.1997.9694727.

Vijayakumar, M P, and V Balakrishnan. 2014. “Effect of Calcium Phosphate Nanoparticles Supplementation on Growth Performance of Broiler Chicken.” *Indian Journal of Science and Technology* 7 (8): 1149–54. www.indjst.org.

Villar, D, S M Rhind, P Dicks, S R Mcmillen, F Nicol, and J R Arthur. 1998. “Effect of Propylthiouracil-Induced Hypothyroidism on Thyroid Hormone Profiles and Tissue Deiodinase Activity in Cashmere Goats.” *Small Ruminant Research* 29: 317–24.

Vyas, V K, A S Kumar, S Prasad, S P Singh, and R Pyare. 2015.

"Bioactivity and Mechanical Behaviour of Cobalt Oxide-Doped Bioactive Glass." *Bulletin of Materials Science* 38 (4): 957–64.

Wallander, M L, E A Leibold, and R S Eisenstein. 2006. "Molecular Control of Vertebrate Iron Homeostasis by Iron Regulatory Proteins." *Biochimica et Biophysica Acta* 1763 (7): 668–89.

Walter, G, J Vogel, U Hoppe, and P Hartmann. 2001. "The Structure of CaO-Na2O-MgO-P2O5 Invert Glass." *Journal of Non-Crystalline Solids* 296 (3): 212–23. https://doi.org/10.1016/S0022-3093(01)00912-7.

Wang, R L, X H Kong, Y Z Zhang, X P Zhu, and Z Jia. 2007. "Influence of Dietary Cobalt on Performance, Nutrient Digestibility and Plasma Metabolites in Lambs." *Animal Feed Science and Technology* 135 (3–4): 346–52. https://doi.org/10.1016/j.anifeedsci.2006.08.011.

Wang, R L, W Zhang, X P Zhu, and Z H Jia. 2010. "Influence of Different Ratios of Cobalt and Copper Supplementation on Vitamin B12 Status and Nutrient Utilization in Sheep." *Agricultural Sciences in China* 9 (12): 1829–35. https://doi.org/10.1016/S1671-2927(09)60282-0.

Wei, G, F Luo, B Li, Y Liu, J Yang, Z Zhang, X Shu, Y Xie, and X Lu. 2021. "Immobilization of Iodine Waste Forms: A Low-Sintering Temperature with Bi2O3-B2O3-ZnO Glass." *Annals of Nuclear Energy* 150: 107817. https://doi.org/10.1016/j.anucene.2020.107817.

Whitehead, David C. 1979. *Chapter 4: Nutrient Elements in Ruminant Animals Outline of Digestive Physiology in Ruminant Animals*. 1st Editio. CABI Publishing.

Wilkinson, J M, J D Allen, R Tunnicliffe, M Smith, and P C Garnsworthy. 2014. "Wilkinson et Al (2014)."

Williams, J R, N E Williams, and N R Kendall. 2017. "The Efficacy of Supplying Supplemental Cobalt, Selenium and Vitamin B12 via the

Oral Drench Route in Sheep.” *Livestock Science* 200 (June): 80–84. https://doi.org/10.1016/j.livsci.2017.04.010.

Wooliams, J A, G Wiener, P H Anderson, and C H McMurray. 1983. “Variation in the Activities of Glutathione Peroxidase and Superoxide Dismutase and in the Concentration of Copper in the Blood in Various Breed Crosses of Sheep.” *Research in Veterinary Science* 34 (3): 253–56. https://doi.org/10.1016/s0034-5288(18)32219-7.

Wu, C, Y Zhou, W Fan, P Han, J Chang, J Yuen, M Zhang, and Y Xiao. 2012. “Hypoxia-Mimicking Mesoporous Bioactive Glass Scaffolds with Controllable Cobalt Ion Release for Bone Tissue Engineering.” *Biomaterials* 33 (7): 2076–85. https://doi.org/10.1016/j.biomaterials.2011.11.042.

Xie, F, T Zhang, P Bryant, V Kurusingal, J M Colwell, and B Laycock. 2019. “Degradation and Stabilization of Polyurethane Elastomers.” *Progress in Polymer Science* 90: 211–68. https://doi.org/10.1016/j.progpolymsci.2018.12.003.

Xu, W, Z Yin, J Yuan, Z Wang, and Y Fang. 2017. “Effects of Sintering Additives on Mechanical Properties and Microstructure of Si3N4 Ceramics by Microwave Sintering.” *Materials Science and Engineering A* 684 (January): 127–34. https://doi.org/10.1016/j.msea.2016.12.031.

Yin, Z, J Ye, D Hong, and W Xu. 2019. “Effect of Molding Pressure on Structural and Densification Behavior of Microwave-Sintered Ceramic Tool Material.” *International Journal of Applied Ceramic Technology* 16 (5): 2085–93. https://doi.org/10.1111/ijac.13237.

Zervas, G., E. Nikolaou, and A. Mantzios. 1990. “Comparative Study of Chronic Copper Poisoning in Lambs and Young Goats.” *Animal Production* 50 (3): 497–506. https://doi.org/10.1017/S0003356100004980.

Zervas, George. 1988. “Treatment of Dairy Sheep with Soluble Glass Boluses Containing Copper, Cobalt and Selenium.” *Animal Feed Science and Technology* 19: 79–83.

Zhang, L, and Q Zhou. 1997. “Water-Resistant Film from Polyurethane/Nitrocellulose Coating to Regenerated Cellulose.” *Industrial and Engineering Chemistry Research* 36 (7): 2651–56. https://doi.org/10.1021/ie960774h.

Zhang, L, and Q I Zhou. 1999. “Effects of Molecular Weight of Nitrocellulose on Structure and Properties of Polyurethane/Nitrocellulose IPNs.” *Journal of Polymer Science, Part B: Polymer Physics* 37 (14): 1623–31. https://doi.org/10.1002/(SICI)1099-0488(19990715)37:14<1623::AID-POLB7>3.0.CO;2-5.

Zhao, C, S Tan, X Xiao, X Qiu, J Pan, and Z Tang. 2014. “Effects of Dietary Zinc Oxide Nanoparticles on Growth Performance and Antioxidative Status in Broilers.” *Biological Trace Elements Research* 160: 361–67. https://doi.org/10.1007/s12011-014-0052-2.

Zhao, H, J Xie, A Mao, A Wang, Y Chen, T Liang, and D Ma. 2018. “Effects of Heating Mode and Temperature on the Microstructures, Electrical and Optical Properties of Molybdenum Thin Films.” *Materials* 11 (9): 1–13. https://doi.org/10.3390/ma11091634.

Zhao, Z, Y Hu, R Hoerle, M Devine, M Raleigh, P Pentel, and C Zhang. 2017. “A Nanoparticle-Based Nicotine Vaccine and the Influence of Particle Size on Its Immunogenicity and Efficacy.” *Nanomedicine: Nanotechnology, Biology, and Medicine* 13 (2): 443–54. https://doi.org/10.1016/j.nano.2016.07.015.

Zhou, Xuxia, Yanbo Wang, Qing Gu, and Weifen Li. 2009. “Effects of Different Dietary Selenium Sources (Selenium Nanoparticle and Selenomethionine) on Growth Performance, Muscle Composition and Glutathione Peroxidase Enzyme Activity of Crucian Carp

(Carassius Auratus Gibelio).” *Aquaculture* 291 (1–2): 78–81. https://doi.org/10.1016/j.aquaculture.2009.03.007.

Zhu, J, D Li, H Chen, X Yang, L Lu, and X Wang. 2004. “Highly Dispersed CuO Nanoparticles Prepared by a Novel Quick-Precipitation Method.” *Materials Letters* 58 (26): 3324–27. https://doi.org/10.1016/j.matlet.2004.06.031.